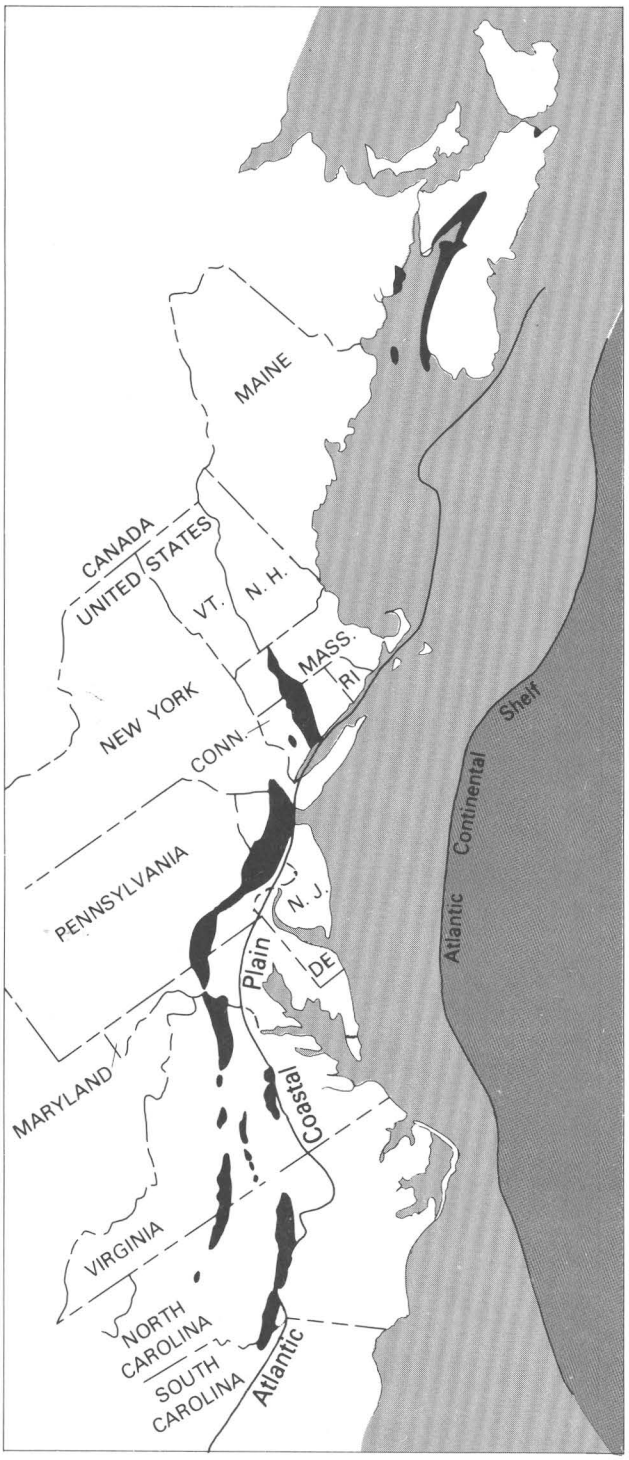

Proceedings of the Second U.S. Geological Survey Workshop on the Early Mesozoic Basins of the Eastern United States

U.S. Geological Survey Circular 946

Errata for Circular 946, Proceedings of the Second U.S. Geological Survey Workshop on the Early Mesozoic Basins of the Eastern United States

Figure 2.3 (p.8) should appear as follows:

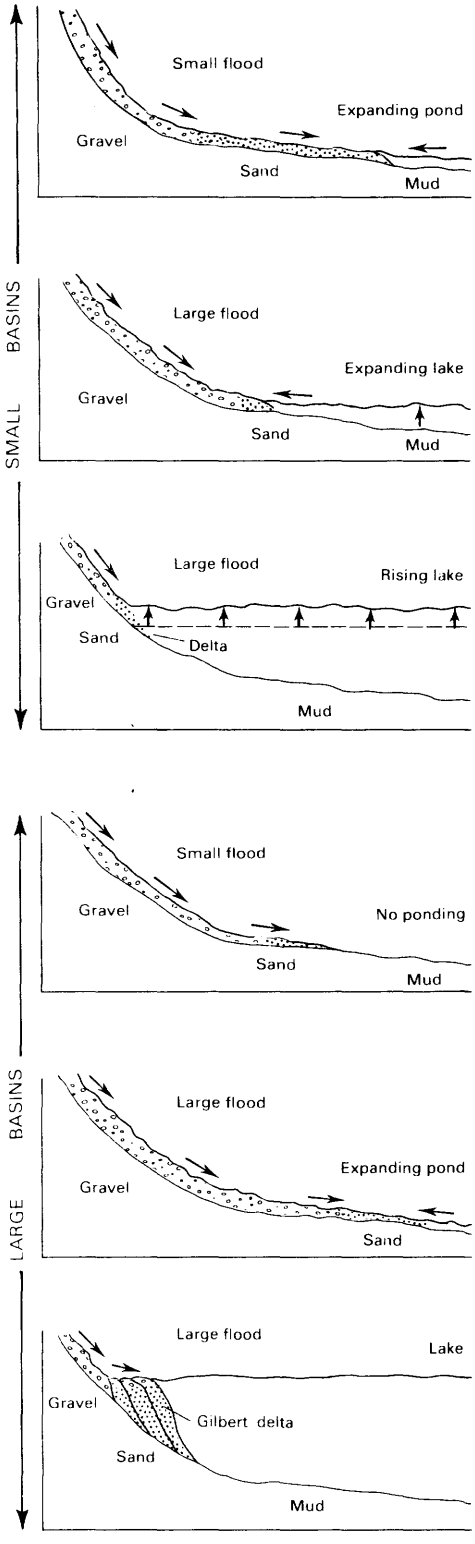

Not enough flood water to cause major ponding. Coarse sediment is transported until stream loses competence.

Flood water causes lake to expand. River deposits its coarse-grained sediment at intersection with the expanding lake.

Flood water causes lake level to rise over river level. Coarse sediment deposition migrates upstream, and the delta topset does not prograde.

Not enough flood water to cause ponding. Stream shallows and seeps into basin floor depositing all sediment.

Flood water causes lake to expand, but far from the river source. Coarse-grained sediment is transported until river shallows or intersects the expanding lake.

Flood water does not significantly affect lake level. Delta topset builds out into the lake.

FIGURE 2.3.—Process models for flood events and coarse-grained fluvial sediment distribution in closed basins. Small basins are tens to hundreds of square kilometers in size; large basins are thousands of square kilometers.

Figure 15.1 (p.82) should show the line of low-TiO_2 diabase in Pennsylvania and Maryland extending down to locality 9 in the Culpeper basin, Virginia. Neither the White Mountain Magma Series in New Hampshire and Vermont nor the nearby dikes to the east and southeast are low-TiO_2 magma types; both belong to a separate New England magmatic province. The Ware dikes are quartz-normative, low-TiO_2. On the explanation (p.83), York Haven (16) should include granophyre (G); 21 should be Barndoor rather than Buttress.

Figure 15.3 (p.85) should appear as follows:

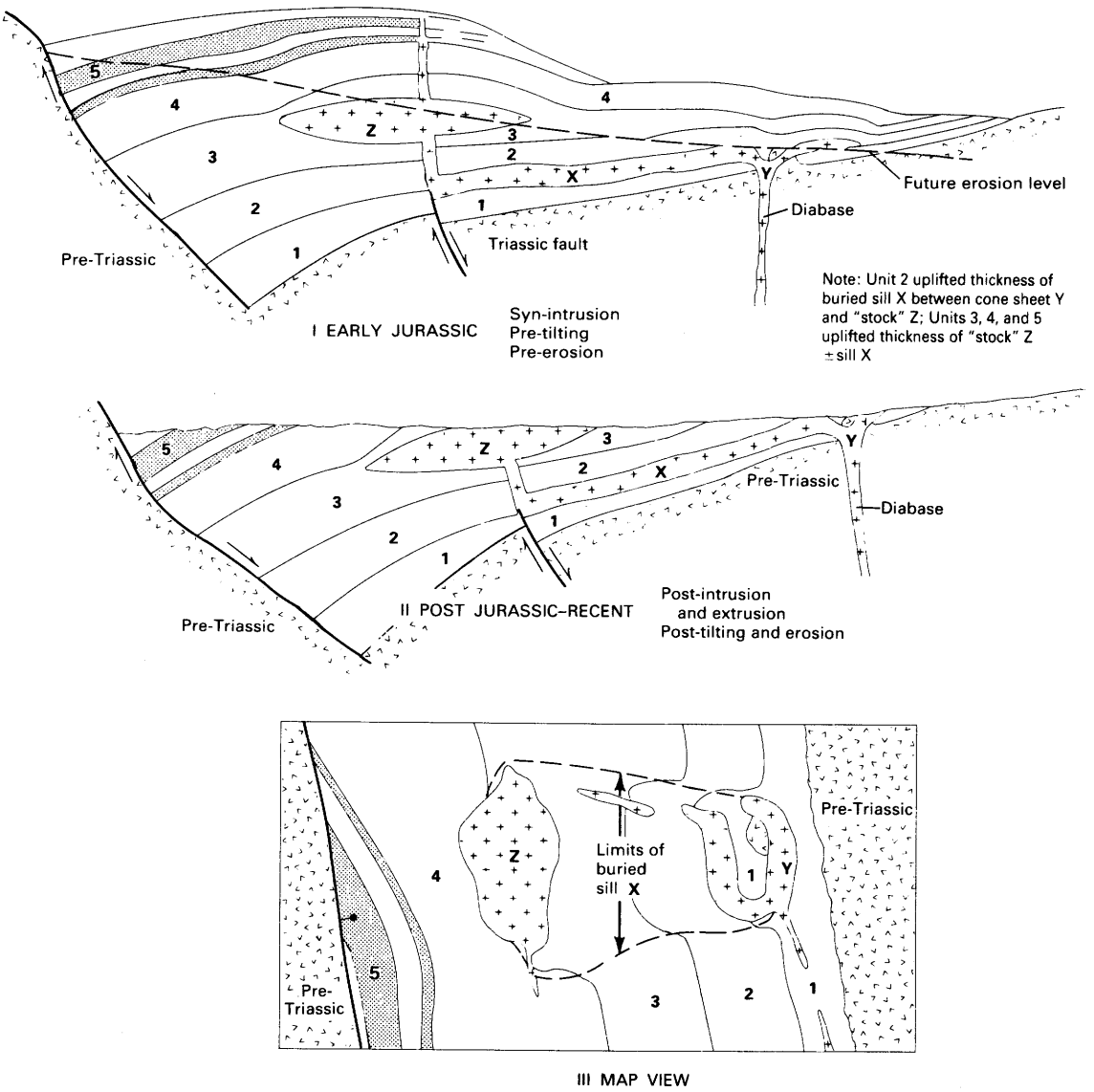

FIGURE 15.3.—Schematic cartoon showing cross sections before (I) and after (II) tilting and erosion; (III) map view of hypothetical early Mesozoic basin containing diabase intrusions and basalt flows.

Add the following sentence to caption for figure 31.1 (p. 140):

Southern boundary of basin (extremely heavy line) is an unconformity.

Proceedings of the Second U.S. Geological Survey Workshop on the Early Mesozoic Basins of the Eastern United States

Gilpin R. Robinson, Jr., and Albert J. Froelich, editors

U.S. Geological Survey Circular 946

1985

DEPARTMENT OF THE INTERIOR
DONALD PAUL HODEL, Secretary

U.S. GEOLOGICAL SURVEY
Dallas L. Peck, Director

Library of Congress Cataloging-in-Publication Data

U.S. Geological Survey Workshop on the Early Mesozoic Basins of the Eastern United States (2nd : 1984 : Reston, Va.)
Proceedings of the Second U.S. Geological Survey Workshop on the Early Mesozoic Basins of the Eastern United States.

(U.S. Geological Survey circular ; 946) Proceedings of the workshop held Nov. 14–16, 1984, Reston, Va.
Supt. of Docs. no. : I 19.4/2:946
1. Geology, Stratigraphic—Mesozoic—Congresses. 2. Geology—United States—Congresses. I. Robinson, Gilpin R. II. Froelich, A. J. (Albert Joseph), 1929– . III. Title. IV. Series.

QE675.U618 1985 551.7'6'0975 85–18829

Free on application to Distribution Branch, Text Products Section,
U.S. Geological Survey, 604 South Pickett Street, Alexandria, VA 22304

CONTENTS

TABLES

ILLUSTRATIONS

FOREWORD

Gilpin R. Robinson, Jr., and Albert J. Froelich

The extended abstracts in this volume are summaries of papers presented orally at the second U.S. Geological Survey (USGS) Workshop on the Early Mesozoic Basins of the Eastern United States, held November 14–16, 1984, at the National Center in Reston, Virginia. The first workshop, limited solely to USGS staff, was held in June of 1982; it was focused on assessing the status of current studies of Mesozoic geology underway in the USGS and on developing a regional overview of the basins as a prelude to initiating an integrated research program to investigate Mesozoic geology along the east coast of the United States. The second workshop was planned as a progress report on ongoing topical studies and was designed to improve communication between members of the various research projects and outside scientists funded by the USGS program. To promote discussion among participants with the goal of testing hypotheses and initiating new approaches to scientific investigation, participants were encouraged to present preliminary and tentative interpretations from work in progress. Consequently, participation in the workshop was generally limited to USGS project scientists, interested USGS managers, and funded outside colleagues from academia.

Support for this team research project is provided jointly by the Strategic and Critical Minerals Program and the Geologic Framework and Synthesis Program at the USGS. A new objective of these programs is to focus comprehensive studies of geology, geophysics, and mineral resources on geological provinces rather than on quadrangles, political provinces, or commodities. Another objective is to initiate new geologic mapping and cooperative interdisciplinary research programs with State geological surveys and universities. These efforts should increase overall knowledge and understanding of regional geology and geological processes and thus enable us to identify possible new frontiers for mineral exploration by industry. An important subtheme of the workshop is this relationship between geologic processes and the development and identification of potential mineral endowment.

Publication of this circular will provide information on this current USGS research program in a timely fashion. Much of the data presented are preliminary, and some of the conclusions are tentative and may change as more data are gathered and results evaluated. Some of the geologic names used in the extended abstracts are informal. Both metric and English units are used in the abstracts; in general, the unit actually used during measurement is reported in each case. Most illustrations were provided by the authors and were not professionally drafted. The papers benefited greatly from careful technical review by Kathleen Krafft of the USGS.

WORKSHOP OVERVIEW

Gilpin R. Robinson, Jr., Joseph P. Smoot, and Albert J. Froelich

The purpose of this USGS workshop was to provide a forum where scientists actively involved in research on the early Mesozoic basins of the Eastern United States could meet informally to exchange ideas, evaluate progress, and chart future research directions.

A unifying theme that emerged from the meeting was the linking of descriptive geology to genetic models of geologic processes, which provides new ways to evaluate existing data and to test hypotheses. This concept is particularly important in poorly exposed regions, such as the Eastern U.S. Mesozoic province, where many geologic relations are poorly known and much geology is inferred from scanty data. These process-oriented models, while strongly limited by the validity of their underlying assumptions, provide predictive constraints on possible lateral and temporal

variation in geologic features. These models can be powerful predictive tools, which can be tested using existing data and which can guide our search for critical information. It was hoped that this meeting would explore the ramifications of these developing geologic models and provide scientific interaction to improve and strengthen them.

The papers presented at the workshop were grouped into five sessions that focused on developing concepts of basin formation, basin sedimentation, organic maturation processes, development and character of igneous provinces, and mineral resources. The session titles are

(1) Stratigraphy, sedimentology, tectonics, and geophysics
(2) Organic geochemistry
(3) Igneous geochemistry
(4) Mineral resources, and
(5) Topical study of the Gettysburg basin, Pennsylvania

Highlights of the five sessions are summarized below. Each paper in this volume was assigned a number; the numbers in parentheses that follow authors' names in this section refer to those papers.

SESSION 1

The presentations on sedimentology and stratigraphy emphasized the use of depositional models as the key to stratigraphic reconstructions. These models can be used to evaluate the relative importance of climate and tectonism in controlling the character of sedimentary deposition. One key problem is distinguishing between regional effects, such as paleolatitude or climate, and local effects of geomorphology. For example, a lithology found in a narrow time-stratigraphic window in many basins could have been produced by a regional climate pattern; a lithology that is locally developed and of limited extent in many basins probably was controlled by local source rocks or geomorphology. The goal of this session was to develop concepts and models that can be applied to areas of limited outcrop to better understand the regional stratigraphic pattern.

Black laminated shale was recognized as a key lithology for stratigraphic correlation, reconstruction of depositional environments, and the development of stratabound mineral deposits. Olsen (7) presented evidence for the deepwater lacustrine origin of these black laminated shale units, which explains their great lateral continuity, and cautioned against uncritical comparison with modern lakes. The lateral intertonguing of lacustrine shales and nonlacustrine mudstones with fluvial deposits, as a function of climatic change or tectonic activity, was examined by Smoot (2), Turner-Peterson and Smoot (3), and LeTourneau (4). They concluded that the style of fluvial deposits is directly related to lacustrine transgressions and regressions and that syndepositional fault activity strongly controls the lateral geometry of fluvial and lacustrine units. A model for recognizing mudstone sequences that formed in different climatic settings was presented by Smoot and Olsen (6). Robbins (5) presented evidence for a narrow time-stratigraphic period of coal formation in the Newark Supergroup, while discussing the problems of distinguishing temporal control of coal formation from latitudinal climatic control (related to variation in paleolatitudes over time).

The structural aspects of basin development were illustrated for the offshore Mesozoic basins by Klitgord and Hutchinson (9); their studies of seismic profiles indicate that in some basins sedimentation was synchronous with faulting, whereas in other basins sedimentation appears to predate the border faults. Ratcliffe and Burton (8) introduced a model for the development of the Newark basin in which the Mesozoic faults inherit their geometry from Paleozoic thrust faults, and the fold structures developed in the Mesozoic strata reflect underlying structures in the thrusted basement rocks. They pointed out that the structural setting of the exposed Triassic-Jurassic basins may differ considerably from that of the offshore basins and proposed a sequential change of basin shape, which would strongly control sedimentary patterns.

Comparison of the offshore buried basins with the onshore exposed basins is dependent upon the quality of geophysical data and on the interpretations drawn from these data. Phillips and Daniels (both oral presentations only) demonstrated that most aeromagnetic and gravity data, respectively, reflect sub-basin lithologic variation; however, various filtering techniques can be used to enhance the effects of sedimentary and igneous basin features. Unger (oral presentation only) illustrated the complexity of interpreting seismic records over basins without subsurface control by using an idealized model of basin geometry and lithotype distribution to generate a synthetic seismic profile.

SESSION 2

The presentations on organic geochemistry focused on the thermal maturity of organic-matter-rich

lacustrine shales and its variability with respect to stratigraphic distribution. Olsen (10) opened with a discussion of the variability of total organic carbon (TOC) within lacustrine transgressive-regressive cycles. He demonstrated that although TOC is greatest in the portions of all cycles representing maximum lake transgression, it is not related to the thickness of the lake units or to the style of layering. The lack of correlation between thermal maturation of organic matter and the apparent depth of burial was demonstrated by Hatcher and Romankiw (11) using nuclear magnetic resonance (NMR) measurements of the organic structure of fossil wood fragments (phytoclasts), and by Pratt and others (13) using pyrolysis measurements from organic-matter-rich shales and stable carbon and oxygen isotopes. Hatcher and Romankiw showed that trends in the nature of altered phytoclasts suggest thermal metamorphism rather than burial coalification. Pratt and others showed that samples from unaltered areas were at maturation levels suitable for oil and gas generation. Spiker (12) indicated that relationships between carbon, hydrogen, and nitrogen isotopes, independent of thermal alteration, could be used to distinguish between organic materials of different origin. Robinson (14) closed the session with an overview of the ways in which organic matter may influence the formation of ore deposits, underscoring the importance of recognizing thermal overprints and fluid pathways.

SESSION 3

The presentations on igneous geochemistry spanned a range of subjects including (1) distribution of diabase sheets in regional provinces, (2) characterization of types of igneous differentiation and fractionation, (3) identification of source dikes feeding basalt flows, and (4) geochronology and isotope geology. Froelich and Gottfried (15) showed that diabase plutons are apparently geographically zoned: olivine-normative bodies are restricted to southern basins, and quartz-normative sheets are confined to northern and central basins. Froelich and Gottfried also found that some thick sheets have olivine cumulate zones, others have cumulus orthopyroxene; some sheets are associated with highly evolved differentiates such as granophyres, pegmatites, and ferrogabbro, others have no associated differentiates preserved. The parent magmas show evidence of different source areas with no systematic relationship in time, possibly due to heterogeneities in the mantle (Gottfried and Froelich, 16) or to multiple pulses of magmatic injection from a chemically evolving chamber in the upper mantle (Ragland and Arthur, 17; J. Philpotts and others, 18). Feeder sources for some basaltic intrusions may be chemically and mineralogically zoned, and this zonation may link magma chemistries once believed to be distinct (Ragland and Arthur, 17; A. Philpotts, 20). A. Philpotts (20) also identified three regional diabase dike systems in Connecticut that fed the three main basalt flow series in the Hartford basin. J. Philpotts (22) and Gottfried and Froelich (16) showed that the trace-element diagrams used to discriminate tectonic provinces cannot be used with these magmas. Many quartz-normative tholeiitic magmas in the province have geochemical trends indicating fractionation of sulfides (Gottfried, 25). The current state of geochronology of Mesozoic igneous rocks in the Eastern United States is such that no temporal resolution is possible between basalt flows and diabase dikes or sheets, but all apparently crystallized between 175 and 200 Ma, probably close to the older end of this range (Sutter, 21).

SESSION 4

The dynamic tectonic setting of the Eastern U.S. early Mesozoic basins provides a suitable environment where many geologic processes may interact favorably to develop local element enrichments and possibly ore deposits.

Ore deposits associated with (1) magma differentiation and interaction with upper crustal materials and (2) the development and migration of metal-bearing brines in sedimentary basins were the focus of presentations in this session. Robinson (23, 26) identified a number of potential ore deposit types:

(1) Magma differentiation and interaction with crustal materials
   (a) diabase-hosted magmatic sulfide deposits (Noril'sk-type)
   (b) magnetite skarn deposits with associated sulfide mineralization (Cornwall, Pa.-type)
(2) Mineralization related to sedimentary brines
   (a) sediment-hosted stratabound sulfide deposits
   (b) organic-matter-rich sediment-hosted uranium deposits
   (c) base-metal-barite vein deposits

Gottfried (25) presented data on nickel, copper, and cobalt systematics in Eastern U.S. Jurassic diabase dikes and flows as a way to differentiate between igneous systems that underwent primarily silicate fractionation and those that underwent sulfide fractionation.

Basaltic systems in which silicate and (or) sulfide fractionation are well documented (Alae lava lake, Hawaii; mid-ocean ridge basalts; Palisades sill, N.J.-N.Y.) were used to define contrasting fractionation trend lines. Although the pattern may be complicated by chemical variation in the mantle source area and other factors, it appears that sulfide-fractionation processes may have modified the chemistry of many quartz-normative tholeiitic magmas in the eastern North America province. This modification implies that segregations of magmatic sulfides, similar to the Noril'sk deposits, may exist in the province. Noril'sk-type magmatic sulfide deposits appear to have formed, in part, in response to contamination of tholeiitic magmas with crustal sulfur, thereby generating an immiscible sulfide liquid that extracts nickel, cobalt, copper, and platinum-group elements from the magma. McNeal (30) presented a sulfur-isotope study of diabase sheets in Pennsylvania with the goal of identifying signatures that may indicate crustal contamination. His data on chilled diabase samples, in general, do not indicate significant crustal contamination of sulfur; however, a trend toward enrichment of isotopically heavy sulfur with increasing fractionation in diabase sheets was seen in some areas. One sheet, the Zora ring complex, appears to have an unusually heavy sulfur isotopic signature, which is not correlated with differentiation trends and which may indicate contamination with crustal sulfur.

Turner-Peterson and others (24) presented data indicating that some black lacustrine mudstones in the Newark basin are enriched in uranium. High uranium concentrations in these black mudstones correlate with high organic carbon and high total sulfur contents in the rocks and are restricted to certain parts of the lacustrine cycles defined by Van Houten and refined by Olsen (10). The greatest uranium concentration (0.29 percent U_3O_8) occurs in a zone containing a high proportion of terrestrial organic material, possibly indicating a connection between uranium mineralization and humic substances. These relationships may be linked to regional sedimentological patterns to identify other targets for possible uranium enrichment.

SESSION 5

The topical study of the Gettysburg basin area, Pennsylvania, focused a number of different disciplines (igneous and aqueous geochemistry, geophysics, remote sensing, and mineral resource studies) on a common target area. Multidisciplinary studies of this pilot area were used to examine relationships among old mining areas, known deposits, geologic features, and anomalous geochemical sites.

Daniels (27) and Phillips (28) presented gravity and aeromagnetic maps, respectively, of the area and showed how modelling of the data could be used to infer the subsurface distribution of diabase sheets. Ficklin and others (29) presented a reconnaissance hydrogeochemical study of the area that identified anomalous sites of metal enrichment. Although human contamination problems were apparent in the data, high metal and anion concentrations in ground water were shown to correlate with areas of known mineralization, and a few new sites of possible mineralization were defined. McNeal (30) presented a sulfur isotope study of Mesozoic diabase sheets. He compared these data with available sulfur isotope data for sedimentary sulfides and sulfates in the Mesozoic strata and with sulfur isotope data from sulfide minerals associated with magnetite skarn deposits bordering some of the diabase sheets. These data indicate that most of the sulfur in the skarn deposits is derived from sedimentary sources. Robinson (26) provided background information on the magnetite-skarn deposits and showed that sulfide-rich variants of these deposits may contain significant cobalt, gold, and silver and may be of interest as a future resource. A preliminary analysis of the linear features of the Gettysburg basin was presented by Krohn and others (31). Three major zones of linear features are aligned with faults, diabase dikes, some ore deposits within the basin, fault offsets along the basin margin, and several different fold and fault structures outside the basin.

FIELD TRIPS

Following the technical sessions, two one-day field trips were held for interested participants. Joe Smoot led a trip to examine lacustrine sedimentation and sedimentary cycles in the central Culpeper basin; Al Froelich and Dave Gottfried led a trip to examine diabase sheets and intrusive relations in the southern Culpeper basin.

Proceedings of the Second U.S. Geological Survey Workshop on the Early Mesozoic Basins of the Eastern United States

Gilpin R. Robinson, Jr., and Albert J. Froelich, editors

1. NEWARK SUPERGROUP, A REVISION OF THE NEWARK GROUP IN EASTERN NORTH AMERICA[1]

Albert J. Froelich and P.E. Olsen[2]

The Newark Supergroup includes the largely continental clastic rocks ("red beds") and interbedded basaltic flow rocks of Late Triassic and Early Jurassic age that crop out in discrete elongate basins parallel to the Appalachian orogen in eastern North America (fig. 1.1). The term "Newark Supergroup" was introduced by Van Houten (1977), referring to an unpublished manuscript by Olsen, to replace "Newark Group" (Redfield, 1856), a term that had been widely used but frequently misapplied in a time-stratigraphic sense (Klein, 1962). The use of the term "Newark Supergroup" preserves a well-established name (North American Stratigraphic Code, art. 7: c), which has increasingly been applied outside the U.S. Geological Survey to the rocks in all of the exposed basins (Geological Society of America, 1983). The Newark Supergroup is a formal assemblage of related groups and formations (North American Stratigraphic Code, art. 29) with close lithologic and structural relationships that are implied through use of the supergroup designation. The term was clearly redefined by Olsen (1978) and was expanded to include subsurface red beds of early Mesozoic age beneath the Atlantic Coastal Plain and Continental Shelf. As these subsurface rocks are poorly understood and apparently of diverse age, lithology, and origin, the term "Newark Supergroup" is here restricted to rocks that crop out, although we recognize that coeval strata are certainly concealed at depth beneath the Coastal Plain.

The Newark Supergroup strata in the exposed basins of eastern North America have variously been considered to be partly or solely of Early Jurassic (Rogers, 1842; Lyell, 1847; Redfield, 1856), Permo-triassic (Emmons, 1857), Jurassic or Late Triassic (Fontaine, 1883), and solely Late Triassic age, at first on the basis of rare vertebrate and plant fossils (Ward, 1891; Eastman, 1913) and subsequently on the basis of vertebrate and plant fossils (Reeside and others, 1957) and radiometric ages of intercalated igneous rocks (Armstrong and Besancon, 1970). Some of the basins, however, have been determined to contain Lower Jurassic as well as Upper Triassic strata, as evidenced by spores, pollen, and well-preserved vertebrate remains in lacustrine mudstones (Cornet and others, 1973; Cornet, 1977; Olsen, 1978; Olsen and others, 1982) interbedded with basalt flows. The Lower Jurassic flows and interbedded strata can be considered informally as the "upper" Newark Supergroup and the Upper Triassic rocks as the "lower" Newark Supergroup.

The basins with only Upper Triassic rocks (with Group names where used) are the Wadesboro-Sanford-Durham (Chatham Group of Emmons, 1857) (1, 2, 3 on fig. 1.1); Davie County (4); Dan River and Danville (Dan River Group of Thayer, 1970) (5); Scottsburg (6);

[1]This paper is reprinted, with modifications, from Stratigraphic Notes, 1983 (U.S. Geological Survey Bulletin 1537-A, 1984, p. A55-A58).

[2]P.E. Olsen, Lamont-Doherty Geological Observatory of Columbia University, Palisades, N.Y. 10964.

basins north of Scottsburg basin (7); Farmville (8); Richmond (Tuckahoe and Chesterfield Groups of Shaler and Woodworth, 1899) (9); Taylorsville (10); Scottsville (11); and Barboursville (Culpeper Group of Lindholm, 1979) (12). The basins in which Upper Triassic rocks are overlain by Lower Jurassic rocks are the Culpeper (Culpeper Group of Lindholm, 1979) (13); Gettysburg (Conewago Group of Ashley, 1931) (14); Newark (15); Pomperaug (16); Hartford with Cherry Valley outlier (Meriden Group of Krynine, 1950) (17); Deerfield (18); Fundy or Minas (Fundy Group of Klein, 1962) (19); and Chedabucto (20).

Older Mesozoic strata of the lower Newark Supergroup (Upper Triassic, middle and upper Carnian), which are commonly coal-bearing, are preserved in the southern basins (1–10, fig. 1.1). Strata in two small, centrally located basins (11, 12, fig. 1.1) are mainly conglomerates and red beds that apparently lack diag-

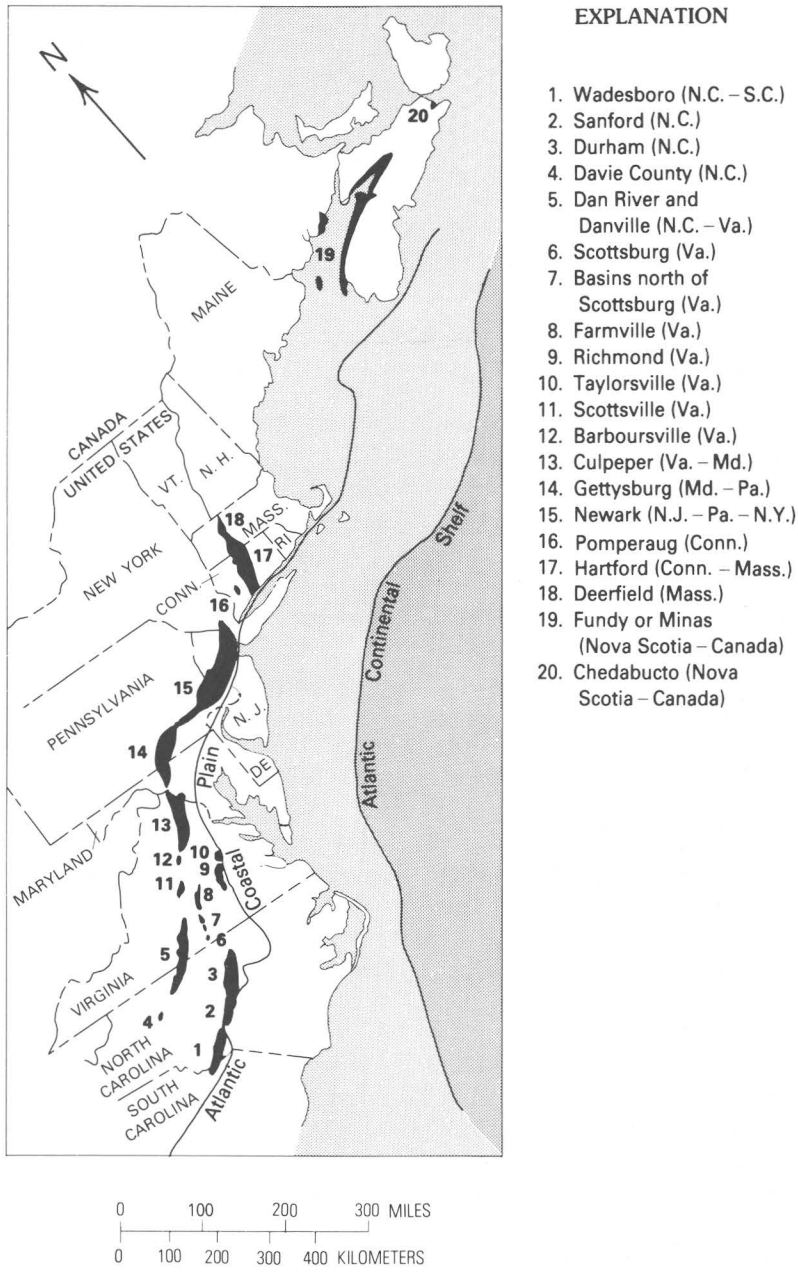

EXPLANATION

1. Wadesboro (N.C. – S.C.)
2. Sanford (N.C.)
3. Durham (N.C.)
4. Davie County (N.C.)
5. Dan River and Danville (N.C. – Va.)
6. Scottsburg (Va.)
7. Basins north of Scottsburg (Va.)
8. Farmville (Va.)
9. Richmond (Va.)
10. Taylorsville (Va.)
11. Scottsville (Va.)
12. Barboursville (Va.)
13. Culpeper (Va. – Md.)
14. Gettysburg (Md. – Pa.)
15. Newark (N.J. – Pa. – N.Y.)
16. Pomperaug (Conn.)
17. Hartford (Conn. – Mass.)
18. Deerfield (Mass.)
19. Fundy or Minas (Nova Scotia – Canada)
20. Chedabucto (Nova Scotia – Canada)

FIGURE 1.1.—Exposed basins of the Newark Supergroup in eastern North America.

nostic fossils but resemble Upper Triassic (upper Carnian and middle and upper Norian) rocks in adjacent basins to the north. Strata from the northern basins contain intercalated basalt flows and younger strata of the upper Newark Supergroup (13–18, fig. 1.1), span Late Triassic (Carnian and Norian) through Early Jurassic (Hettangian to Toarcian) time, and in the Hartford basin (17, fig. 1.1) perhaps extend into Middle Jurassic (Bajocian) time. In the extreme northeast, the Fundy (Minas) basin (19, fig. 1.1) is anomalous to this regional pattern because it contains Upper and possibly Middle Triassic (Ladinian) strata at the base and Lower Jurassic strata and basalt flows of the upper Newark Supergroup at the top.

As Olsen (1978) pointed out: "* * * Raising the rank of the term Newark to Supergroup preserves the original and familiar meaning of Redfield's designation, allows the formations of individual basins to be included in specific groups while remaining in a strictly rock-stratigraphic hierarchy, and permits the maximum amount of flexibility for future subdivision. * * *"

REFERENCES

Armstrong, R.L., and Besancon, J., 1970, A Triassic time scale dilemma: K–Ar dating of Upper Triassic mafic igneous rocks, eastern U.S.A. and Canada and post-Triassic plutons, western Idaho, U.S.A.: Eclogae Geologicae Helvetiae, v. 63, p. 15–28.

Ashley, G.H., 1931, A syllabus of Pennsylvania geology and mineral resources: Pennsylvania Topographic and Geologic Survey, 4th Series, Bulletin no. G–1, 159 p.

Cornet, Bruce, 1977, The palynostratigraphy and age of the Newark Supergroup: University Park, Pennsylvania State University, unpub. Ph.D. thesis, 506 p.

Cornet, Bruce, Traverse, Alfred, and McDonald, N.G., 1973, Fossil spores, pollen and fishes from Connecticut indicate Early Jurassic age for part of the Newark Group: Science, v. 182, p. 1243–1246.

Eastman, C.R., 1913, Notes on Triassic fishes belonging to the Families Catopteridae and Semionotidae: Annals of the Carnegie Museum, v. 9, p. 139–148.

Emmons, E.E., 1857, American geology, part VI [III]; Albany, New York, 152 p.

Fontaine, W.M., 1883, Contributions to the knowledge of the older Mesozoic flora of Virginia: U.S. Geological Survey Monograph 6, 144 p.

Geological Society of America, 1983, Symposium: Advances in paleontology and paleoecology—Newark Supergroup (Early Mesozoic): Northeastern Section Abstracts with Programs, v. 15, no. 3, p. 156.

Klein, G.D., 1962, Triassic sedimentation, Maritime Provinces, Canada: Geological Society of America Bulletin, v. 73, p. 1127–1146.

Krynine, P.D., 1950, Petrology, stratigraphy, and origin of the Triassic sedimentary rocks of Connecticut: Geological and Natural History Survey Bulletin no. 73, 247 p.

Lindholm, R.C., 1979, Geologic history and stratigraphy of the Triassic-Jurassic Culpeper basin, Virginia: Geological Society of America Bulletin (pt. 2, microfiche), v. 90, no. 11, p. 1702–1736.

Lyell, Charles, 1847, On the structure and probable age of the coal field of the James River near Richmond, Virginia: Quarterly Journal of the Geological Society of London, v. 3, p. 261–280.

North American Commission on Stratigraphic Nomenclature, 1983, North American Stratigraphic Code: American Association of Petroleum Geologists Bulletin, v. 67, no. 5, p. 841–875.

Olsen, P.E., 1978, On the use of the term Newark for Triassic and Early Jurassic rocks of eastern North America: Newsletters on Stratigraphy, v. 7, no. 2, p. 90–95.

Olsen, P.E., McCune, A.R., and Thomson, R.S., 1982, Correlation of the early Mesozoic Supergroup by vertebrates, principally fishes: American Journal of Science, v. 282, p. 1–44.

Redfield, W.C., 1856, On the relations of the fossil fishes of the sandstone of Connecticut and the Atlantic States to the Liassic and Oolitic periods: American Journal of Science (ser. 2), v. 22, p. 357–363.

Reeside, J.B., Jr. (Chairman, Triassic Subcommittee), and others, 1957, Correlation of Triassic formations of North America: Geological Society of America Bulletin, v. 68, p. 1451–1514.

Rogers, W.B., 1842, Report of the progress of the Geological Survey of the State of Virginia for the year 1841: Richmond, Va., 12 p. (*reprinted in* Geology of the Virginias, 1884, p. 537–546.)

Shaler, N.S., and Woodworth, J.B., 1899, Geology of the Richmond Basin, Virginia: U.S. Geological Survey Annual Report 19, 1897–1898, pt. 2, p. 385–515.

Thayer, P.A., 1970, Stratigraphy and geology of the Dan River Triassic basin, North Carolina: Southeastern Geology, v. 12, p. 1–37.

Van Houten, F.B., 1977, Triassic-Liassic deposits of Morocco and Eastern North America: Comparison: American Association of Petroleum Geologists Bulletin, v. 61, no. 1, p. 79–99.

Ward, L.F., 1891, The plant-bearing deposits of the American Triassic: Science, v. 18, p. 287–288.

2. THE CLOSED-BASIN HYPOTHESIS AND ITS USE IN FACIES ANALYSIS OF THE NEWARK SUPERGROUP

Joseph P. Smoot

INTRODUCTION

A major objective of sedimentological analysis of the Newark Supergroup is predicting the distribution of its unexposed lithologies. To accomplish this, depositional models of sufficient refinement to locate 1-m-thick lithologies within kilometers of stratigraphic section must be constructed. The lack of large, continuous outcrops in which the vertical and lateral relationships of sedimentary features can be observed is the greatest obstacle to this task. Each Newark Supergroup basin contains limited exposures of a complex array of sedimentary lithologies, structures, and fabrics, which suggest a diversity of fluvial and lacustrine depositional environments. It is difficult to ascertain whether the different sedimentary features represent minor perturbations of relatively simple facies relationships (for instance, river-delta-lake facies or alluvial fan-sand-flat-playa facies) or major variations in climate, basin geometry, tectonic conditions, or ecology.

THE PROBLEM OF LIMITED EXPOSURE

A new exposure in the Durham basin in the Triangle Brick Quarry near Glenlee, N.C., demonstrates the difficulty of producing predictive facies models when exposures are limited. The middle part of the Chatham Group of Emmons (1857) in the Durham basin commonly consists of thin-bedded, extensively bioturbated sandy mudstone and clayey sandstone. At intervals of 3 to 4 m within these muddy, bioturbated sediments are zones consisting of several 5- to 10-m-wide lenses of trough cross-laminated, medium- to coarse-grained sandstone. Each coarse sandstone lens, 20 to 30 cm thick, is graded, with mudstone intraclasts at the base and fine-grained sandstone, commonly in the form of low-angle climbing-ripple cross-lamination, near the top. Similar sedimentary sequences occur in parts of the Passaic Formation of Olsen (1980) in the Newark basin and in parts of the Balls Bluff Siltstone in the Culpeper basin. A typical interpretation of this type of deposit is that the sandstone lenses are channel-fill deposits of shallow, braided streams and that the bioturbated sandstones and mudstones were deposited on the adjacent flood plains (see, for example, Froelich and others, 1982, p. 60–61). The new continuous exposure of this sequence in the Triangle Brick Quarry revealed that the bioturbated muddy sandstone and sandy mudstone are *not* horizontally bedded flood-plain deposits but are actually sets of low-angle cross-strata. Furthermore, the sandstone beds of the cross-strata dip into the coarser grained, trough cross-laminated sandstone lenses at their bases (fig. 2.1). These large-scale, low-angle cross-sets probably are laterally accreted beds of a point bar of a meandering stream at least 3 m deep. Cross-sets of bioturbated sandstone and mudstone within similar facies were subsequently recognized in the Culpeper and Newark basins.

This example of the reinterpretation of a depositional environment due to the exposure of unexpected vertical and lateral lithologic relationships is particularly germane to the problem of limited exposure in the Newark Supergroup. There is a tendency to assume that changes or lack of changes seen in an outcrop represent the significant variability of a depositional environment. However, very few Newark Supergroup outcrops are of sufficient size to show the vertical or lateral variability of a large delta (fig. 2.2) or of a large meandering river–flood plain complex. One could argue, for instance, that the vertical succession of the shales of the Vinita beds to the Otterdale Sandstone, both of Shaler and Woodworth (1899), in the Richmond basin in Virginia represents a deltaic progradational sequence and that the interbedded sandstones and mudstones of the Passaic Formation of Olsen (1980) in the Newark basin in New Jersey are the overbank–flood plain deposits of a large river. The outcrops of these units are generally too small and too widely scattered to confirm or deny these hypotheses conclusively, however; a different approach is needed.

THE WORKING MODEL AS AN AID TO STRATIGRAPHIC RECONSTRUCTIONS

An inductive approach toward sedimentological analysis is to assume a model that predicts the origin or shape of a rock body and then to test the model in the field by finding outcrops that support or refute the predicted trend or the inherent implications of the model. For example, Olsen (1984) produced a strikingly

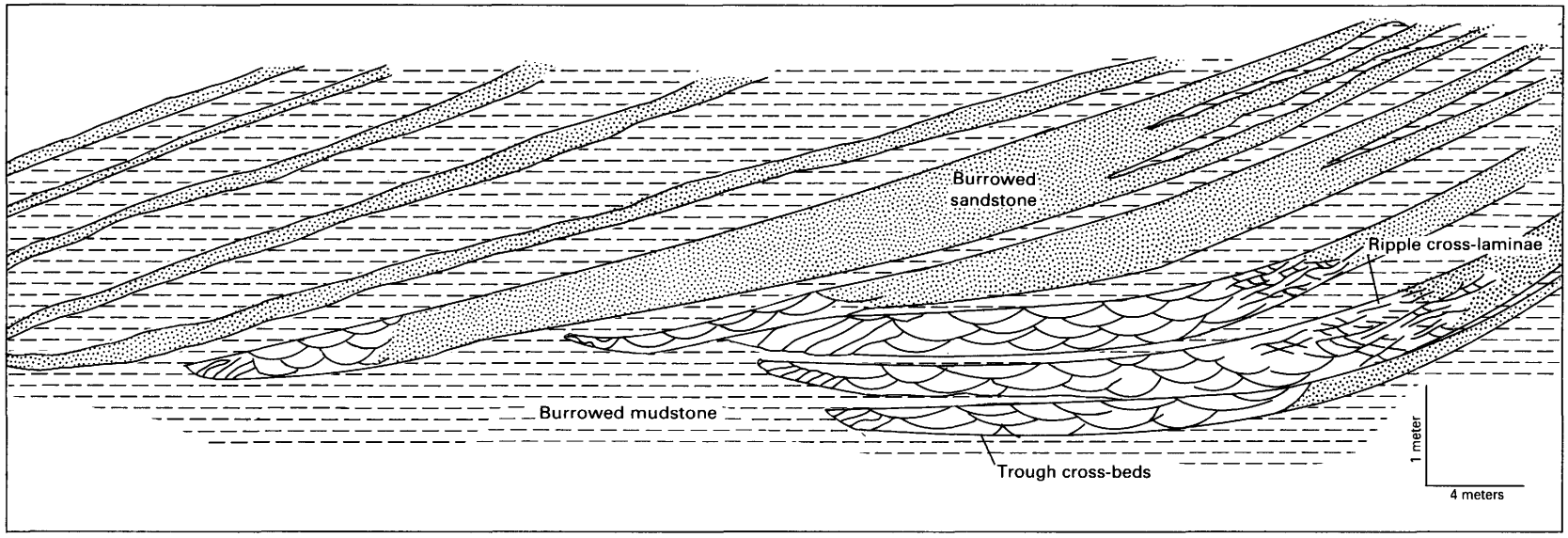

FIGURE 2.1.—Simplified sketch of sedimentary features exposed in the Triangle Brick Quarry near Glenlee, N.C. Trough cross-bedded areas are coarse-grained sandstone with mud intraclasts, and the ripple cross-laminated areas are medium- to fine-grained sandstone. The stippled areas represent internally massive, burrowed muddy sandstones, and the dashed areas represent internally massive, burrowed mudstones. The transitions from the cross-bedded sandstones to the burrowed sandstones and the contacts between the burrowed mudstones and the burrowed sandstones are diffuse, presumably because of bioturbation. Vertical exaggeration (×4) has increased the apparent dip of bedding (about 5°). Paleocurrent direction, as indicated by the trough cross beds, is out of the page and to the right.

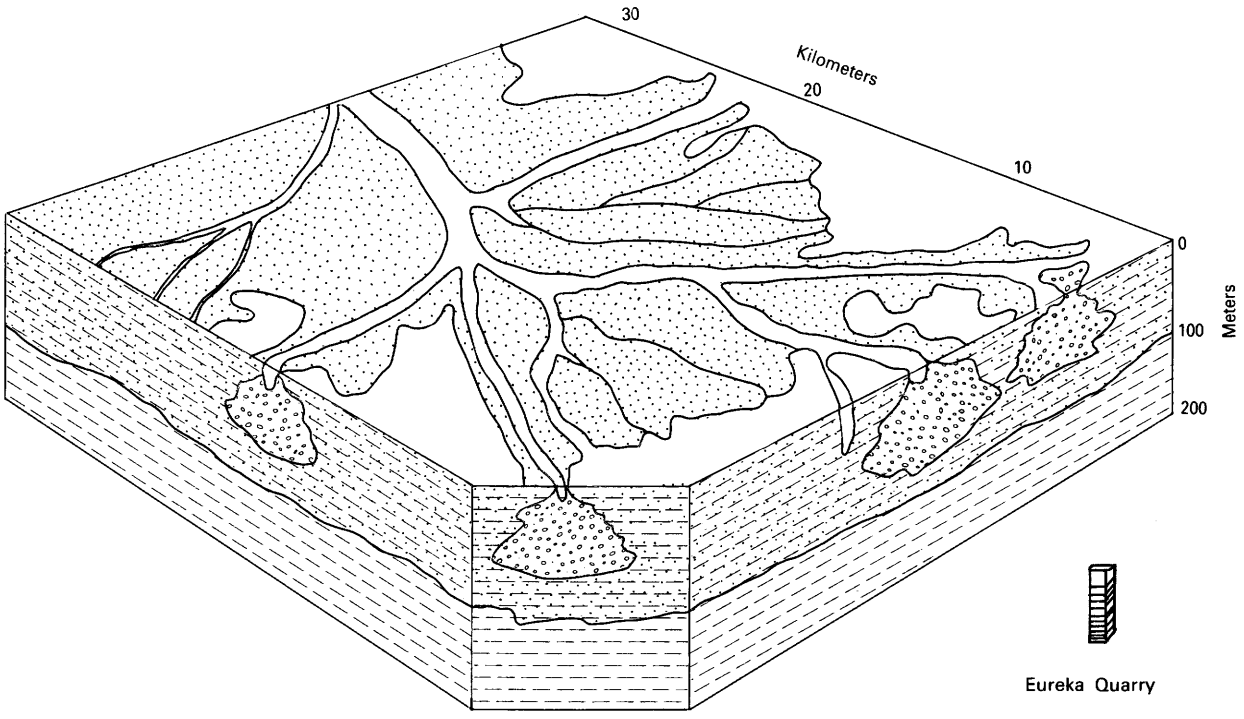

FIGURE 2.2.—Comparison of the area and thickness of a lobe of the Mississippi River delta complex to the Eureka Quarry section of the Lockatong Formation in Pennsylvania. Eureka Quarry is one of the largest areal exposures in the Newark Supergroup. Most outcrops are an order of magnitude or two smaller and are widely scattered. Vertical exaggeration is about ×50. (Simplified from Mathews, 1974.)

detailed lithostratigraphic map of parts of the Newark basin by using lithostratigraphic models. His first model assumed that the Jurassic basalts were deposited essentially instantaneously, the base of each flow representing a unique time line. His second working model assumed in addition that black, laminated shales were deposited in large, basin-filling lakes and that their positions in the stratigraphic sequence defined correspondingly unique times. Diagnostic lithological and biological features of some shale layers helped confirm both initial hypotheses and provided a framework to extend them further.

A different type of working model assumes that a process or set of processes controlled sedimentation; the model then constrains the possible variation within a stratigraphic unit. An example of a working process model is that of rhythmic climatic fluctuations controlling cyclicity of Newark Supergroup sediments (Van Houten, 1964; Olsen, 1984). This model suggests that variations in net rainfall and evaporation produce recognizable differences in the sedimentary record and predicts that the same sense of change will be exhibited across lithofacies boundaries in coeval units. Therefore, lateral relationships of mudstone to sandstone to conglomerate should enable us to distinguish periods of aridity from periods of high rainfall (see Olsen, chapter 10; Turner-Peterson and Smoot, chapter 3; and LeTourneau, chapter 4, this volume)

The strength of a working model is that it provides a conceptual framework within which systematic observations can be applied to test the initial hypotheses. The best working models present a variety of implications, evidence of which can be recognized in the rocks. The remainder of this paper is a discussion of the closed-basin hypothesis for the Newark Supergroup deposits and some working models for stratigraphic reconstructions. This hypothesis has been frequently cited for Newark Supergroup basins but has not been systematically applied to the rocks.

WORKING MODELS BASED ON THE CLOSED-BASIN HYPOTHESIS

A closed basin has no drainage outlet, so that all surface drainage and groundwater that enters the basin leaves primarily by evaporation (Langbein, 1961), although evapotranspiration and subsurface seepage

out of the basin may also be important. A closed-basin paleohydrology has been postulated for all basins of the Newark Supergroup for at least some part of their accumulation histories. There is some disagreement, however, as to whether or not the present extent of exposed deposits reflects the original depositional basins (see, for instance, Klein, 1969, or Olsen, 1984). The most commonly cited reasons for postulating closed-basin deposition in the Newark Supergroup are (1) the systematic increase of grain size towards all boundaries of a basin, (2) paleocurrent patterns indicating flow away from each border of a basin, (3) the local provenance of the coarse-grained sediments near the basin margins, (4) the occurrence of evaporites or evaporite-crystal casts, and (5) the cyclicity of the fine-grained sedimentary rocks in the central portions of the basin. These five criteria result from direct comparisons to modern closed basins, such as the block-fault basins of the Basin and Range of the Western United States and the rift basins of East Africa. Since these criteria are not uniformly applicable to every stratigraphic horizon in each basin, it is possible that some basins were open intermittently and that some basins were never closed. The assumption of closed-basin conditions for a Newark Supergroup basin, however, may be tested by looking for the presence or absence of sedimentary features or relationships that the model implies.

In closed basins, the basin size, the amount of inflow, and the presence or absence of a lake influence the distribution of coarse-grained, fluvial sediments on the basin floor. Figure 2.3 is a schematic representation of six working process models that show effects of these variables on fluvial sedimentation during individual flood events in a closed-basin setting. Coarse-grained sediments enter the basin carried by streams, by debris flows on alluvial fans, or as bedload in perennial or ephemeral streams and rivers. Small floods are defined as short-lived (less than 1-day duration) flash floods on alluvial fans or along axial streams. Large floods indicate greater volumes of water introduced by sustained flow (many days in duration or seasonal) in large streams on alluvial fans or brought in by rivers. A small basin in figure 2.3 is on the scale of tens to hundreds of square kilometers in area, or near the size of North Panamint Valley in California or the Pomperaug basin of the Newark Supergroup in Connecticut. A large basin is thousands of square kilometers in area, the size of Lake Eyre in Australia or the Newark basin in Pennsylvania and New Jersey. The closed-basin model has many implications that can be tested. A perennial river or stream entering a closed basin will result in a permanent lake, whose size depends upon the size and frequency of inflow and the net annual evaporation. If perennial inflow into a closed basin exceeds evaporation, the lake will eventually fill the basin and spill out, thus ending closure. Streams and rivers entering a closed basin will probably lose some of their hydraulic head, because of the change in slope, and thus lose some of their sediment-transport capability. Small floods into large basins may soak into the ground before ponding water in the hydrologic low areas, but a large flood will cause an area of ponded water to expand rapidly. A flooding stream or river that intersects a lake or shallow ponded water will decelerate and deposit its coarser grained sediments; if the body of standing water is expanding rapidly, this intersection point will migrate upflow or towards the basin margins. A large, flash-flooding river in a small closed basin will intersect the transgressing lake surface near the basin margin; if a lake already covers the floor of the basin, the river mouth and channel will be "drowned" by the rising lake water. The shorelines of lakes that cover most of the floors of large closed basins will transgress less noticeably during flooding events than would those of smaller lakes in the same basin. Perennial lakes in closed basins have fluctuating shorelines because lake level is a function of the ratio of inflow to evaporation.

The process models in figure 2.3 and the conditions resulting from a closed-basin setting described above provide constraints for facies distributions. Almost all the coarse-grained, fluvial sediments (coarse sand and gravel) in small closed basins should be deposited near the edges of the basin floor laterally adjacent to lacustrine or playa muds. Perennial rivers should produce perennial lakes that cover the entire basin floor. Large, flash-flooding ephemeral rivers should cause rapidly expanding, temporary lakes, which also restrict most of the coarse-grained sediments close to the basin edge. Small, short-lived floods may locally transport sand and gravel towards the center of the basin floor, but the size of the coarse-grained deposit will be very small. Hooke (1968) noted the above relationships for the Basin and Range playas and argued that this is why their alluvial fan deposits are always restricted to the basin margins, even when annual rainfall increases markedly.

Coarse-grained fluvial deposits in large closed basins may have greater extents within the basins than those in small closed basins. Large ephemeral rivers can deposit sediments far into a large closed basin before intersecting ponded water. Still, the coarse-grained fluvial sediments must intertongue with finer

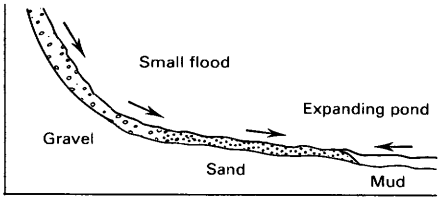

Not enough flood water to cause major ponding. Coarse sediment is transported until stream loses competence.

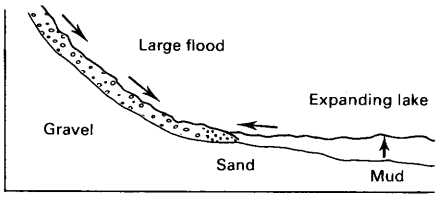

Flood water causes lake to expand. River deposits its coarse-grained sediment at intersection with the expanding lake.

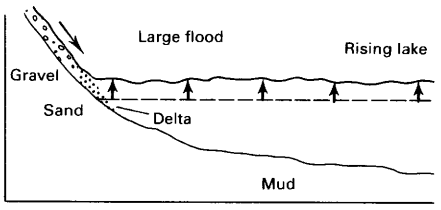

Flood water causes lake level to rise over river level. Coarse sediment deposition migrates upstream, and the delta topset does not prograde.

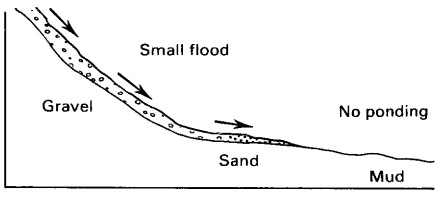

Not enough flood water to cause ponding. Stream shallows and seeps into basin floor depositing all sediment.

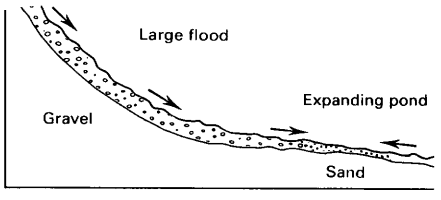

Flood water causes lake to expand, but far from the river source. Coarse-grained sediment is transported until river shallows or intersects the expanding lake.

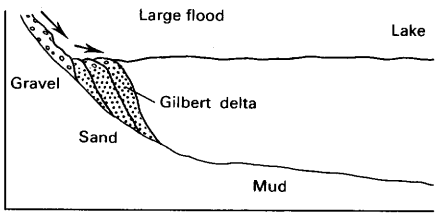

Flood water does not significantly affect lake level. Delta topset builds out into the lake.

FIGURE 2.3.—Process models for flood events and coarse-grained fluvial sediment distribution in closed basins. Small basins are tens to hundreds of square kilometers in size; large basins are thousands of square kilometers.

grained lacustrine deposits, at least near the lowest point of the basin. A large, perennial river flowing into a large closed basin will produce a lake that will probably cover most, if not all, of the basin floor. Therefore, the perennial river deposits should be mostly restricted to the outer portions of the basin floor and should intertongue with deltaic or lacustrine deposits. The coarse-grained deposits of small floods in large basins will probably be confined to the edges of the basin floor because the flood waters will soak into the ground.

Delta deposits in closed basins should be affected by the frequent rising and falling of lake levels. The rapid transgression of small lakes during flood events will cause the point where the river or stream intersects the lake to shift continuously upstream, inhibiting the development of steep delta foresets and the formation of coarsening-upward bottomset-foreset-topset sequences. Even relatively deep lakes in small basins should demonstrate this drowning of the river mouth during floods. Large, shallow lakes in large basins will not transgress as much as small lakes during each flooding event. In these large, shallow lakes, broad, thin deltaic deposits dominated by the fluvial component may accumulate. Where rivers enter deep lakes in large basins, classical Gilbert-type deltas (Gilbert, 1890) will probably develop. The frequent change of lake depth in closed basins will cause small delta foresets to develop over the topsets of lower lake stands and cause the shorelines of higher lake stands to be dissected by streams or rivers.

POSSIBLE APPLICATIONS OF THE CLOSED-BASIN HYPOTHESIS TO THE NEWARK SUPERGROUP

The working models of the closed-basin hypothesis may be used primarily to check for the consistency of the predicted depositional conditions in coeval stratigraphic levels and for differences in successive stratigraphic sequences. If a local stratigraphic unit conforms to a closed-basin working model, the laterally equivalent deposits should reflect similar conditions. These working models may help distinguish between closed- and open-drainage basins in the rock record, but the actual conclusions that can be drawn are often equivocal. Some possible applications of closed-basin working models to Newark Supergroup sedimentary rocks are presented below.

Thick sandstone units containing 2- to 4-m-thick packages of dune-scale, trough cross-bedding occur in several basins of the Newark Supergroup. These sandstones indicate deposition in relatively deep fluvial channels. The presence of areally extensive fluvial sandstones of this type, in particular the occurrences near the bases of several sections, suggests the possibility of open-drainage conditions in some basins for part of their history. The cross-bedding characteristics and sorting of some of these sandstones suggest that the sands were deposited by perennial rivers, whereas flash-flooding ephemeral rivers, which flowed at least on the scale of days, are indicated by other deposits. The working models described above indicate that perennial river deposits should occur only on the margins of a closed basin and that these fluvial deposits will be laterally equivalent to perennial lake deposits. Sandstones deposited by ephemeral rivers may extend far into a large closed basin, but they should intertongue at some point in the basin with lacustrine shales or possibly with playa mudstones. If a sandstone deposited by a perennial river is found near the center of a basin, then either the basin was not closed or its present configuration is only a small remnant of a larger basin. If the mudstones and sandstones of the Passaic Formation of Olsen (1980) are interpreted as being part of a large meandering-river–flood-plain complex, some problems of basin geometry result whether we allow the proposed through-flowing river to enter and leave the basin or enlarge the basin to accommodate it. In the Richmond basin, which is small, the occurrence of large-scale cross-bedded sandstones of the Otterdale Sandstone indicates either that the present outline of the basin is a small part of the original depositional basin or that the basin was not closed. This is true even if the Otterdale Sandstone represents deposits of ephemeral streams.

The nature of deltaic shoreline deposits in the Newark Supergroup may provide information on the extent of associated lacustrine sedimentary rocks and may reflect changes from closed-basin to open-basin conditions, which could have been caused by lake level rising to the height of a spillway. Vertical sequences of 2- to 3-m-thick foreset beds, which appear to be deposits of small Gilbert-type deltas, are found in several stratigraphic units in the Newark basin. This type of deltaic deposit is consistent with closed-basin conditions, where rising and falling lake levels cause relatively thin sets of delta-foreset beds to be deposited on and preserved beneath the delta plain and in river valleys adjacent to the lake. The small delta fronts in the

Newark basin, therefore, could be laterally equivalent to deep-lake laminated shale deposits that extend over a large area. Apparent deltaic deposits that consist only of very low angle foreset beds with no overlying topsets are also found in the Newark basin. These deposits may reflect development of a small, very shallow lake in a closed basin and, therefore, would be laterally equivalent to mudcracked mudstones rather than laminated shales. A thick topset-foreset-bottomset sequence, similar to glacial-lake deltas or to the Mississippi River delta, would if present indicate a deeper, more persistent lake, which is more consistent with open-basin conditions than with closed-basin conditions.

SUMMARY

The depositional constraints implied by the working models derived from a closed-basin paleohydrology hypothesis for the Newark Supergroup basins may lead to recognition of whether each basin was closed or open. If a closed-basin setting is confirmed locally, the possible lateral changes of coeval lithologies are further constrained. Considering the implications of these models in conjunction with the other stratigraphic, paleontological, chemical, and climatic constraints may help resolve many of the problems of facies reconstruction in the Newark Supergroup.

REFERENCES

Emmons, E., 1857, American geology, part VI [III]: Albany, N.Y., 152 p.

Froelich, A.J., Leavy, B.D., and Lindholm, R.C., 1982, Geologic traverse across the Culpeper basin (Triassic-Jurassic) of northern Virginia, *in* Lyttle, P.T., ed., Central Appalachian geology — Joint Northeastern-Southeastern Sections, Geological Society of America Field Trip Guidebooks: American Geological Institute, Falls Church, Va., p. 55–81.

Gilbert, G.K., 1890, Lake Bonneville: U.S. Geological Survey Monograph 1, 483 p.

Hooke, R.L., 1968, Steady-state relationships on arid-region alluvial fans in closed basins: American Journal of Science, v. 266, p. 609–629.

Klein, G.D., 1969, Deposition of Triassic sedimentary rocks in separate basins, eastern North America: Geological Society of America Bulletin, v. 80, p. 1825–1832.

Langbein, W. B., 1961, Salinity and hydrology of closed lakes: U.S. Geological Survey Professional Paper 412, 20 p.

Mathews, R.K., 1974, Dynamic stratigraphy: Englewood Cliffs, N.J., Prentice Hall, 367 p.

Olsen, P.E., 1980, The latest Triassic and Early Jurassic formations of the Newark basin (eastern North America, Newark Supergroup): Stratigraphy, structure and correlation: New Jersey Academy of Science Bulletin 25, p. 25–51.

———1984, Comparative paleolimnology of the Newark Supergroup — A study of ecosystem evolution: New Haven, Conn., Yale University, unpub. Ph.D. dissertation, 726 p.

Shaler, N.S., and Woodworth, J.B., 1899, Geology of the Richmond basin, Va.: U.S. Geological Survey 19th Annual Report, 1897–98, pt. II, p. 385–519.

Van Houten, F. B., 1964, Cyclic lacustrine sedimentation, Upper Triassic Lockatong Formation, central New Jersey and adjacent Pennsylvania: Kansas Geological Survey Bulletin 169, p. 497–531.

3. NEW THOUGHTS ON FACIES RELATIONSHIPS IN THE TRIASSIC STOCKTON AND LOCKATONG FORMATIONS, PENNSYLVANIA AND NEW JERSEY

Christine E. Turner-Peterson and Joseph P. Smoot

INTRODUCTION

Sedimentation in the Triassic-Jurassic Newark basin of Pennsylvania and New Jersey was the result of infilling of a rift basin formed during incipient stages of continental breakup. Following deposition, Newark strata were tilted, uplifted, and eroded so that a representative portion of the entire section is exposed in a northwest-dipping homocline (fig. 3.1). The section has a maximum stratigraphic thickness of 7,800 m (Olsen, 1984) and is repeated by faulting in the central portion of the basin. Subdivision of the sedimentary units in this tilted sequence into formations that are stacked vertically, with the oldest to the southeast and the youngest to the northwest, has encouraged the ideas that each formation represents a discrete episode in basin filling and that each formation can be interpreted in terms of a depositional environment or group of

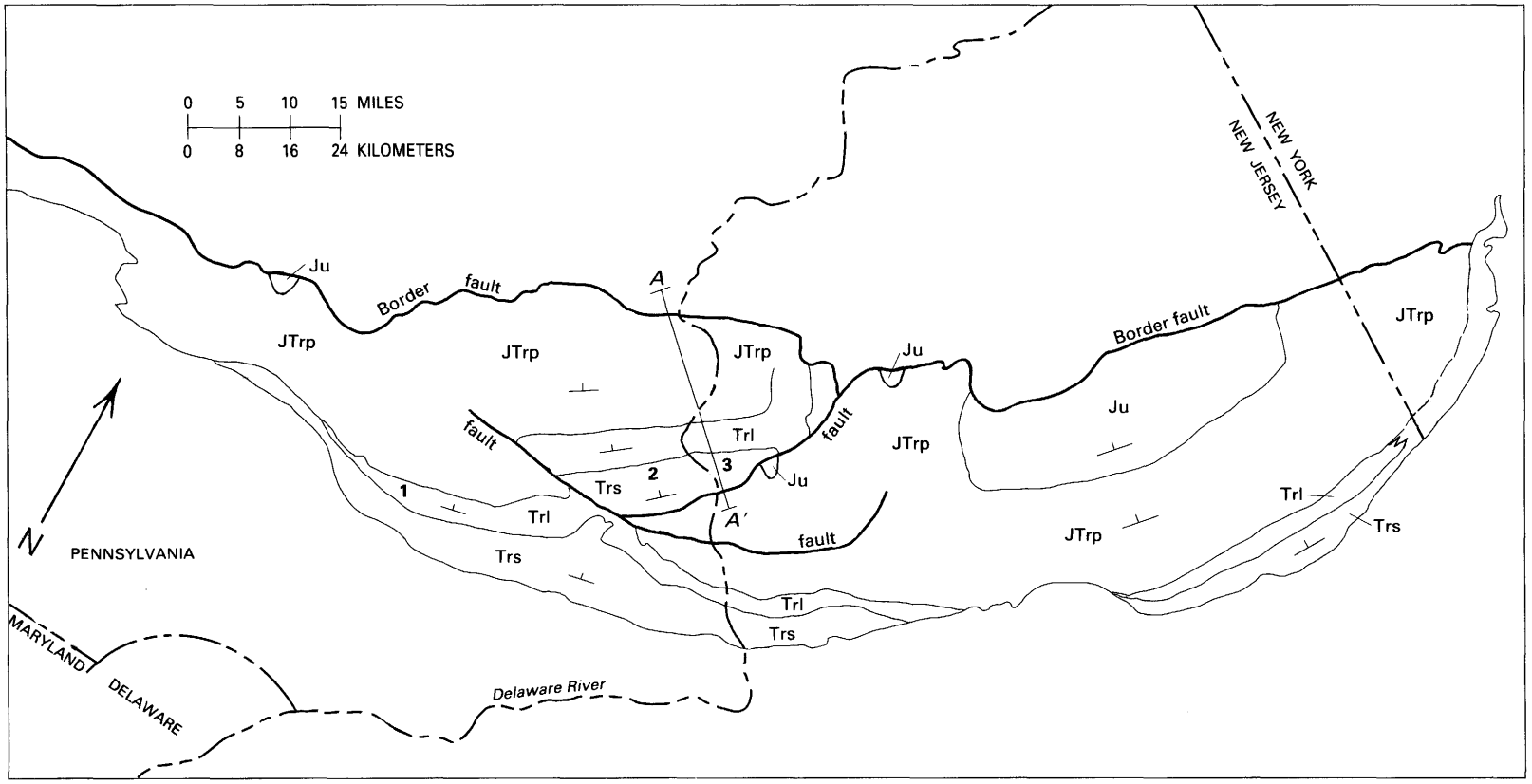

FIGURE 3.1.—Generalized geologic map of Newark basin (modified from Glaeser, 1966). Units dip to the north and northwest toward the northern border fault, and the section is repeated by faulting near the Delaware River. The stratigraphic units shown are the Stockton (Trs), Lockatong (Trl), and Passaic (JTrp) Formations and the Jurassic basalts and interbedded sedimentary rocks, shown here as Jurassic undifferentiated (Ju). Numbered localities are as follows: 1) State Park Quarry, Pennsylvania, 2) Carversville, Pennsylvania, and 3) Wickecheoke Creek, New Jersey. Cross section *A*–*A*' is shown on figure 3.3.

environments more or less distinct from those in other formations (Van Houten, 1969). For example, the concept of a basal fluvial episode (Stockton Formation) followed by a lacustrine episode (Lockatong Formation) had its origins in this concept of basin filling (fig. 3.2).

Alternatively, the formations can be viewed as large-scale time-transgressive facies, whose distribution is due to the tectonic asymmetry of the basin (Turner-Peterson, 1980; fig. 3.3). In the second hypothesis, inferred recurrent movement of major faults along the northwestern margin during deposition maintained a steep slope, resulting in the interfingering of fine-grained basinal units with coarse, poorly sorted marginal conglomerates. In contrast, the southeastern margin is thought to have been characterized by minor faulting; the resulting gentle slope permitted efficient sorting of detritus delivered to the basin and thus more gradual facies transitions. Figure 3.4 shows the inferred primary distribution of facies based on this interpretation. These two hypotheses of facies relationships and several new ones are currently being tested in detailed sedimentologic studies comparing the depositional environment of sandstone intervals in the Stockton Formation and Lockatong Formation. Preliminary results of these more detailed studies and their implications for basin reconstruction are discussed below.

Any interpretation of basin filling through time will need to accommodate the complications inherent in the history of a tectonically active basin that received sediment over a period of tens of millions of years. Pulses of tectonic activity and climatic changes would be accompanied by fluctuations in sediment input, causing migration of facies belts and boundaries. These external controls were probably the most significant factors in determining the relative proportions of fluvial and lacustrine depositional environments. Changes along depositional strike within the same formation will add second-order variations that must be considered with other fundamental differences observed between the individual formations.

NEW RESULTS

Possible deltaic sequences are present in exposures of sandstone within the Stockton and Lockatong Formations. These intervals contain large-scale (3- to 4-m), low-angle, inclined cross-strata, which typically are intercalated with shaley units in their downdip portions. Grain size in the cross-strata decreases downdip, accompanied by a downdip change in internal sedimentary structures. A similar decrease in grain size and change in sedimentary structures occurs from the base to the top of each cross-stratum. Ripples in the lower part of the cross-strata have erosional stoss sides with a low angle of climb, whereas ripples in the upper part of the foresets have draped laminae and a steep angle of climb, a vertical transition similar to that reported in deltaic foresets (Jopling and Walker, 1968; Hunter, 1977). A waning of flow in both the downdip and the vertical directions in these cross-strata is inferred from the changes in grain size and transitions in ripple geometry. Abundant soft-sediment deformation includes load casts, pseudonodules, and soft-sediment folding. All of these features suggest that the cross-strata are small "Gilbert" delta foresets (Gilbert, 1890). Obvious topset fluvial beds are absent, however, except for a lenticular bed of trough cross-laminated sandstone at one outcrop. Foresets are typically overlain either by bioturbated red mudstones or by more foresets. The inferred deltaic cross-strata that are vertically stacked consist of fine-grained sandstone strata with low-angle dips at the bases of the sequences and coarser grained strata with higher angle dips near the tops of the sequences. These cross-strata sequences may be portions of large-scale, deltaic, coarsening-upward sequences (see Smoot, chapter 2, this volume).

A sequence of the stacked deltaic foresets has been inferred in sandstones in State Park Quarry, Pa. This exposure is along the projected strike of cyclic black shales and red mudstones of the lower Lockatong (Olsen, 1984). The sandstones with foresets are interpreted as shoreline facies of the lacustrine shales. Similar deltaic foresets in the Stockton Formation near Carversville, Pa., are roughly on strike with black, conchostracan-bearing shales along Wickecheoke Creek, N.J., about 10 miles (16 km) to the east. This suggests that the two formations contain similar facies that show transitions from fluvial to lacustrine conditions.

DISCUSSION

Recognition of deltaic and lacustrine sequences in both the Stockton and Lockatong Formations has important implications for facies distribution and thus provides additional constraints on basin reconstruction. One important consequence of the new observations is that the presence of deltaic beds in the Stockton implies the lateral existence of lacustrine conditions basinward. Thus, the Stockton probably has lacustrine shales basinward from the deltaic sandstones, possibly like those in the Lockatong. The similar deltaic deposits

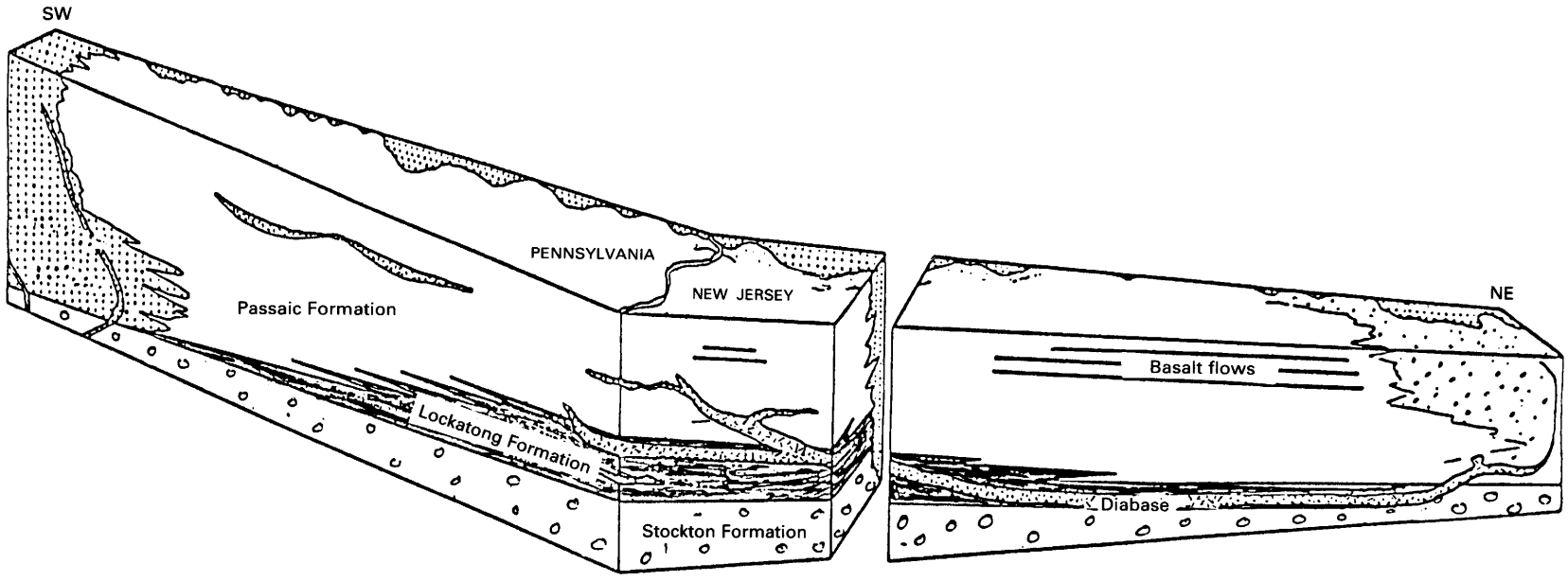

FIGURE 3.2.—Schematic southwest-northeast block diagram of the Newark basin showing original configuration of Triassic formations and lithofacies of the Newark Supergroup, as interpreted by Van Houten (1969).

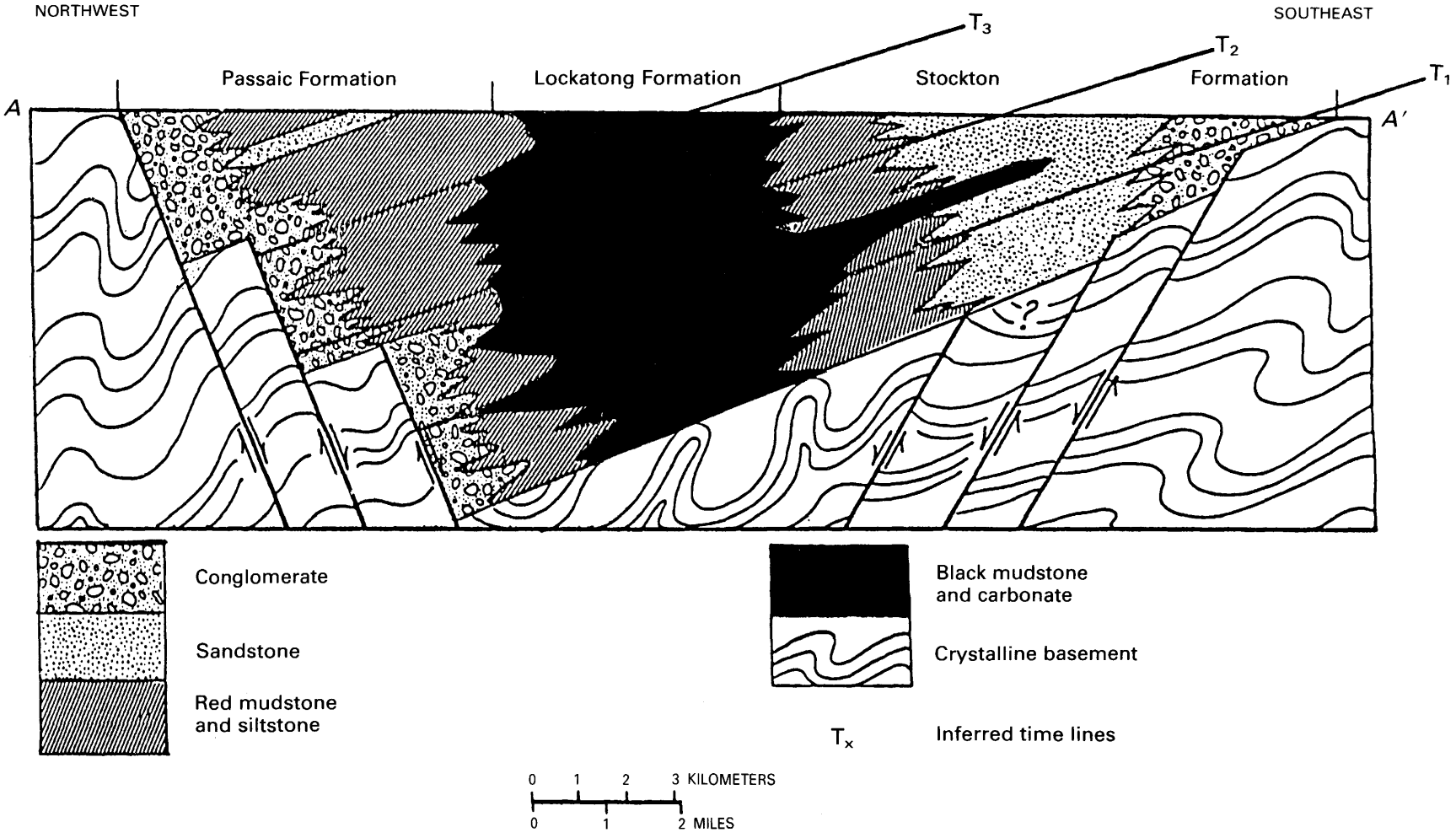

FIGURE 3.3.—Cross section showing structural and facies relationships within the Newark basin as interpreted by Turner-Peterson (1980). The section is drawn approximately parallel to the Delaware River (*A*–*A*' in fig. 3.1). T1, T2, and T3 are inferred time lines. (Modified slightly from Turner-Peterson, 1980.)

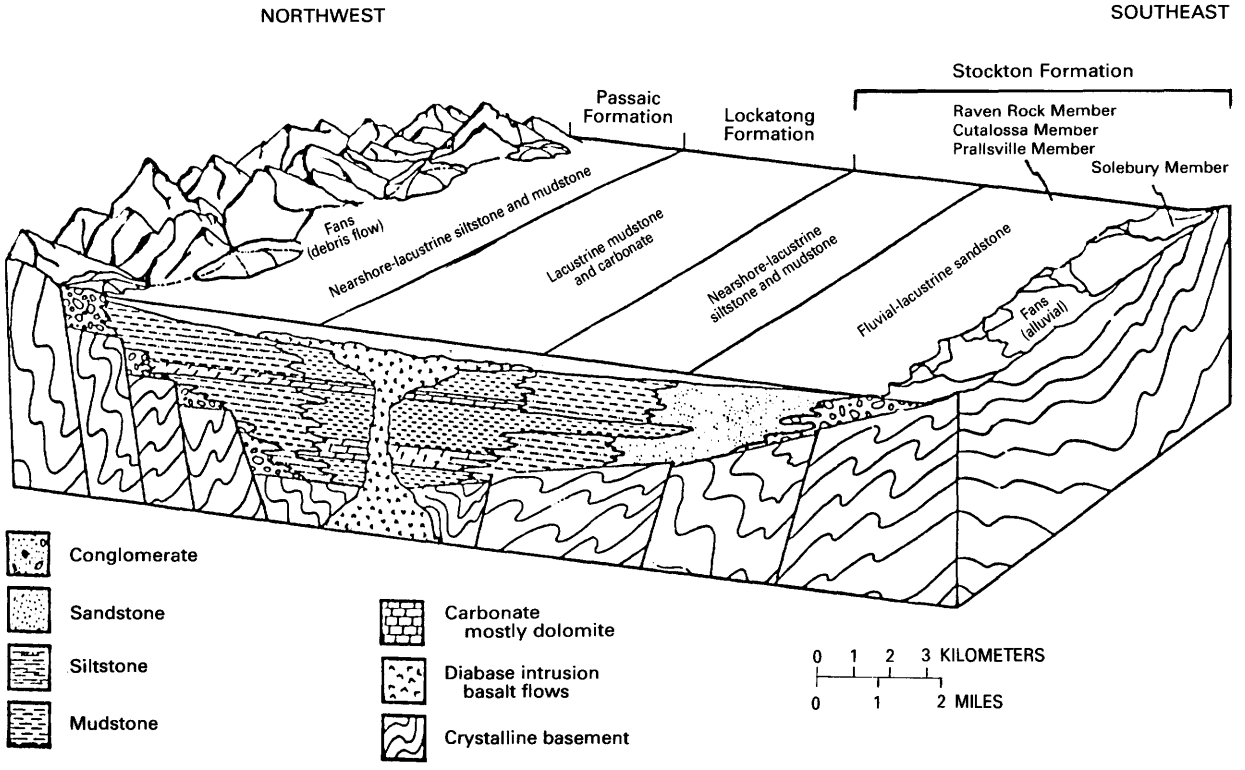

FIGURE 3.4.—Primary distribution of facies in the Newark basin, inferred from the cross section in figure 3.3. (Modified slightly from Turner-Peterson, 1980.)

in the Lockatong also suggest that Stockton-like fluvial sandstones may have been deposited near the original basin margin.

In spite of the local similarity of facies within the Stockton and Lockatong Formations and the implications for facies distribution, some problems still remain with the concept of the formations as large-scale, time-transgressive facies. For instance, repetition of similar lithologic sequences in the two fault blocks (shown in fig. 3.1) suggests that the named formations are discrete lithologic entities. In addition, if the formations are indeed facies of one another, one would expect to see more distal facies of each formation farthest from the inferred basin margin, with exposures in the northern fault block containing more distal facies than those exposed in the southern fault block. This has not been demonstrated.

One possible explanation for the repetition of formations in the two fault blocks is that the exposed Stockton is mostly fluvial-deltaic and the exposed Lockatong is dominantly lacustrine. Dominance of one facies in each formation may reflect a variation of the relative importance of fluvial versus lacustrine deposition through time, perhaps as a consequence of expansion and contraction of a lake in the center of the basin (fig. 3.5). Fluvial sedimentation may have been the dominant process during the early history of the basin, accounting for Stockton lithologies, while subsequent expansion of a central lake may account for the dominant lacustrine facies of the Lockatong Formation. If this model is correct, the concept of each formation generally representing a specific period of deposition, as proposed by Van Houten (1969) and corroborated by Cornet (1977) and Olsen (1984) on paleontological grounds, is largely valid. Probably at no time, however, was the entire basin characterized by either fluvial or lacustrine sedimentation. It would be difficult to imagine an extensive deep lake such as that postulated during Lockatong deposition (Olsen, 1984), especially with deltas building into it, without streams to supply water and sediment to the lake. Similarly, recognition of deltaic sequences within the Stockton Formation requires that some sort of lake existed basinward, or deltas could not have developed. Still, the evidence is insufficient to prove that the fluvial sandstones of the Lockatong resemble those of the Stockton, or that the Stockton lacustrine beds resemble lacustrine units of the Lockatong. Thus, the implication of the new findings in terms of basin reconstruction is that both of the initially proposed models of basin reconstruction have

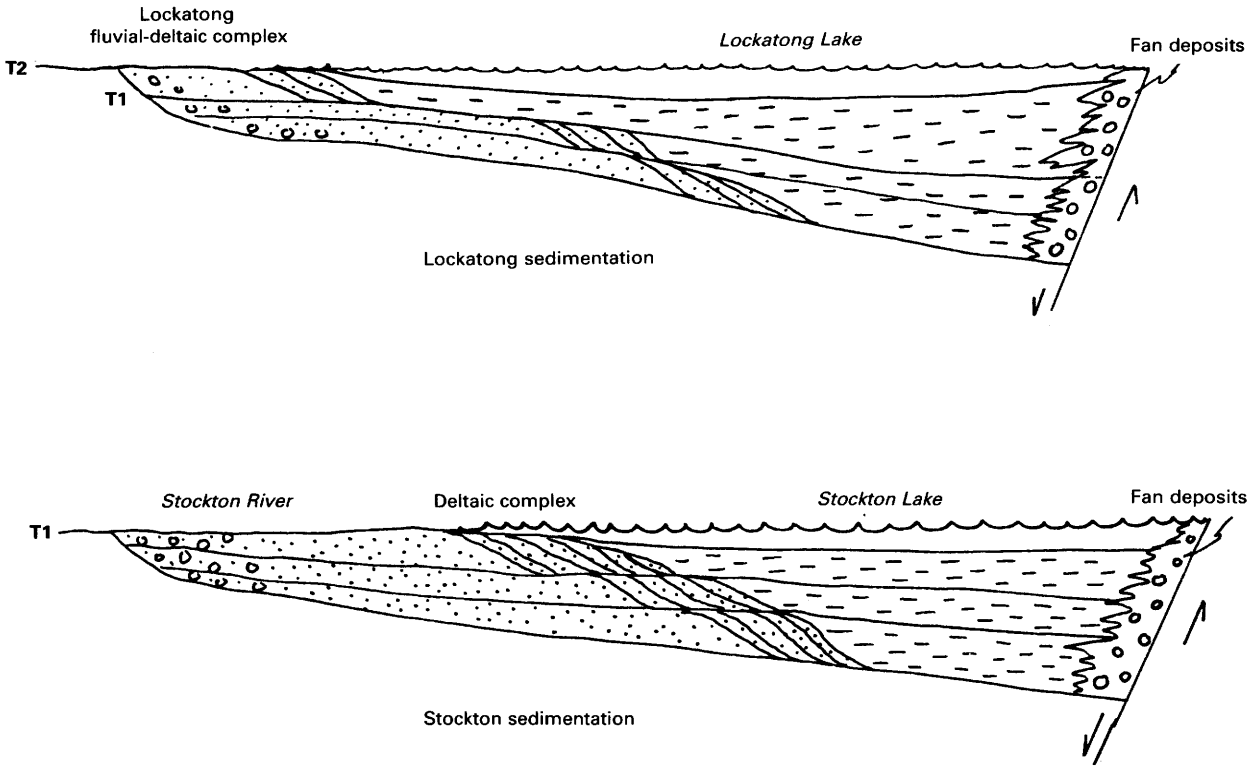

FIGURE 3.5.—Schematic cross sections of hypothetical facies distributions in the Stockton and Lockatong Formations as they change with time. During time 1 (T1), lacustrine conditions are restricted to a narrow belt adjacent to the border fault, while fluvial deposits extend well into the basin. During time 2 (T2), a tectonic shift in basin shape or a change in the nature of inflow causes the lake to expand over a larger area, restricting fluvial sedimentation to the margins.

some validity. Whether or not equivalent lithologies downdip are similar to the outcropping formations remains uncertain.

Several other possible explanations for the observed facies relationships exist. One possibility is that the basin widened to the southeast with time, in response to step faulting in that direction. This widening would have superimposed more distal facies on more proximal facies, resulting in the observed vertical transitions in lithologies. Another possibility is that the basin was not closed during initial Stockton deposition, so that fluvial sediments could conceivably have extended from margin to margin across the present-day basin. Later closing of the basin may then have led to lake development and deltaic deposition. Expansion of a smaller lake into a much larger lake would have permitted deposition of the extensive black mudstones of the Lockatong Formation. Climatic change may have affected the Stockton-Lockatong transition by changing the style of fluvial input.

Understanding the overall facies distribution in the basin is crucial to determining the hydrocarbon and mineral resource potential. If good petroleum source rocks occur, it is important to know if a potential sandstone reservoir exists near the source rocks, either laterally or vertically. Similarly, if a particular facies is favorable for mineralization, it is important to know if that facies occurred only once during basin filling or if it was an integral part of the depositional system recurring throughout basin evolution. Before any solid conclusions can be made, more detailed comparisons of Stockton and Lockatong sandstone intervals are needed, as well as reliable subsurface controls in the form of cores or deep drill holes tied to seismic lines and outcrops.

REFERENCES

Cornet, Bruce, 1977, The palynostratigraphy and age of the Newark Supergroup: University Park, Pennsylvania State University, unpub. Ph.D. thesis, 506 p.

Gilbert, G.K., 1890, Lake Bonneville: U.S. Geological Survey Monograph 1, 483 p.

Glaeser, J.D., 1966, Provenance, dispersal, and depositional environments of Triassic sediments in the Newark-Gettysburg basin: Pennsylvania Geological Survey Bulletin G43, 168 p.

Hunter, R.E., 1977, Terminology of cross-stratified sedimentary layers and climbing-ripple structures: Journal of Sedimentary Petrology, v. 47, p. 697–706.

Jopling, A.V., and Walker, R.G., 1968, Morphology and origin of ripple-drift cross-lamination, with examples from the Pleistocene of Massachusetts: Journal of Sedimentary Petrology, v. 38, p. 971–984.

Olsen, P.E., 1980, The latest Triassic and Early Jurassic formations of the Newark basin (eastern North America, Newark Supergroup): Stratigraphy, structure, and correlation: New Jersey Academy of Science Bulletin, v. 25, p. 25–51.

———1984, Comparative paleolimnology of the Newark Supergroup—A study of ecosystem evolution: New Haven, Conn., Yale University, unpub. Ph.D. thesis, 726 p.

Turner-Peterson, C.E., 1980, Sedimentology and uranium mineralization in the Triassic-Jurassic Newark basin, Pennsylvania and New Jersey, *in* Turner-Peterson, C.E., ed., Uranium in sedimentary rocks—Application of the facies concept to exploration: Short Course Notes, Rocky Mountain Section, Society of Economic Paleontologists and Mineralogists, p. 149–175.

Van Houten, F.B., 1969, Stratigraphy and sedimentology of Triassic rocks of eastern North America: Atomic Energy Commission Report GJO-7402, 77 p.

4. ALLUVIAL FAN DEVELOPMENT IN THE LOWER JURASSIC PORTLAND FORMATION, CENTRAL CONNECTICUT—IMPLICATIONS FOR TECTONICS AND CLIMATE

Peter M. LeTourneau[3]

INTRODUCTION

Continental rift basins of the early Mesozoic Newark Supergroup are exposed along the eastern flank of the Appalachian orogen from Nova Scotia to South Carolina. The Hartford basin, in central Connecticut and Massachusetts (fig. 4.1), is an east-dipping half-graben 140 km long and 30 km wide, which contains 4–7 km of Upper Triassic and Lower Jurassic continental sedimentary rocks and tholeiitic basalts (Krynine, 1950; Olsen and others, 1982; Burger and Atman, 1984). West-dipping, listric, normal faults define the eastern margin of the Hartford basin (Hamblin, 1965; Hubert and others, 1982; Wise and Robinson, 1982). Postdepositional deformation produced large open folds in the basin fill along the eastern fault margin and northeast-trending normal faults throughout the basin (Sanders, 1963). Three laterally continuous basalt flows that form prominent ridges on the uplifted edges of tilted fault blocks have helped define the stratigraphy of the Hartford basin (table 4.1). Sedimentary rocks are assigned to specific formations according to their position relative to the basalt flows.

The sedimentary rocks of the Hartford basin are coarsest within 4 km of the eastern margin and become progressively finer grained toward the center of the basin. This study investigated the sedimentology and stratigraphy of the conglomerate, sandstone, siltstone, and dark shale of the Lower Jurassic Portland Formation exposed along the eastern margin of the basin in central Connecticut (fig. 4.1). The strata in the study area strike roughly north and dip 12–20°E., forming steep west-facing outcrops 3–15 m high, parallel to the strike of the beds. Within 1 km of the eastern border fault, the dip of the bedding increases to more than 45°.

[3]Wesleyan University, Middletown, Connecticut 06457.

LITHOSOME DISTRIBUTION

More than 1000 m of detailed measured sections, consisting of a 700-m-long vertical reference section

TABLE 4.1.—*Stratigraphy of the Hartford basin in Connecticut*

[Thicknesses estimated from Krynine (1950) and Olsen and others (1982). All units are Jurassic except the New Haven Arkose, which is Triassic and possibly earliest Jurassic in Connecticut]

Stratigraphic unit	Estimated average thickness (meters)
Portland Formation	1500
Hampden Basalt	100
East Berlin Formation	170
Holyoke Basalt	150
Shuttle Meadow Formation	100
Talcott Basalt	65
New Haven Arkose	2250

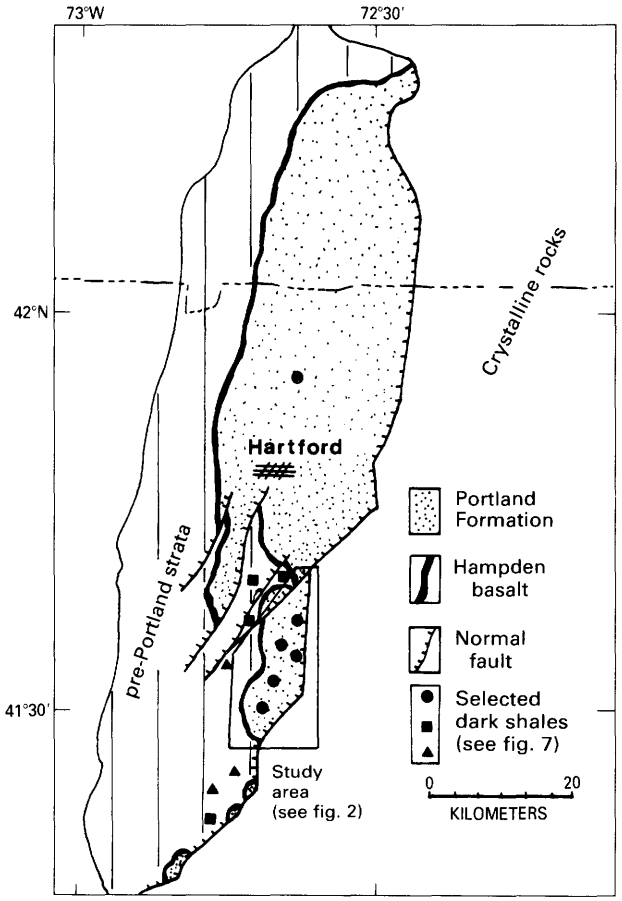

FIGURE 4.1.—Simplified geologic map of the Hartford basin in Connecticut and Massachusetts (modified from Hubert and others, 1982).

and 300 m of additional, laterally correlative measured sections, document the vertical succession and lateral variability of coarse sedimentary rocks in part of the Portland Formation. In addition, the sedimentary rocks at more than 100 other localities in the study area were described to map the distribution of the various lithologies. Sedimentary rocks of similar texture, composition, and depositional style are grouped as lithosomes, which are "***masses of essentially uniform lithologic character which have intertonguing relationships with adjacent masses of different lithology***" (Krumbein and Sloss, 1963, p. 301). The distribution of lithosomes is shown in figure 4.2.

The conglomerate lithosome includes the following lithologies (which will be referred to by number). (1) Poorly sorted, matrix-supported boulder and cobble conglomerate with a disorganized or chaotic internal fabric. Beds are commonly lenticular with hummocky or irregular upper contacts and planar to undulatory lower contacts. The largest clasts in the study area are associated with this lithology. (2) Poorly sorted pebbly sandstone and clast-supported conglomerate. Laminated silt drapes 5 to 10 cm thick form the upper layers of these 20- to 60-cm-thick, fining-up beds. (3) Pebbly sandstone and clast-supported pebble and cobble conglomerate with imbricated clasts and trough and tabular cross-stratification features 20 to 150 cm in thickness. These conglomerate lithologies are interpreted, respectively, as (1) debris flow deposits (Hooke, 1967; Rust, 1979; Nilsen, 1982); (2) shallow, ephemeral braided-stream deposits (Miall, 1978, Rust, 1979); (3) moderately deep, possibly perennial braided-stream deposits (Schumm, 1977; Miall, 1978; Rust, 1979).

The sandstone lithosome consists of the following lithologies: (4) fine sandstone with horizontal, planar lamination and ripple cross-lamination and (5) pebbly, medium to coarse sandstone with mud intraclasts and

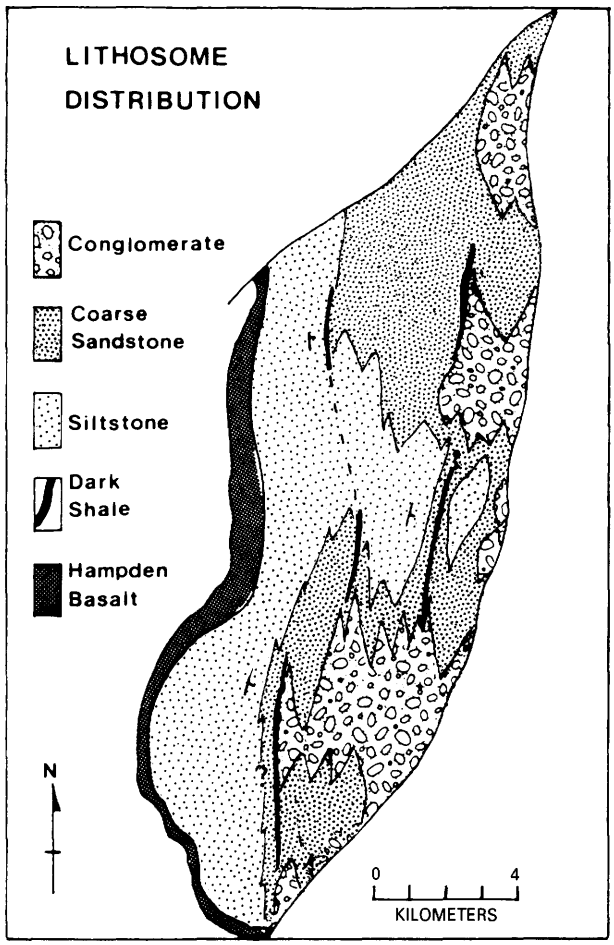

FIGURE 4.2.—Distribution of lithosomes in the Hartford basin. Strike and dip symbols indicate orientation of sedimentary layering.

thin, burrowed and mudcracked, laminated siltstone interbeds. These sandstone lithologies are interpreted, respectively, as (4) shallow sheetflow deposits (Hubert and Hyde, 1982; Smoot, 1983) and (5) channel sand and overbank silt deposits of ephemeral braided streams (Miall, 1978; Steel and Aasheim, 1978).

The siltstone lithosome is composed of (6) red siltstone containing horizontal, planar lamination and climbing-ripple cross-lamination, mudcracks, and interbeds of medium to coarse sandstone with trough cross-stratification. This lithology is interpreted as fine-grained floodplain deposits and associated ephemeral braided-stream channel sand (Miall, 1978; Steel and Aasheim, 1978; Hubert and others, 1982).

The dark shale lithosome contains the following lithologies. (7) Gray, well-sorted, coarse sandstone with oscillatory ripple cross-lamination and interbedded gray siltstone. Fossilized plant fragments are common in this lithology. (8) Organic-matter-rich black shale containing well-preserved fish fossils, which have been identified as freshwater species (Olsen and others, 1982). These rocks are interpreted, respectively, as (7) wave-worked shallow-water and shoreline deposits and (8) quiet-water lacustrine deposits. The sedimentary structures and fossils of the dark shale lithosome are similar to those described from modern and ancient lacustrine deposits (Van de Kamp, 1973; Raaf and others, 1977; Link and Osborne, 1978; Picard and High, 1981; Fouch and Dean, 1982).

The vertical and lateral distribution of lithosomes is indicated in figure 4.2. The conglomerate lithosome forms discrete sedimentary prisms along the eastern margin of the basin. At a distance of about 2 km west of the eastern basin margin, the beds of conglomerate and associated coarse sandstone thin and intertongue laterally with finer sandstone and siltstone. The dark shale lithosome is interbedded with the conglomerate and sandstone beds at five localities in the study area.

PALEOENVIRONMENTAL RECONSTRUCTION

Comparison with descriptions of modern and ancient alluvial fan conglomerates and sandstones (Bull, 1968, 1972; Steel and Wilson, 1975; Heward, 1978a; Steel and Aasheim, 1978; Rachocki, 1981; Nilsen, 1982; Galloway and Hobday, 1983) suggests that the coarse sedimentary rocks of the conglomerate and sandstone lithosomes are an excellent example of ancient alluvial fan deposits. This interpretation is consistent with the conclusions of previous investigations of the Hartford basin and the Portland Formation (Longwell, 1922; Russell, 1922; Krynine, 1950; Gilchrist, 1979). The distribution and geometry of the conglomerate lithosomes (fig. 4.2) define seven discrete alluvial fan prisms along the eastern fault margin of the basin. The largest of these alluvial fan deposits appears to have persisted throughout much of the deposition of the Portland Formation in central Connecticut.

The lithosomes, each consisting of one or more of the numbered lithologies, are interpreted as three distinct depositional facies as summarized in figure 4.3. Depositional facies A combines numbered lithologies 1–4 of the conglomerate and sandstone lithosomes, facies B combines part of the sandstone lithosome (lithology 5) and the siltstone lithosome (lithology 6), and facies C corresponds to the dark shale lithosome (lithologies 7, 8). The lithosomes describe texturally similar rock types; the depositional facies incorporate the sedimentary rocks that are characteristic of a particular depositional environment.

Figure 4.4 is a paleoenvironmental reconstruction of the study area showing the hypothesized areal distribution of alluvial fans and a perennial lake in the Early Jurassic based on the locations of corresponding lithologies in the study area. During periods of maximum lake expansion, progressively finer grained lacustrine deposits formed a transgressive sequence over the distal margins of the alluvial fans, and several lake shoreline siltstones and sandstones were deposited within 0.75 km of the eastern fault margin of the basin. The perennial lake, at times, was replaced by playas or floodplains.

The alluvial fan reconstruction is based on the geometry of the conglomerate and associated sandstone lithologies of facies A and paleocurrent dispersal patterns. Comparison with modern alluvial fans suggests that the coarse-grained sedimentary rocks may represent only the mid- and lower fan deposits. The upper fan lithologies may have been removed by post-depositional uplift and erosion along the eastern margin of the basin.

The different lithologies commonly form regular vertical sequences (for example, a coarsening-upward sequence of siltstone through conglomerate) that are repeated in the stratigraphic column. The vertical and lateral relations of the lithologies provide an indication of possible controls on sedimentation along the margin of an ancient rift basin, including climatic variation and tectonic activity.

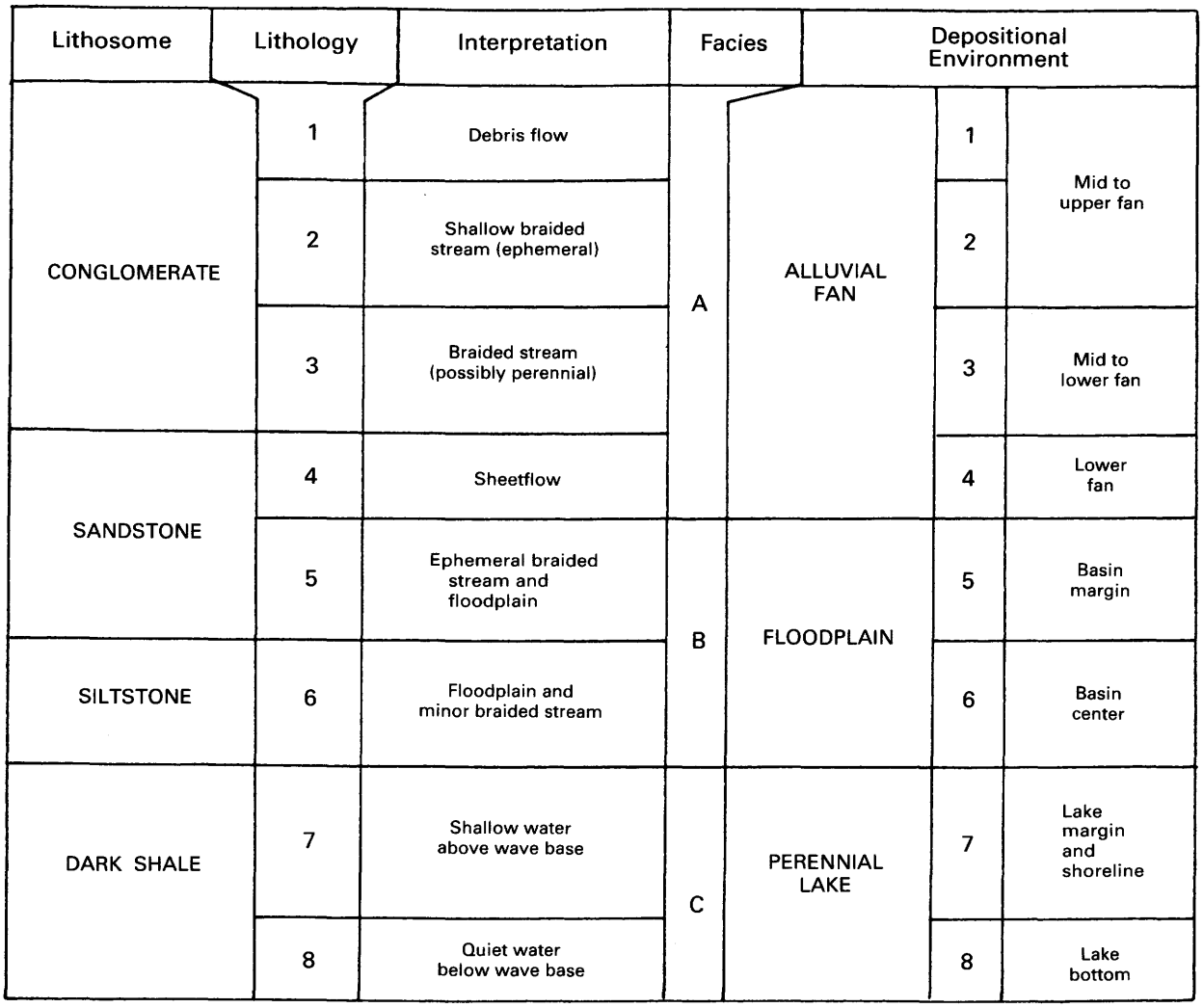

FIGURE 4.3.—Interpreted depositional environments for sedimentary rocks of the Portland Formation in central Connecticut.

CLIMATE HYPOTHESIS

Lithologies 3, 7, and 8, of facies A and C, are associated in the vertical succession. The abundant, dune-scale cross-bedding of lithology 3 suggests persistent fluvial activity in moderately deep braided streams (Schumm, 1977; Heward, 1978a; Galloway and Hobday, 1983). Lithologies 7 and 8 are interpreted as a perennial-lake depositional environment. These three lithologies typically occur in 5- to 10-m-thick sequences, in a 3–7–8–7 order upsection, indicating the transgression of the lake over the stream-dominated distal alluvial fan deposits. This depositional sequence may be the result of humid climatic conditions that favored the development of perennial lakes and persistent fluvial activity (Lustig, 1965; Schumm, 1977; Galloway and Hobday, 1983).

Lithologies 1, 2, 4, 5, and 6, of facies A and B, are characterized by poor stratification, poor sorting, and sedimentary features indicative of ephemeral and episodic fluvial activity (Bluck, 1965; Lustig, 1965; Rust, 1979). The debris-flow deposits of lithology 1 are associated with episodic fluvial activity in arid and semiarid climates (Blackwelder, 1928; Lustig, 1965; Galloway and Hobday, 1983, p. 25–50). The fining-up depositional units of lithology 2 represent decelerating flow sequences associated with ephemeral fluvial activity (Miall, 1978; Tunbridge, 1981). These lithologies are

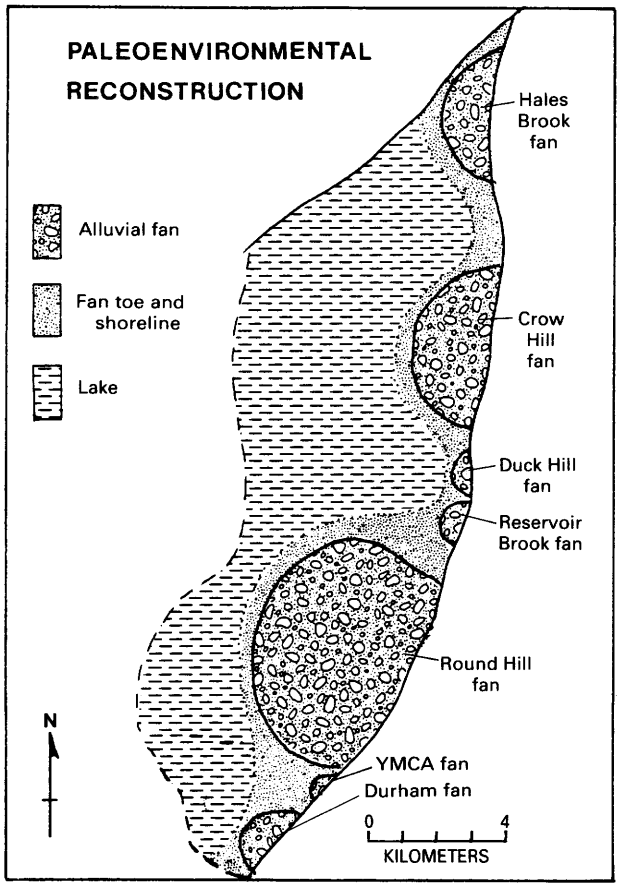

FIGURE 4.4.—Reconstruction of paleoenvironments in the study area during a period of maximum lake expansion.

found as an upward-coarsening sequence, 6–5–4–2–1, indicating the progradation of the alluvial fan over the floodplain deposits of the basin floor.

Figure 4.5 summarizes the lateral relationships of the inferred "wet" and "dry" phases of deposition based on the sedimentological criteria discussed above. In the vertical section the "wet" or "dry" lithologies repeat to form stacked sequences approximately 175 m thick. These 175-m-thick sequences are formed of smaller scale, 5- to 10-m-thick coarsening- or fining-up sequences that may be the result of autocyclic depositional processes due to channel avulsion, resulting in shifting sites of deposition on the alluvial fan (Heward, 1978b). It is proposed that the larger scale, cyclic alternation of the two distinct "wet" and "dry" phases of deposition may record the oscillation from humid to arid or semi-arid climatic conditions.

TECTONIC HYPOTHESIS

The influence of syndepositional tectonic activity on the sedimentary deposits along the basin margin is shown by several lines of evidence. The alluvial fan deposits mapped along the eastern basin margin extend from 1 to 3 km into the basin and delineate discrete alluvial fans with a radial pattern of sediment dispersal. In modern rift basins, the rapidly subsiding basin margins typically have separate, small, steep, alluvial fans (Hunt and Mabey, 1966; Hooke, 1972; Steel, 1976; Heward, 1978b; Gloppen and Steel, 1981). Figure 4.6 shows the map-view geometry of modern alluvial fans on the east side of Death Valley, for comparison with the reconstructed fans from the study area (fig. 4.4). Syndepositional tectonic tilting of the basin floor may have prevented the prograding alluvial fans from extending far into the basin by continually burying the coarse sands and gravels under finer basin floor deposits (Hooke, 1972; Gloppen and Steel, 1981).

Upward-coarsening sequences of conglomerate and sandstone, 10 to 30 m thick, represent progradational alluvial fan lobes. Similar vertical successions described by Steel (1976) and Heward (1978b) suggest that these sequences may represent the tectonic rejuvenation of the basin margin and relative uplift of the source area that resulted in a progradational depositional sequence. Syndepositional subsidence and eastward tilting of the basin floor in the study area is also suggested by the inferred geometry of the lacustrine sequences. Figure 4.7 is a plot of the thickness of black shale units versus the distance from the eastern fault margin. In the Shuttle Meadow, East Berlin, and Portland Formations, the black shale units all thin progressively away from the eastern basin margin. The thickest black shale units are within 1.5 km of the eastern margin. Several lacustrine deposits located within 1 km of the basin margin contain beds with soft-sediment deformation features, including slump folds with fold axes oriented subparallel to the eastern border fault. Sims (1973) described similar features in the bottom sediment of a modern lake that had been subjected to recent seismic activity.

The distribution of the black shale units suggests that the lake waters persisted longer and were possibly deeper near the eastern basin margin and where high sedimentation rates contributed to the thick accumulations of organic-matter-rich sediment. Gloppen and Steel (1981) suggested that tectonic tilting of the basin floor may control the geographic distribution of lakes in rapidly subsiding basins. Figure 4.8 is a schematic diagram of a "wet" phase relationship of lake and fan

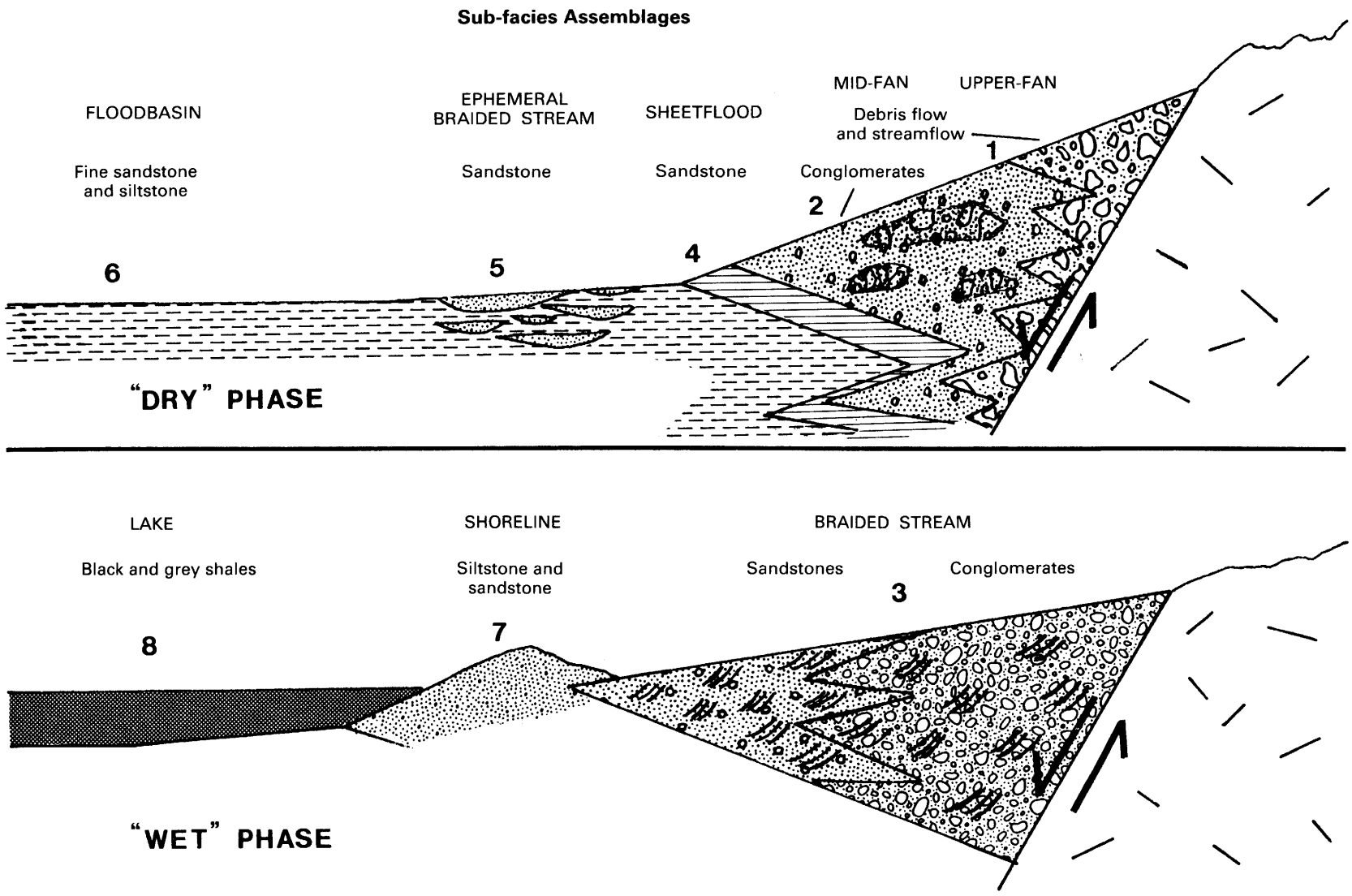

FIGURE 4.5.—Lateral relations of depositional environments of the two climate types in the study area.

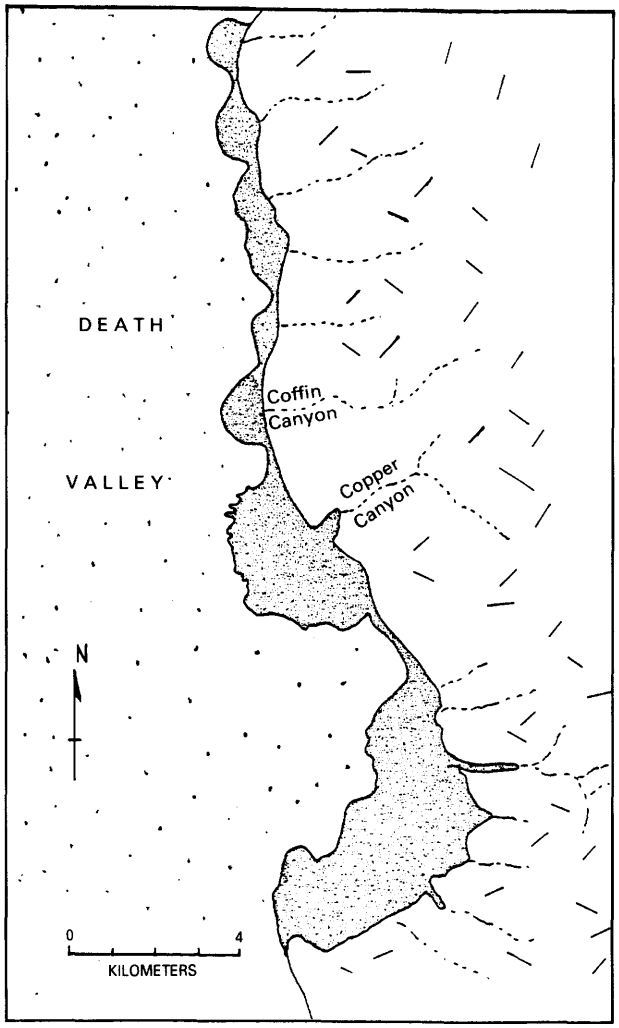

FIGURE 4.6.—Map-view geometry of modern alluvial fans in Death Valley, Calif., showing deposition patterns (from Hunt and Mabey, 1966).

deposits and the inferred lake geometry for the Early Jurassic lakes in the Hartford basin.

SUMMARY

The most extensive exposures of sedimentary rocks in the Lower Jurassic Portland Formation occur along the eastern margin of the Hartford basin in central Connecticut. This investigation mapped the distribution of conglomerate, sandstone, siltstone, and dark shale and described the vertical succession of these rocks in more than 1000 m of detailed measured section. The conglomerate and sandstone beds form discrete sedimentary prisms that thin away from the basin margin and intertongue laterally with finer sandstone and siltstone beds toward the basin center; they are interpreted to be ancient alluvial fan deposits on the basis of grain-size distributions, paleocurrent patterns, and depositional style. Thin dark shale beds interpreted to be lacustrine deposits are intercalated with the conglomerate and sandstone beds in the study area.

These alluvial fan and lacustrine rocks may provide a record of the tectonic and climatic controls on sedimentation along the margin of an ancient rift basin. Two distinct styles of fluvial sedimentation, interpreted as ephemeral braided-stream deposits and perennial braided-stream deposits, occur as approximately 175-m-thick sequences along the measured section and may indicate alternating semi-arid and humid climatic conditions.

Syndepositional tectonic subsidence of the basin margin is suggested by the geometry of the alluvial fan and lacustrine deposits. The reconstructed alluvial fans from the Portland Formation are small, discrete bodies with a radial pattern. The depositional geometry of these fans is similar to that of modern fans in rapidly subsiding basins. The thickest black shale beds are within 2 km of the basin margin. The tectonic tilting of the basin floor may have caused the lakes to be longest lived and possibly deepest adjacent to the fault margin. Figure 4.9 is a graphic representation of the various scales at which the inferred controls on sedimentation may be recognized.

This study provides a detailed description of the stratigraphy and depositional environments of the Portland Formation in central Connecticut and describes the evolution of the rift basin depositional system and its response to regional tectonic activity and long-term climatic change. The methods and results from this study may assist investigations of the coarse sedimentary rocks found along the margins of other rift basins in the Newark Supergroup by suggesting that possible climatic and tectonic controls on sedimentation can be recognized in the stratigraphic record. Similar depositional environments have been described from the Jurassic strata of the Deerfield basin in Massachusetts (Wessel, 1969) and the Waterfall Formation in the Culpeper basin, Virginia (Hentz, 1981). These strata may also contain the features that are attributed to climatic and tectonic controls in the Portland Formation.

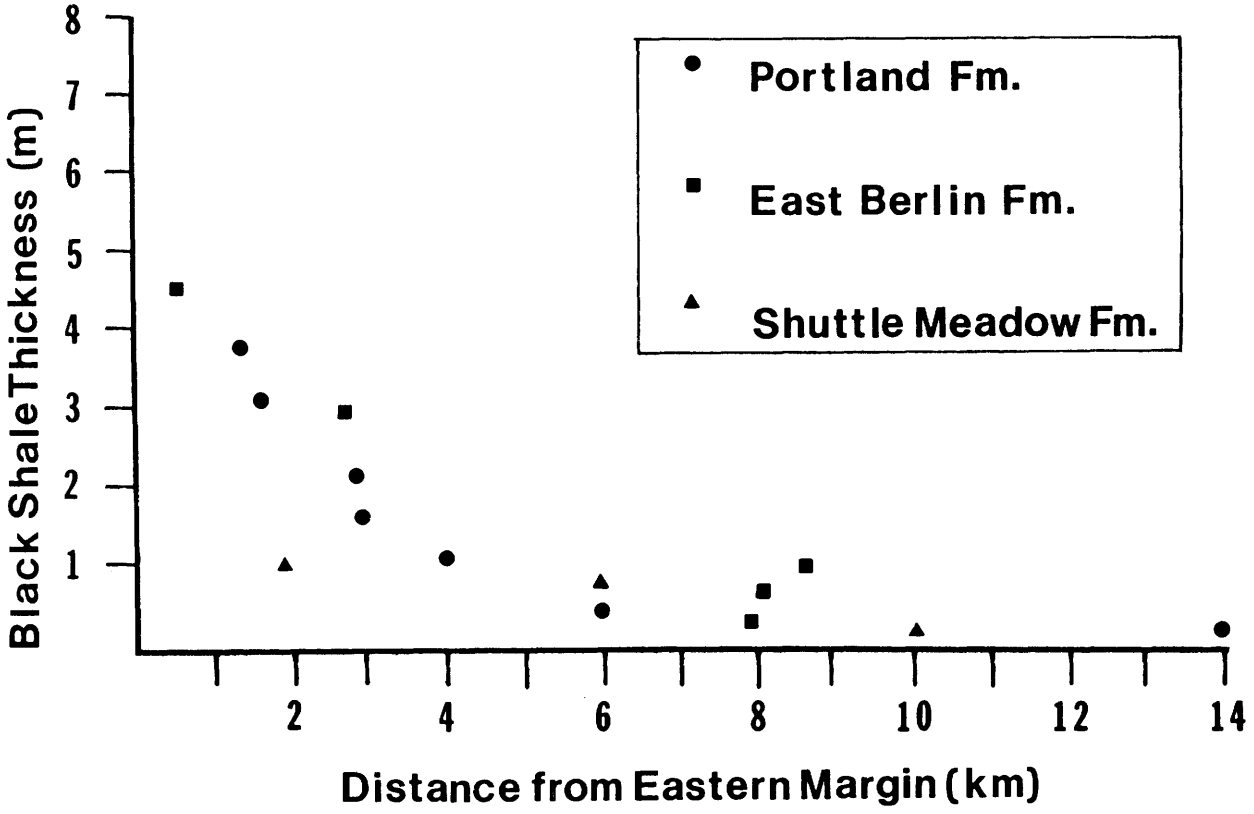

FIGURE 4.7.—Relation between thickness of black shale beds and distance from the eastern fault margin of the Hartford basin.

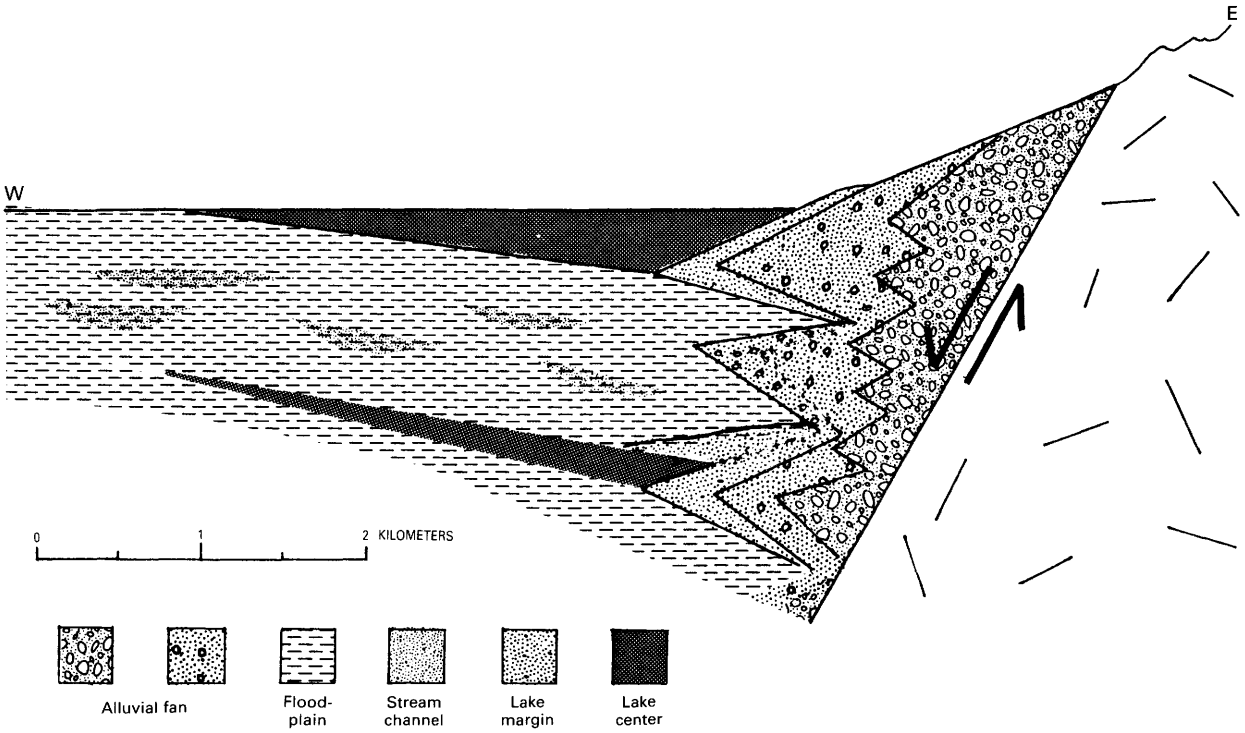

FIGURE 4.8.—Schematic diagram of inferred geometry of Early Jurassic lakes in the Hartford basin.

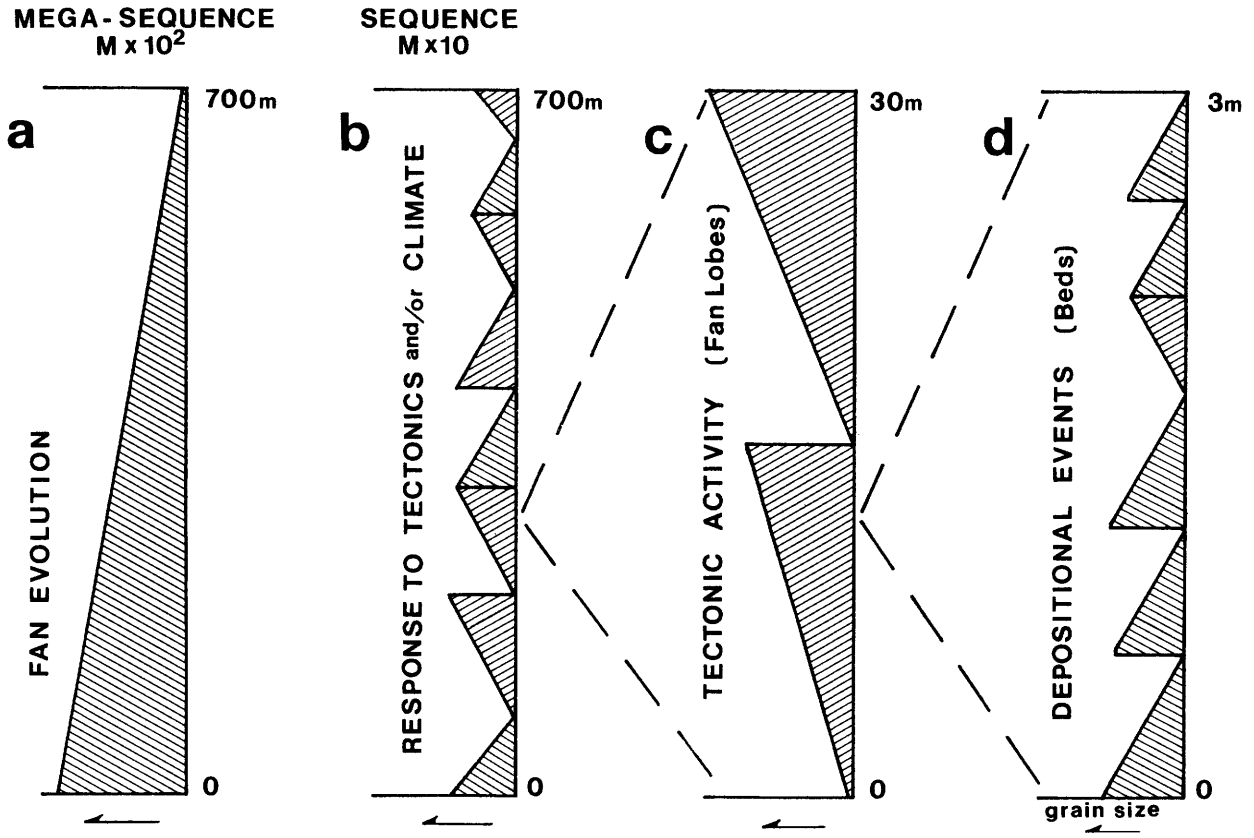

FIGURE 4.9.—Schematic diagram showing relative scales of depositional sequences in the vertical section.

REFERENCES

Blackwelder, E., 1928, Mudflow as a geologic agent in semiarid mountains: Geological Society of America Bulletin, v. 39, p. 465–483.

Bluck, B.J., 1965, The sedimentary history of some Triassic conglomerates in the Vale of Glamorgan, South Wales: Sedimentology, v. 4, p. 225–245.

Bull, W.B., 1968, Alluvial fans: Journal of Geological Education, v. 16, p. 101–106.

———1972, Recognition of alluvial fan deposits in the stratigraphic record, *in* Rigby, J.K., and Hamblin, W.K., eds., Recognition of ancient sedimentary deposits: Society of Economic Paleontologists and Mineralogists, Special Publication 6, p. 63–83.

Burger, R.H., and Atman, P., 1984, Thicknesses of Mesozoic sedimentary rocks, Hartford Basin, Massachusetts, as interpreted from Bouguer gravity [abs.]: Geological Society of America Abstracts with Programs, v. 16, no. 1, p. 7.

Fouch, T.D., and Dean, W.E., 1982, Lacustrine environments, *in* Scholle, P.A., and Spearing, D., eds., Sandstone depositional environments: American Association of Petroleum Geologists Memoir 31, p. 87–114.

Galloway, W.E., and Hobday, D.K., 1983, Terrigenous clastic depositional environments: Applications to petroleum, coal, and uranium exploration: New York, Springer-Verlag, 423 p.

Gilchrist, J.M., 1979, Sedimentology of the Lower to Middle Jurassic Portland Arkose of central Connecticut: Amherst, University of Massachusetts, unpub. M.S. thesis, 165 p.

Gloppen, T.G., and Steel, R.J., 1981, The deposits, internal structure and geometry in six alluvial fan-fan delta bodies (Devonian, Norway) — A study in the significance of bedding sequence in conglomerates, *in* Ethridge, F.G., and Flores, R.M., eds., Recent and ancient non-marine depositional environments: Models for exploration: Society of Economic Paleontologists and Mineralogists, Special Publication 31, p. 49–69.

Hamblin, W.K., 1965, Origin of "reverse drag" on the downthrown side of normal faults: Geological Society of America Bulletin, v. 76, p. 1145–1164.

Hentz, T.F., 1981, Sedimentology and structure of Culpeper Group lake beds (Lower Jurassic) at Thorofare Gap, Virginia: Lawrence, University of Kansas, unpub. M.S. thesis, 166 p.

Heward, A.P., 1978a, Alluvial fan and lacustrine sediments from the Stephanian A and B (La Magdalena, Cinera - Matallana, and Sabero) coalfields, northern Spain: Sedimentology, v. 25, p. 451–488.

———1978b, Alluvial fan sequence and megasequence models: with examples from Westphalian D–Stephanian B coalfields, northern Spain, *in* Miall, A.D., ed., Fluvial sedimentology: Canadian Society of Petroleum Geologists Memoir 5, p. 669–702.

Hooke, R.L., 1967, Processes on arid-region alluvial fans: Journal of Geology, v. 75, p. 438–460.

———1972, Geomorphic evidence for Late Wisconsin and Holocene tectonic deformation, California: Geological Society of America Bulletin, v. 83, p. 2073–2098.

Hubert, J.F., Gilchrist, J.M., and Reed, M.G., 1982, Jurassic redbeds of the Connecticut Valley, *in* Joesten, R., and Quarrier, S.S., eds., New England Intercollegiate Geological Conference, Guidebook for fieldtrips in Connecticut and south-central Massachusetts: Connecticut State Geological and Natural History Survey, Guidebook 5, p. 103–141

Hubert, J.F., and Hyde, M.G. 1982, Sheet-flow deposits of graded beds and mudstones on an alluvial sandflat-playa system: Upper Triassic Blomidon Redbeds, St. Mary's Bay, Nova Scotia: Sedimentology, v. 29, p. 457–474.

Hunt, C.B., and Mabey, D.R., 1966, Stratigraphy and structure of Death Valley, California: U.S. Geological Survey Professional Paper 494–A, 162 p.

Krumbein, W.C., and Sloss, L.L., 1963, Stratigraphy and sedimentation: San Francisco, Freeman, 660 p.

Krynine, P.D., 1950, Petrology, stratigraphy, and origin of Triassic sedimentary rocks of Connecticut: Connecticut State Geological and Natural History Survey Bulletin 73, 247 p.

Lindholm, R.C., 1979, Geologic history and stratigraphy of the Triassic-Jurassic Culpeper basin, Virginia: Geological Society of America Bulletin, pt. 1, v. 90, no. 11, p. 995–997; pt. 2, v. 90, p. 1702–1736.

Link, M.H., and Osborne, R.H., 1978, Lacustrine facies in the Pliocene Ridge Basin Group: Ridge Basin, California, *in* Matter, A., and Tucker, M.E., eds., Modern and ancient lake sediments: International Association of Sedimentologists Special Publication 2, p. 169–187.

Longwell, C.R., 1922, Notes on the structure of the Triassic rocks in Southern Connecticut: American Journal of Science, v. 4, p. 223–236.

Lustig, L.K., 1965, Clastic sedimentation in Deep Springs Valley, California: erosion and sedimentation in a semiarid environment: U.S. Geological Survey Professional Paper 352–F, p. 131–192.

Miall, A.D., 1978, Lithofacies types and vertical profile models in braided river deposits, *in* Miall, A.D., ed., Fluvial sedimentology: Canadian Society of Petroleum Geologists Memoir 5, p. 597–604.

Nilsen, T.H., 1982, Alluvial fan deposits, *in* Scholle, P.A., and Spearing, D., eds., Sandstone depositional environments: American Association of Petroleum Geologists Memoir 31, p. 49–86.

Olsen, P.E., McCune, A.R., and Thomson, K.S., 1982, Correlation of the early Mesozoic Newark Supergroup by vertebrates, principally fishes: American Journal of Science, v. 282, p. 1–45.

Picard, M.D., and High, L.R., 1981, Physical stratigraphy of ancient lacustrine deposits, *in* Ethridge, F.G., and Flores, R.M., eds., Recent and ancient non-marine depositional environments: Models for exploration: Society of Economic Paleontologists and Mineralogists, Special Publication 31, p. 233–259.

Raaf, J.F.M. de, Boersma, J.R., and Van Gelder, A., 1977, Wave-generated structures and sequences from a shallow marine succession, Lower Carboniferous, County Cork, Ireland: Sedimentology, v. 24, p. 451–483.

Rachocki, A., 1981, Alluvial fans: New York, Wiley, 157 p.

Russell, W.L., 1922, The structural and stratigraphic relations of the great Triassic fault of southern Connecticut: American Journal of Science, fifth series, v. 4, p. 483–497.

Rust, B.R., 1979, Coarse alluvial deposits, *in* Walker, R.G., ed., Facies models: Geoscience Canada Reprint Series 1, p. 9–21.

Sanders, J.E., 1963, Late Triassic tectonic history of the northeastern United States: American Journal of Science, v. 261, p. 501–524.

Schumm, S.A., 1977, The fluvial system: New York, Wiley-Interscience, 335 p.

Sims, J.D., 1973, Earthquake induced structures in sediments of Van Norman Lake, San Fernando, California: Science, v. 102, p. 161–163.

Smoot, J.P., 1983, Depositional subenvironments in an arid closed basin; the Wilkins Peak Member of the Green River Formation (Eocene), Wyoming, U.S.A.: Sedimentology, v. 30, p. 801–827.

Steel, R.J., 1976, Devonian basins of western Norway—Sedimentary response to tectonism and varying tectonic context: Tectonophysics, v. 36, p. 207–224.

Steel, R.J., and Aasheim, S.M., 1978, Alluvial sand deposition in a rapidly subsiding basin (Devonian, Norway), *in* Miall, A.D., ed., Fluvial sedimentology: Canadian Society of Petroleum Geologists Memoir 5, p. 385–412.

Steel, R.J., and Wilson, A.C., 1975, Sedimentation and tectonism (Permo-Triassic?) on the margin of the North Minch Basin: Journal of the Geological Society of London, v. 131, p. 183–202.

Tunbridge, I.P., 1981, Sandy high energy fluvial sedimentation: some criteria for recognition, with an example from the Devonian of Southwest England: Sedimentary Geology, v. 28, p. 79–96.

Van de Kamp, P.C., 1973, Holocene continental sedimentation in the Salton Basin, California: A reconnaissance: Geological Society of America Bulletin, v. 84, p. 827–848.

Wessel, J.M., 1969, Sedimentary history of Upper Triassic alluvial fan complexes in north central Massachusetts: Amherst, University of Massachusetts, Department of Geology and Geography, Contribution 2, 157 p.

Wise, D.U., and Robinson, P., 1982, Tectonics of the Mesozoic Connecticut Valley graben [abs.]: Geological Society of America Abstracts with Programs, v. 14, no. 1, p. 96.

5. PALYNOSTRATIGRAPHY OF COAL-BEARING SEQUENCES IN EARLY MESOZOIC BASINS OF THE EASTERN UNITED STATES

Eleanora I. Robbins

INTRODUCTION

One of the earliest discoveries of coal in the United States was in the Richmond basin of Virginia in 1701; by 1858, gas manufactured from Richmond basin coal was used to light the streets of New York City (Eavenson, 1942; Wadleigh, 1938). Early Mesozoic rift basin coal has been produced commercially in both the Richmond and Deep River (Sanford-Durham) basins (Eavenson, 1942; Reinemund, 1955; Robbins, 1981). Recent estimates by the Virginia Polytechnic Institute (1981) suggest that 4 billion tons of coal resources remain in the Richmond basin. Coal beds in the Dan River-Danville and Farmville basins are thin but have been mined for local consumption (Stone, 1910; Wilkes, 1982). Nonrecoverable resources in isolated coal beds less than 14 inches thick (Wood and others, 1983) have been observed in the Taylorsville and Gettysburg basins (McCreath, 1879; Weems, 1980). Coalified logs have been collected in the Newark, Culpeper, and Hartford basins.

Most of the coal is high-volatile and medium-volatile bituminous in rank (Woodworth, 1902; Roberts, 1928; Reinemund, 1955; Virginia Polytechnic Institute, 1981). There are reports of lignite in the Taylorsville basin, semianthracite coal in the Dan River-Danville basin, and natural coke in the vicinity of dikes in the Deep River (Sanford-Durham) basin (Rogers, 1884; Reinemund, 1955; Robbins, 1982). The total sulfur content of the coals ranges from 0.49 to 7.2 percent on an as-received basis (Stone, 1910; G.P. Wilkes, written commun., 1984).

The coal beds of the early Mesozoic rift basins are not considered to be of economic importance at present, primarily because they are generally thin and dipping and because numerous faults pose difficulties to mining. However, the abundant methane in Richmond basin coal, which has caused deaths associated with mining (Woodworth, 1902), has led to recent studies to consider the possibility of extraction of the methane (Virginia Polytechnic Institute, 1981).

Coal, impure coal, and associated carbonaceous shale were studied for this report. Carbonaceous shale is defined here as dark gray or black shale that consists of more than 60 volume percent organic matter in which wood cells are the dominant tissue. In all, 21 samples were collected from the coal-bearing sequences of five early Mesozoic basins. Eight samples were from the Coal Measures in the Richmond basin (Va.), two from the Cumnock Formation in the Deep River (Sanford) basin (N.C.), four from the Cow Branch Formation of Meyertons (1963) in the Dan River-Danville basin (N.C.-Va.), six from the Coal Measures in the Farmville basin (Va.), and one from the Doswell Formation in the Taylorsville basin (Va.). Samples were processed according to standard palynological methods. Fifty-gram samples of coal and impure coal were subjected to sequential treatment in 10 percent HCl, 48 percent HF, Schulze solution with saturated $KClO_3$ and the 90 percent HNO_3 modification for high-rank coals suggested by R.M. Kosanke (written commun., 1984), and 10 percent KOH. Ten-gram samples of carbonaceous shale were each subjected to treatment only in 10 percent HCl and 48 percent HF.

DATA

Table 5.1 lists 63 species of palynomorphs that were identified in the coal-bearing sequences: 18 trilete and monolete spore species; 21 bisaccate pollen species; 13 monosaccate, circumpolloid, and inaperturate pollen species; and 11 monosulcate and plicate pollen species. Several taxa were found in three or more basins; *Alisporites parvus* and *Paracirculina scurrilis* were found in the coal-bearing sequences from four of the five basins, and *Alisporites ovatus, Deltoidospora magna,* and *Placopollis raymondii* were found in three.

Cysts of an alga similar to those of the green alga *Volvox* were identified in the samples from the Farmville basin. The globular cysts average 15 μm in diameter.

INTERPRETATIONS AND CONCLUSIONS

Most of the palynomorphs identified in the samples are species that have long time ranges and are not diagnostic for specific age. However, taxa that are restricted in time to the middle Carnian stage of the

TABLE 5.1.—*Palynomorphs in coal-bearing sequences of Triassic basins*

[X, positive identification; ?, possible identification; ..., not seen in samples]

	Dan River-Danville	Deep River	Farmville	Richmond	Taylorsville
Trilete and monolete spores					
Aratrisporites fimbriatus				X	
A. saturnii	X			X	
cf. Callialasporites	X				
Calamospora nathorstii				X	
Concentricisporites sp.	X				
Cyathidites minor				X	
Cyclotriletes oligogranifer				X	
Deltoidospora hallii				X	
D. magna		X		X	X
Neoraistrickia sp.				X	
Polycingulatisporites mooniensis			?		
P. sp. A (D. Benson, Amoco, pers. commun.)					X
Punctatisporites major				X	
P. sp.		X			
Pyramidosporites traversei	X				
Reticulatisporites sp.	X				
Stereisporites perforatus	X				
Todisporites major				X	
Bisaccate pollen					
Alisporites grandis	?				X
A. ovatus	X			X	X
A. parvus	X	X	X	X	X
A. sp.					X
Brachysaccus neomundanus	X				
Colpectopollis ellipsoideus		X		X	X
Haplosporites varius				?	
Klausipollenites gouldii	X	X			
K. schaubergeri		X			
Microcachryidites sp. 143 (Cornet, 1977)			X		
Pityosporites devolvens					X
P. inclusus		X			
P. scaurus		X			
P. sp. A (Robbins, 1982)	X				
P. spp.	X				
Platysaccus sp.	X				
Plicatisaccus badius		X			
Protodiploxypinus sp.	X				
Protohaploxypinus sp.				X	
Sulcatisporites australis	X			X	
Vitreisporites pallidus			X	X	
Monosaccate, circumpolloid, and inaperturate pollen					
Araucariacites fissus	X	X		X	
A. sp.			?		
Corollina meyeriana			X	X	X
Enzonalasporites vigens	X				
Guthoerlisporites cancellosus	X				
Paracirculina scurrilis	X	X	X	X	X
Parallinites pauper		X		X	
Patinasporites densus	X			X	
Praecirculina granifer	?		X	X	
Vallasporites ignacii	X				
Monosaccate sp. A (Robbins, 1982)	X				
Monosulcate and plicate pollen					
Cycadopites deterius	X	X			
C. subgranulosus	X				
C. wielandii	X		X		
C. sp. 103 (Cornet, 1977)		X			
Equisetosporites sp.	X				
Ginkgocycadophytus sp.				X	
Monocolpopollenites sp.				X	
Monosulcites sp. A. (Robbins, 1982)	X				
M. spp.				X	
Ovalipollis ovalis			X		
Placopollis raymondii			X	X	X
Other					
Volvox sp.			?		

Late Triassic were identified from every basin. These diagnostic taxa, which include *Cyclotriletes oligogranifer, Klausipollenites gouldii, Plicatisaccus badius,* and *Placopollis raymondii,* indicate that the major deposition of coal was during the middle Carnian. The samples from the Richmond and Taylorsville basins contain an assemblage of undisputed middle Carnian age that represents the oldest Triassic palynoflora in the Eastern United States (Cornet, 1977). This paper is the first report of palynomorphs in the Farmville basin, which contains an assemblage similar to that of the Richmond-Taylorsville palynoflora. The palynoflora of the Deep River and Dan River-Danville basin coals is clearly later than the Richmond-Taylorsville sequence (Cornet, 1977), but there is a problem with the dating of the assemblages. The Carnian section in the Eastern United States is much thicker than the European type section (Cornet and Olsen, in press). Collections presently being made will allow future zonal differentiation between the late middle Carnian and the early late Carnian along the east coast (Bruce Cornet, written commun., 1984). Until this is done, it is not possible to be entirely certain that the coal-bearing sequences in the Deep River and Dan River-Danville basins are late middle Carnian rather than early late Carnian in age.

The palynomorphs in these coal-bearing sequences are of bryophytes, lycopods, ferns, seed ferns, conifers, cycadeoids and cycads, and unknown affinities. It is difficult to assess whether the palynomorphs are the remains of plants that grew under closed canopies in swamps or were carried into open-canopied swamps by the wind or both. Certainly the presence of megafossils of *Macrotaeniopteris* spp., *Equisetosporites* sp., and fern fronds in the coals (Fontaine, 1883) strongly supports the presence of true cycads, horsetails, and ferns, and (or) tree ferns growing in the swamps of the Richmond basin. Five palynotaxa were found in at least three of the basins and thus probably were produced by plants growing in the swamps. *Alisporites ovatus* and *A. parvus* are from voltzialian conifers, *Patinasporites densus* and probably *Paracirculina scurrilis* are from conifers, and *Cycadopites deterius* is from a cycadeoid or cycad (Retallack, 1975; A. Traverse, written commun., 1978; Grauvogel-Stamm, 1978).

REFERENCES

Cornet, Bruce, 1977, The palynostratigraphy and age of the Newark Supergroup: University Park, Pennsylvania State University, unpub. Ph.D. dissertation, 501 p.

Cornet, Bruce, and Olsen, P.E., in press, A summary of the biostratigraphy of the Newark Supergroup of eastern North America with comments on early Mesozoic provinciality: 3rd Latin American Paleobotanical Congress Symposium on Triassic Global Distribution.

Eavenson, H.N., 1942, The first century and a quarter of American coal industry: Pittsburgh, Pa., privately printed, Koppers Building, 701 p.

Fontaine, W.M., 1883, Contributions to the knowledge of the older Mesozoic flora of Virginia: U.S. Geological Survey Monograph 6, 144 p.

Grauvogel-Stamm, Lea, 1978, La flore du Gres à Voltzia (Buntsandstein Supérieur) des Vosges du nord (France); Morphologie, anatomie, interprétations phylogéniques et paléogéographiques: Sciences Géologiques Mémoire 50, 225 p.

McCreath, A.S., 1879, Second report on progress in the laboratory of the Survey at Harrisburg: Second Geological Survey of Pennsylvania, 1876–1878, MM, p. 102–103.

Meyertons, C.T., 1963, Triassic formations of the Danville basin: Virginia Division of Mineral Resources Report of Investigations 6, 65 p.

Reinemund, J.A., 1955, Geology of the Deep River coal field, North Carolina: U.S. Geological Survey Professional Paper 246, 159 p.

Retallack, G.J., 1975, The life and times of a Triassic lycopod: Alcheringa, v. 1, p. 3–29.

Robbins, E.I., 1981, A preliminary account of the Newark rift system: Lunar and Planetary Institute Contribution 456, Papers presented at the Conference on the Processes of Planetary Rifting, St. Helena, Calif., p. 107–109.

———1982, "Fossil Lake Danville": The paleoecology of a Late Triassic ecosystem on the North Carolina-Virginia border: University Park, Pennsylvania State University, unpub. Ph.D. dissertation, 400 p.

Roberts, J.K., 1928, The geology of the Virginia Triassic: Virginia Geological Survey Bulletin 29, 205 p.

Rogers, W.B., 1884, Reprint of annual reports and other papers on the geology of the Virginias: Appleton, New York, p. 315–330.

Stone, R.W., 1910, Coal on Dan River, North Carolina: U.S. Geological Survey Bulletin 471, p. 137–169.

Virginia Polytechnic Institute, 1981, The methane potential from coal seams in the Richmond basin of Virginia: Department of Mining and Minerals Engineering, Virginia Polytechnic Institute and State University, U.S. Department of Energy Contract No. DE–AC21–78MC08089, 93 p. and appendices.

Wadleigh, F.R., 1938, The story of the Richmond, Va., coal field and its development, 1700–1934, *in* Davis, I.F., and Evans, L.S., eds., The Richmond coal basin: a compilation in three parts, Part II, 163 p.

Weems, R.E., 1980, Geology of the Taylorsville basin, Hanover County, Virginia: Virginia Division of Mineral Resources Publication 27, p. 23–38.

Wilkes, G.P., 1982, Geology and mineral resources of the Farmville Triassic basin, Virginia: Virginia Minerals, v. 28, no. 3, p. 25–32.

Wood, G.H., Jr., Kehn, T.M., Carter, M.D., and Culbertson, W.C., 1983, Coal resource classification system of the U.S. Geological Survey: U.S. Geological Survey Circular 891, 65 p.

Woodworth, J.B., 1902, The Atlantic coast Triassic coal fields: U.S. Geological Survey 22nd Annual Report, Part III, 1900–1901, p. 25–53.

6. MASSIVE MUDSTONES IN BASIN ANALYSIS AND PALEOCLIMATIC INTERPRETATION OF THE NEWARK SUPERGROUP

Joseph P. Smoot and P.E. Olsen[4]

INTRODUCTION

Massive red or gray mudstones make up much of the fine-grained sedimentary rocks of the Newark Supergroup. In fact, the upper third of most sedimentary cycles in the fine-grained facies of most Newark basins is massive mudstone (division 3 of Olsen, 1984). Massive mudstones have not, however, been studied or described nearly as fully as conglomerates, sandstones, and laminated shales. This lack is due primarily to the difficulty in making textural descriptions from weathered outcrop exposures of massive mudstones and to the dearth of published depositional models for them. The widespread distribution and facies associations of massive mudstones in the early Mesozoic basins suggest that they are potentially useful in stratigraphic basin analysis. Furthermore, distinctive characteristics of massive mudstone textures suggest that they may be used for paleoclimatic interpretation, particularly in the context of their surrounding facies.

TYPES OF MASSIVE MUDSTONES

Four major types of massive mudstone texture are proposed for the Newark Supergroup, on the basis of a limited number of observations in most of the exposed early Mesozoic basins. These four types are (1) mud-cracked massive mudstone, (2) burrowed massive mudstone, (3) root-disrupted massive mudstone, and (4) sand-patch massive mudstone. Gradations exist between each of the massive mudstone types, so each is treated as an end member with dominant, distinctive fabrics and particular associations with other sedimentary features. The four types of massive mudstone oc-

[4]P.E. Olsen, Lamont-Doherty Geological Observatory of Columbia University, Palisades, N.Y. 10964.

cur in a variety of sedimentary sequences of which seven are shown in figure 6.1. These sequences show characteristic associations of the massive mudstone textures with other sedimentary features.

Mudcracked massive mudstone is characterized by abundant small (1–5 cm deep), narrow, jagged cracks, which form a polygonal pattern in plan view. The cracks are filled with sandstone or mudstone (the broader cracks having complex, cross-cutting or stratified fillings) or are partially filled with cements of carbonate minerals or analcime. Mudcracked massive mudstone generally contains different proportions of two fabrics: a breccia fabric and an overlying "crumb" fabric (fig. 6.1, sequence 1). The breccia fabric is defined by polygonal cracks, which separate isolated blocks of mudstone. The mudstone blocks show no evidence of displacement or rotation where they are internally thin-bedded. The "crumb" fabric is composed of millimeter-scale mud clumps and abundant laminoid and ovoid, cement-filled vesicles, which also commonly have thin clay linings. The cracks in the "crumb" fabric are typically narrower and form smaller polygonal patterns than those in the breccia fabric.

Mudcracked massive mudstone typically overlies laminated to thin-bedded, lacustrine mudstone with large polygonal cracks and rare reptile footprints. It is also associated with centimeter-scale siltstone beds, which form concave-upward polygonal curls, and with thin, scour-based, muddy sandstone lenses. Pseudomorphs after a bladed evaporite mineral, possibly gypsum, have been found in a few occurrences of brecciated mudstone (fig. 6.1, sequence 4).

Mudcracked massive mudstone with the breccia fabric is interpreted as lacustrine beds disrupted by desiccation cracks formed by repeated wetting and drying during long periods of nondeposition. The massive mudstone with the "crumb" fabric is believed to be the basin-floor deposit of an aggrading playa mudflat (Smoot and Katz, 1982; Katz, 1983).

Burrowed massive mudstone is dominated by numerous tubes 0.5–1.0 cm in diameter, which are typically randomly oriented, have constant diameters, and are filled with sandstone or mudstone. These tubes are interpreted as burrows. The most distinctive types of tube are *Scoyenia* (Bain and Harvey, 1977), which are characterized by "spreiten" (convex laminae in the burrows, defined by small grain-size changes) and textured outer walls, but other tubes with simple fillings also occur and may be the dominant variety. There is a common minor component of small, often less than 1 mm in diameter, flattened tubes, which bifurcate and taper, associated with this massive mudstone type. These tubes may be lined with tangentially oriented clays, which commonly define the entire tube shape. These branching tubes are interpreted as the casts and molds of rootlets. Large polygonal cracks, 10–20 cm deep, may also be present in these mudstones.

Burrowed massive mudstone is associated with two types of sequences. The most common association is with fine-grained, micaceous sandstone showing climbing-ripple cross-lamination and soft-sediment deformation (load casts, "pseudonodules," and oversteepened ripple cross-laminae) and with laminated shales, which commonly contain abundant conchostracans, ostracodes, and other aquatic fossils (fig. 6.1, sequence 5). Reptile footprints often occur on the bedding planes that are not obscured by burrows, and disarticulated fish fossils and reptile bones occur rarely. The other association is with thick packages of microlaminated mudstone, which grade into wispy thin beds and finally into massive mudstone by a gradual loss of layer definition (fig. 6.1, sequences 6 and 7), apparently owing to bioturbation (Olsen, 1984, p. 521–527). The burrows in the massive mudstones in these sequences lack "spreiten" and are generally smaller than typical *Scoyenia*.

The burrowed massive mudstone probably represents several different depositional environments, including shallow margins of lakes, delta plains, and fluvial floodplain-overbank settings. The most likely burrowers include worms, crayfish-like crustaceans (Olsen, 1980), and insects (beetles?).

Root-disrupted massive mudstone is characterized by abundant downward bifurcating and tapering tubes, ranging in diameter from less than 1 mm to several centimeters. These characteristics are believed to be diagnostic of root casts and molds. The tubes are predominantly oriented perpendicular to bedding, but some are parallel. Large tubes are filled with sandstone and mudstone, whereas smaller tubes are generally lined with clays, which are tangentially oriented, and filled with carbonate mineral cements. Small, spherical nodules of micritic calcite and dolomite are common and are concentrated in the larger tubes or scattered in the surrounding matrix. These nodules are interpreted as caliche concretions. *Scoyenia* burrows and polygonal cracks (5–10 cm deep) may also be present. Remnant patches of laminated mudstone or ripple cross-laminated sandstone are common.

Root-disrupted massive mudstones have two associations: (1) overlying, and laterally equivalent to, burrowed massive mudstone (fig. 6.1, sequences 5 and 6); the contacts are gradational, resulting from an increase of root and carbonate nodule abundances; and

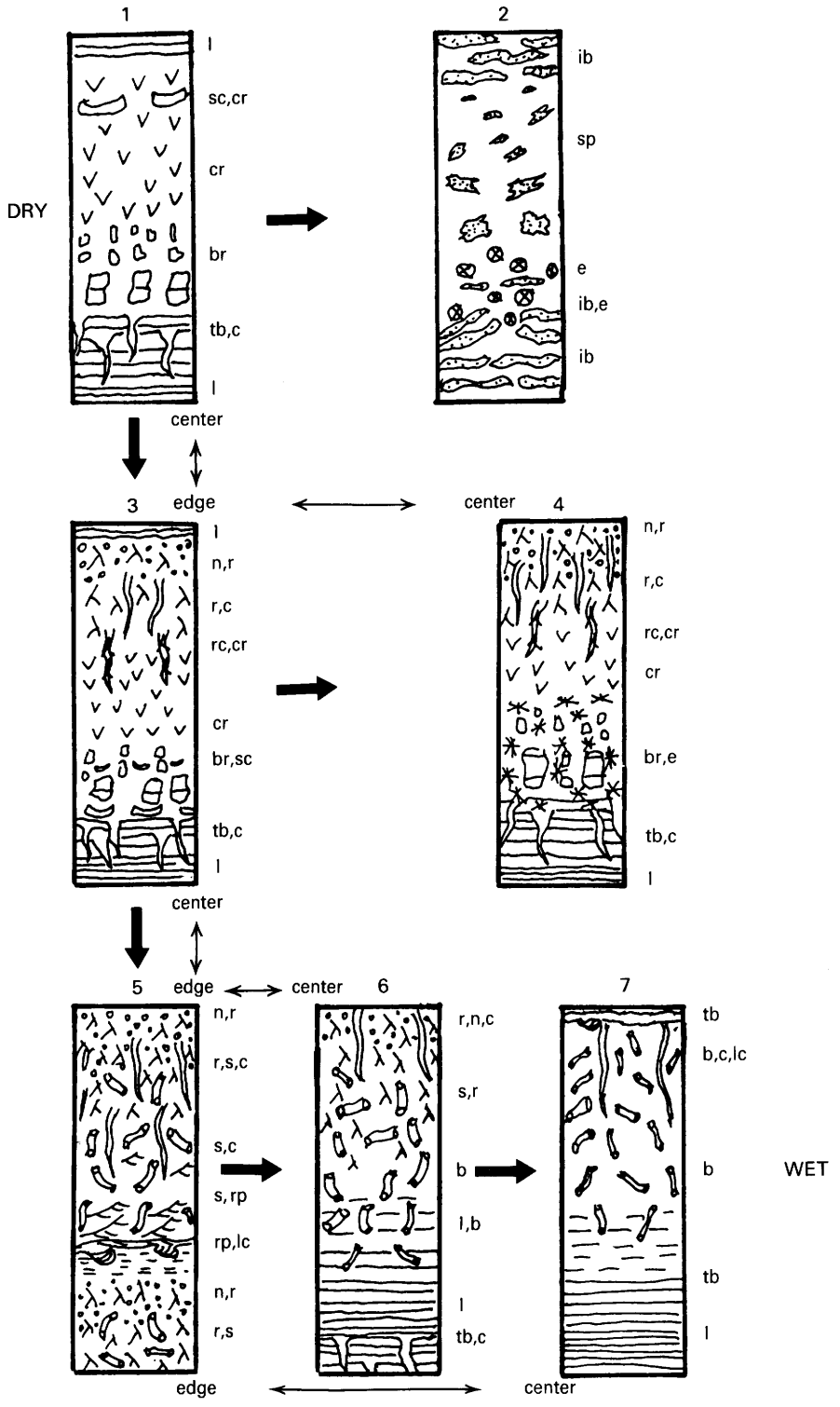

FIGURE 6.1.—Schematic drawing of sedimentary sequences containing massive mudstones. Thick arrows point to relatively wetter depositional environments. The "driest" sequence is at the upper left and the "wettest" is at the lower right. Thinner arrows show possible geographic relationships between sequences within a basin. Thicknesses range from 1–3 m in sequence 2 to as much as 20 m for sequence 5. Symbols: b—burrows, br—breccia fabric, c—cracks, cr—crumb fabric, e—evaporite molds, ib—irregular bedding, l—flat lamination, lc—load casts, n—carbonate nodules, r—root structures, rc—roots within cracks, rp—ripple cross-laminae, s—*Scoyenia*, sc—siltstone curls, sp—sand-patch fabric, tb—thin bedding.

(2) gradationally overlying mudcracked massive mudstone (fig. 6.1, sequences 3 and 4), as shown by tubes that first preferentially follow crack polygons then dominate the mudstone fabric, commonly with an increase in carbonate nodules. In the Newark basin, a number of articulated reptile skeletons were found in massive mudstones that are probably of this type.

The root-disrupted mudstones are interpreted as deposits formed on vegetated floodplains of a basin floor, river overbanks, or the margins of lakes, on which a soil containing caliche was developed.

Sand-patch massive mudstone contains small (1–5 cm long), irregular-shaped pods of sandstone and siltstone with the following diagnostic characteristics: angular margins; internal jagged, mud-filled cracks; internal zones of different grain sizes; and cuspate contacts with the surrounding mudstone. The sand pods may have internal cross-laminae, which are randomly oriented with respect to cross-laminae in adjacent pods.

Sand-patch massive mudstone is associated with eolian sandstone lenses and cross-strata and with mudstone containing evaporite molds and irregular thin beds and lenses of sandstone (fig. 6.1, sequence 2). Hubert and Hyde (1982) interpreted the sand patches as eolian "adhesion ripples." However, the patches strongly resemble fabrics produced by accretional saline mudflats where the sand pods are wind-blown and stream-deposited material trapped in surface irregularities of a subsequently dissolved efflorescent salt crust (Smoot and Castens-Seidel, 1982). No fossils have been found in association with this fabric.

DISCUSSION

Mudcracked massive mudstone and sand-patch massive mudstone are interpreted as deposits formed under relatively arid basin-floor conditions. The "crumb" fabric in mudcracked massive mudstone is believed to represent a playa floor that is inundated by flood water for a few days then totally dry for several years. The breccia fabric probably indicates slightly wetter conditions of formation, since the polygonal cracks in it are wider and deeper than those in the "crumb" fabric. Sand-patch massive mudstones required an evaporitic setting but also needed a shallow, persistent, saline ground-water table to precipitate the salts. This suggests a slightly wetter depositional setting for sand-patch massive mudstone than for mudcracked massive mudstone, or at least for mudstone with the "crumb" fabric.

The burrowed and root-disrupted massive mudstones are interpreted as representing wetter depositional conditions than the mudcracked and sand-patch massive mudstones. The organisms responsible for the burrows in the burrowed massive mudstone probably required water-saturated sediments. The association of this massive mudstone type with low-energy fluvial deposits, soft-sediment deformation structures, lacustrine deposits, and deep, widely spaced mudcracks supports this interpretation. If the abundant tubes in the root-disrupted massive mudstone are properly identified as roots, the environments of their formation must have had enough water to support a vegetative cover. It is difficult to ascertain how much vegetation was growing, or if the growth occurred throughout the accumulation of the massive mudstone, or if the roots are superimposed over another depositional fabric. The common presence of carbonate nodules, which are interpreted as caliche nodules, suggests a dry setting (Gile and others, 1966), at least intermittently. A dry setting is also suggested by the transition upward from mudcracked massive mudstone, at places including evaporite mineral molds (fig. 6.1, sequence 4), to root-disrupted massive mudstone. For these reasons the root-disrupted massive mudstones are believed to indicate generally drier depositional conditions than the burrowed massive mudstones.

The sedimentary sequences containing massive mudstones shown in figure 6.1 are organized from those representing the driest conditions at the top left to those indicating the wettest at the bottom right. A thick accumulation of the "crumb" fabric, as in sequence 1, is believed to indicate drier conditions than the accumulation of the sand-patch fabric in sequence 2. Sequence 1 may represent a greater variation in depositional aridity, however, since the mudcracked massive mudstone grades up from lake deposits, while the sand-patch massive mudstone overlies subaerial deposits. The root-disrupted massive mudstones in sequences 3 and 4 indicate wetter conditions than for sequences 1 and 2. Both overlie mudcracked massive mudstone, suggesting a decrease of aridity in the younger portions. Sequence 4 is interpreted as indicating a wetter depositional setting than sequence 3 because the evaporite crystals in the breccia fabric require a near-surface brine table to precipitate. Sequences 5, 6, and 7 are interpreted as representing progressively wetter settings of formation. Sequence 5 contains fluvial sandstones and common mudcracks and root structures, sequence 6 is mostly lacustrine with mudcracked, root-disrupted massive mudstone at the top, and sequence 7 has only burrowed massive mudstone overlying the lake deposits.

Sand-patch massive mudstone has only been found in the Fundy basin, and mudcracked massive mudstone is apparently more common in the Hartford, Newark, Culpeper, and Danville basins than in the Richmond, Dan River, Durham, Sanford, or Wadesboro basins. In the latter five basins, the burrowed or root-disrupted massive mudstones are apparently the dominant varieties. This general change from "drier" massive mudstone textures in the northern basins to "wetter" massive mudstones in the southern basins supports the hypothesis that the sediments preserved in the exposed Newark basins reflect increasing aridity towards the north, due to the change in paleolatitude (Hubert and others, 1978). One problem with this interpretation is that the burrowed and root-disrupted massive mudstones are present in all of the basins, including the Fundy basin. The distribution of the massive mudstone types may also be influenced or controlled by (1) local environments, such as the margins of shallow lakes on playa floors or desiccated ponds on fluvial flood plains, (2) local climates, such as orographic deserts in a temperate climate belt, and (3) changes in climate over time, such as a wetter Carnian and a drier Norian. Some of the possible coeval lateral relationships of massive mudstone sequences within a basin are shown in figure 6.1. The stratigraphic correlations of Olsen (1984, p. 85, 115–119) in the Newark basin established the lateral equivalence of sequence 3 (center) to sequence 5 (edge), of 4 (center) to 3 (edge), and of 7 (center) to 5 (edge). The other lateral relationships shown in figure 6.1 are suggested by less well constrained correlations in other basins. A change in the depositional conditions from drier to wetter settings within the basins of the Newark Supergroup, as envisioned for some of the massive mudstone sequences, has been suggested by others on the basis of the nature of sedimentary cycles (for instance, Van Houten, 1964; Olsen, 1984) and on fossil pollen and spore assemblages (Cornet, 1977, p. 61–71).

The climatic implications of the massive mudstone textures suggest possible application as constraints for stratigraphic reconstructions. Mudstone cycles dominated by "dry" characteristics (sand-patch or mudcracked massive mudstone textures) may be laterally correlated to sandstones and conglomerates also reflecting dry conditions (such as debris flows and sheet floods); mudstone cycles dominated by "wet" characteristics (burrowed and root-disrupted massive mudstone textures) may be similarly correlated to the sandstones and conglomerates reflecting deposition under sustained higher discharges (such as braided or meandering river deposits with large-scale cross-bedding). More information is needed concerning the lateral variability of massive mudstone fabrics. We also need to determine if subtle differences occur within a specific type of massive mudstone; if so, a more complex breakdown of types or stronger affinities between them may be necessary. Even if massive mudstones ultimately prove to have limited climatic or stratigraphic utility, our understanding of the depositional environments of the Newark Supergroup can be improved by recognition of the differences within massive mudstones.

REFERENCES

Bain, G.L., and Harvey, B.W., 1977, Field guide to the geology of the Durham Triassic basin — Carolina Geological Society, 40th Anniversary Meeting, Raleigh: North Carolina Department of Natural Resources and Community Development, Geological Survey Section, 83 p.

Cornet, Bruce, 1977, The palynostratigraphy and age of the Newark Supergroup: University Park, Pennsylvania State University, unpub. Ph.D. thesis, 506 p.

Gile, L.H., Peterson, F.F., and Grossman, R.B., 1966, Morphological and genetic sequences of carbonate accumulation in desert soils: Soil Science, v. 101, p. 347–360.

Hubert, J.F., and Hyde, M.G., 1982, Sheetflow deposits of graded beds and mudstones on an alluvial sandflat-playa system: Upper Triassic Blomidon redbeds, St. Mary's Bay, Nova Scotia: Sedimentology, v. 29, p. 457–474.

Hubert, J.F., Reed, A.A., Dowdall, W.L., and Gilchrist, J.M., 1978, Guide to the redbeds of central Connecticut: State Geologic and Natural History Survey of Connecticut, Guidebook 4, 129 p.

Katz, S.B., 1983, Sedimentary features and soil-like fabrics in chemical cycles of the Lockatong Formation, Newark Supergroup (Late Triassic), New Jersey and Pennsylvania: Stony Brook, State University of New York at Stony Brook, unpub. M.S. thesis, 134 p.

Olsen, P.E., 1980, Fossil great lakes of the Newark Supergroup in New Jersey, *in* Manspeizer, Warren, ed., Field studies in New Jersey geology and guide to field trips, 52nd Annual Meeting of New York State Geological Association: Newark, N.J., Rutgers University, p. 352–398.

———1984, Comparative paleolimnology of the Newark Supergroup — A study of ecosystem evolution: New Haven, Conn., Yale University, unpub. Ph.D. thesis, 726 p.

Smoot, J.P., and Castens-Seidel, Barbara, 1982, Sedimentary fabrics produced in playa sediments by efflorescent salt crusts: an explanation for "adhesion ripples" [abs.], *in* Abstracts of Papers, 11th International Congress on Sedimentology, McMaster University, Hamilton, Ontario: International Association of Sedimentologists, p. 10.

Smoot, J.P., and Katz, S.B., 1982, Comparison of modern playa mudflat fabrics to cycles in the Triassic Lockatong Formation of New Jersey [abs.]: Geological Society of America Abstracts with Program, v. 14, no. 1–2, p. 83.

Van Houten, F.B., 1964, Cyclic lacustrine sedimentation, Upper Triassic Lockatong Formation, central New Jersey and adjacent Pennsylvania: Kansas Geological Survey Bulletin 169, p. 497–531.

7. CONSTRAINTS ON THE FORMATION OF LACUSTRINE MICROLAMINATED SEDIMENTS

P.E. Olsen[5]

Microlaminated sediments have very thin (less than 1 mm), usually laterally continuous laminae. Many ancient examples, including those of the lower Mesozoic Newark Supergroup and the Eocene Green River Formation, are relatively rich in organic matter (total organic carbon greater than 1 weight percent) and contain complete fossil fish and other delicate organisms.

The main controls on the distribution of microlaminated sediments are bottom energy conditions and bioturbation. Microlaminated sediments can retain their structure in high-energy conditions only if they are bound by microbial communities. The microbial communities can be dominated by blue-green algae or by sulfur-oxidizing bacteria such as *Beggiatoa*. Such microbial mats exist today only where grazing organisms are limited by such factors as high salinity or toxic waters. Modern algal mats typically form in very shallow water where they are commonly desiccated. Fish have not been found preserved under these conditions. However, fish can be preserved on deeper water lake bottoms, where sulfur-oxidizing microbial mats flourish in microenvironments devoid of bottom feeders.

Microlaminated sediments not bound by microbial mats can form only in water where there is no bottom turbulence (that is, below wave base). The depth at which microlaminated sediments can form is controlled by the surface area of a lake and the modal wind velocity (Manspeizer and Olsen, 1981; Olsen, 1984). A lake must be relatively deep compared to its surface area for this type of microlaminated sediment to form. In strongly density-stratified lakes, wave propagation can be impeded, causing wave base to be shallower than in unstratified lakes.

The third factor controlling the distribution of microlaminated units is protection from bioturbation. Bioturbators today are limited by primary productivity levels in the lakes. Microlaminated sediments form today at two ends of the productivity spectrum (fig. 7.1). Very low productivity excludes macroscopic bioturbators, as in Lake Brienz, Switzerland; sediments in such

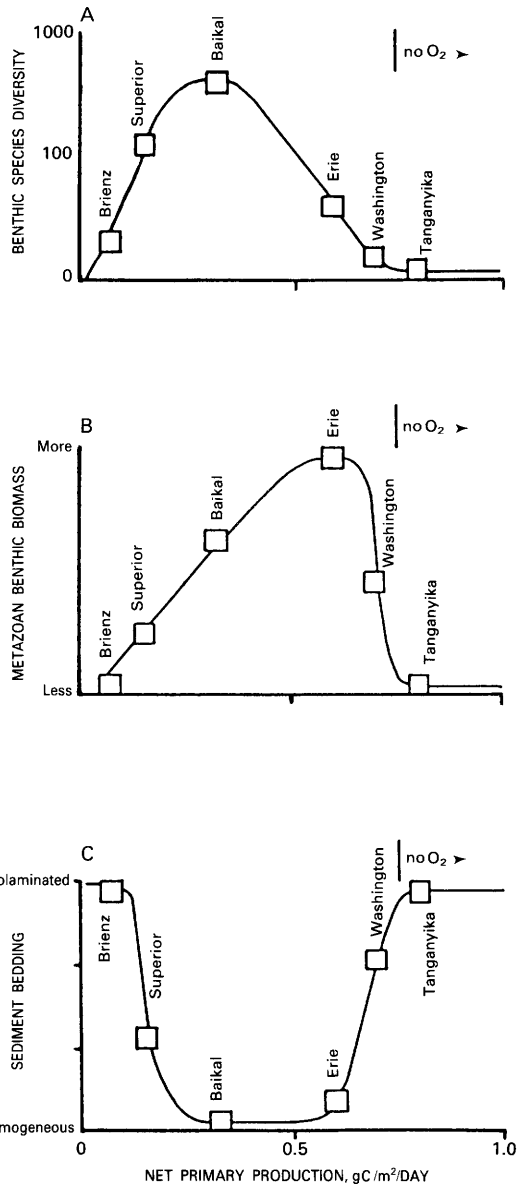

FIGURE 7.1.—Theoretical relationships between primary production and properties of the benthos of lakes. If benthic bioturbators needed higher oxygen levels in the past than they need now to survive, these curves would all be narrowed, shifted to the left, and probably made more symmetrical. (A) Relationship between primary production and benthic species richness in modern deep lakes. (B) Relationship between primary production and metazoan benthic biomass in modern lakes. (C) Relationship between primary production and sediment lamination development in modern lakes.

[5]P.E. Olsen, Lamont-Doherty Geological Observatory of Columbia University, Palisades, N.Y. 10964.

lakes contain little organic carbon. In other lakes, there is so much primary production that oxygen taken up by consumers exceeds oxygen supply, as in Lake Tanganyika. In a given lake, benthic species diversity first increases with increased productivity, then drops as the tolerances of bioturbators to low oxygen are reached, ultimately dropping to zero. Metazoan benthic biomass, and hence the degree of bioturbation, also first increases with productivity and lowered oxygen levels, continues to rise or levels off where benthic diversity is very low, and then decreases dramatically as oxygen levels drop off to zero. The oxygen tolerances of bioturbators limit them to the region between the two productivity extremes (fig. 7.1). Therefore, the distribution of non-microbial-mat microlaminated sediments is, in part, limited by the tolerances of the range of bioturbators available to colonize the lakes.

The history of major groups of bioturbating organisms is thus critical to the understanding of the paleoecological meaning of microlaminated beds. In the early Precambrian, there was no bioturbation and all sediments deposited below wave base could be microlaminated. Sometime between then and now, the modern groups of bioturbators became important. Tubificid worms, ostracodes, and fly larvae are the most important modern lacustrine bioturbators; their oldest known occurrences are unknown, Ordovician, and Late Triassic (late Carnian), respectively. I hypothesize that, through the Phanerozoic, sediments of increasingly lower oxygen levels were colonized by bioturbators. Examination of broad suites of sediments of different ages supports this hypothesis: as the sediments get younger, bioturbation becomes more important (and water turbulence proportionally less important) in limiting the distribution of microlaminated sediments. Therefore, simply extrapolating from modern conditions that limit bioturbation may lead to erroneous estimates of the frequency of ancient lakes with anoxic bottom waters.

Similarly, the distribution of modern microbial mats depends both on the range of grazers available and on their tolerances to high salinity and low oxygen or toxic water. In the Precambrian, we can imagine a continuum from shallow-water, blue-green microbial mats, formed under high-energy conditions, to deeper water microbial mats, and, ultimately, to unbound microlaminated sediments below wave base. The range of conditions under which microbial mats were formed may have been much wider then, simply because of differences in predation pressure.

REFERENCES

Manspeizer, Warren, and Olsen, P.E., 1981, Rift basins of the passive margin; tectonics, organic-rich lacustrine sediments, basin analysis, *in* Hobbs, G.W., III, ed., Field guide to the geology of the Paleozoic, Mesozoic, and Tertiary rocks of New Jersey and the central Hudson Valley, New York: Petroleum Exploration Society of New York, p. 25–105.

Olsen, P.E., 1984, Periodicity of lake-level cycles in the Late Triassic Lockatong Formation of the Newark Basin (Newark Supergroup, New Jersey and Pennsylvania), *in* Berger, Andre, Imbrie, John, Hays, James, Kukla, George, and Saltzman, Barry, eds., Milankovitch and climate, NATO Symposium: D. Reidel, Dordrecht, Part 1, p. 129–146.

8. FAULT REACTIVATION MODELS FOR ORIGIN OF THE NEWARK BASIN AND STUDIES RELATED TO EASTERN U.S. SEISMICITY

Nicholas M. Ratcliffe and William C. Burton

INTRODUCTION

Extensive core drilling, geologic mapping, and VIBROSEIS[6] reflection profiling (conducted by John Costain of Virginia Polytechnic Institute and State University and the U.S. Geological Survey) of the Newark basin and of contiguous Middle Proterozoic and Paleozoic rocks of the footwall blocks show a strong correspondence between the dip of Mesozoic border faults and the dip of mylonite zones of Paleozoic age in their foot walls. This correspondence is greatest at the preserved basin margins where Mesozoic faults such as the Ramapo, Flemington, and other unnamed border faults coincide with Paleozoic thrust faults that exhibit abundant evidence of Mesozoic reactivation. The overall structure of the basin appears to be closely controlled by reactivation of Paleozoic ramps and thrusts. The present location of the Newark basin and structural style within the Newark basin are directly relatable to position over the ancestral ramp-thrust complex. Southeastward extension was dominant in the early Mesozoic, and the resolution of this extension, acting on the preexisting curvilinear concave-upward thrust-fault and convex-upwards ramp-fault geometry, may explain many of the variations in structural style that occur north to south along the trend of the basin.

The character of internal deformation within the basin, fold orientations, fault attitudes, and movement senses all appear to be directly explained by the geometry of the reactivated structures rather than by changes in the stress field that are imperfectly known at present. Most importantly, acceptance of the fault reactivation model means that the interpretation of specific tectonic features, such as dike orientations, fold axes, and slip directions on faults and stress orientations, inferred from these features may be locally controlled by the configuration of the master faults in the basement rocks.

BACKGROUND AND SCOPE OF WORK

Study of the Mesozoic fault systems in New York and New Jersey and their relationship to ancestral faults and to current seismicity has been conducted under funding by the Earthquake and Reactor Hazards Programs of the U.S. Geological Survey (USGS). The aim of these investigations is to determine what association exists between the instrumentally located seismicity and geologic structure in the Ramapo seismic zone. Specifically these studies are concerned with the extent to which current seismicity can be causally linked to the reactivation of Mesozoic faults such as the Ramapo. In the past 2 years approximately 180 km of 12- and 24-fold VIBROSEIS reflection data have been collected across the northern end of the Newark basin in a cooperative USGS and Virginia Polytechnic Institute and State University (VPISU) program funded by the Nuclear Regulatory Commission (fig. 8.1). In addition one proprietary industry (VIBROSEIS) line has been acquired. The approximate position of USGS seismic lines is indicated on figure 8.1. These lines are in various stages of processing and are not available at present. We are attempting to complete detailed fault mapping and coring along each of the VIBROSEIS lines, looking especially at areas critical to the interpretation of the profiles. Results of coring of the border faults at localities identified in figure 8.1 are presented in table 8.1.

The ideas presented here are the result of about 7 years of detailed geologic mapping, coring, and mineralogic studies of fault-zone materials, both in the Mesozoic rocks of the Newark basin and in the Proterozoic and Paleozoic rocks outside the basin. Our data have been made available to members of the early Mesozoic basin project, and we welcome the extensive cooperation this project has generated.

OBLIQUE-SLIP MOVEMENT ON MESOZOIC BORDER FAULTS: HOW IMPORTANT?

The data we have collected indicate clearly that few of the Mesozoic faults in figure 8.1 moved in a pure dip-slip mode. Instead evidence for right-oblique normal faulting is widespread. The combination of low rakes of slickenlines and widespread compressional

[6]The use of trade names is for identification purposes and does not constitute endorsement by the U.S. Geological Survey.

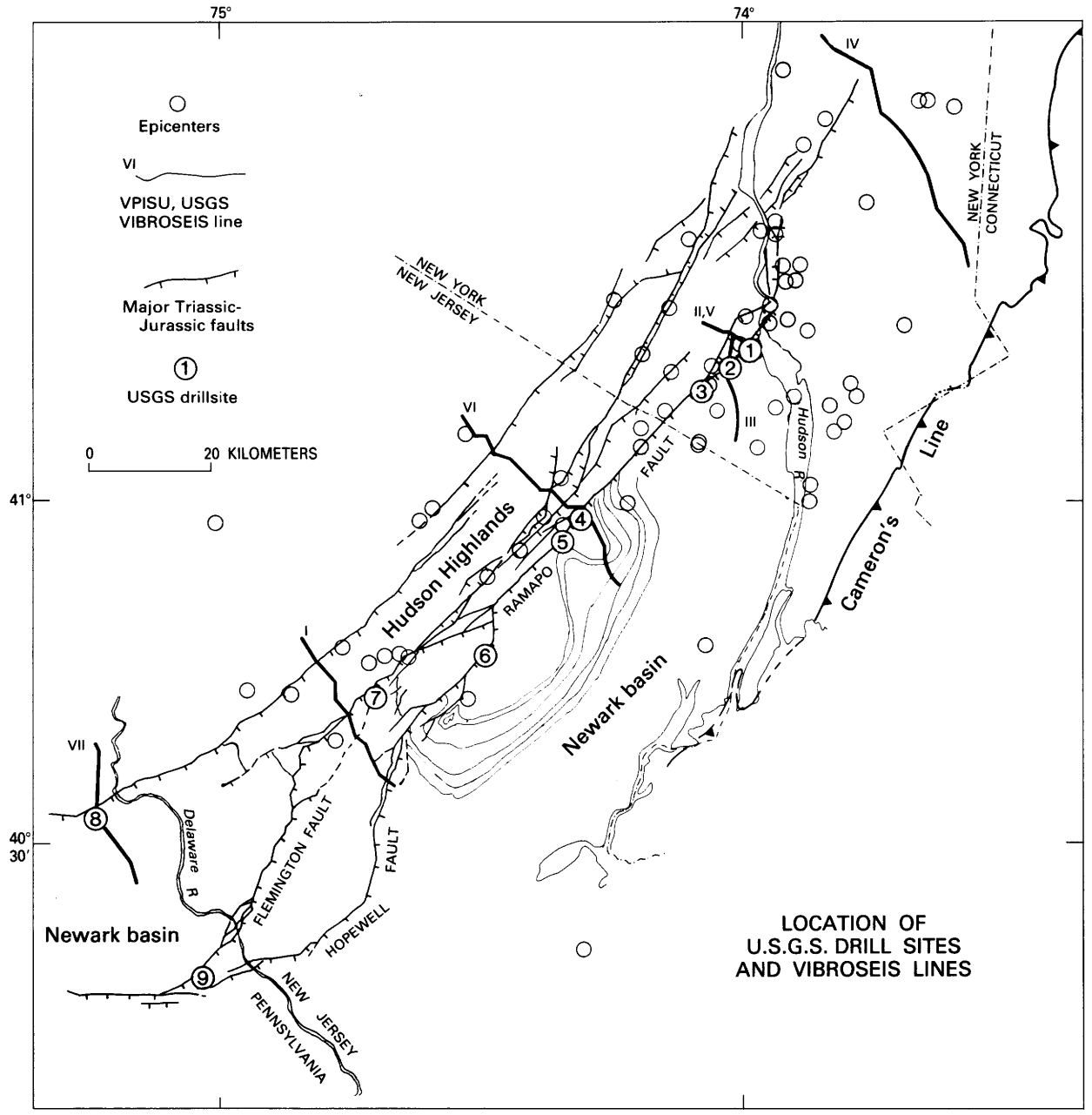

FIGURE 8.1.—Generalized fault map of the Newark basin showing location of the Ramapo fault, Hopewell fault, Flemington fault, and other Mesozoic border faults (hachured lines) in relationship to epicenters and USGS–VPISU VIBROSEIS profiles. Cameron's Line (saw-toothed line) is the trace of the Ordovician suture zone. Numbers refer to drill sites identified in table 8.1. Epicenters from Aggarwal and Sykes (1978).

features (folds) in the Newark basin lead to the proposition that Mesozoic rifting involved a significant component of right-lateral strike-slip faulting. This idea was presented by Manspeizer (1980) and by Ratcliffe (1980). At the 1982 early Mesozoic basin workshop, Ratcliffe presented a review of Manspeizer's ideas regarding a strike-slip origin of the basin as shown by the model of Aydin and Nur (1982) (fig. 8.2).

TABLE 8.1.—*Results of coring of Newark basin border faults at localities identified in figure 8.1*
[More than one hole was drilled at most sites; depths given are depths at which fault was encountered]

No.	Drill site	Feature drilled	Depth (feet)	Rocks of hanging wall	Rocks of footwall	Dip of fault	Comments
1	Cemetery	Thiells fault	46 153	Triassic fanglomerate.	Middle Proterozoic.....	70°	Narrow gouge zone, steep fractures throughout, unfractured to end; on lines 2, 5.
2	Letchworth.....	Thiells fault	1496	Triassic siltstone and fanglomerate.	Not penetrated	>45°	Located on line 3.
3	Sky Meadow ...	Ramapo fault ...	269 463	Jurassic diabase.	Middle Proterozoic.....	55°	Complete recovery of fault contacts.
4	Riverdale	Ramapo fault ...	152 263 337	Jurassic fanglomerate.	Middle Proterozoic.....	50°	Complete recovery of fault contact; on line 6.
5	N.J. Dept. of Transportation.	Ramapo fault ...	127 224 230 200	Jurassic diabase fanglomerate.	Middle Proterozoic.....	50°	Complete recovery of fault contacts; near line 6.
6	Mt. Kemble	Ramapo fault ...	55 172 83 106	Hook Mt. basalt.	Middle Proterozoic.....	44°	Poor recovery of fault zone.
7	Oldwick	Flemington fault.	110 174	Triassic fanglomerate.	Middle Proterozoic.....	34°	Good recovery of fault zone materials; on line 1.
8	Riegelsville.....	Triassic border fault.	311 117	Triassic siltstone.	Middle Proterozoic and Cambrian dolostone.	25-30°	Good recovery of faults; on line 7.
9	Buckingham....	Furlong fault ...	— —	Triassic mudstone.	Cambrian dolostone, diabase.	≅45–50°	Good recovery of faults; drilling in progress.

In this model the basin floor is differentially downfaulted or remains relatively high depending upon the stepping sense of the interconnected faults. Steep faults with dips greater than 55° are the general rule, and compressional features (thrust faults and folds) are related to the buttressing effect of horst blocks. The data on slip direction and attitude of the faults known from the central and northern part of the Newark basin in 1982 supported elements of this model. Assuming a right-slip model, the movement sense and dip of the opposed border faults of the Newark and Hartford basins could also be explained (fig. 8.3).

Since 1982 we have extended our mapping and coring of the border faults south into New Jersey (Ratcliffe and Burton, 1984). These data, in conjunction with the VIBROSEIS results, confirm a shallowing of the border fault southward. The Hopewell and Flemington faults and the border faults in eastern Pennsylvania appear to dip about 30° SE., on the basis of drill data and analysis of water-well data.

The overall deformation plan for rocks of the Mesozoic Newark basin and for faults related to basin formation is consistent from the northern end of the basin south to the Delaware River. This plan is shown in figure 8.4. Bulk extension was in the southeast quadrant, and the dominant sense of strike-slip faulting, fold orientations, and minor thrust faults indicates that the intermediate principal stress, σ_2, was in the northeast quadrant.

Our new analysis suggests that the strike-slip pull-apart model does not fully apply. In this paper we propose that *simple extensional reactivation of a complex system of curvilinear thrust-ramp structures can explain both the fault geometry and the deformational structures found in the basin. The new model explains in a very simple way how the attributes of a strike-slip pull-apart basin are developed without calling upon a model such as is shown in figure 8.2.*

We hasten to point out that the extent of fault reactivation in the northern Newark basin is unknown, although this is the most thoroughly studied Eastern U.S. early Mesozoic basin from that standpoint. The ideas presented in this paper are not intended to be a complete explanation of the origin of the Newark basin

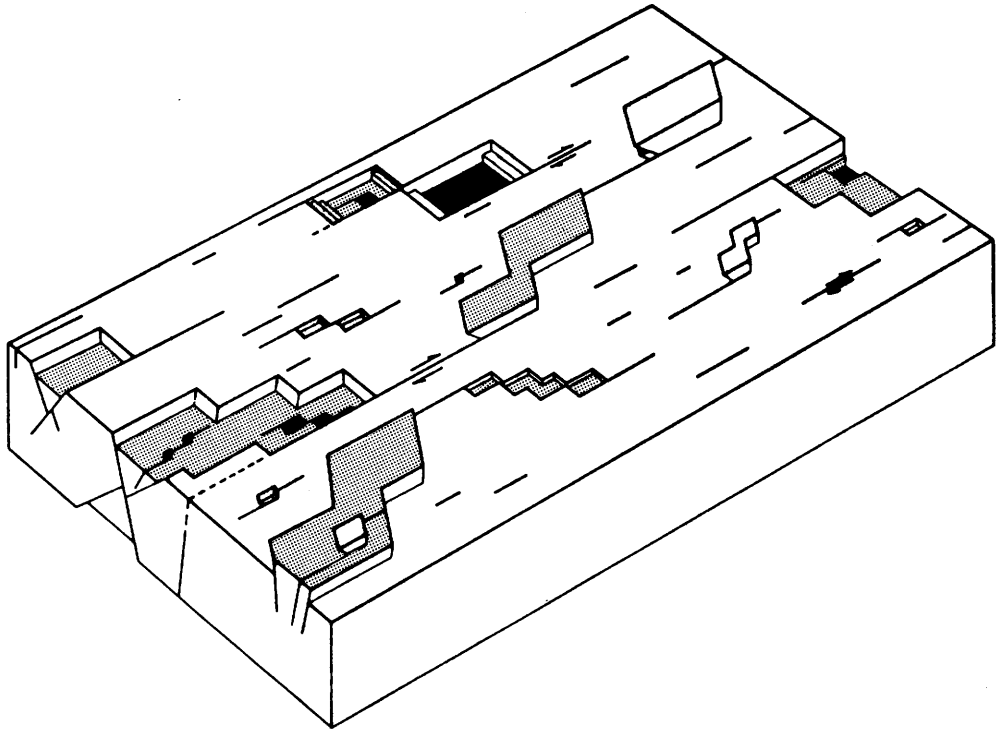

FIGURE 8.2.—A hypothetical dimensionless block diagram illustrating a right-lateral strike-slip regime and the evolution of right-slip pull-apart basins. Darker areas represent basins; light stippled areas represent uplifted areas (horsts). Left-stepping faults induce uplift and compression; right-stepping faults induce basins. Diagram reproduced from Aydin and Nur (1982, Tectonics, v. 1, no. 1, fig. 10; reprinted with permission of editors). In this model the basin floor is irregular, and the basin-forming faults or growth faults are hidden beneath transgressing sedimentary cover. Although form of the faults and senses of movement agree closely with those determined from the Ramapo and other faults of the Newark basin and the border faults of the Hartford basin, this model cannot entirely explain the extensional history of the Newark basin.

but are intended to direct attention to some of the important implications of the fault reactivation model.

GEOMETRY OF THE BORDER FAULTS AND ASSOCIATED MYLONITES

Core drilling and field studies along the length of the Ramapo and other border faults, from the northern end of the Newark basin in Rockland County, N.Y., to the Delaware River in Pennsylvania, reveal a systematic decrease in the dip of the border faults from northeast to southwest. In Rockland County at the north end of the basin, the Ramapo fault dips 70° SE. (loc. 1, fig. 8.1); 55° SE. at Suffern, N.Y. (loc. 3); 48° SE. at Riverdale, N.J. (loc. 4); 40° SE. at Bernardsville, N.J. (loc. 6); 35° SE. at Oldwick, N.J. (loc. 7); and 30° SE. near Riegelsville, Pa. (loc. 8). This decrease in dip is closely paralleled by a decreasing dip of Paleozoic thrust faults southward (fig. 8.6). VIBROSEIS profiles in New York and New Jersey also confirm this decrease in dip (Ratcliffe and Costain, 1985 and unpub. data).

This variation in dip of Paleozoic mylonite zones and thrust faults also coincides with a westward transgression of the Newark basin strata across the ancestral ramp-thrust system, from a position in the north over steeply dipping internal ramp zones to a position in the south over relatively more foreland types of thrusts in Pennsylvania. The widest part of the Newark basin in Pennsylvania overlaps the area of the most shallowly dipping reactivated thrusts, and the termination of the basin in the north is situated over the most steeply dipping thrust faults.

MOVEMENT SENSE AND DEFORMATION PLAN IN TRIASSIC-JURASSIC STRATA

Major Mesozoic faults such as the Ramapo, Hopewell, Flemington, and other unnamed border faults have a consistent plan of deformation that indicates right-oblique normal faulting on southeast- and

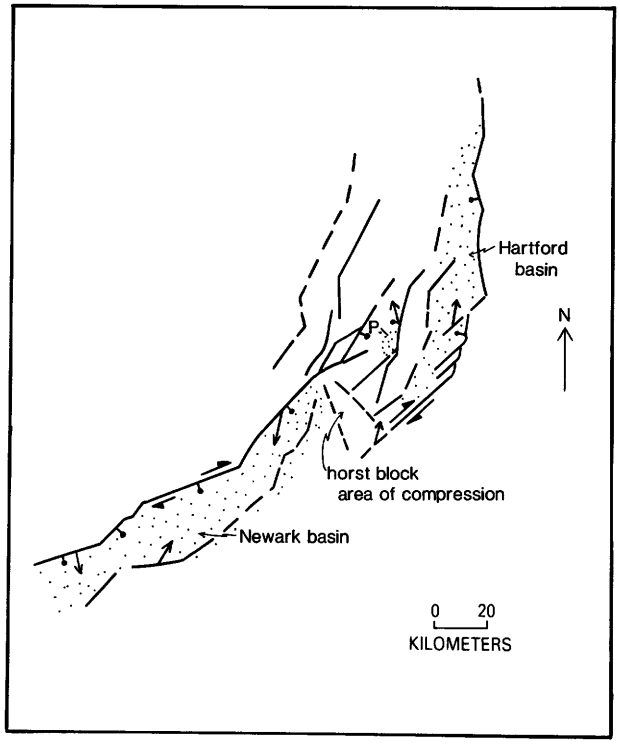

FIGURE 8.3.—A schematic diagram showing the Newark and Hartford basins (stippled) as separate non-coalesced, right-slip, pull-apart basins. This interpretation is consistent with the observed slip directions on Newark and Hartford border faults, namely that northeast-striking, southeast-dipping faults show right-oblique normal movement, and northeast-striking, northwest-dipping faults show left-oblique normal movement. P = Pomperaug basin. Scale approximate.

east-dipping surfaces. Slickenlines, calcite fiber growth in extension fractures, drag folds, and fabric of exposed or cored fault zones document a consistent deformation plan with extension in the southeast quadrant and compression in the northeast quadrant (fig. 8.4).

Fold sets in the basin vary in direction, amplitude, and intensity with position in the basin and with proximity to the border or other major faults. Major left-stepping splays from the border faults, such as the Flemington and Hopewell faults, have high-amplitude, short-wavelength, northwest-trending folds developed in their hanging walls adjacent to the faults. Near major faults these northwest transverse folds interfere with northeast-trending drag synclines to produce a pattern of tight elongated basins separated by areas of gentle warping. Away from the faults these interference folds pass into broadly warped homoclines.

The fold systems in the basin appear to be directly related to syn-faulting deformation in which both compression and extension are important. In many ways the patterns of faults and folds in the Newark basin resemble those found in right-slip, pull-apart basins formed in a strike-slip regime. However, the widespread development of antithetic normal faults and near-vertical extension fractures that strike east-northeast points to dominant southeast extension throughout the northern end of the basin. Pure strike-slip displacement of significant magnitude appears to be absent, as are the master en-echelon strike-slip faults called for in the Aydin and Nur (1982) model.

FAULT REACTIVATION MODELS FOR ORIGIN OF EASTERN NORTH AMERICAN HALF-GRABENS OF MESOZOIC AGE

The asymmetry of many Appalachian Mesozoic basins is well known and differs markedly from more classical symmetrical rift basins such as the Rhine, Red Sea, and Ethiopian. The asymmetry, width, and thickness of sediments within some eastern North American Mesozoic half-grabens may be related to the position and attitude of fault systems in the basement rocks. In this paper west-dipping asymmetric basins like the Newark are related to reactivation of either (*A*) concave listric foreland thrusts or (*B*) convex ramp systems (fig. 8.5). When reactivation by extension along concave thrusts occurs, broad shallow sedimentary basins with characteristic listric normal faulting develop, leading to a west-dipping homoclinal section. When reactivation of a convex-upward ramp system occurs, a relatively narrow and rapidly subsiding fold basin with less asymmetry is developed. Strong counterclockwise rotation of strata is expected east of the inflection point between concave and convex portions of the reactivated thrust system.

Reactivation of an entire thrust-ramp configuration (fig. 8.5*C*), therefore, leads to a characteristic basin form with a shallow, wide western flange developed over the ancestral shallow thrusts and a deepening axial portion with an anticlinal bulge of basement roughly coinciding with the inflection point between thrusts and ramps.

The variation in structural style and cross-sectional form of the Newark basin from New York south to Pennsylvania is believed to be largely the result of variations in the geometry of reactivated Paleozoic ramp-thrusts. The Mesozoic strata extend farther west in Pennsylvania (fig. 8.6) where they rest on shallow-dipping reactivated thrusts and have transgressed well beyond the inflection point between gentle thrusts and steep ramps. Because the extension direction was in the southeast quadrant (fig. 8.3) and apparently was

consistent in orientation through time, both the dip and the strike of the reactivated faults directly controlled the amounts of subsidence along the basin axis (fig. 8.7*A*). The marked narrowing of the basin to the southwest, where the ancient structural grain is east-west, may have been the result of predominant left-

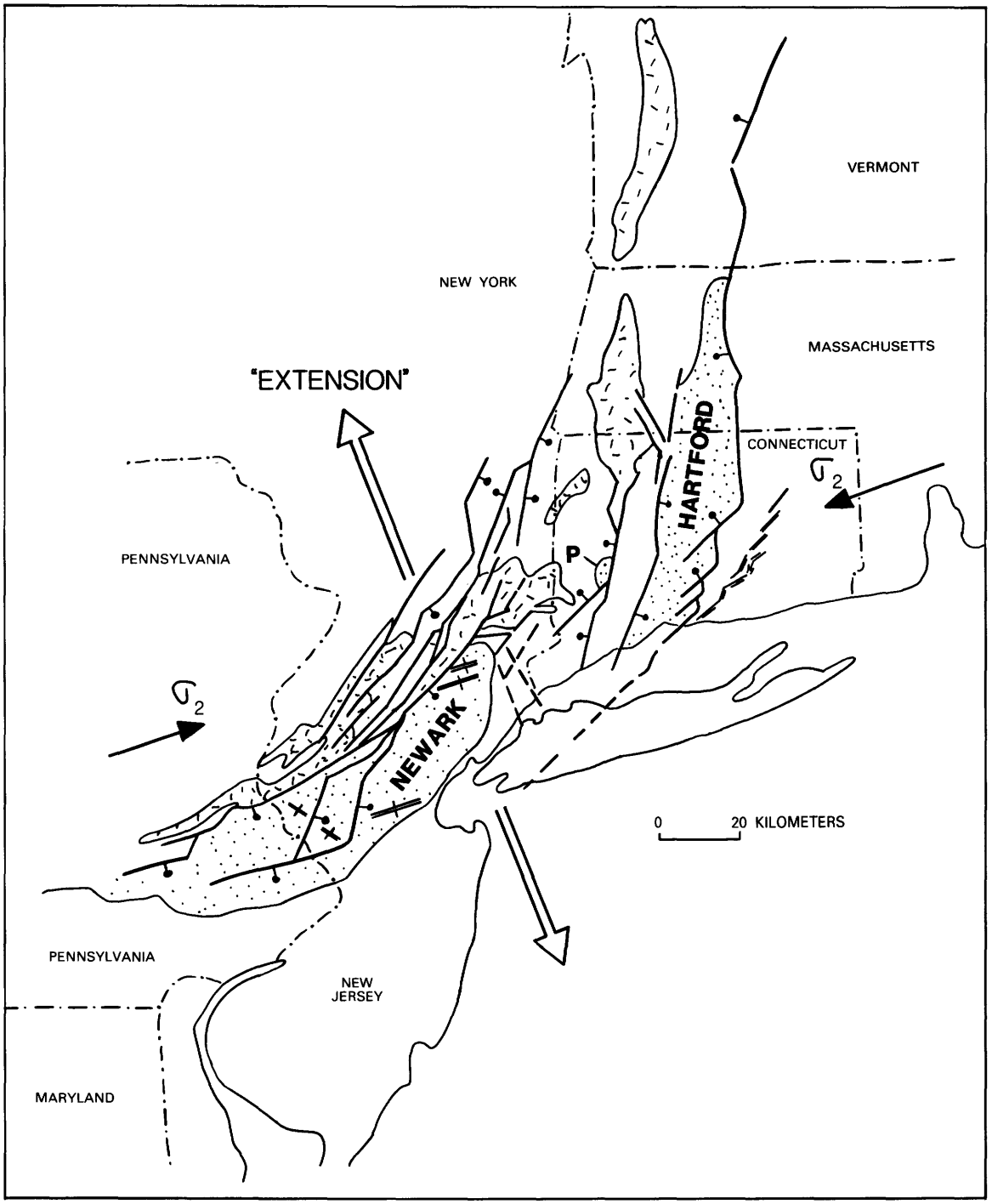

FIGURE 8.4.—Major fault patterns of the Newark and Hartford basins (stippled) in relationship to dominant northwest-southeast extension direction and inferred location of the intermediate principal stress direction, σ_2, as determined from analysis of slickenlines, extension fiber growths, and compressional features in the Newark basin. Various deformational features such as folds and thrust faults within the basin are relatable to this general stress field and to the stepping character of the faults as in figure 8.1.

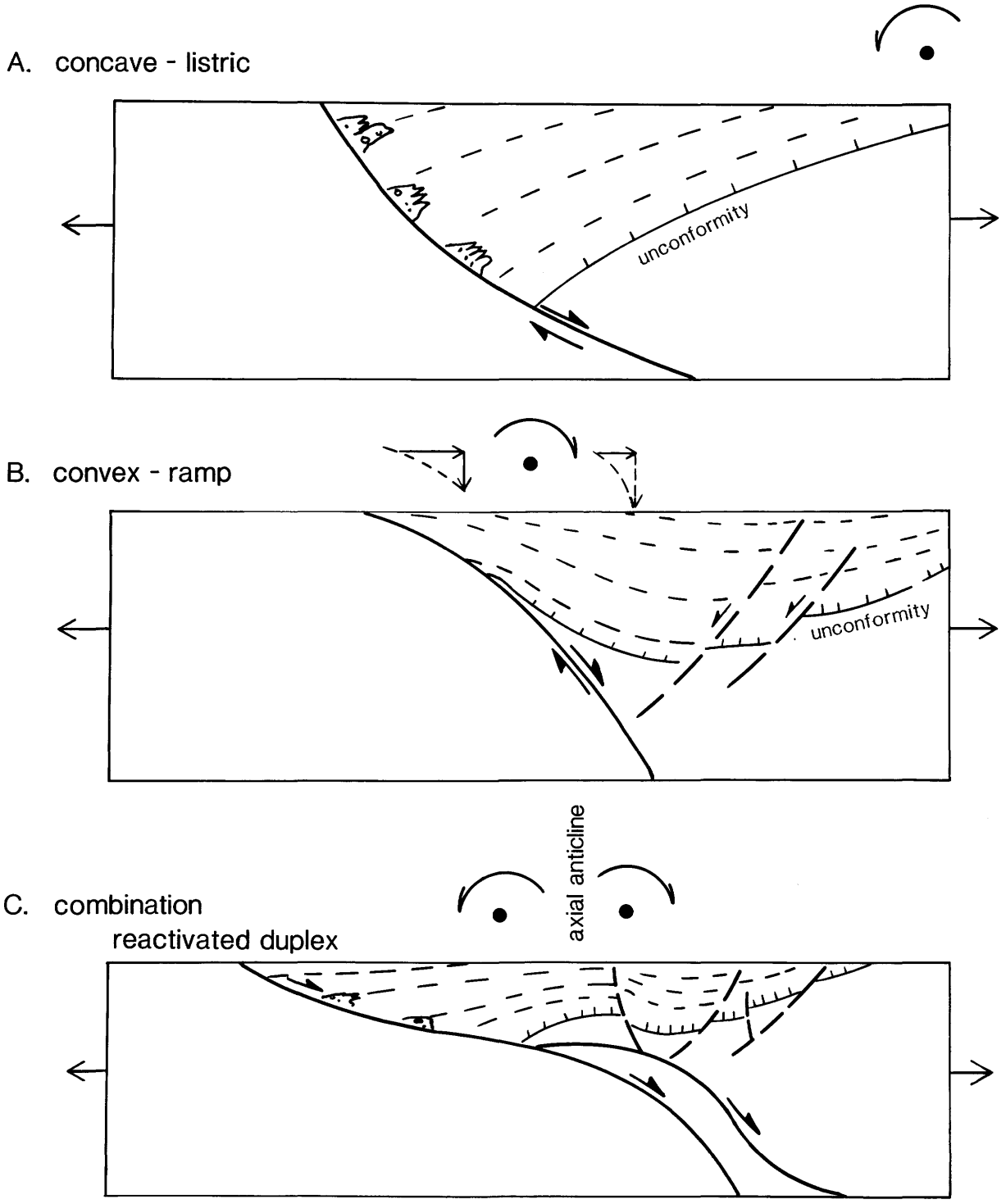

FIGURE 8.5.—Hypothetical models for subsidence and characteristic forms of basins developed by extension on (*A*) concave and (*B*) convex faults showing opposed rotation senses. In (*C*) a geologically reasonable model that shows extension on a reactivated thrust-ramp system is shown. At the point of inflection between thrusts and ramps an axial anticline is developed. This model could account for some sections across Mesozoic basins that are developed over Paleozoic west-verging duplexes such as the Newark basin in Pennsylvania and New Jersey and the Culpeper and Riddlesville basins (Petersen and others, 1984). The model shows how reactivation of west-verging Paleozoic thrust systems can explain the form of the west-dipping half-grabens of the Appalachians. East-dipping basins are not explained by this model.

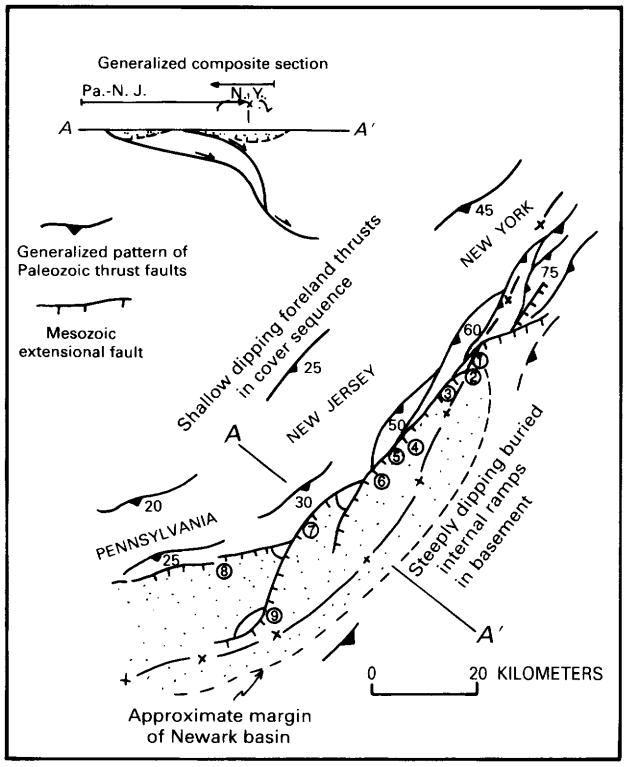

FIGURE 8.6.—Position of Newark basin in relation to Paleozoic thrust faults (sawtoothed lines) that have been reactivated to form the basin. Some Mesozoic faults shown by hachured lines. From New York southward the basin trangresses westward across shallower dipping thrust faults and may be situated farther northwest of the inflection point (long dashed line with x's) between concave and convex fault systems. In the diagrammatic section *A–A'*, the position of the New York and Pennsylvania-New Jersey parts of the basin are shown in relation to their position on a hypothetical thrust-ramp system, at an early stage in the evolution.

oblique normal faulting with minor dip-slip movement. The northern termination of the basin in New York coincides with an area of right-oblique normal movement on reactivated N. 20° E.-striking, steeply dipping, convex ramps that resulted in development of a narrow, southwestwardly deepening basin. The widest and deepest part of the basin is located in Pennsylvania where southeast extension was normal to the strike of the ancestral thrust-ramp complex (fig. 8.7*A*).

The model outlined above explains in a simple way the correspondence between reactivated fault systems and the overall form of the Newark basin. South from the New York recess (fig. 8.7*A*), the widest parts of the basins occur on salients and recesses, where the strike of the reactivated structures is normal to the extension direction, and the narrowest parts occur where predominantly strike-slip movement would be expected. Evidence for Mesozoic reactivation of Proterozoic and Paleozoic structures in and around the Newark basin is overwhelming at all levels of examination, from thin section to outcrop to quadrangle scale, and it is known that such processes operated well beyond the limits of the present Newark basin (Ratcliffe, 1980). The map distribution of certain offshore (buried) basins at the latitude of the Newark basin does not resemble that of their onshore counterparts (see Klitgord and Hutchinson, chapter 9, this volume), further suggesting that reactivation of continental foreland thrust systems endemic to Paleozoic and older North American crust was instrumental in localizing some but not all zones of Mesozoic extension. In the reactivation model, the present onshore early Mesozoic basins mark the response of previously disrupted continental crust to extensional tectonic forces generated far to the east, rather than the response to local rift or juvenile spreading centers developed beneath each basin.

IMPLICATIONS OF REACTIVATION CONTROL FOR BASIN TECTONICS AND SEDIMENTATION

Reactivation of fault systems with different curvatures such as shown in figure 8.5*C* will produce different rates of subsidence depending upon location of features within the basin above points on the curved surfaces (figs. 8.5*A*, *B*). At any instant, therefore, rates of subsidence will vary across the basin. In addition, inasmuch as the model is dynamic and the position of the sediments above the curved surface varies with the amount of extension, the subsidence rates related to that position migrate through space with time. In the combination model (fig. 8.5*C*), one might predict a broad shallow basin over the shallow concave part of the fault system, a high or emergent area over the inflection point, and a more sharply defined subsiding basin over the convex surface. In this model, for example, one could envision an axial anticline that migrates upwards and westward through time. This axial region might separate two sedimentologically distinct basins. In an area situated on steeply dipping or convex surfaces, such as the northernmost end of the Newark basin, a narrow basin with infilling from the north and northeast might develop. The greater subsidence to the south-southwest might induce southerly drainage. The relationship of sedimentary facies, thickness of sediments, patterns of igneous activity, and growth folds to the curvature and form of basin-forming faults is likely to be a fruitful area of investigation. To what extent

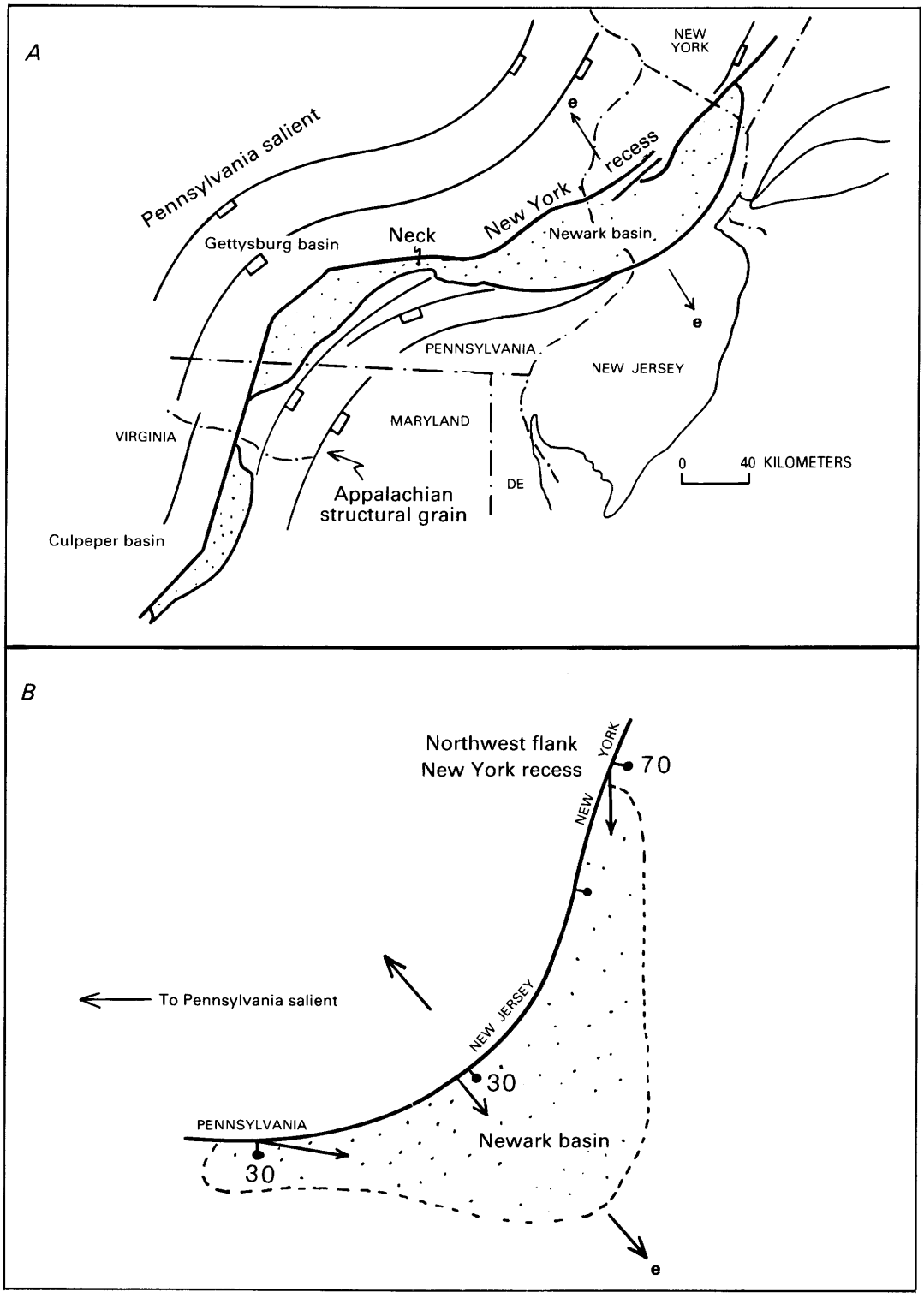

FIGURE 8.7.—*A*, Newark-Gettysburg and Culpeper basins in relation to Pennsylvania structural salient and New York recess. "e" shows probable extension direction. *B*, Diagram showing that the widest part of Newark basin occurs where extension was normal to the Paleozoic grain. Necking of the basin southward and termination northward are explained by increasing oblique slip to the north and to the south and consequent decrease in horizontal separation and (or) vertical slip. In the fault-reactivation model, the width and depth of the basin are related to both strike and dip of the reactivated surfaces. Cross sections drawn at various places could differ markedly depending upon the dip and strike of the faults in relation to the extension direction.

fault reactivation and the geometry of reactivated surfaces are important remains to be determined. In this paper we have emphasized the role of reactivation and some of the important implications of the acceptance of this model.

SELECTED REFERENCES

Aggarwal, Y.P., and Sykes, L.R., 1978, Earthquakes, faults and nuclear power plants in southern New York and northern New Jersey: Science, v. 200, p. 425–429.

Aydin, Atilla, and Nur, Amos, 1982, Evolution of pull-apart basins and their scale independence: Tectonics, v. 1, no. 1, p. 91–105.

Burton, W.C., and Ratcliffe, N.M., 1985, Attitude, movement history and structure of cataclastic rocks of the Flemington fault based on core drilling near Oldwick, New Jersey: U.S. Geological Survey Miscellaneous Field Studies Map MF–1781.

_____1985, Compressional structures associated with right-oblique normal faulting of Triassic-Jurassic strata of the Newark basin near Flemington, New Jersey [abs.]: Geological Society of America Abstracts with Programs, v. 17, no. 1, p. 9.

Manspeizer, Warren, 1980, Rift tectonics inferred for volcanic and clastic structures, *in* Manspeizer, Warren, ed., Field studies of New Jersey geology and guide to field trips, 52nd Annual Meeting of the New York State Geological Association: Newark, N.J., Rutgers University, p. 315–350.

Petersen, T.A., Brown, L.D., Cook, F.A., Kaufman, Sidney, and Oliver, J.E., 1984, Structure of the Riddleville basin from COCORP seismic data and implications for reactivation tectonics: Journal of Geology, v. 92, p. 261–271.

Ratcliffe, N.M., 1980, Brittle faults (Ramapo fault) and phyllonitic ductile shear zones in basement rocks of the Ramapo seismic zone, New York and New Jersey, and their relationship to current seismicity, *in* Manspeizer, Warren, ed., Field studies of New Jersey geology and guide to field trips, 52nd Annual Meeting of the New York State Geological Association: Newark, N.J., Rutgers University, p. 278–311.

_____1982, Results of core drillings of the Ramapo fault at Sky Meadow Road, Rockland County, New York, and assessment of evidence for reactivation to produce current seismicity: U.S. Geological Survey Miscellaneous Investigations Map I–1401, scale 1:62,500.

_____1982, Fault reactivation and seismicity in the Ramapo seismic zone, New York-New Jersey: Seismological Society of America, Eastern Section Meeting, Airlie House.

_____1984, Brittle-ductile transition zone in a Barrovian gradient: Implications for tectonic emplacement of isograds [abs.]: Geological Society of America Abstracts with Programs, v. 16, no. 1, p. 57.

Ratcliffe, N.M., and Burton, W.C., 1984, Brittle fault fabrics, mineralogy and geometry of the border faults of the Newark basin, N.Y.-N.J., from drill-core information [abs.]: Geological Society of America Abstracts with Programs, v. 16, no. 1, p. 57.

Ratcliffe, N.M., and Costain, J.K., 1985, Northeastern seismology and tectonics: U.S. Geological Survey Open-File Report 85–464, p. 54–58.

See also brief reports by Ratcliffe since 1978 in the semiannual Summaries of Technical Reports (from v. 5 on) of the National Earthquake Hazards Reduction program for progress reports and brief statements of work planned and completed. Starting in 1980, these volumes were assigned Open-File Report numbers; from 1980 till now, those numbers are 80–6, 80–842, 81–167, 81–833, 82–65, 82–840, 83–90, 83–525, 83–918, 84–628, 85–22, and 85–464.

9. DISTRIBUTION AND GEOPHYSICAL SIGNATURES OF EARLY MESOZOIC RIFT BASINS BENEATH THE U.S. ATLANTIC CONTINENTAL MARGIN

Kim D. Klitgord and Deborah R. Hutchinson

INTRODUCTION

Basement structures associated with early Mesozoic extensional tectonic activity have been mapped on the U.S. Atlantic margin (fig. 9.1) by means of seismic-reflection and magnetic data (Klitgord and Behrendt, 1979; Hutchinson, 1984). On the shallow basement platforms, these structures include isolated basins (graben or half-graben structures) and faults that extend into the crust. At the basement hinge zone, which separates shallow platforms from deep marginal sedimentary basins, is a series of parallel half-graben structures that deepen seaward. These half-grabens are bounded on one side by normal faults, which can be traced on seismic records into the crust. Many of these basins are characterized by broad magnetic-anomaly lows and are flanked by magnetic and gravity anomaly highs at their edges. Thus, contoured magnetic data can be used to map the shapes of basement structures that have been identified from seismic-reflection data. We shall discuss examples of these structures on the Long Island and Gulf of Maine platforms and along the landward edges of the Georges Bank basin and the Baltimore Canyon trough.

LONG ISLAND PLATFORM

Four major buried basins are located on the Long Island platform: the New York Bight, Long Island,

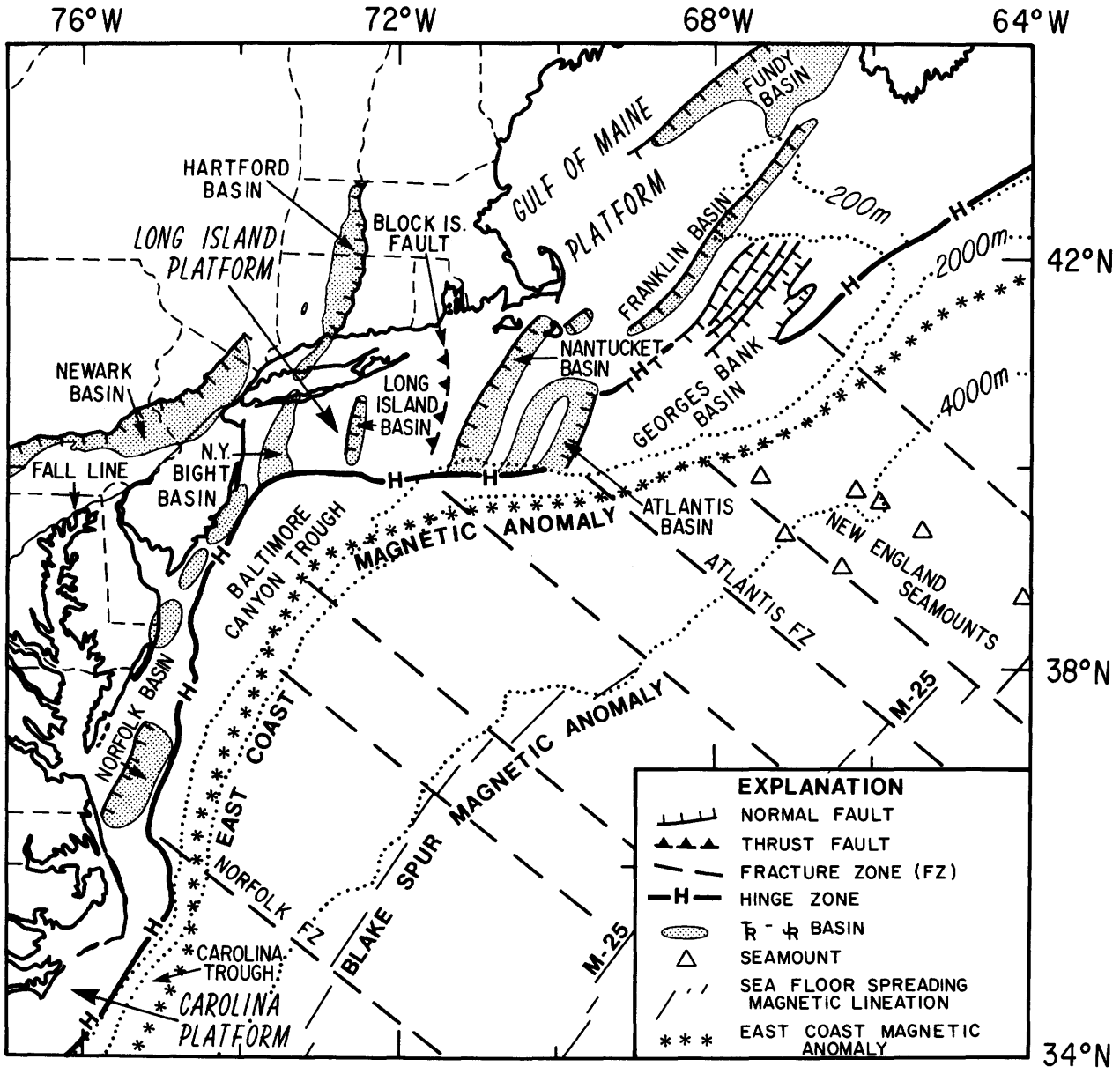

FIGURE 9.1.—Tectonic framework of the U.S. Atlantic continental margin. From Klitgord (1983).

Nantucket, and Atlantis basins (Hutchinson and others, in press; Hutchinson, 1984). Several kilometers of sediment have filled isolated basins beneath the postrift unconformity. The sedimentary units dip steeply in these small basins and are truncated updip at the postrift unconformity, suggesting that a significant section of sedimentary and crystalline rock has been eroded.

The New York Bight basin and associated faults form a chaotic set of basement structures that may connect with the Hartford basin onshore (fig. 9.1). The broad magnetic-anomaly low over the basin (fig. 9.2*A*) terminates to the south at the basement hinge zone and extends northward across Long Island. The continuity of this magnetic low with the magnetic low over the Hartford basin indicates a connection between the onshore and offshore basins. The flanking magnetic highs are also regions of gravity-anomaly highs; this combination indicates more mafic material is present along the edges of the basin. The basement structure recorded on seismic profiles (fig. 9.2*B*) is more chaotic than is suggested by the magnetic data (Hutchinson and Grow, 1985; Hutchinson, 1984). This difference may be a result of tectonic activity after the basin was

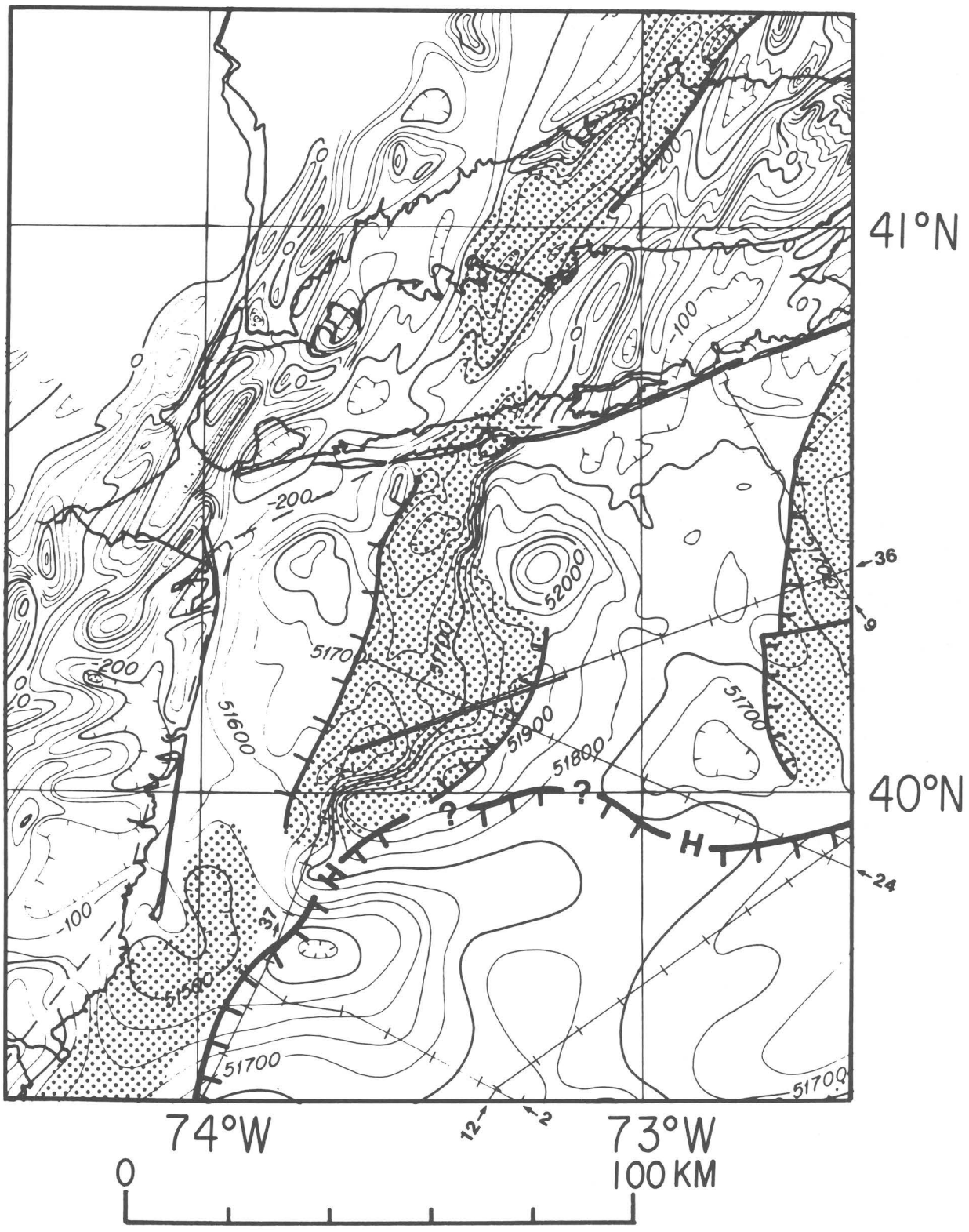

FIGURE 9.2*A*.—Magnetic anomaly map of the New York Bight basin area. Limits of basin (shaded region), faults (heavy hachured lines), basement hinge zone (heavy hachured line with H's), multichannel seismic lines (light hachured lines), and location of seismic line 36 (heavy line) are indicated. Modified from Klitgord and Behrendt (1979) and Hutchinson and others (in press).

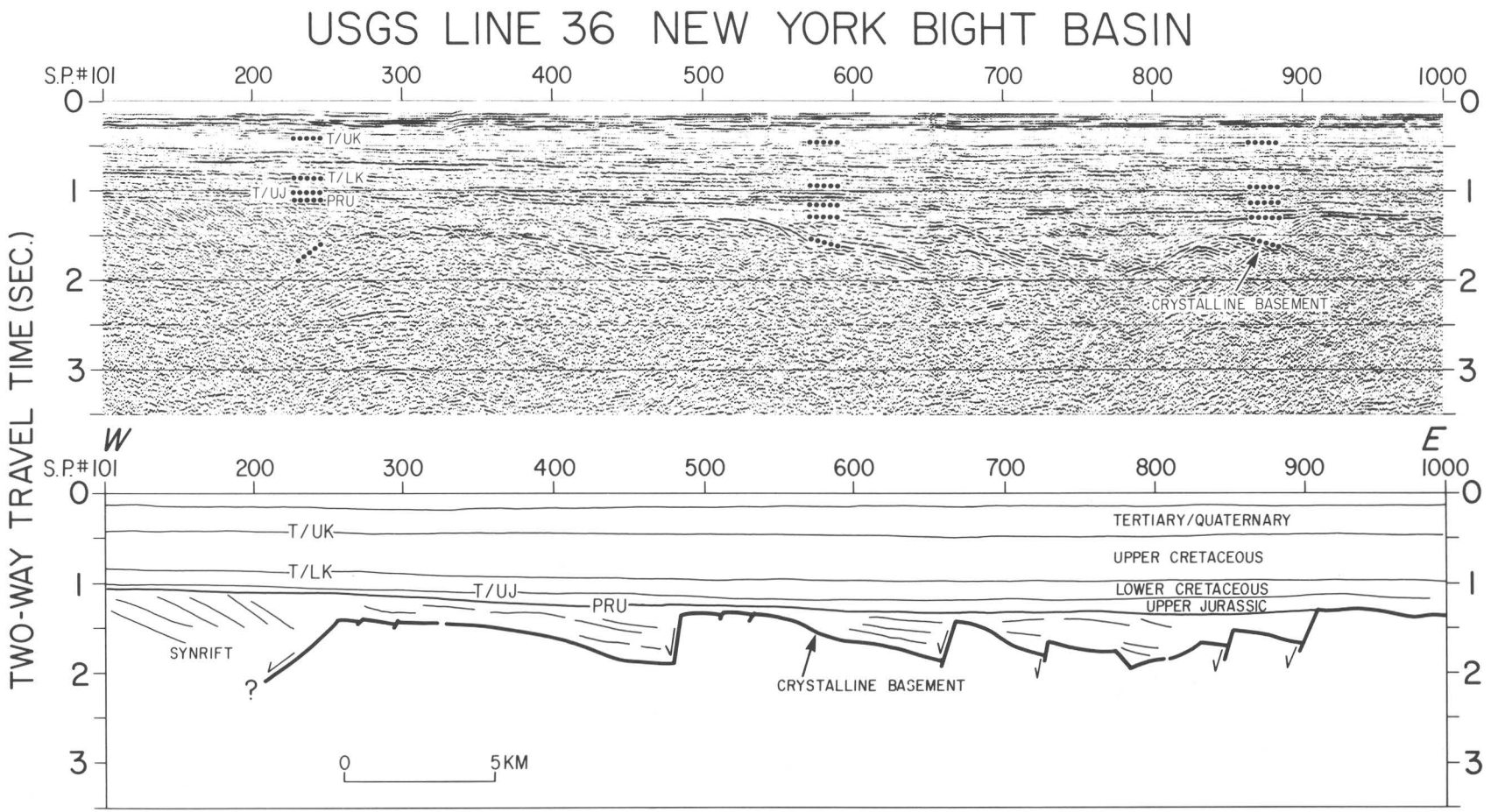

FIGURE 9.2*B*.—Seismic record of part of USGS line 36 over the New York Bight basin showing dipping reflectors and a zone of chaotic basement faults within the basin. Lower record shows interpretation. PRU, postrift unconformity. From Hutchinson and others (in press).

originally formed (for example, uplift and erosion or hinge zone subsidence and faulting).

Long Island basin (fig. 9.3) is a typical half-graben structure with a northeast trend. The primary fault

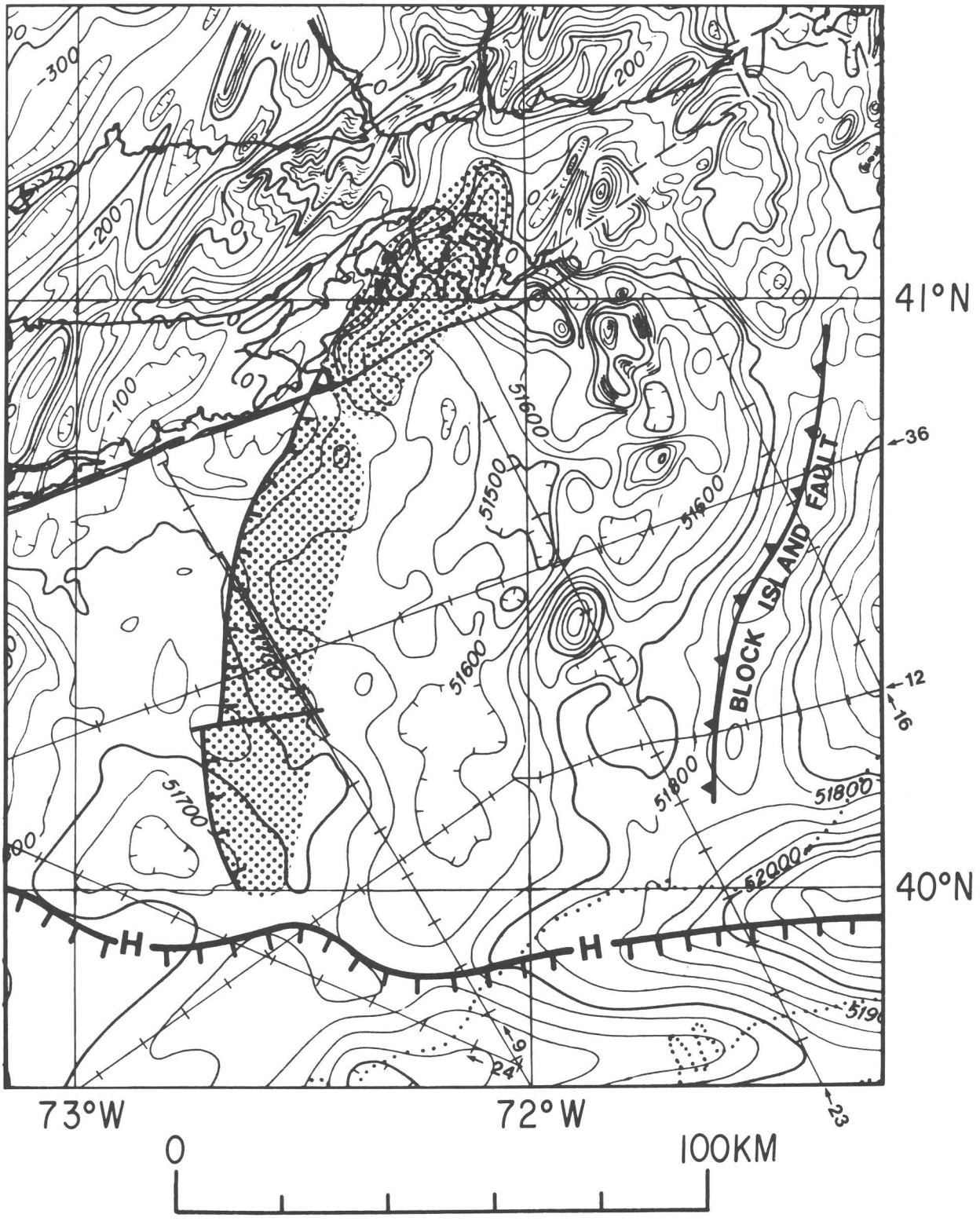

FIGURE 9.3A.—Magnetic anomaly map of the Long Island basin area. Limits of basin (shaded region), faults (heavy hachured lines), basement hinge zone (heavy hachured line with H's), multichannel seismic lines (light hachured lines), and location of seismic line 9 (heavy line) are indicated. Modified from Klitgord and Behrendt (1979) and Hutchinson and others (in press).

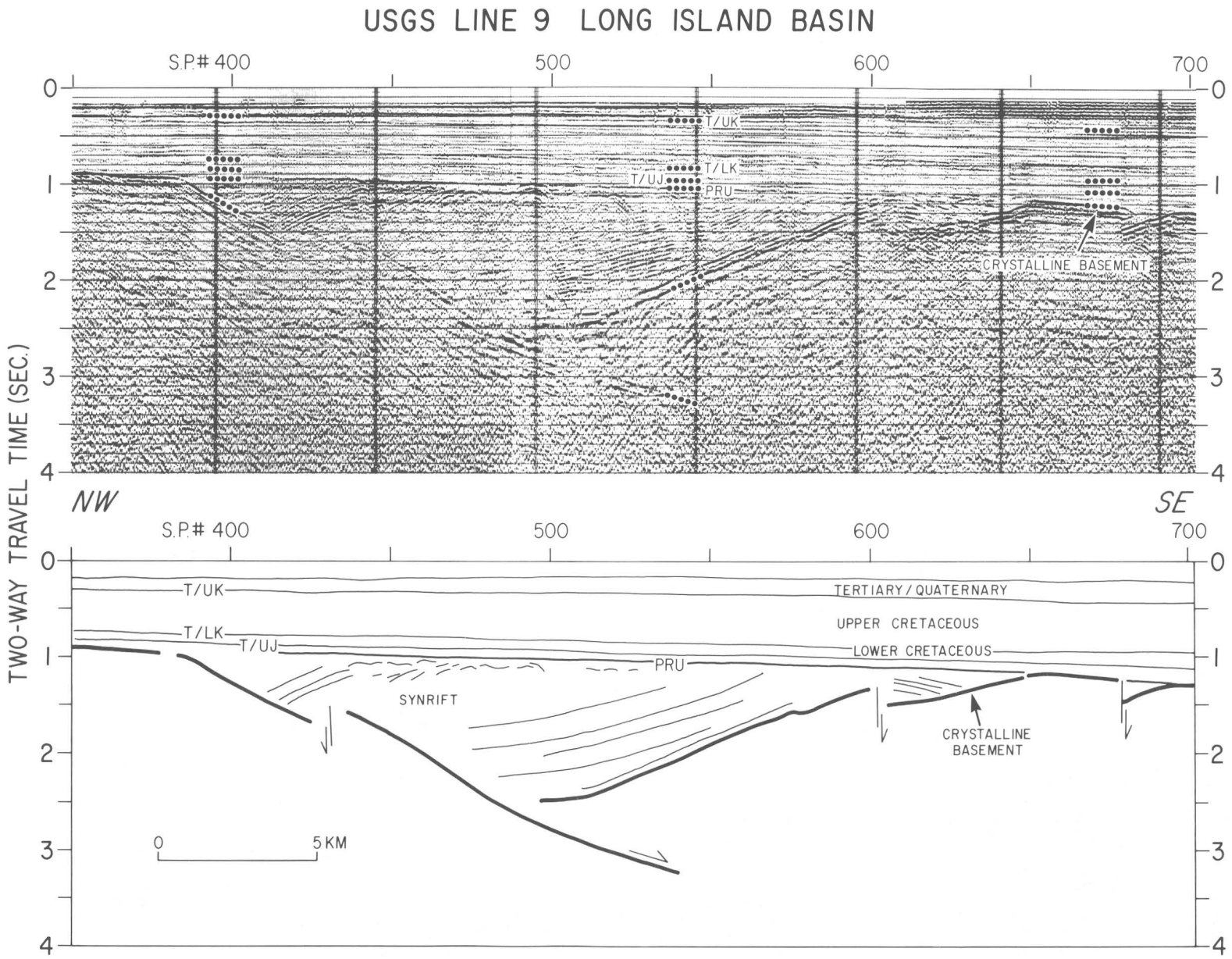

FIGURE 9.3*B*.—Seismic record of part of USGS line 9 over Long Island basin showing west-dipping synrift or prerift sediments and an east-southeast-dipping crust-cutting fault. PRU, postrift unconformity. From Hutchinson and others (in press).

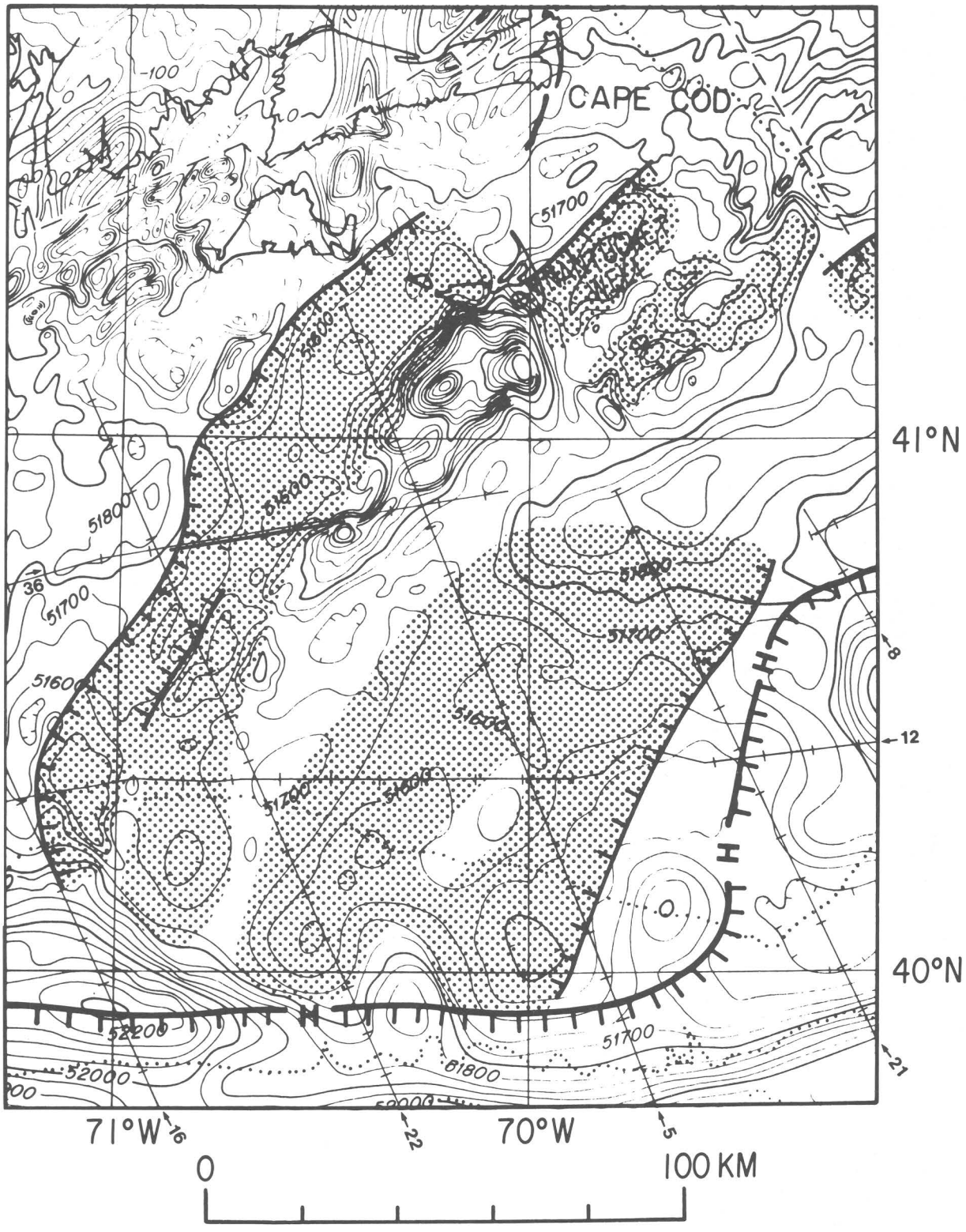

FIGURE 9.4A.—Magnetic anomaly map of the Nantucket basin area. Limits of basin (shaded region), faults (heavy hachured lines), basement hinge zone (heavy hachured line with H's), multichannel seismic lines (light hachured lines), and location of seismic line 36 (heavy line) are indicated. Modified from Klitgord and Behrendt (1979) and Hutchinson and others (in press).

surface dips eastward (southeastward?) and can be traced almost to the base of the crust. This half graben is filled with west-dipping sedimentary rock units that may be synrift or prerift material. Unlike many of the other basins, it is not situated over a simple, broad magnetic low. However, the western border fault is located along the steep gradient of a north-northwest-trending magnetic high. The numerous circular magnetic highs near the basin indicate small igneous bodies.

Nantucket basin (fig. 9.4) is located between the islands of Martha's Vineyard and Nantucket and has a well-defined magnetic low over it. The basin contains northwest-dipping sedimentary units and is bordered on its western flank by an east-dipping fault. The large, northeast-trending magnetic-anomaly high and a large gravity high along the eastern edge of the basin are probably caused by a shallow mafic body.

A fourth basin, the Atlantis basin, is on the eastern end of the Long Island platform at the edge of Georges Bank basin. The most conspicuous structure of the basin is a west-dipping fault along its eastern edge. On some seismic profiles, the basin is divided into several smaller basins in the west and a single larger basin along its eastern half. Our grid of seismic-reflection profiles is not adequate to resolve whether the basin is a series of interconnected smaller rift basins or the remnants of a single large basin (Hutchinson, 1984).

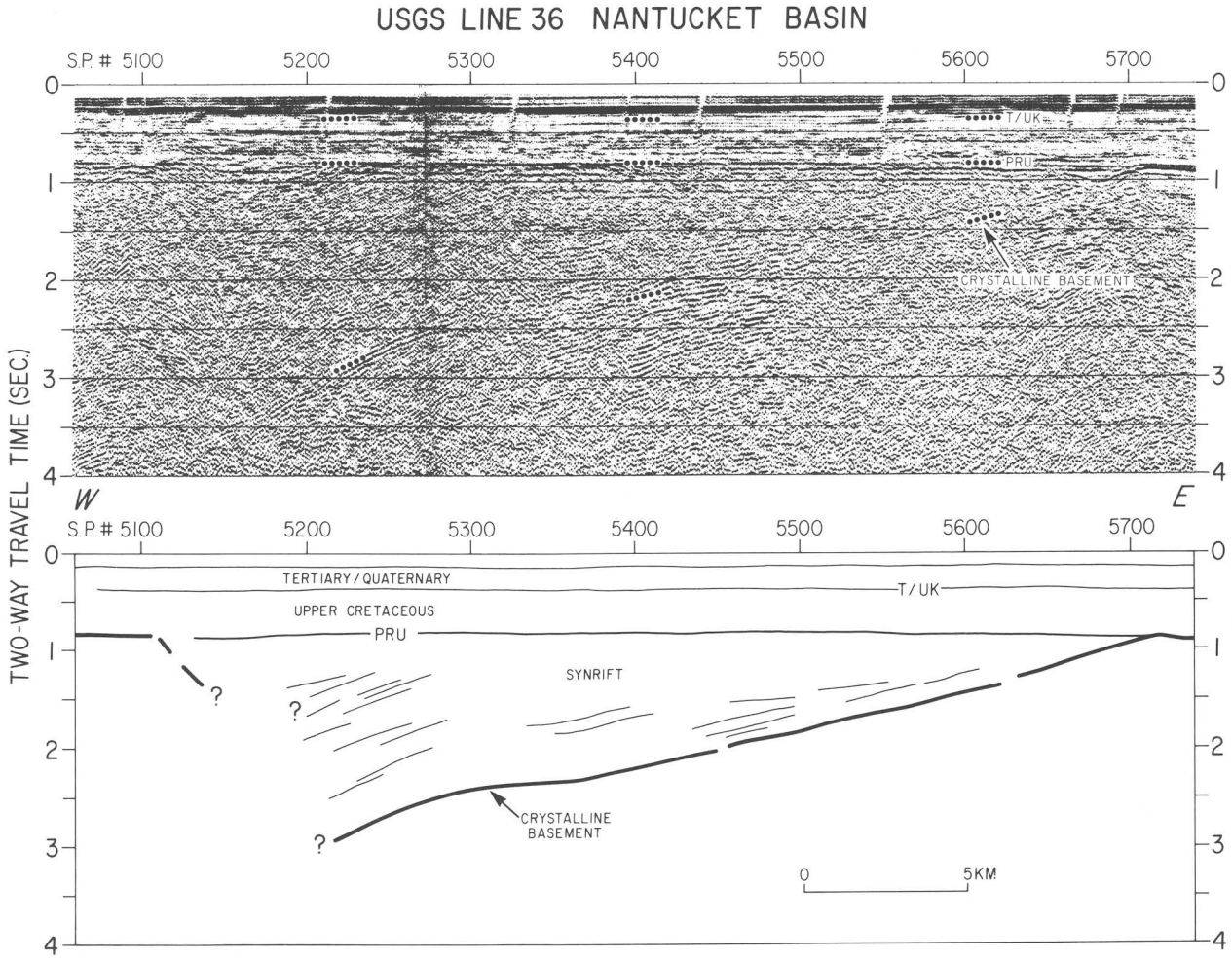

FIGURE 9.4*B*.—Seismic record of part of USGS line 36 over Nantucket basin showing the west-northwest-dipping synrift or prerift sedimentary units beneath the postrift unconformity (PRU). From Hutchinson (1984).

GULF OF MAINE PLATFORM

Numerous small basins have been mapped by Ballard and Uchupi (1975) on the Gulf of Maine platform. The most seaward of these basins is the Franklin basin. Unlike sedimentation patterns in the Long Island platform basins, on the Gulf of Maine platform the late Mesozoic and Cenozoic deposition patterns continued to reflect this basin structure, forming a bathymetric basin (Franklin Basin) on the northern edge of Georges Bank. Franklin basin parallels the hinge zone along the edge of the Gulf of Maine platform. A distinctive magnetic low is located along the axis of the basin (fig. 9.5*A*) and a superimposed pair of magnetic and gravity highs, indicative of a mafic body, is at its seaward edge (fig. 9.5*B*). Sediment fill of this basin dips westward and is truncated updip by the postrift unconformity.

GEORGES BANK BASIN

The block-faulted basement hinge zone at the edge of the Gulf of Maine platform deepens in a series of steps into a broad crustal depression that forms the Georges Bank basin (fig. 9.6*A*) (Klitgord and others, 1982). Each "step" is a small half graben formed by a backtilted block that has rotated along a southeast-dipping normal fault. These half grabens contain wedges of fanshaped sedimentary deposits (fig. 9.6*B*), indicating syndeformational sediment deposition, that have not been eroded into as deeply as the sedimentary units found in the basins on the Long Island platform. The postrift unconformity separates landward-dipping, rift-related sedimentary units from more conformable postrift sedimentary units (fig. 9.6*B*).

Crystalline basement (upper surface of crystalline rock) is not easy to identify at the hinge zone. The rough character of acoustic basement at the updip side of some half grabens (see, for example, shot point number 1200, fig. 9.6*B*) may indicate crystalline basement. On some seismic profiles, this rough basement can be traced beneath the west-dipping sedimentary reflectors. Crystalline-basement depths at the uptilted edges of the grabens range from less than 2 km to more than 6 km below sea level.

BALTIMORE CANYON TROUGH

The basement hinge zone of the Baltimore Canyon trough, which is located near the coastline of New Jersey, steps seaward to the south until it is nearly 75 km offshore near Norfolk, Virginia (fig. 9.1). Marine seismic data collected in the northern part of the Baltimore Canyon trough do not extend to the hinge zone at the coastline because of shallow water. However, in the southern part of the Baltimore Canyon trough, the seismic lines cross a well-defined hinge zone (fig. 9.7) (Klitgord and Behrendt, 1979; Klitgord, 1983; Benson, 1984; Klitgord and Schouten, unpub. data). The large Norfolk basin is between the hinge zone and coastline just north of Norfolk. A broad magnetic low marks the areal extent of the basin and two small, circular magnetic highs indicate intrusive bodies within the basin (fig. 9.8*A*). Norfolk basin contains northwest-dipping sedimentary units and a set of southeast-dipping normal faults (fig. 9.8*B*). The sedimentary units within the basin are truncated updip by the postrift unconformity.

SUMMARY

We have characterized some of the small basins and half grabens along the Atlantic margin with seismic-reflection and magnetic data. Sedimentary rocks within the basins have never been sampled, but our inferred connection of the New York Bight basin with the Hartford basin suggests that the basin fill should be similar — early Mesozoic clastic material intruded by dikes and sills. Sedimentary fill of the basins landward of the basement hinge zone forms steeply dipping units that are truncated updip by the postrift unconformity. This style of sediment fill and truncation is similar to that of the onshore Triassic-Jurassic basins. In contrast, the sedimentary units within the half grabens of the hinge zone form a fanshaped pattern; the upper layers are nearly conformable with the postrift unconformity. The original sediment fill pattern of the basins landward of the hinge zone may have had this same fan shape before erosion along the postrift unconformity. Most basins have crust-cutting faults along one edge, and some of these faults can be traced on seismic records to the Moho surface.

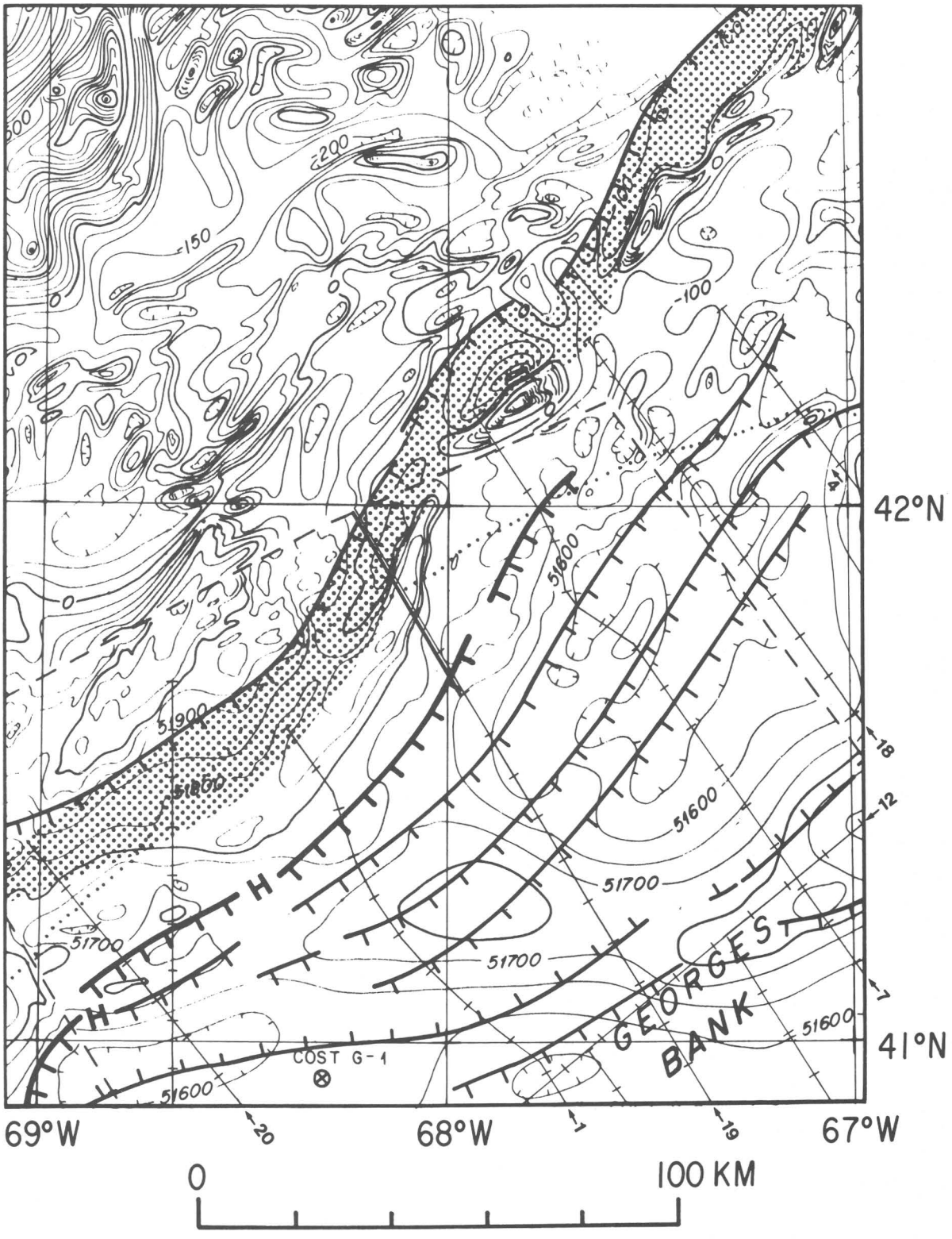

FIGURE 9.5*A*.—Magnetic anomaly map of the Franklin basin area at the edge of the Gulf of Maine platform. Limits of basin (shaded region), faults (heavy hachured lines), basement hinge zone (heavy hachured line with H's), multichannel seismic lines (light hachured lines), and location of seismic line 19 (heavy line) are indicated. Modified from Klitgord and others (1982, fig. 73).

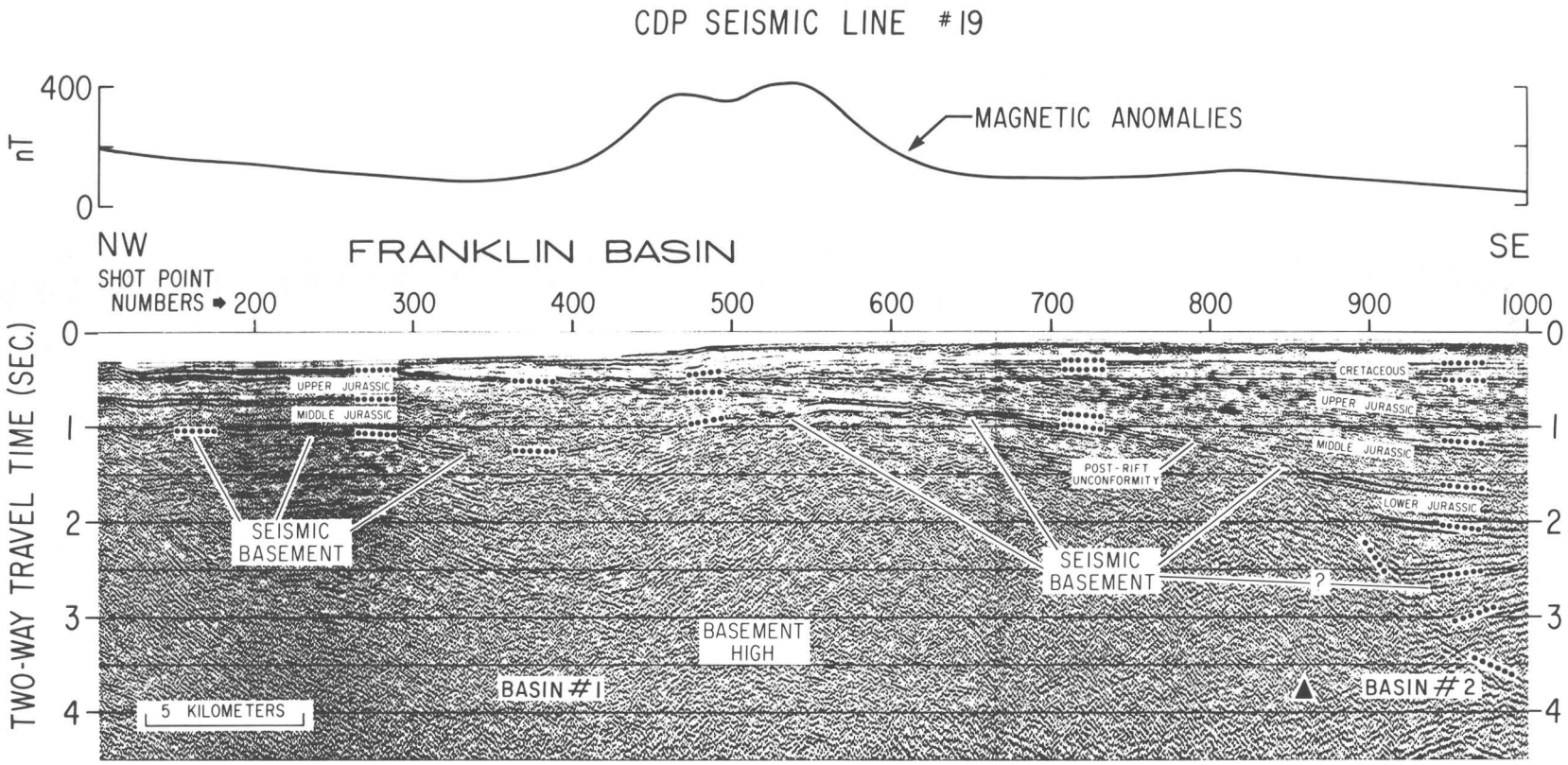

FIGURE 9.5*B*.—Seismic record of part of USGS line 19 over the Franklin basin (shotpoints 200-500). The magnetic anomaly peak at the edge of the Franklin basin may indicate a dike at the edge of the basin. Solid triangle marks faulted edge of basin 2. From Klitgord and others (1982, fig. 75).

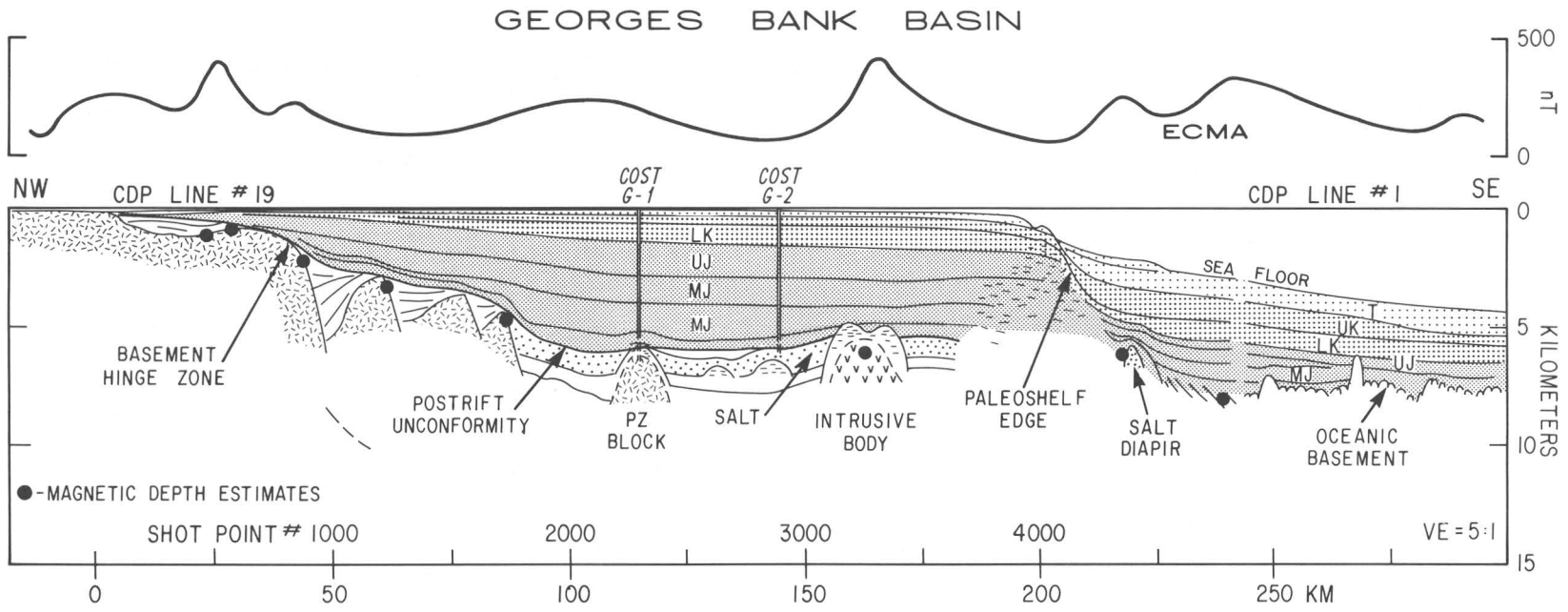

FIGURE 9.6*A*.—Line drawing of USGS line 19 showing formation of the basement hinge zone by a series of block-faulted steps containing rift basins. ECMA, east coast magnetic anomaly. From Klitgord and others (1982, fig. 72).

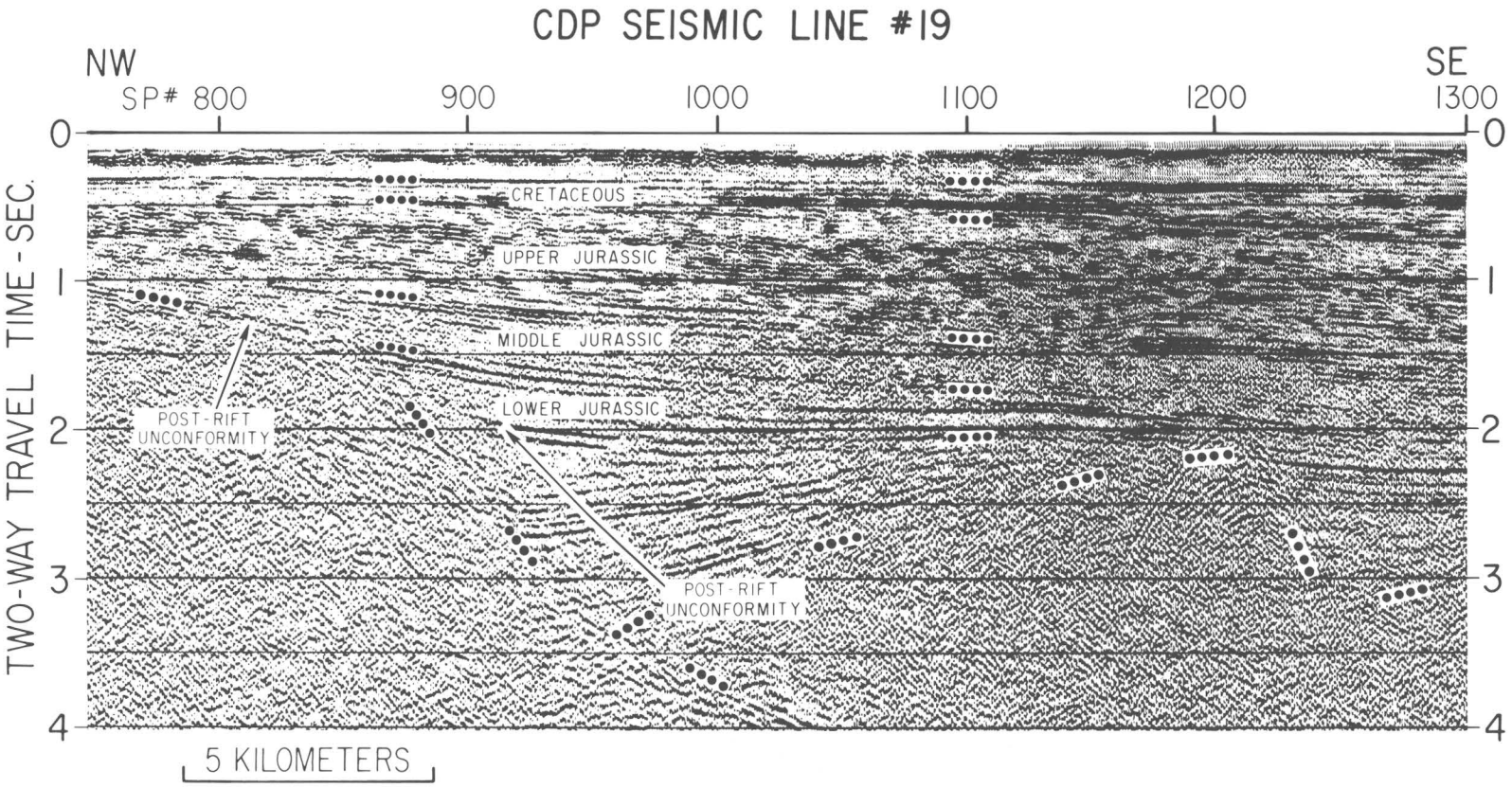

FIGURE 9.6*B*.—Seismic record of part of USGS line 19 showing the graben structures at the Georges Bank hinge zone. From Klitgord and others (1982, fig. 78).

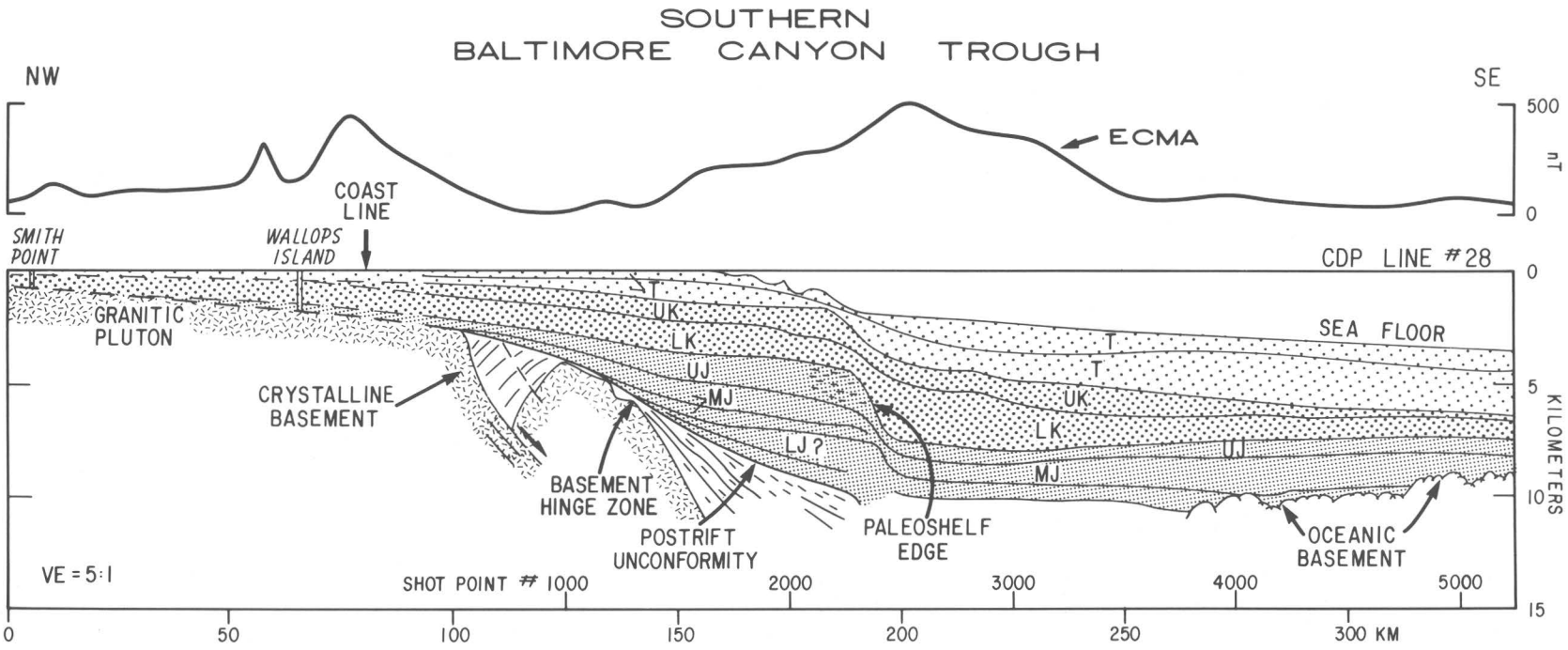

FIGURE 9.7.—Line drawing of USGS line 28 across the southern Baltimore Canyon Trough; Norfolk basin is between the coastline and the basement hinge zone. ECMA, east coast magnetic anomaly. From Klitgord (1983).

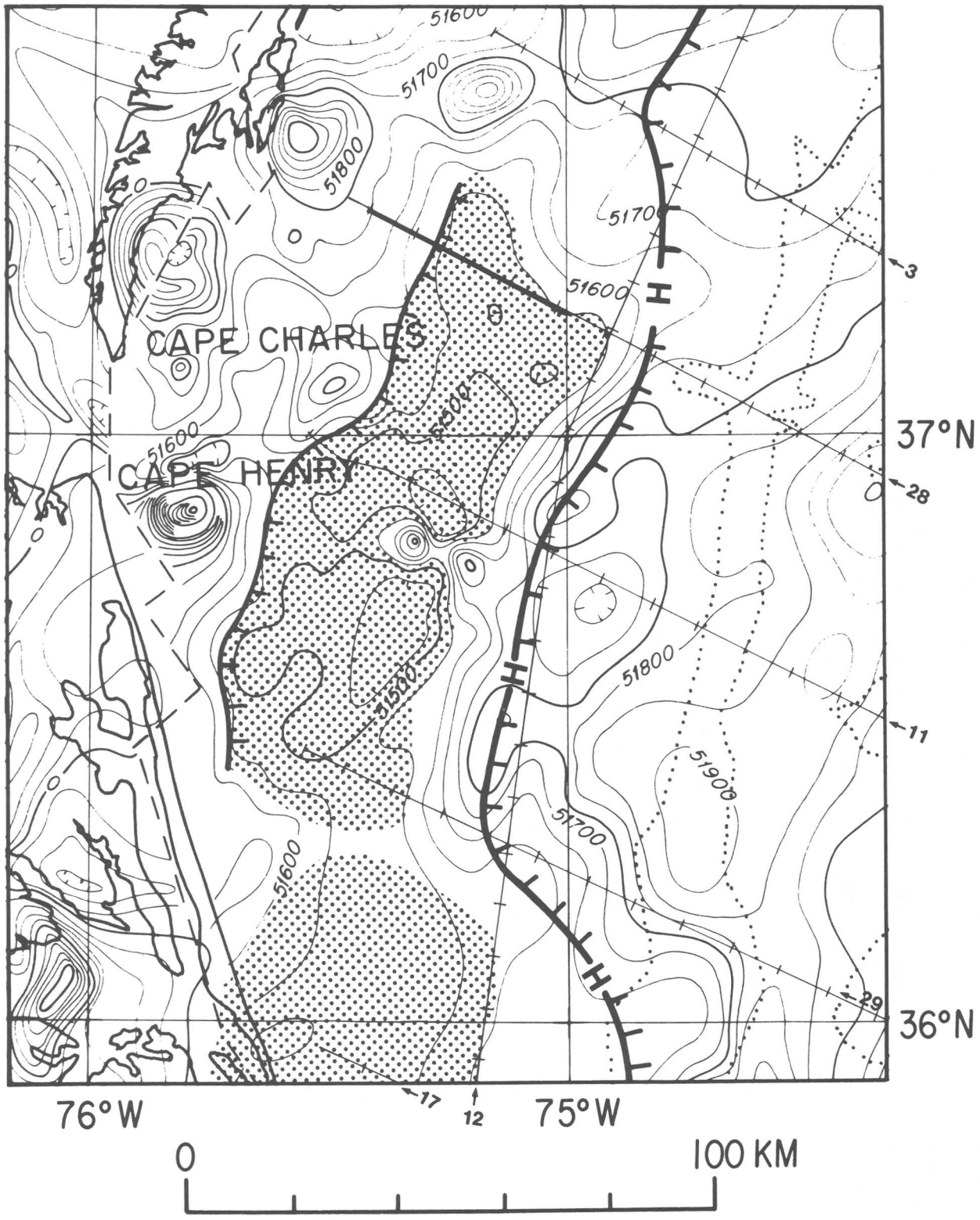

FIGURE 9.8A.—Magnetic anomaly map of the Norfolk basin area, Baltimore Canyon Trough. Limits of basins (shaded regions), faults (heavy hachured lines), basement hinge zone (heavy hachured line with H's), multichannel seismic lines (light hachured lines), and location of seismic line 28 (heavy line) are indicated. From Klitgord and Schouten (unpub. data) and Klitgord and Behrendt (1979).

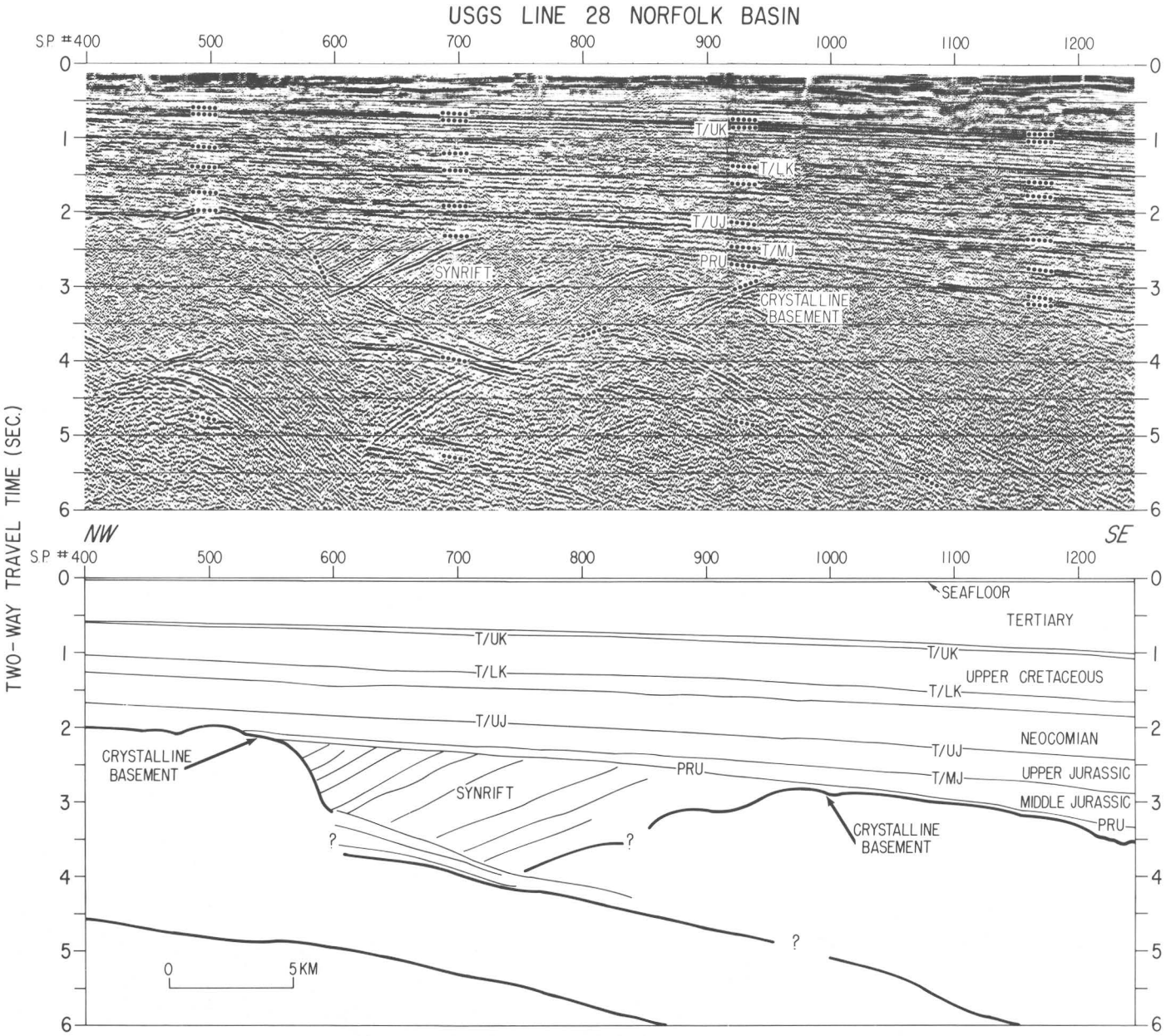

FIGURE 9.8*B*.—Seismic record of part of USGS line 28 showing the buried Norfolk basin (shotpoints 500 to 1000). Diffractions obscure some of the deeper reflectors. Upper limit of northwest-dipping units in basin is truncated by the postrift unconformity (PRU).

REFERENCES

Ballard, R.D., and Uchupi, E., 1975, Triassic rift structure in Gulf of Maine: American Association of Petroleum Geologists Bulletin, v. 59, no. 7, p. 1041–1072.

Benson, R.N., 1984, Structure contour map of pre-Mesozoic basement, landward margin of Baltimore Canyon trough: Delaware Geological Survey Miscellaneous Map Series No. 2, scale 1:500,000.

Hutchinson, D.R., 1984, Structure and tectonics of the Long Island platform: Kingston, University of Rhode Island, unpub. Ph.D thesis, 289 p.

Hutchinson, D.R., and Grow, J.A., 1985, New York Bight fault: Geological Society of America Bulletin, v. 96, p. 975–989.

Hutchinson, D.R., Klitgord, K.D., and Detrick, R.S., in press, Rift basins of the Long Island platform: Geological Society of America Bulletin.

Klitgord, K.D., 1983, Structure and evolution of the U.S. Atlantic Continental Margin [abs.]: Programme and Abstracts, Interunion Commission on the Lithosphere, XVIII General Assembly, International Union of Geodesy and Geophysics, p. 57.

Klitgord, K.D., and Behrendt, J.C., 1979, Basin structure of the U.S. Atlantic margin, *in* Watkins, J.S., Montadert, Lucien, and Dickerson, P.W., eds., Geological and geophysical investigations of the continental margins: American Association of Petroleum Geologists Memoir 29, p. 85–112.

Klitgord, K.D., Schlee, J.S., and Hinz, K., 1982, Basement structure, sedimentation, and tectonic history of the Georges Bank basin, *in* Scholle, P.A., and Wenkam, C.R., eds., Geological studies of the COST Nos. G–1 and G–2 Wells, United States North Atlantic Outer Continental Shelf: U.S. Geological Survey Circular 861, p. 160–186.

10. DISTRIBUTION OF ORGANIC-MATTER-RICH LACUSTRINE ROCKS IN THE EARLY MESOZOIC NEWARK SUPERGROUP

P.E. Olsen[7]

Most major, relatively fine grained Newark Supergroup sequences show a pattern of recurring lithologies making up sedimentary cycles (Van Houten, 1969, 1977; Olsen, 1980a, 1984a,b; Manspeizer and Olsen, 1981). These cycles consist of a strongly asymmetrical sequence of lithologically identifiable units that record the transgression, high stand, regression, and low stand of lakes. I propose that these cycles in the Newark Supergroup be termed "Van Houten cycles" for the worker who first recognized them. Each Van Houten cycle can be divided into three lithologically defined divisions (fig. 10.1), which have already been described for a number of Newark sequences (Olsen, 1981; Hentz, 1981). (I include division 4 of Towaco cycles (Olsen, 1980) within division 3 of Van Houten cycles.) In this paper I will focus on division 2, which has the greatest percentage of total organic carbon (TOC).

Division 1 is a relatively thin, platy to massive siltstone to conglomerate, which generally has a higher TOC (0.5–1.0 percent) than division 3 of the preceding cycle and shows fewer signs of desiccation. Current bedding, algal tufa, pisolites, oncolites, root zones, and reptile footprints are sometimes present.

Division 2 is commonly a laminated to microlaminated (laminae less than 1 mm) black siltstone, claystone, or carbonate showing few or no signs of desiccation, which commonly is rich in organic carbon (TOC locally more than 20 percent). In its most extreme form, division 2 contains abundant and well-preserved fossil fish, reptiles, arthropods, and sometimes plants. In its least developed form, division 2 consists of a red laminated siltstone that has desiccation cracks and is much better bedded than surrounding divisions 1 and 3.

Division 3 is generally thicker than the other two divisions. It consists of a massive, commonly red mudstone grading to a coarsening upwards sequence of sandy tilted beds showing current bedding and structures indicating deceleration of flow or to a fining upwards sequence with high-flow-regime structures at the base and low-flow-regime structures near the top. Desiccation structures are pervasive, commonly obliterating most bedding. Root and burrow zones and reptile footprints are common.

Both division 2 and the entire Van Houten cycle can be usefully thought of as varying along four independent lithologic axes (three of which are shown in fig. 10.2), which are (1) the desiccation-bioturbation axis, which reflects the amount of exposure to air and oxygenated water (largely a function of lake depth);

[7]Lamont-Doherty Geological Observatory of Columbia University, Palisades, N.Y. 10964.

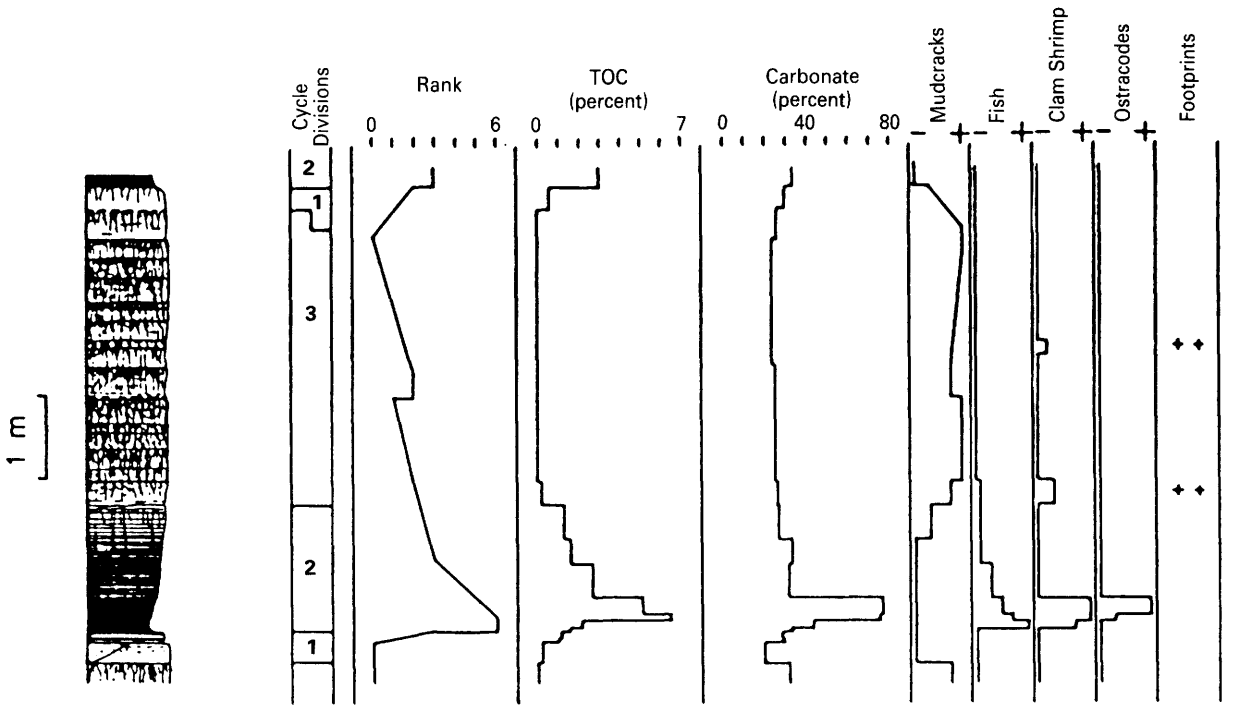

FIGURE 10.1.—Measured section through a single Van Houten cycle comprising the Skunk Hollow fish bed in the Lockatong Formation, showing common characteristics of a cycle near the microlaminated side of the desiccation-bioturbation axis (from Olsen, 1984a). Closeness of horizontal lines in the lithologic section indicates degree of lamination; solid black indicates microlamination. Irregular near-vertical lines indicate the density and depth of desiccation cracks. Rank is an indication of the position of *single beds* along the desiccation-bioturbation axis in figure 10.2; rank 6 indicates a microlaminated unit showing no signs of bioturbation or desiccation.

(2) the thickness axis, which is a measure of net sedimentation rate; (3) the coarseness axis, which reflects proximity to the basin edge; and (4) the chemical axis, which in part reflects the salinity of the lake water. At one end of the desiccation-bioturbation axis are beds showing very little or no signs of desiccation or bioturbation, while at the other end the sediments are massively disrupted by desiccation cracks and (or) bioturbation. For division 2, one end member along this axis is a microlaminated siltstone containing complete fish, while the opposite end member is a mud-cracked siltstone containing *Scoyenia*, roots, and reptile footprints. Extremes in the thickness axis are about 2 cm to 15 m for division 2 and 1 m to more than 50 m for the whole cycle. The coarseness axis for division 2 ranges from siltstone sequences containing thin conglomerate beds and abundant sandy graded beds (interpreted as turbidites) to claystones. Finally, along the chemical axis, division 2 ranges from a nearly pure limestone or dolomite to a noncalcareous claystone.

In a single Van Houten cycle, percentages of TOC are always highest in division 2. Within a single cycle, organic-matter content is closely related to the desiccation-bioturbation axis, increasing in beds as disturbance decreases. This relationship also holds for comparisons between cycles in single formations and suites of related formations in single basins, but it does not hold for comparisons between units in different basins. There also seems to be no correlation between increasing thickness of a cycle and increasing TOC. There is a general trend to have substantially greater TOC contents in more southern basins, however. Within the Triassic Lockatong Formation (late Carnian age) in the Newark basin, calcareous microlaminated portions of division 2 contain the most organic carbon (TOC 2.5–8.0 percent). Other cycles of the Lockatong in which division 2 is not microlaminated are not as rich in organic carbon. In contrast, the Cumnock Formation (Late Triassic, middle Carnian) in the Deep River (Sanford) basin contains no microlaminated sediments or beds producing whole fish, and Van Houten cycles there are quite thin (about 2 m). Many of the laminated siltstones of division 2, however, contain much more organic carbon (TOC 5–30 percent) than most other

parts of the Newark Supergroup. The interbeds of coal (Cumnock and Gulf seams) low in the section are within division 2 and contain the same aquatic fossils as the overlying black siltstones.

Visual examination of kerogen from organic-matter-rich parts of division 2 commonly shows a large amorphous fraction made up of possible fecal pellets (E.I. Robbins, oral commun., 1984) and what is presumably algal and bacterial matter. Small amounts of pollen and spores and even smaller amounts of leaf cuticle and wood tracheids are also present. However, woody matter can become the dominant component, as in some lacustrine Newark coals. The kerogen in divisions 1 and 3 is, in contrast, almost always dominated by pollen, spores, cuticle, and wood tracheids.

The organic-carbon-rich parts of division 2 generally are a small fraction of the total volume of formations. However, this fraction is substantially larger in the Cumnock Formation, the lower 500 m of the Lockatong Formation, much of the Portland Formation (Early Jurassic, Hettangian to Toarcian) in the Hartford basin, and the Waterfall Formation (Early Jurassic, Hettangian to ?Sinemurian) in the Culpeper basin. Some formations have very thick Van Houten cycles, and, since the thickness of division 2 correlates strongly with total cycle thickness, the organic-matter-rich examples of division 2 can be quite thick. The Richmond basin section (Late Triassic, middle Carnian) seems to have very thick transgressive-regressive cycles, which may fall within a broad definition of Van

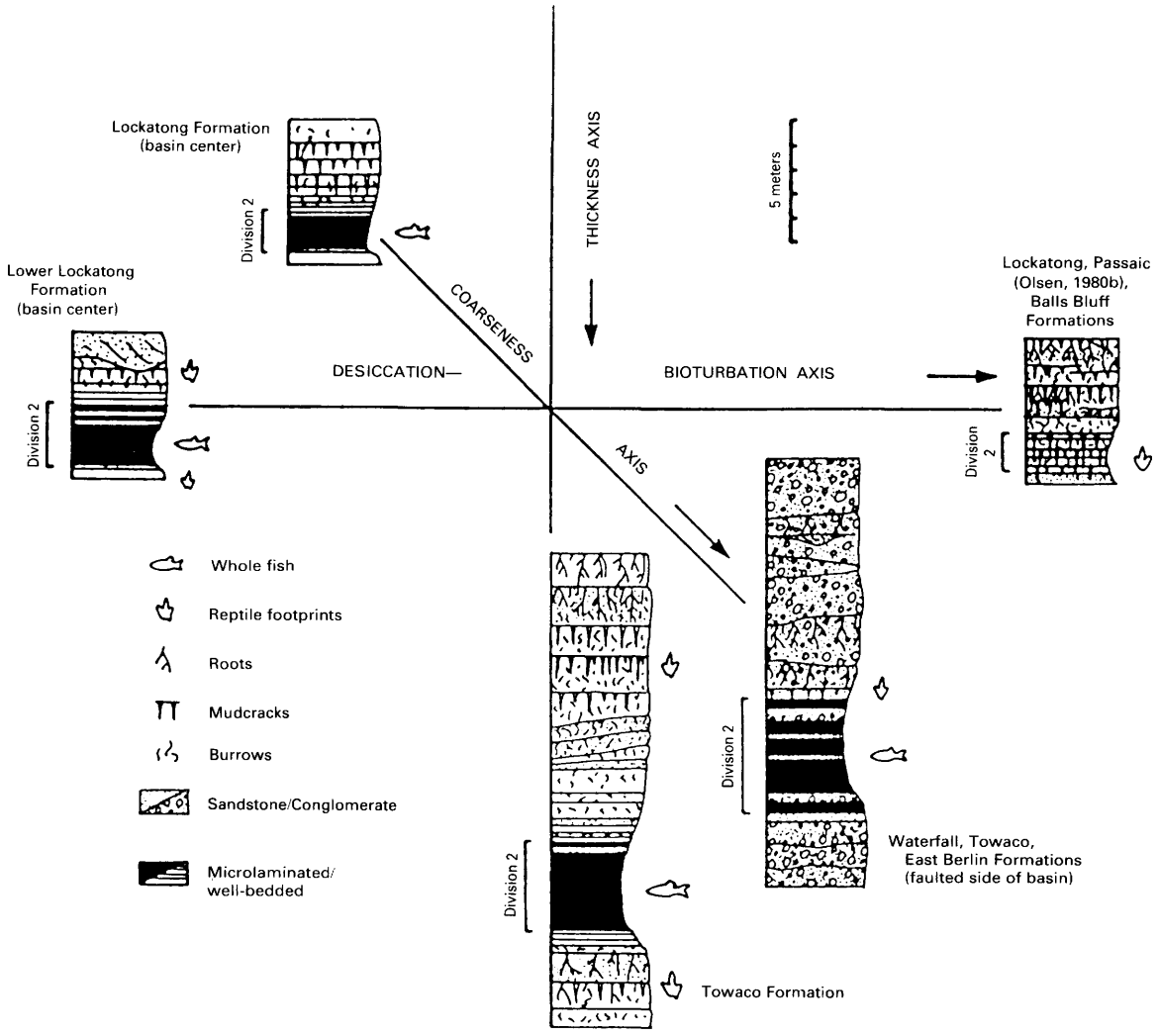

FIGURE 10.2.—Diagram of the relationship between the desiccation-bioturbation axis, the thickness axis, and the coarseness axis of Van Houten cycles and specific examples of classes of cycles from various Newark Supergroup formations in various basins. Division 2 is marked by brackets to the left of the columns.

Houten cycles (B. Cornet, oral commun., 1984). The deep-water parts of these cycles can be more than 15 m thick and consist of microlaminated black siltstones containing whole fish (TOC in the range of 10 percent) interbedded with sandstone beds showing no signs of desiccation. Similarly, the Towaco Formation (Early Jurassic, Hettangian) in the Newark basin has Van Houten cycles with a mean thickness of 25 m on the western side of the basin. Division 2 of these cycles is commonly as much as 5 m thick and contains more than 1.5 percent TOC.

Cycles in the Fundy basin commonly contain a conspicuous eolian and evaporitic component, substantially different from cycles in the other exposed Newark Supergroup basins. However, some can still be broadly classed as Van Houten cycles. The Blomidon Formation (Late Triassic, late Carnian to Norian) is made up of thin cycles (about 1.5 m thick), which consist mostly of a lower fissile red siltstone and an upper, highly disrupted siltstone or sandstone apparently containing eolian sand. The upper parts of these cycles seem to have been disrupted by evaporite crystal growth and possibly by efflorescent salt crusts (Smoot and Olsen, chapter 6, this volume). The overlying Scots Bay Formation (Early Jurassic) seems to consist of at least two 3-m-thick transgressive-regressive cycles, which are made up almost entirely of white and green limestone and chert. The coeval McCoy Brook Formation resembles the older Blomidon Formation, except that bioturbation seems more important than the evaporite-disrupted fabric in the upper parts of cycles and the sequences have much more fluvial sediment. Apart from some very thin beds just below the North Mountain Basalt, there are no organic-carbon-rich beds in the Fundy basin. The deepest water deposits, even those that are finely laminated and contain complete fish and invertebrates, have no carbonaceous organic matter.

Even Van Houten cycles that are otherwise rich in organic carbon can have very low TOC's near sills and other plutons where the sediments are metamorphosed. The most dramatic changes in the TOC occur within 50 m of the intrusive bodies, well within their zone of metamorphic alteration.

REFERENCES

Hentz, T.F., 1981, Sedimentology and structure of Culpeper Group lake beds (Lower Jurassic) at Thoroughfare Gap, Virginia: Lawrence, University of Kansas, unpub. M.S. thesis, 166 p.

Manspeizer, Warren, and Olsen, P.E., 1981, Rift basins of the passive margin: tectonics, organic-rich lacustrine sediments, basin analysis, *in* Hobbs, G.W., III, ed., Field guide to the geology of the Paleozoic, Mesozoic, and Tertiary rocks of New Jersey and the central Hudson Valley, New York: Petroleum Exploration Society of New York, p. 25–105.

Olsen, P.E., 1980a, Fossil great lakes of the Newark Supergroup in New Jersey, *in* Manspeizer, Warren, ed., Field studies in New Jersey geology and guide to field trips, 52nd Annual Meeting, New York State Geological Association: Newark, N.J., Rutgers University, p. 352–398.

———1980b, The latest Triassic and Early Jurassic formations of the Newark basin (eastern North America, Newark Supergroup); stratigraphy, structure, and correlation: New Jersey Academy of Science Bulletin, v. 25, p. 25–51.

———1981, Comment on "Eolian dune field of Late Triassic age, Fundy Basin, Nova Scotia": Geology, v. 9, p. 557–561.

———1984a, Comparative paleolimnology of the Newark Supergroup: a study of ecosystem evolution: New Haven, Conn., Yale University, unpub. Ph.D. thesis, 726 p.

———1984b, Periodicity of lake-level cycles in the Late Triassic Lockatong Formation of the Newark Basin (Newark Supergroup, New Jersey and Pennsylvania), *in* Berger, Andre, Imbrie, John, Hays, James, Kukla, George, and Saltzman, Barry, eds., Milankovitch and climate, NATO Symposium: D. Reidel, Dordrecht, Part 1, p. 129–146.

Van Houten, F.B., 1969, Late Triassic Newark Group, north central New Jersey, and adjacent Pennsylvania and New York, *in* Subitzky, Seymour, ed., Geology of selected areas in New Jersey and eastern Pennsylvania: New Brunswick, N.J., Rutgers University Press, p. 314–347.

———1977, Triassic-Liassic deposits in Morocco and eastern North America: American Association of Petroleum Geologists Bulletin, v. 61, p. 79–99.

11. NUCLEAR MAGNETIC RESONANCE STUDIES OF ORGANIC-MATTER-RICH SEDIMENTARY ROCKS OF SOME EARLY MESOZOIC BASINS OF THE EASTERN UNITED STATES

Patrick G. Hatcher and Lisa A. Romankiw

INTRODUCTION

As part of a multidisciplinary study to understand burial history and hydrocarbon potential of organic-matter-rich lacustrine shales and the role of sedimentary organic matter in ore-forming processes in early Mesozoic basins of the Eastern United States, we examined organic matter associated with these lacustrine shales by using solid-state ^{13}C nuclear magnetic resonance (NMR). This technique provides a direct, nondestructive analysis of the chemical structural composition of organic matter. Maturation, rank, the hydrocarbon-generating potential of organic matter, and possibly the time-temperature history of the sediment can be directly correlated to the chemical structural composition of kerogen. Kerogen derived from the decomposed remains of nonvascular plants (algae) and microorganisms is highly aliphatic in composition and, when it undergoes maturation or thermal alteration, yields abundant amounts of liquid hydrocarbons (Breger, 1963; Tissot and Welte, 1978). This type of kerogen is said to be oil-prone. Vascular plant remains, however, yield humic coal-like kerogen that is highly aromatic and prone to producing natural gas rather than oil (Forsman, 1963; Hunt, 1979). As maturation progresses beyond the "oil window," both types of kerogen produce natural gas and their chemical structural compositions become exceedingly aromatic. The temperature of formation of many commercial ore deposits is thought to be the same as that of hydrocarbon generation (50–200° C). If changes in the chemical structural nature of organic matter could be correlated to the temperature of hydrothermal events, we could develop an accurate and sensitive means of delineating regions of possible hydrothermal activity.

The sedimentary units that constitute part of the Newark Supergroup show evidence that both vascular and nonvascular plants contributed to the lacustrine organic matter (Olsen and others, 1982). In many instances, coalified plant remains (phytoclasts) are found within and associated with finely laminated organic-matter-rich shales. Because both types of organic matter contributed to the lacustrine sediments, we could presumably discriminate the source of organic matter based simply on the structural nature of the kerogen as determined by NMR. If the kerogen were highly aromatic, we could conclude that vascular plant residues were the dominant source, whereas if it were mostly aliphatic, we would assign it a predominantly algal or microbial source (Breger and others, 1983).

Unfortunately, maturation above a coal rank equivalent to high-volatile A bituminous coal (vitrinite reflectance $R_o \cong 1.0$) or carbonization induced by hydrothermal stress leads to loss of the aliphatic structures in kerogen (both algal and humic). This effect negates the possibility of using aromaticity as a source discriminant in rocks having experienced a high degree of maturation or heating (Hatcher and others, 1983). The source of organic matter can only be discerned for low-rank kerogen (below high-volatile A bituminous coal). The loss of aliphatic structures can be gauged by NMR and consequently used as a guide to the degree of maturation or temperature of hydrothermal activity if the source of the organic matter is known.

NMR studies of coal and coalified logs have shown that aromaticity (f_a) can be correlated with rank and, therefore, used as a rank parameter (Miknis and others, 1981; Wilson and others, 1984). Figure 11.1 shows NMR spectra for a series of coalified logs that range in rank from lignite to low-volatile bituminous coal. Note that all spectra show two major, broad peaks at 130 and 30 ppm for aromatic and aliphatic carbons, respectively. Aromaticity, measured as the ratio of the area for aromatic carbons to the total peak area, increases progressively with rank, consistent with other results from studies of coal (Wilson and others, 1984). Anthracite is essentially 100 percent aromatic. Thus, changes in the chemical structural composition of phytoclasts, namely the aromaticity, can be used to determine the degree of coalification or thermal stress if other processes such as weathering or fusinization have not affected the phytoclasts. Studies of coalified logs additionally demonstrate that the relative intensity of specific peaks of lower rank coal, notably the smaller phenolic-carbon and methoxyl-carbon peaks at 150 and 55 ppm, respectively, that are superimposed over the larger peaks for aromatic and aliphatic carbons can be used to discriminate between lignite, subbituminous, and bituminous coal as is shown in figure 11.1 (Hatcher and others, 1982). At such low ranks, measurements

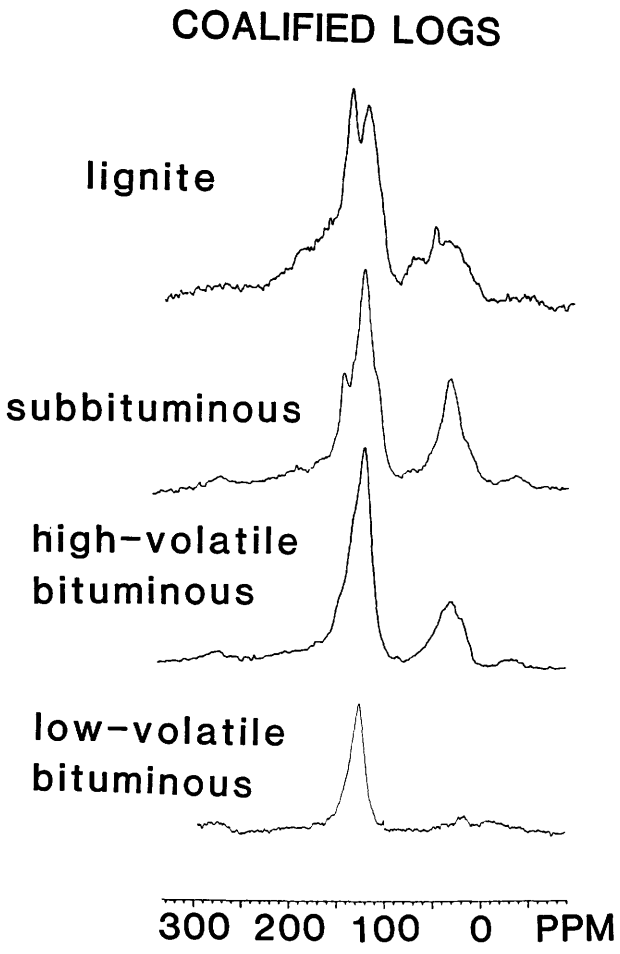

FIGURE 11.1.—Solid-state ^{13}C NMR spectra of logs that have been coalified to various ranks as indicated.

such as carbon content and vitrinite reflectance are not as sensitive rank parameters.

In the current investigation of organic matter from early Mesozoic basins of the Eastern United States, our preliminary focus is to establish the rank of the organic matter or its level of maturation by using phytoclasts isolated from lacustrine organic-matter-rich shales and associated units. We also plan to isolate the kerogen from these shales in order to compare its structural composition with that of the phytoclasts. This comparison may allow us to determine its source and degree of maturation. In this preliminary report we present results of our study of phytoclasts.

SAMPLING AND EXPERIMENTAL WORK

Coalified phytoclasts were collected from shales, sandstones, and tufas associated with Triassic and Jurassic rocks from the Newark, Hartford, Culpeper, and Taylorsville basins. Table 11.1 lists the samples, their locations, stratigraphic positions, and ages. Air-dried phytoclast samples were removed from the rock matrix by hand with the aid of forceps or spatulas and were ground in a mortar and pestle before analysis.

For solid-state ^{13}C NMR analysis, approximately 300 mg of the ground samples was placed in a Kel-F spinner and inserted into the NMR probe. The spectra were obtained on approximately 10,000 scans by employing the technique of magic-angle spinning with cross polarization (Schaefer and others, 1975; Bartuska and others, 1977). The scale, in parts per million (ppm) chemical shift downfield of tetramethylsilane, is a relative frequency-based scale that denotes the types of carbon in a sample (aliphatic, aromatic, alcoholic, and so on). Elemental analyses (C, H, N, O, and ash by difference) were performed on a Carlo Erba 1106 elemental analyzer using approximately 1 mg of sample per analysis. These data are reported on a moisture- and ash-free basis.

RESULTS AND DISCUSSION

ELEMENTAL COMPOSITIONS

Elemental compositions reported on an ash-free basis and corresponding atomic H/C and O/C ratios of phytoclasts are listed in table 11.2. Carbon contents range from 71 to 91 percent. The highest values are characteristic of high-rank coal (anthracite or semianthracite), whereas the lowest values (71.11 and 74.15) are characteristic of subbituminous coal or lignite. On the basis of carbon contents used as a rank parameter, the phytoclasts range from subbituminous coal to anthracite. The samples appear to cluster at the extremes of this range. The elemental hydrogen and oxygen data show a similar trend.

Plotting elemental compositions on a van Krevelen diagram, where atomic H/C ratios are plotted against atomic O/C ratios, provides a good approximation of the level of maturation or degree of coalification. Vitrains or coalified xylem tissue plots on a trendline shown in figure 11.2. Coalified wood tracks this trendline quite well, whereas wood or coal that has been carbonized (heated to temperatures above those normally associated with coalification) or fusinized deviates from the trend, effectively cutting across the normal coalification trend (van Krevelen, 1950). At higher ranks (for example, anthracite), the elemental composition of the end product of carbonization or

TABLE 11.1.—*Location, stratigraphic position, and age of phytoclast samples from Eastern Mesozoic basins*

Sample	Location	Age
Newark basin:		
NB584–14 . .	H and K quarry near Chalfont, PA; Skunk Hollow member of Olsen (1984) of the Lockatong Formation.	Late Carnian.
NB584–16 . .	H and K quarry near Chalfont, PA; Skunk Hollow member of Olsen (1984) of the Lockatong Formation.	Late Carnian.
NB584–24 . .	Pompton Lakes, NJ; middle carbon-rich laminated zone of the Towaco Formation.	Hettangian.
NB584–25 . .	Pompton Lakes, NJ; tufa-encrusted phytoclast from the lower laminated zone of the Towaco Formation.	Hettangian.
NB584–26 . .	Gill quarry, off Potshot road near Fairview Village, PA; Weehawken member of Olsen (1984) of the Lockatong Formation.	Late Carnian.
SP1	State Park quarry near Eagleville, PA; Gwynedd 1 member of Olsen (1984) of the Lockatong Formation.	Late Carnian.
SP3	State Park quarry near Eagleville, PA; Gwynedd 1 member of Olsen (1984) of the Lockatong Formation.	Late Carnian.
A. Feranti . .	A. Feranti quarry near Bernardsville, NJ; near top of Feltville Formation approx. 10 m below the Preakness Basalt.	Hettangian.
Blue Brook	Ravine along Blue Brook, 1 km south of Lake Surprise near Feltville, NJ; Feltville Formation, 13 m above the Orange Mountain Basalt.	Hettangian.
Hartford basin:		
Portland, CT	Longbrook, CT; near the base of the Portland Formation.	Pliensbachian.
Portland, MA	Suffield, MA; middle to lower part of Portland Formation.	Pliensbachian.
Culpeper basin:		
CB784–13 . .	Licking Creek locale, Midland, VA; Midland Formation fish bed.	Hettangian.
Culpeper log	Millbrook quarry, Thoroughfare Gap, VA; Waterfall Formation.	Sinemurian/ Pliensbachian.
Taylorsville basin:		
ASH–1	479 ft in a core taken 1 mile south of Taylorsville, VA; Falling Creek Member of Doswell Formation.	Middle Carnian.

fusinization is the same as that of coalification. However, intermediate carbonized products tend to have higher O/C ratios and lower H/C ratios.

The elemental data for phytoclasts from Eastern U.S. early Mesozoic basins are plotted in figure 11.2. Note that the points do not follow the coalification trendline but cut across it, as would be expected from a carbonization or fusinization process. If the logs were carbonized, then the phytoclasts have been heated to temperatures higher than those expected from normal geothermal gradients. Phytoclasts from the Jurassic Towaco Formation, which are subbituminous-coal rank, appear to be essentially unaffected by this heating because their elemental compositions plot on or near the coalification line. Phytoclasts from the Jurassic Feltville Formation, which is stratigraphically lower than the Towaco Formation, appear to be carbonized. We are uncertain whether this heating is from localized thermal events at the sampling site (for example, basalt flows or diabase intrusions) or from regional heating. The latter is more likely, considering that all phytoclasts from the Triassic Lockatong Formation are thermally altered regardless of their proximity to possible local heat sources.

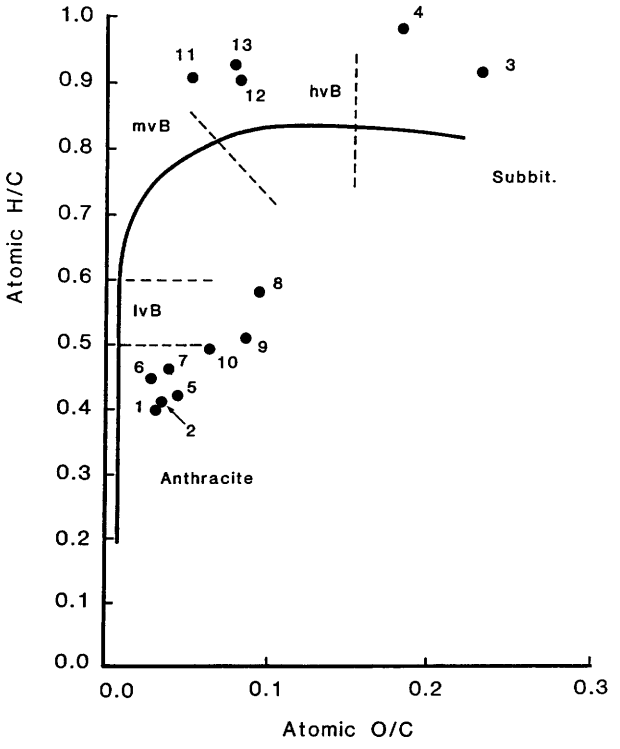

FIGURE 11.2.—van Krevelen plot of the elemental compositions of phytoclasts from Eastern U.S. early Mesozoic basins. The sample numbers correspond to those in table 11.2. The developmental line is that of vitrains (van Krevelen, 1950) and coalified logs (Hatcher and others, 1982). Subbit., subbituminous coal; B, bituminous coal; lv, mv, hv, low-, middle-, and high-volatile.

TABLE 11.2.—*Elemental data for phytoclasts*

[C, H, N, and O in weight percent, on a moisture- and ash-free basis, direct analysis. Data from Hatcher and others, 1982]

Sample	C	H	N	O	H/C	O/C
Newark basin:						
1. NB584-14	90.50	3.07	2.42	4.00	0.41	0.033
2. NB584-16	91.00	3.00	2.40	3.60	.40	.030
3. NB584-24	71.11	5.42	1.98	21.5	.92	.23
4. NB584-25	74.15	6.03	1.85	18.0	.98	.18
5. NB584-26	88.69	3.11	3.15	5.0	.42	.043
6. SP1	90.30	3.37	2.16	4.17	.45	.028
7. SP3	89.94	3.48	2.05	4.52	.46	.038
8. A. Feranti	84.25	4.07	1.14	10.5	.58	.094
Hartford basin:						
9. Portland, Conn.	85.63	3.64	.92	9.82	.51	.086
10. Portland, Mass.	86.44	3.54	2.58	7.44	.49	.065
Culpeper basin:						
11. CB784-13	85.46	6.45	2.17	5.92	.91	.052
12. Culpeper log	82.80	6.27	2.10	9.00	.91	.082
Taylorsville basin:						
13. ASH-1	82.76	6.38	2.17	8.68	.92	.079

As pointed out by van Krevelen (1950), fusinization could also lead to changes in elemental composition that are similar to those observed for carbonization. In fact, this observation has contributed to the predominant belief that fusinization is, in part, though not solely, a carbonization process. Visual inspection of all recovered phytoclasts suggests that fusinization was not important in causing the observed changes in elemental compositions. First, all phytoclasts have a vitreous appearance on a macroscopic scale, a characteristic that is atypical of fusinite. Second, the phytoclasts appear intact: they have retained many of the original morphological features of the original plant. Fusinization at an early depositional stage, on the other hand, would have rendered the phytoclasts brittle, preventing the observed morphological preservation during compaction and lithification.

NMR DATA

NMR spectra of phytoclasts are shown in figure 11.3. Note that most spectra show a broad aromatic peak at about 130 ppm and associated spinning sidebands (denoted by an asterisk). Aliphatic carbons are represented by a broad peak at about 30 ppm. Other peaks observed in some spectra are at 150 ppm (phenolic carbon), 175 ppm (carboxyl carbon), and 200 ppm (carbonyl carbon). These peaks, representing oxygenated functional groups, are usually present only in low-rank coals (fig. 11.1; Hatcher and others, 1982).

The NMR data show that the ranks of phytoclasts vary considerably, from subbituminous coal to anthracite, which is consistent with the elemental data. The phytoclasts from the Lockatong and Feltville Formations in the Newark basin and the Portland Formation in the Hartford basin all appear to be essentially aromatic in nature with virtually no aliphatic character. The spectra of these samples are similar to those of coal and coalified logs (fig. 11.1) having ranks greater than medium-volatile bituminous coal (Miknis and others, 1981). This rank is equivalent to or greater than that considered to be the late stages of oil generation (oil window) for kerogen (Tissot and Welte, 1978). Thus, if the associated shales were good source rocks for petroleum, they probably have already produced it and now produce only thermogenic gas.

Phytoclasts from the Portland and Feltville Formations have NMR spectra showing a peak at 150 ppm. This peak, that of phenolic carbon, is usually absent from coalified logs having ranks greater than high-volatile A bituminous coal. The coalification process effectively induces a rapid decrease of phenolic carbon above this rank. The spectra of the Portland and Feltville phytoclasts are unusual in that their high aromaticity and elemental data implies a high rank, whereas the presence of phenolic carbon implies that structures usually associated with low-rank coal are still present. We suggest that carbonization, rather than coalification, is responsible for these effects. During carbonization the aliphatic groups would be lost more rapidly than phenolic groups. Thus, the atomic

H/C ratio would decrease more rapidly than the atomic O/C, and the aromaticity would increase faster than the rate of loss of phenolic peaks in the NMR spectra.

Four samples have NMR spectra that show significant amounts of aliphatic carbon. Two of these samples are from the Jurassic Towaco Formation in the Newark basin, one is from the Jurassic Midland Formation in the Culpeper basin, and the fourth is from the Triassic Doswell Formation in the Taylorsville basin. The relative intensity of the aliphatic peak (lower f_a) and the presence of a peak or shoulder at 150 ppm in the spectra indicate that these samples are relatively low rank — high-volatile bituminous to subbituminous coal. Again the NMR data are consistent with the elemental data for the phytoclasts.

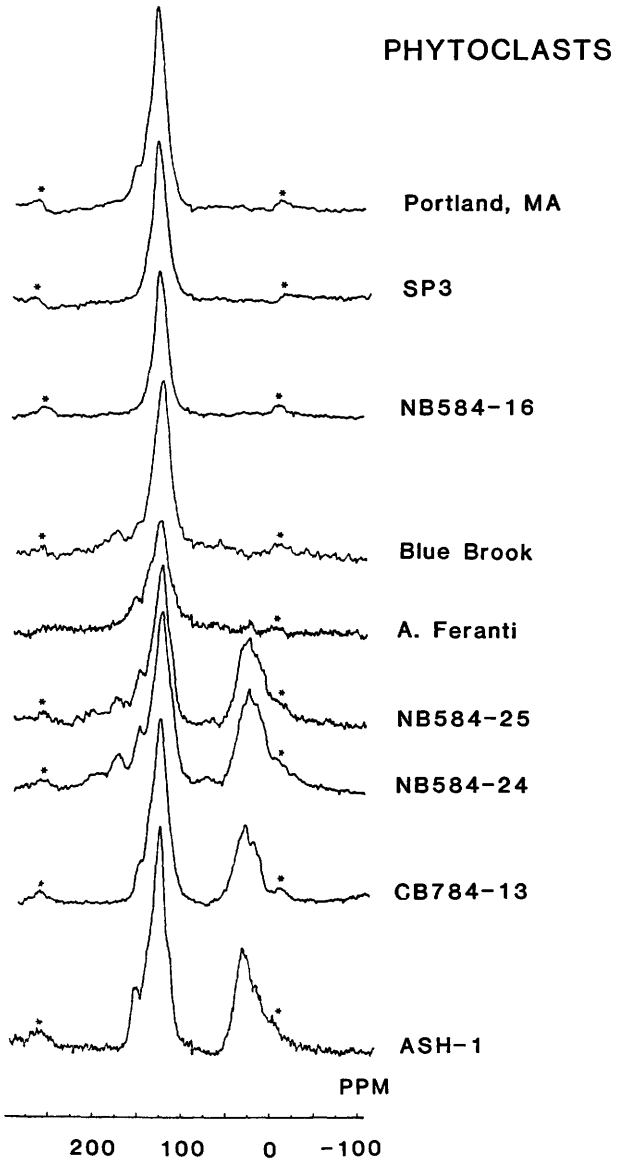

FIGURE 11.3.—Solid-state ^{13}C NMR spectra of phytoclasts. The asterisk denotes spinning sidebands.

CONCLUSIONS

Organic geochemical studies of phytoclasts suggest that the organic matter of continental sedimentary rocks of the Newark Supergroup shows a wide range of apparent maturation. However, there is no distinct gradational trend. The samples are either low in rank or are thermally altered to a rank of low-volatile bituminous coal or greater. The paucity of samples precludes any conclusions regarding an explanation for such behavior; however, the van Krevelen plot of the data suggests that the phytoclasts of higher rank have been carbonized rather than coalified. The data suggest that the samples have experienced heating greater than the normal geothermal gradient that induces coalification. The data are too limited to allow for a definite conclusion as to the timing of the thermal event, though it is noteworthy that no correlation of rank with age is observed. This might imply that the heating was of a regional nature. Indeed, the phytoclasts from younger Jurassic rocks in the Hartford basin have been carbonized whereas phytoclasts from older Triassic and Jurassic rocks from the Newark, Culpeper, and Taylorsville basins have not.

REFERENCES

Bartuska, V.J., Maciel, G.E., Schaefer, J., and Stejskal, E.O., 1977, Prospects for carbon-13 nuclear magnetic resonance analysis of solid fossil fuel materials: Fuel, v. 56, p. 354–358.

Breger, I.A., 1963, Origin and classification of naturally occurring carbonaceous substances, *in* Breger, I.A., ed., Organic geochemistry: New York, Pergamon, p. 50–86.

Breger, I.A., Hatcher, P.G., Romankiw, L.A., Miknis, F.P., and Maciel, G.E., 1983, Upper Devonian black shales of the Eastern United States—Organic geochemical studies—past and present, *in* Miknis, F.P. and McKay, J.F., eds., Geochemistry and chemistry of oil shales: American Chemical Society Symposium Series No. 230, p. 181–198.

Forsman, J.P., 1963, Geochemistry of kerogen, *in* Breger, I.A., ed., Organic geochemistry: New York, Pergamon, p. 148–182.

Hatcher, P.G., Breger, I.A., Szeverenyi, N., and Maciel, G.E., 1982, Nuclear magnetic resonance studies of ancient buried wood—II. Observations on the origin of coal from lignite to bituminous coal: Organic Geochemistry, v. 4, p. 9–18.

Hatcher, P.G., Romankiw, L.A., Szeverenyi, N.M., and Maciel, G.E., 1983, Solid-state ^{13}C NMR studies of kerogen in Upper Devonian shales of the Appalachian basin: Proceedings of the 1983 Eastern Oil Shale Symposium, Lexington, Ky., November 13–16, 1983, p. 217–224.

Hunt, J.M., 1979, Petroleum geochemistry and geology: San Francisco, Freeman, 617 p.

Miknis, F.P., Sullivan, M., Bartuska, V.J., and Maciel, G.E., 1981, Cross polarization magic-angle spinning ^{13}C NMR spectra of coals of varying rank: Organic Geochemistry, v. 3, p. 19–28.

Olsen, P.E., 1984, Comparative paleolimnology of the Newark Supergroup: A study of ecosystem evolution: New Haven, Conn., Yale University, unpub. Ph.D. thesis, 726 p.

Olsen, P.E., McCune, A.R., and Thomson, K.S., 1982, Correlation of the early Mesozoic Newark Supergroup by vertebrates, principally fishes: American Journal of Science, v. 282, p. 1–44.

Schaefer, J., Stejskal, E.O., and Buchdahl, R., 1975, High resolution carbon-13 nuclear magnetic resonance study of some solid glassy polymers: Macromolecules, v. 8, p. 291–296.

Tissot, B., and Welte, D.H., 1978, Petroleum formation and occurrence: Berlin, Springer-Verlag, 538 p.

van Krevelen, D.W., 1950, Graphical-statistical method for the study of structure and reaction processes of coal: Fuel, v. 29, p. 269–284.

Wilson, M.A., Pugmire, R.J., Karas, J., Alemany, L.B., Woolfenden, W.R., Grant, D.M., and Given, P.H., 1984, Carbon distribution in coals and coal macerals by cross polarization magic angle spinning carbon-13 nuclear magnetic resonance spectrometry: Analytical Chemistry, v. 56, p. 933–943.

12. STABLE-ISOTOPE CHARACTERIZATION OF ORGANIC MATTER IN THE EARLY MESOZOIC BASINS OF THE EASTERN UNITED STATES

Elliott C. Spiker

INTRODUCTION

The stable-isotopic composition of organic matter in the lacustrine shales of the early Mesozoic basins of the Eastern United States is being examined as part of a multidisciplinary study of the history of the basins and the role of organic matter in sedimentary ore deposits. The effects on organic matter of source differences, diagenesis, and maturation can combine to produce complexity that is difficult to interpret. For this reason, the analysis of several isotopes (^{13}C, ^{15}N, and deuterium) is useful because each isotope may behave differently, thus allowing a better distinction to be made between diagenetic processes and sources.

The source of sedimentary organic matter may be determined from its isotopic composition. Marine organic matter and terrestrial vascular plant remains can often be differentiated by their ^{13}C and ^{15}N compositions (Deines, 1980; Letolle, 1980). Source distinction on the basis of D/H ratio may also be possible because algae tend to have much less deuterium than do vascular land plants (Epstein and others, 1976; Estep and Hoering, 1980).

The early Mesozoic basins of the Newark Supergroup contained fresh or alkaline lakes and were not truly open-marine systems. The stable-isotope composition of lacustrine algae is expected to differ from that of marine algae and may reflect variations in productivity, species, and lake chemistry and salinity. Isotopic variations in the organic matter may therefore provide evidence for such changes in the Newark lacustrine systems. Also, comparison with ^{13}C and ^{18}O in associated primary carbonates, which reflect lake chemistry (Buchardt and Fritz, 1980; Magaritz and Turner, 1982; Spiker and Hatcher, 1984), may help confirm such changes.

Diagenesis and maturation of organic matter can have a significant isotope effect that needs to be understood to allow a better distinction of the source of the organic matter (Stuermer and others, 1978; Peters and others, 1981). Our previous studies have shown the possibility of significant carbon isotope fractionation during early diagenesis and the selective preservation of isotopically distinct biomolecules (Hatcher and others, 1983; Spiker and Hatcher, 1984). Also, humic acids and bitumens produced and mobilized during diagenesis and maturation may be isotopically distinctive because their sources may be different. For example, humic acids may be derived mostly from woody plant remains, whereas bitumens may be derived mostly from algal remains.

A potentially fruitful approach to these studies is to first determine the effects of diagenesis and maturation on organic matter of known source. By examining woody plant fragments (phytoclasts), separate from the finer grained organic matter (kerogen) in the whole-rock matrix, which is presumably derived mostly from aquatic sources, we can begin to delineate diagenetic and maturation effects on these different types of organic matter. Some preliminary results from

the Newark, Hartford, Culpeper, and Taylorsville basins are discussed here.

RESULTS AND DISCUSSION

The isotopic compositions of phytoclasts and kerogen from the Newark Supergroup are plotted against the corresponding H/C ratios in figure 12.1. Sample descriptions and a discussion of the elemental compositions of the phytoclasts are given by Hatcher and Romankiw (chapter 11, this volume). The H/C ratio of phytoclasts provides a good approximation of the level of maturation or coalification. Lower H/C ratios are characteristic of higher rank coal, while higher values are characteristic of subbituminous coal or lignite.

The $\delta^{13}C$ values of the phytoclasts range from about -20 to -27 per mil, similar to values of modern woody plants. No clear trend with maturation, which in this study is denoted by H/C ratios, is apparent. This lack of correlation is consistent with the apparent lack of significant ^{13}C fractionation during coalification (see Deines, 1980). The $\delta^{13}C$ of lignite is similar to that of low- and high-rank coals. Peters and others (1981) observed no significant ^{13}C fractionation during pyrolysis of wood in laboratory experiments simulating thermal maturation. They found only about a 0.5 per mil increase in the $\delta^{13}C$ of the heated peat samples in the H/C range observed here (about 0.9 to 0.4). Thus, it appears that much of the approximately 7 per mil range of $\delta^{13}C$ in the phytoclasts is due to original variations in the plants. Different samples from the same locality differ by at most only 1 per mil. $\delta^{13}C$ variations in woody plants typically reflect local environmental conditions. Apparently, the 7 per mil range in $\delta^{13}C$ primarily reflects differing environmental conditions during growth of the plants.

Also shown in figure 12.1 are the $\delta^{13}C$ values of the kerogen in the whole-rock matrix associated with phytoclasts at two localities. The $\delta^{13}C$ values of the kerogen samples are -27.5 and -30.9 per mil, similar to most values measured in modern lacustrine sediments, in the Green River Formation, and in marine organic matter of middle Cretaceous and older age (Deines, 1980; Maynard, 1981; Arthur and others, 1985). The $\delta^{13}C$ values of the kerogen are about 4 to 5.4 per mil more negative than those of the associated phytoclasts. $\delta^{13}C$ clearly distinguishes between the kerogen and the phytoclasts.

The difference in $\delta^{13}C$ between the two kerogen samples (3.4 per mil) may be primary, reflecting a change in source or possibly a shift in the $\delta^{13}C$ of the precursor lacustrine algae. Differences in the $\delta^{13}C$ of the kerogen could be interpreted as being due to differing contents of fine-grained woody debris. Thus, the 3.4 per mil difference between the two kerogens may be due to more land-plant carbon in the more ^{13}C-rich kerogen. Another possible cause is a shift in the $\delta^{13}C$ of the precursor lacustrine algae, corresponding to a change in lake chemistry and a shift in the $\delta^{13}C$ of dissolved carbonate in the lake. Comparison with $\delta^{13}C$ in primary carbonates should help confirm this possibility.

Much of the $\delta^{13}C$ difference between the two kerogen samples, however, is probably due to maturation. The more positive value is from the more mature sample, as indicated by its lower H/C. A similar ^{13}C enrichment in more mature samples was observed in thermal maturation experiments on algal organic matter by Peters and others (1981).

The δD values of the phytoclasts range from about -65 to -95 per mil, similar to values of modern woody plants. No correlation with H/C was observed, consistent with the results of Redding and others (1980) who found, at most, a 20 per mil increase in δD in "humic" kerogen and no trend in δD of coals of various ranks. However, Peters and others (1981) observed about a 60 per mil increase in the δD value of heated peat samples, as H/C decreased from about 0.9 to 0.4. They attributed this deuterium enrichment during heating to the loss of deuterium-depleted methane. This apparent discrepancy needs further study. Although the phytoclasts have about a 30 per mil range, the δD values of different samples from the same locality differ by at most only about 8 per mil, probably reflecting local environmental conditions as $\delta^{13}C$ does.

All the δD values are somewhat low relative to modern trees in the low latitudes. δD values of about -70 per mil are more typical of regions of relatively low average temperature (about 7°C) or high latitude (Yapp and Epstein, 1982). This deuterium depletion may be due to the presence of a small amount of resin or possibly adsorbed algal derived material from the matrix sediment, which can be highly depleted in deuterium. Further examination of these hypotheses awaits δD analysis of the kerogen derived mostly from lacustrine sources, which will also help us to determine the δD of the lake water. The paleoclimatic significance of these data can then be considered.

The $\delta^{15}N$ values of the phytoclasts range from about 4 to 10 per mil, similar to values of modern woody plants, though more positive than is typical.

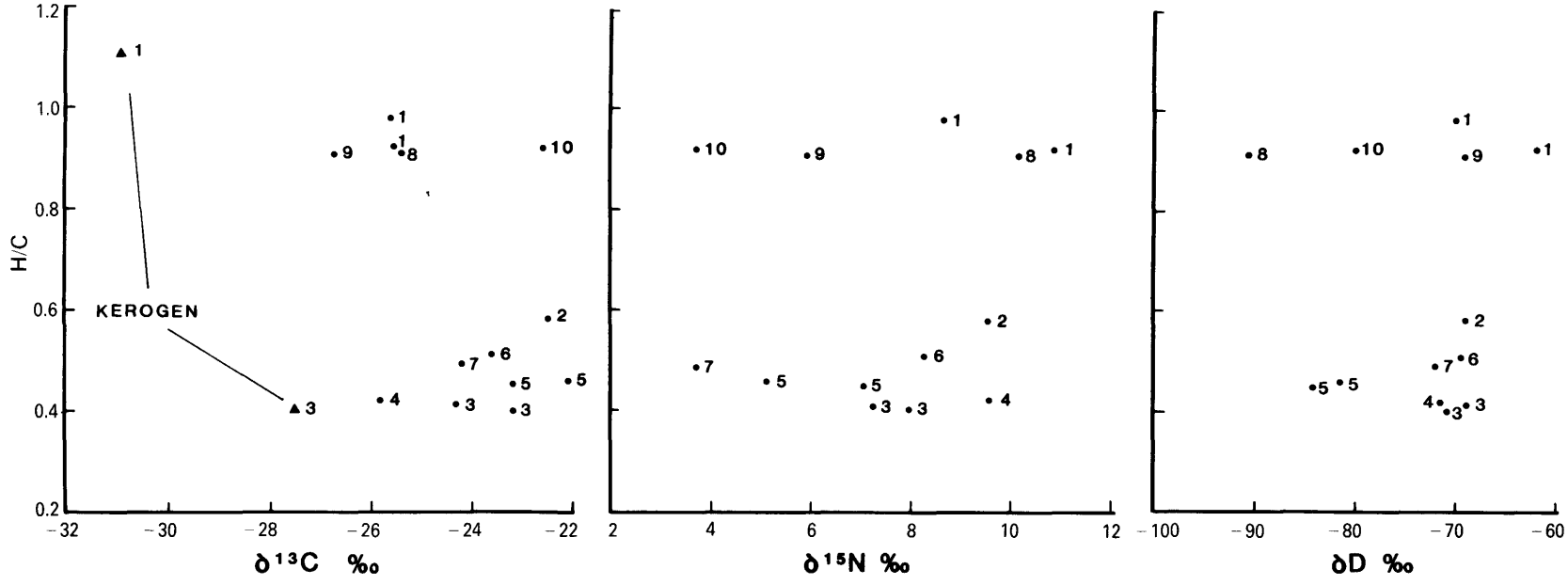

FIGURE 12.1.—Stable-isotope ($\delta^{13}C$, δD, $\delta^{15}N$) ratios of phytoclasts and $\delta^{13}C$ of two associated whole-rock kerogen samples (solid triangles), plotted against the respective atomic H/C ratios. Newark basin (N.J.-Pa.): 1, Towaco Formation; 2, Feltville Formation; 3, Lockatong Formation, Skunk Hollow member of Olsen (1984); 4, Lockatong Formation, Weehawken member of Olsen (1984); 5, Lockatong Formation, Gwynedd 1 member of Olsen (1984). Hartford basin (Conn.-Mass.): 6, Portland Formation in Connecticut; 7, Portland Formation in Massachusetts. Culpeper basin (Va.): 8, Waterfall Formation; 9, Midland Formation. Taylorsville basin (Va.): 10, Doswell Formation, Falling Creek Member.

$\delta^{15}N$ does not correlate with H/C. Few data for $\delta^{15}N$ in shale and coal have been published (see LeTolle, 1980), and no $\delta^{15}N$ trends with maturation have been reported. The $\delta^{15}N$ of different samples from the same locality differ by at most 2 per mil, possibly reflecting local environmental conditions as suggested for $\delta^{13}C$ and δD. The relatively high nitrogen content of these phytoclasts ($N/C \cong 0.022$; see Hatcher and Romankiw, this volume, table 11.2), may be due to the adsorption of nitrogen-rich compounds from algal or microbial sources in the matrix sediment. These sources may cause the somewhat high $\delta^{15}N$ values in the phytoclasts, because organic nitrogen from algal and microbial sources tends to be enriched in ^{15}N. $\delta^{15}N$ analysis of the kerogen in the rock matrix is needed to confirm this possibility.

CONCLUSIONS

Preliminary isotopic analyses of C, H, and N in the phytoclasts show no trend with maturation. The range of isotope values in the phytoclasts is mostly premetamorphic and primarily reflects variations in the original woody plants. The isotope values observed here are generally within the range of values found in modern vascular plants and peat.

$\delta^{13}C$ values of two whole-rock kerogen samples are 4 to 5 per mil more negative than the associated phytoclasts, suggesting that $\delta^{13}C$ may be a useful indicator of woody debris in these lacustrine sediments. Variations in the isotopic composition of the whole-rock kerogen may be due to changes in source composition or to the effects of maturation. Comparison with associated phytoclasts is helpful in interpreting these variations. Further work will be greatly facilitated by more extensive sampling to establish regional patterns and by analyzing samples representing more intermediate stages of maturation.

REFERENCES

Arthur, M.A., Dean, W.E., and Claypool, G.E., 1985, Anomalous ^{13}C enrichment in modern marine organic carbon: Nature (in press).

Buchardt, B., and Fritz, P., 1980, Environmental isotopes as environmental and climatological indicators, *in* Fritz, P., and Fontes, J.C., eds., Handbook of environmental isotope geochemistry, v. 1: Amsterdam, Elsevier, p. 473–504.

Deines, P., 1980, The isotopic composition of reduced organic carbon, *in* Fritz, P., and Fontes, J.C., eds., Handbook of environmental isotope geochemistry, v. 1: Amsterdam, Elsevier, p. 329–406.

Epstein, S., Yapp, C.J., and Hall, J., 1976, The determination of the D/H ratio of non-exchangeable hydrogen in cellulose extracted from aquatic and land plants: Earth and Planetary Science Letters, v. 30, p. 241–251.

Estep, M.F., and Hoering, T.C., 1980, Biogeochemistry of the stable hydrogen isotopes: Geochimica et Cosmochimica Acta, v. 44, p. 1197–1206.

Hatcher, P.G., Spiker, E.C., Szeverenyi, N.M., and Maciel, G.E., 1983, Selective preservation and origin of petroleum-forming aquatic kerogen: Nature, v. 305, p. 498–501.

Letolle, R., 1980, Nitrogen-15 in the natural environment, *in* Fritz, P., and Fontes, J.C., eds., Handbook of environmental isotope geochemistry, v. 1: Amsterdam, Elsevier, p. 407–433.

Magaritz, M., and Turner, P., 1982, Carbon cycle changes of the Zechstein Sea: Isotopic transition zone in Marl Slate: Nature, v. 297, p. 389–390.

Maynard, J.B., 1981, Carbon isotopes as indicators of dispersal patterns in Devonian-Mississippian shales of the Appalachian Basin: Geology, v. 9, p. 262–265.

Olsen, P.E., 1984, Comparative paleolimnology of the Newark Supergroup — A study of ecosystem evolution: New Haven, Conn., Yale University, unpub. Ph.D. thesis, 726 p.

Peters, K.E., Rohrback, B.G., and Kaplan, I.R., 1981, Carbon and hydrogen stable isotope variations in kerogen during laboratory — Simulated thermal maturation: American Association of Petroleum Geologists Bulletin, v. 65, p. 501–508.

Redding, C. E., Schoell, M., Monin, J.C., and Derand, B., 1980, Hydrogen and carbon isotopic composition of coal and kerogen, *in* Douglas, A.G., and Maxwell, J.R., eds., Advances in organic geochemistry 1979: Oxford, Pergamon, p. 711–723.

Spiker, E.C., and Hatcher, P.G., 1984, Carbon isotope fractionation of sapropelic organic matter during early diagenesis: Organic Geochemistry, v. 5, p. 283–290.

Stuermer, D.H., Peters, K.E., and Kaplan, I.R., 1978, Source indicators of humic substances and proto-kerogen: Stable isotope ratios, elemental compositions and electron spin resonance spectra: Geochimica et Cosmochimica Acta, v. 42, p. 989–997.

Yapp, C.J., and Epstein, S., 1982, Climatic significance of the hydrogen isotope ratios in tree cellulose: Nature, v. 297, p. 636–639.

13. GEOCHEMICAL AND ISOTOPIC CHARACTERIZATION OF ORGANIC MATTER IN ROCKS OF THE NEWARK SUPERGROUP

Lisa M. Pratt, April K. Vuletich, and Ted A. Daws

INTRODUCTION

Sixty-five samples of Newark Supergroup rocks collected from six of the early Mesozoic basins exposed in the Eastern United States have been studied. Organic carbon (C_{org}) and carbonate carbon (C_{carb}) contents of the samples were determined, and Rock-Eval pyrolysis was used to characterize the composition and thermal maturity of the organic matter. Results of these analyses indicate that many sedimentary units of latest Triassic to Jurassic age exposed in the Hartford, Newark, Culpeper, Richmond, Taylorsville, and Deep River (Sanford) basins are thermally mature with respect to petroleum generation. The extractable organic matter in four samples of the Jurassic Towaco Formation in the Newark basin was studied in detail by gas chromatography. Rocks from the Towaco Formation are less thermally altered and are immature to marginally mature. Nearly all of the older Triassic samples and a few of the latest Triassic to Jurassic samples are highly thermally altered but may still have some potential for dry gas generation. Carbon isotopic ratios ($\delta^{13}C$) of the total organic matter were determined for 39 samples from the Newark, Richmond, Culpeper, and Hartford basins. For 27 of these samples, the $\delta^{13}C$ and $\delta^{18}O$ values of whole-rock carbonate also were determined. Results of the isotopic analyses suggest that these four basins differ significantly in source of organic matter and water chemistry.

THERMAL MATURITY

The temperature of maximum pyrolytic yield (T_{max}) determined for organic matter during Rock-Eval pyrolysis is a useful index of thermal maturity. Peak petroleum and wet-gas generation occurs during the catagenic stage of thermal alteration and is indicated by T_{max} values between about 435°C and 460°C (Tissot and Welte, 1978). Table 13.1 shows the pyrolytic data for those samples that produced measurable quantities of hydrocarbons and yielded reliable T_{max} values. Samples from many of the upper Triassic and Jurassic formations in the Eastern U.S. early Mesozoic basins have T_{max}values indicative of a mid-catagenic stage of alteration. The Towaco samples from the Newark basin are unusual in that they are characterized by relatively low T_{max} values and are in a late diagenetic to early catagenic stage of thermal alteration. Data are not shown for rocks that are highly thermally altered and did not yield measurable quantities of hydrocarbons below 550°C; this category includes samples of the Balls Bluff Siltstone in the Culpeper basin, Stockton and Lockatong Formations in the Newark basin, Cumnock Formation in the Deep River (Sanford) basin, and some of the samples from the Blackheath coal measures in the Richmond basin.

The observed degree of thermal maturity, together with assumptions about past geothermal gradients and the rate of burial and uplift, permits some constraints to be placed on the maximum depth of burial. Assuming the thermal gradient was about 50°C km^{-1} during rifting and cooled to about 30° km^{-1} over a period of 50 Ma, effects of a rapid burial history can be compared with effects of a slower burial history. Assuming that the Towaco Formation was at maximum burial depth for 10 Ma, if it underwent relatively rapid burial and reached maximum depth of burial while the thermal gradient was 40°C km^{-1}, then the maximum burial depth was probably no more than 1.5 km. If the Towaco Formation was buried more slowly and reached maximum burial depths after the thermal gradient had cooled to 30° km^{-1}, then the maximum burial depth was probably about 2 km.

TABLE 13.1.—*Temperatures of maximum pyrolytic yield determined by Rock-Eval pyrolysis for samples from six of the exposed early Mesozoic basins in the Eastern United States*

[T_{max} values (in degrees Celsius) between about 435 and 460 indicate catagenic stage of maturation]

Basin	Lithologic unit	No. of samples analyzed	T_{max}
Culpeper	Midland Formation	4	445
Taylorsville	Falling Creek Member of Doswell Formation.	2	437
Newark	Towaco Formation	5	426
Newark	Feltville Formation	1	443
Richmond	Blackheath coal	5	455
Richmond	Otterdale Sandstone of Shaler and Woodworth (1899).	2	452
Deep River (Sanford)	Cumnock Formation	2	451
Hartford	Portland Formation	1	441

TYPES OF ORGANIC MATTER

The type of organic matter preserved in Newark Supergroup strata is highly variable. The organic matter in rocks that are not highly thermally altered and contain more than about 0.2 percent organic carbon can be usefully described in terms of hydrogen index (HI) and oxygen index (OI) from Rock-Eval pyrolysis (Espitalie and others, 1977). These terms are derived, respectively, from the pyrolytic hydrocarbon and CO_2 yields normalized to the organic carbon content. Compositional data on the samples listed in table 13.1 are given in figure 13.1. Upper Triassic and Lower Jurassic samples from the Hartford, Newark, Culpeper, Deep River (Sanford), and Taylorsville basins contain moderately hydrogen-rich types of organic matter (Type II) that are probably derived mostly from lacustrine-algal debris with variable proportions of vascular plant debris. The position along the HI axis of samples from the various basins is related to both original hydrogen content of the organic matter and to thermal maturity. Thus, samples with HI values of about 200 to 300 mg/g C_{org} (Deep River (Sanford), Richmond, Culpeper) may have originally been as hydrogen-rich as the less thermally altered samples with HI values of 300 to 400 mg/g C_{org} (Newark, Taylorsville, Hartford). Samples analyzed from the Richmond basin contain mostly hydrogen-poor organic matter that is probably derived from a swamp-vascular flora. The low oxygen content of samples from the Blackheath coal measures in the Richmond basin is probably related to their being in a middle to late catagenic stage of thermal alteration.

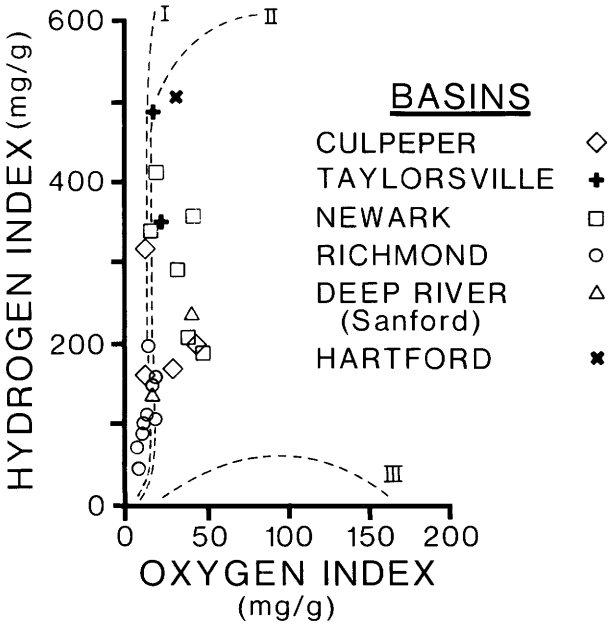

FIGURE 13.1.—Plot showing hydrogen indexes versus oxygen indexes determined by Rock-Eval pyrolysis. Lines I, II, and III are inferred maturation pathways for three kerogen types defined by Espitalie and others (1977).

EXTRACTABLE ORGANIC MATTER

Four samples of the Towaco Formation were extracted with chloroform and gave moderate to high yields of extractable organic matter (600–2900 ppm). The aliphatic hydrocarbons were studied by capillary gas chromatography (fig. 13.2). Pristane and phytane are dominant compounds in all samples. Two of the samples have a smooth distribution of *n*-alkanes with a

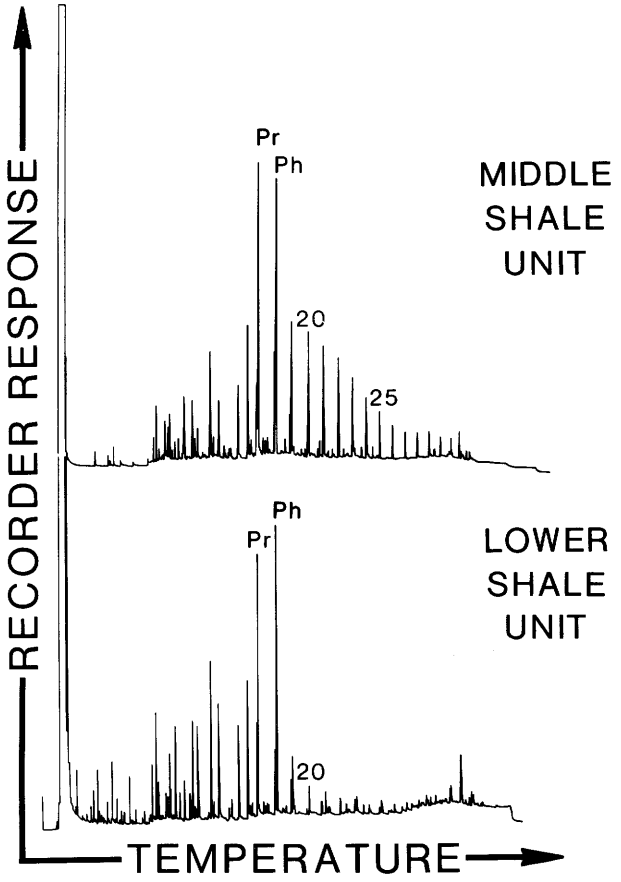

FIGURE 13.2.—Capillary gas chromatograms for samples of the Towaco Formation from the Newark basin. In both samples, pristane (Pr) and phytane (Ph) are dominant compounds and the Pr/Ph ratio is close to 1. Upper chromatogram shows relatively abundant and smoothly distributed *n*-alkanes (numbered peaks) and a single maximum at *n*-C_{19}. Lower chromatogram shows mostly light branched and cyclic compounds.

single maximum at n-C_{19} (upper chromatogram, fig. 13.2), whereas the other two samples contain mostly light branched and cyclic compounds (lower chromatogram, fig. 13.2). Both types have pristane/phytane ratios close to 1 and contain a diverse and abundant suite of polycylic biomarkers in the elution range of n-C_{26} to n-C_{33}. The overall distribution of compounds shown on the gas chromatograms supports an interpretation of a late diagenetic to early catagenic stage of thermal alteration for these samples (Tissot and Welte, 1978). The n-alkane maximum at n-C_{19} as well as the low abundance and lack of odd-carbon predominance in the heavier n-alkanes suggests that the extractable organic matter in these samples is largely algal or bacterial in origin (Phillipi, 1965; Han and Calvin, 1969; Powell and McKirdy, 1973).

CARBON ISOTOPIC RATIOS OF ORGANIC MATTER

Carbon isotopic ratios of total organic matter were determined for 39 samples from the Newark, Richmond, Culpeper, and Hartford basins. Figure 13.3 shows a crossplot of $\delta^{13}C_{org}$ and C_{org} data. With one exception, values of $\delta^{13}C_{org}$ for rocks from the Richmond basin (range -22 to -27 per mil) are heavier than those for rocks from the Newark, Culpeper, and Hartford basins (range -25 to -32 per mil). In conjunction with the pyrolysis data, this suggests that swamp-vascular deposits in these basins have heavier $^{13}C_{org}$ values than do lacustrine-algal deposits.

There is a marked difference in $\delta^{13}C_{org}$ values between the Jurassic Towaco Formation (average $\delta^{13}C_{org} = -30.9$) and the Triassic Stockton and Lockatong Formations (average $\delta^{13}C_{org} = -27.2$) in the Newark basin (fig. 13.4). The Triassic samples have about a 3 per mil range of $\delta^{13}C_{org}$ values, the samples with abundant organic matter being 0.5 to 1.0 per mil heavier than the samples with less organic matter. Thermal cracking and loss of isotopically light volatiles may account for the somewhat heavier $\delta^{13}C_{org}$ values of the organic-matter-rich Triassic samples, but differences in paleoenvironmental conditions in the Newark basin are probably the major cause of the 4 per mil shift toward lighter $\delta^{13}C_{org}$ values from the Triassic to Jurassic. Paleoenvironmental factors such as temperature, water chemistry, and extent of mixing between water layers can strongly influence $\delta^{13}C$ values of sedimented organic matter (Wong and Sackett, 1978; Rau and others, 1982).

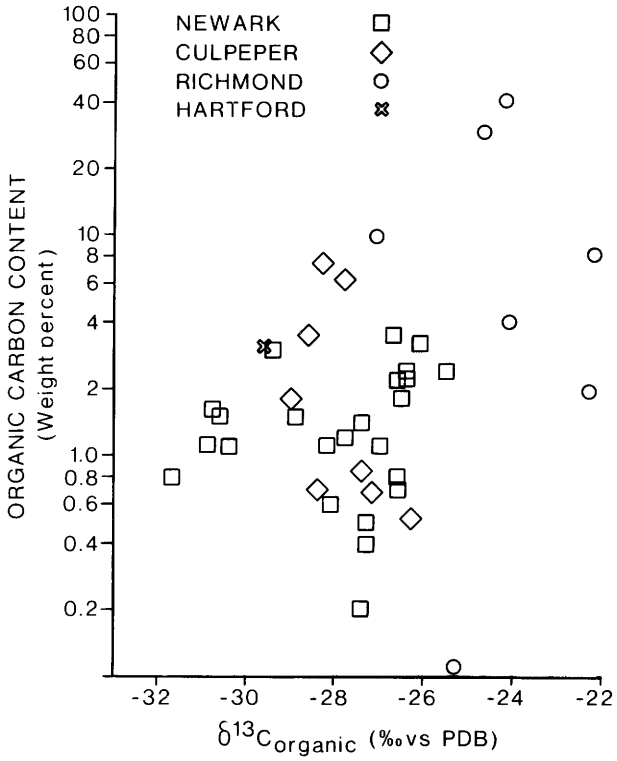

FIGURE 13.3.—Plot showing organic carbon content versus $\delta^{13}C_{org}$ for samples from the Newark, Culpeper, Richmond, and Hartford basins. Samples from the Richmond basin are isotopically heavier (less negative) than samples from the other basins regardless of the organic-carbon content. PDB, Peedee belemnite standard.

CARBON AND OXYGEN ISOTOPIC RATIOS OF CARBONATES

Values of $\delta^{13}C$ and $\delta^{18}O$ for whole-rock carbonate were determined for 27 samples from the Newark, Culpeper, Richmond, and Hartford basins (fig. 13.5). Although the mineralogy and origin of the carbonate have yet to be determined, it is worth noting that the carbonate samples from these four basins plot in four distinct regions on figure 13.5. Numerous primary paleoenvironmental and subsequent diagenetic factors could have influenced this isotopic pattern (see, for example, Keith and Weber, 1964; Hudson and Friedman, 1976; Irwing and others, 1977; Kroopnick and others, 1977). The wide range of $\delta^{18}O$ values, however, suggests that evaporation may have been a principal factor governing the isotopic composition of water in these basins (Craig, 1961) and, consequently, the isotopic composition of primary and early diagenetic carbonates. It is inferred that open-basin circulation would

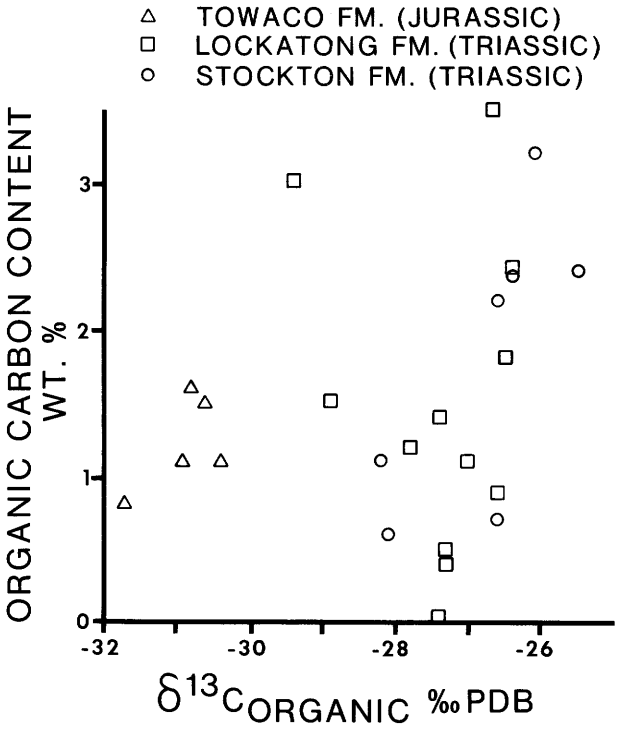

FIGURE 13.4.—Plot showing organic carbon contents versus $\delta^{13}C_{org}$ for samples from the Newark basin. Note that Triassic samples are about 4 per mil lighter (more negative) than Jurassic samples. The more organic-matter-rich Triassic samples tend to be 0.5 to 1 per mil heavier in $\delta^{13}C_{org}$ than the organic-matter-lean Triassic samples. PDB, Peedee belemnite standard.

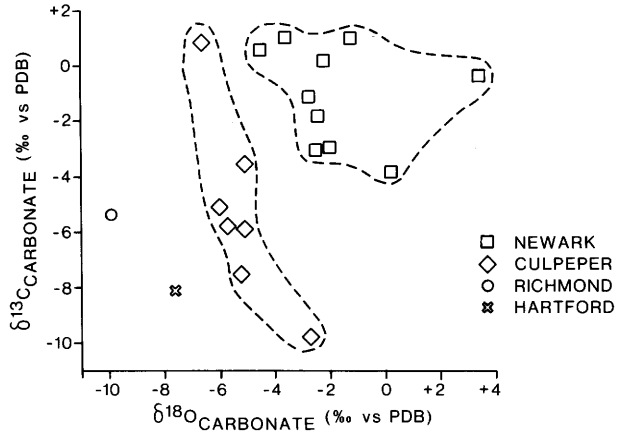

FIGURE 13.5.—Plot of isotopic compositions of whole-rock carbonate from the Newark, Culpeper, Richmond, and Hartford basins. Although there is a wide range of $\delta^{13}C$ and $\delta^{18}O$ values, the samples from each basin plot in distinct regions. PDB, Peedee belemnite standard.

be reflected in more negative $\delta^{18}O$ values (−4 to −10 per mil), and closed-basin circulation would be reflected in less negative to positive $\delta^{18}O$ values (−2 to +4 per mil).

CONCLUSIONS

(1) Pyrolysis and gas-chromatography data indicate that the Jurassic Towaco Formation in the Newark basin is at a late diagenetic to early catagenic stage of thermal alteration. Reconstruction of the time-temperature history suggests that the Towaco Formation probably was not buried at depths greater than about 2 km.

(2) Our current set of samples consists of highly thermally altered rocks and relatively unaltered rocks without transitional samples. This suggests unusually high heat flow at some times in some parts of these early Mesozoic basins.

(3) Isotopic data on organic matter and carbonates show a wide range of values for $\delta^{13}C_{org}$, $\delta^{13}C_{carb}$, and $\delta^{18}O_{carb}$. This range is inferred to reflect different sources of organic matter and different physical and chemical paleoenvironmental conditions in the different basins.

REFERENCES

Craig, H., 1961, Isotopic variations in meteoric waters: Science, v. 133, p. 1702–1703.

Espitalie, J., Laporte, J.L., Madec, M., Marquis, F., Leplat, P., Paulet, J., and Boutefeu, A., 1977, Méthode rapide de caractérisation des roches mères, de leur potentiel petrolier et de leur degré d'évolution [Rapid method for characterization of source rocks, their petroleum potential, and their degree of evolution]: Revue de l'Institut français du pétrole, v. 32, p. 23–42.

Han, Jerry, and Calvin, Melvin, 1969, Hydrocarbon distribution of algae and bacteria, and microbiological activity in sediments: National Academy of Sciences Proceedings, v. 64, no. 2, p. 436–443.

Hudson, J.D., and Friedman, I., 1976, Carbon and oxygen isotopes in concretions; Relationship to pore-water changes during diagenesis, *in* Cadek, J., and Paces, T., eds., Proceedings of the International Symposium on Water-Rock Interaction: Czech Geological Survey, p. 331–339.

Irwing, H., Curtis, C., and Coleman, M., 1977, Isotopic evidence for source of diagenetic carbonates formed during burial of organic-rich sediments: Nature, v. 269, p. 209–213.

Keith, M.L., and Weber, J.N., 1964, Carbon and oxygen isotopic composition of selected limestones and fossils: Geochimica et Cosmochimica Acta, v. 28, p. 1787–1816.

Kroopnick, P.M., Margolis, S.V., and Wong, C.S., 1977, $\delta^{13}C$ variations in marine carbonate sediments as indicators of the CO_2 balance between the atmosphere and oceans, *in* Andersen, N.R., and Malahoff, A., eds., The fate of fossil fuel CO_2 in the oceans: New York, Plenum Press, p. 295–321.

Phillipi, G.T., 1965, On the depth, time and mechanism of petroleum generation: Geochimica et Cosmochimica Acta, v. 29, p. 1021–1049.

Powell, T.G., and McKirdy, D.M., 1973, The effect of source material, rock type and diagenesis on the *n*-alkane content of sediments: Geochimica et Cosmochimica Acta, v. 37, p. 623–633.

Rau, G.H., Sweeney, R.E., and Kaplan, I.R., 1982, Plankton ^{13}C:^{12}C ratio changes with latitude; differences between northern and southern oceans: Deep-Sea Research, v. 29, p. 1034–1039.

Shaler, N.S., and Woodworth, J.B., 1899, Geology of the Richmond basin, Virginia: U.S. Geological Survey 19th Annual Report, Part 2, p. 385–516.

Tissot, B.P., and Welte, D.H., 1978, Petroleum formation and occurrence: Berlin, Springer-Verlag, 538 p.

Waples, D.W., 1980, Time and temperature in petroleum formation; Application of Lopatin's method to petroleum exploration: American Association of Petroleum Geologists Bulletin, v. 64, p. 916–926.

Wong, W.W., and Sackett, W.M., 1978, Fractionation of stable carbon isotopes by marine phytoplankton: Geochimica et Cosmochimica Acta, v. 42, p. 1809–1816.

14. ORGANIC GEOCHEMISTRY IN SEDIMENTARY BASINS AND ORE DEPOSITS—THE MANY ROLES OF ORGANIC MATTER

Gilpin R. Robinson, Jr.

Studies characterizing the organic geochemistry of sedimentary rocks in the Eastern U.S. Triassic-Jurassic basins are useful, both directly and indirectly, in mineral resource studies. This presentation is designed to focus consideration by the organic geochemists on roles that their research may play in understanding the formation of sedimentary ore deposits.

By definition, ore deposits are abnormal concentrations of elements in the earth's crust. These concentrations are the result of a number of processes related to element *sources*, *transport*, and *traps*. *Energy* is needed to drive transport and possibly trapping processes. A chain of coincidence where all these features occur in proper sequence may result in an ore deposit; large deposits may form when these processes are maximized; small deposits may form when one or more of the processes are inefficient.

Some of the roles organic matter may play in the source, transport, trap, and energy processes leading to an ore deposit are explored below. Organic material may influence the chemical characteristics of source rocks through both organic and inorganic interactions and provide early element enrichments, which influence the nature of future additional element enrichments leading to an ore deposit. Organic processes leading to source rock enrichment include all processes that lead to element enrichment in living tissue, which is also preserved in the dead material. Robbins (1983) emphasized the role of these processes in the development of metal enrichment in organic-matter-rich shales. However, inorganic processes, such as the control of redox reactions on metal-complex solubilities and adsorption reactions of metals on organic material, may play a dominant role in concentrating metals in sediments. Whatever the dominant processes controlling metal enrichment in organic sediments may be, it is clear from many recent studies that organic-matter-rich shales contain significantly higher amounts of many metals than do other rocks (Vine and Tourtelot, 1970; Coveney and Martin, 1983).

However, a "source" rock cannot normally influence the development of an ore deposit unless it can release metals to a transport medium to be further concentrated elsewhere. Organic matter may play an important role in the transport of metals. Much organic material in rocks is unstable and is slowly degraded over time. Metals that are bound in this organic material may be released during degradation. In addition, organic compounds created during degradation may transport metals through organometallic complexing or chelation. The influence of organic material on fluid Eh and pH may strongly control metal concentrations in the transporting fluid. This organic degradation frequently increases CO_2 pressure in the pore fluids, with the result that metal-CO_2 complexes may transport material. In addition, immiscible water- and hydrocarbon-rich fluids may be influential in the formation of some ore deposits. The degradation of sulfur-rich hydrocarbon fluids tranported with metal-bearing brines may cause sulfide deposition with metal enrichment.

Metal trapping processes are similar to the processes required to form enriched source rocks. Chemical changes to the transporting fluid that cause mineral deposition form the deposit. Organic material may influence the redox potential or pH of the fluid and cause mineral deposition. Organic material may act as an absorbant for metals, or it may locally provide sulfur, immobilizing transported metals as relatively insoluble sulfides.

In addition, organic matter may provide energy to drive the metal transport or trapping processes. Organic matter may be the food (fuel) for organisms to change fluid chemistry, affecting metal transport or deposition. Unstable organic matter may provide chemical energy driving some inorganic reactions, such as sulfate reduction. The rates of these reactions are strongly influenced by temperature and fluid chemistry, so kinetics may play an important role as well. In addition, organic matter may act as a catalyst for some inorganic reactions and thus influence mineral deposition or element transport.

Studies of organic matter also play a role in mineral resource evaluation and exploration. Organic matter may concentrate trace elements useful for geochemical exploration. Studies of organic material can be used to characterize the thermal and chemical history of the rocks and possibly to identify the pathways of heated fluids. Supporting isotopic studies may be used to identify fluid sources and rock-fluid ratios.

These ideas are only sketchily developed here; they are largely restatements of ideas expressed by others (for example, Barton, 1982). Furthermore, additional roles for organic matter in the formation, study, and evaluation of ore deposits could be added to the ones presented here. However, consideration of these relationships relative to the many ongoing studies of the organic character, maturation, and evolution in the Eastern U.S. early Mesozoic basins may provide new tools and techniques to locate and understand sedimentary ore deposits in these basins.

REFERENCES

Barton, P.B., Jr., 1982, The many roles of organic matter in the genesis of mineral deposits [abs.]: Geological Society of America Abstracts with Programs, v. 14, no. 7, p. 440.

Coveney, R.M., Jr., and Martin, S.P., 1983, Molybdenum and other heavy metals of the Mecca Quarry and Logan Quarry Shales: Economic Geology, v. 28, p. 132–149.

Robbins, E.I., 1983, Accumulation of fossil fuels and metallic minerals in active and ancient rift lakes: Tectonophysics, v. 94, p. 633–658.

Vine, J.D., and Tourtelot, E.B., 1970, Geochemistry of black shales—A summary report: Economic Geology, v. 65, p. 253–273.

15. EARLY JURASSIC DIABASE SHEETS OF THE EASTERN UNITED STATES — A PRELIMINARY OVERVIEW

Albert J. Froelich and David Gottfried

INTRODUCTION

Before 1970, lower Mesozoic diabase intrusive rocks in the Eastern United States were considered essentially uniform in chemical and mineralogical composition (Dana, 1873; Walker, 1940; De Boer, 1967). Almost simultaneously, Weigand and Ragland (1970), in North Carolina, and Smith and Rose (1970), in Pennsylvania, reported on a variety of "Triassic" diabase dikes and sheets whose parental magmas could be characterized by their geochemical signatures as follows: olivine-normative tholeiite, or Quarryville type; quartz-normative tholeiite, high TiO_2, or York Haven type; and quartz-normative tholeiite, low TiO_2, or Rossville type. We have used this foundation and their subsequent published refinements (Ragland and others, 1971; Ragland and Hatcher, 1980; Ragland and Whittington, 1983a,b; Smith, 1973; Smith and others, 1975), as well as new data from others (Justus and Weigand, 1971; Gottfried and others, 1983; Husch and others, 1984; McHone, 1978) and our own largely unpublished recent results (see Gottfried and Froelich, chapter 16; J. Philpotts and others, chapter 18; Brown and others, chapter 19; and J. Philpotts, chapter 22, this volume), to construct a preliminary geochemical framework of magma types that encompasses the diverse early Mesozoic igneous rocks in the Eastern United States that are generally classified as diabase or

dolerite. This paper summarizes preliminary results of geochemical work in progress and presents a tentative field classification of diabase sheets largely on the basis of mineralogical and textural zonation, cumulate layering, and lateral flow differentiation. However, much of the regional geochemical basis, except in Pennsylvania, stems from research and publications on continental tholeiite dikes, supplemented by our own sparse analytical results from sheets contiguous to analyzed dikes.

The general term "sheet" is used here to embrace all of the great variety of forms displayed by the intrusive diabase other than vertical or steeply inclined dikes — that is, sills, stocks, and ring-, spoon-, or saucer-shaped bodies having one margin nearly conformable to bedding but the other margins commonly crosscutting stratification. The areal extent, thickness, and geometrical form of the sheets are highly variable, but the original morphologies have been only slightly modified by later tectonic deformation. Delineation of subsurface form is largely dependent on geophysical interpretation, supplemented by sparse local drill-hole information. One of our long-term goals is to use all our geophysical techniques to locate zones of maximum thickness.

DISTRIBUTION AND DEPTH OF EMPLACEMENT

Nearly all the plutons in the Eastern United States are within or adjoin the early Mesozoic basins. Exposed sheets are most abundant, thickest, and most diverse in form and geochemistry in the Culpeper, Gettysburg, and Newark basins; they are sparse but present in the Hartford basin to the north and in the Danville, Durham, and Sanford basins to the south. Large sheets are absent from most of the other basins (fig. 15.1).

The sheets are considered to be hypabyssal intrusives injected at high temperatures but under relatively low pressures, partly on the basis of their near-exclusive association with early Mesozoic continental sedimentary rocks. Theoretical chemical and thermodynamic considerations of the diabase mineralogy, as well as the geothermometry and geobarometry of minerals developed in the enclosing thermal aureole, support this conclusion.

GEOCHEMICAL AND PHYSICAL CHARACTERISTICS

The southern sheets, mainly those in North Carolina, are distinctly different from those to the north in several ways. (1) They are probably all olivine-normative tholeiites and are more mafic ("primitive") than the central and northern sheets. Ragland and Whittington (1983b) have recently subdivided nearby olivine-normative dikes into high-LIL (large-ion lithophile) and low-LIL varieties, but no similar work has yet been completed on the sheets. (2) In places, they are characterized by coarsely porphyritic (glomeroporphyritic?) pyroxene-rich cumulate(?) zones that have a distinctive clotted or knobby appearance. Megascopically the main body of each sheet is medium to coarsely crystalline, but a variety of textural zones near the margins, which may be related to assimilation or differentiation, are recognizable in cores. (3) The southern sheets are only rarely associated with late-stage differentiates of granophyre or pegmatite (or few are preserved at the surface). (4) Both the chilled border zone and the surrounding aureole of thermally metamorphosed sedimentary rock are relatively thin — the metamorphic aureole is commonly less than 10–20 percent of the estimated thickness of the sheet. (5) They are probably thinner than sheets to the north. In the Durham basin, rarely more than 500 feet (150 m) thickness is preserved after erosion, although sparse geophysical data suggest that some thicker lobes are present at depth. In other southern sheets, scattered core hole data indicate that generally less than 300 feet (90 m) total thickness is present.

The central and northern sheets in northern Virginia, Maryland, Pennsylvania, New Jersey, and Connecticut resemble each other and differ from the southern sheets in the following ways. (1) They are predominantly quartz-normative tholeiites with two distinct populations of trace and minor elements: York Haven-type sheets are characterized geochemically by chilled margins with high TiO_2 (and high Cu); Rossville-type sheets are characterized by chilled margins with low TiO_2 (and low Cu). A possible variant of the high-TiO_2 quartz-normative type is a high-iron type (Weigand and Ragland, 1970; Husch and others, 1984), but its regional significance is still being evaluated. (2) The sheets can be divided into two main populations having basal to medial cumulate zones of either abundant olivine (Palisades type) or abundant orthopyroxene (bronzite-hypersthene) in addition to clinopyroxene (augite, pigeonite) (York Haven type). (3) Central and northern diabase sheets, unlike southern sheets, are strongly differentiated, containing thick, well-developed granophyric masses, magnetite-rich quartz gabbro, coarse pegmatite, and syenitic to granitic or aplitic lenses. (4) The chilled border zone is moderately thick, and the sheet is surrounded by a

thick, well-zoned thermal aureole, commonly 25–35 percent of the thickness of the intrusive sheet. (5) The northern sheets are much thicker than those to the south. In the Culpeper basin, diabase may exceed 1500 ft (450 m), and in the Gettysburg and Newark basins it may exceed 2500 feet (750 m) in preserved thickness.

Smith and others (1975, p. 947) have evaluated the metallic sulfide and oxide associations in Rossville and York Haven sheets and Quarryville dikes in Pennsylvania. Their observations and conclusions, summarized in table 15.1, appear to be generally valid for most of the early Mesozoic diabase sheets in the Eastern United States.

CONTACT ZONES: CHILLED MARGINS OR BORDERS AND THERMAL AUREOLES

To study the composition of the parent magma and to avoid the complications of differentiation in place, the most reliable sampling site for geochemical analysis has long been held to be the chilled borders of sheets and dikes (Smith and others, 1975, p. 943). Recent U.S. Geological Survey sampling of chill margins exposed in quarries or from core (for which we have diagnostic thin sections as well as complete chemistry) has shown that in many cases chilled diabase from some large quartz-normative sheets contains major- or trace-element components characteristic of hornfels, and hornfels near the contact may contain components of diabase. This is not true for chilled margins of dikes nor for all sheets, nor does it negate published analytical results, especially where meticulous care in sampling was taken (Smith and others, 1975). Clearly, however, wall-rock–diabase reactions are very complex and may involve wholesale interactions that are easily overlooked and that must be critically evaluated before using such analyses to determine the composition of the parental magma. Several aspects of diabase–wall-rock interaction relating to "diabasization," assimilation, and hybridization are the subject of current or planned research.

STRUCTURAL SETTING AND FORM OF DIABASE SHEETS

Diabase sheets in the Eastern United States are almost totally restricted to the early Mesozoic sedimentary basins containing Triassic and Jurassic layered rocks. Smith and others (1975) observed that locally diabase sheets of the northwestern Gettysburg and Newark basins extend outside and intrude Precambrian and Paleozoic rocks; however, the sheet form is usually retained.

Carey (1958b, p. 165–169) has pointed out that in areas of folded and consolidated "basement" rocks (density 2.8–2.9 + g/cm^3), dolerite (diabase) magma (density 2.7 g/cm^3) should occur in the form of dikes or steep cone sheets of restricted thickness but that basaltic magma ascending into sedimentary basins would do less work by lifting the sediments (density 2.2–2.4 g/cm^3) than by continuing to the surface. Furthermore, in basins with about 10,000 feet (3000 m) of sediment fill, trumpet-shaped cone sheets should develop in the sediments, and basalts should *not* be extruded until after the sediments are intruded by dolerite sheets. Du Toit (1920, p. 33), and Walker and Poldervaart (1949, p. 685), on the other hand, believed that the order of dolerite injection was from the top downward, the first

TABLE 15.1.—*Sulfide and oxide mineral resource implications of the three diabase types*
[From Smith and others, 1975, table 3, p. 947]

Diabase type	Expected mineral resource	
	Sulfides	Oxides
York Haven (Quartz-normative, high TiO_2).	Subrounded chalcopyrite blebs and irregular pyrite grains.	Approximately 3–5% separate, homogeneous, subrounded grains of ilmenite and magnetite, ilmenite roughly twice as abundant.
Rossville (Quartz-normative, low TiO_2).	Subrounded blebs of pyrrhotite, some with chalcopyrite lamellae; some chalcopyrite grains; pyrite as subrounded blebs and stringers.	Approximately 2% interstitial, subhedral to anhedral ilmenite and magnetite in roughly equal amounts.
Quarryville (Olivine-normative, very low TiO_2).	Tiny, subrounded mixed blebs of pyrrhotite and pentlandite(?); abundant very fine grained (2 μm) yellow sulfides (chalcopyrite?).	Approximately 2–3% anhedral magnetite with traces of ilmenite.

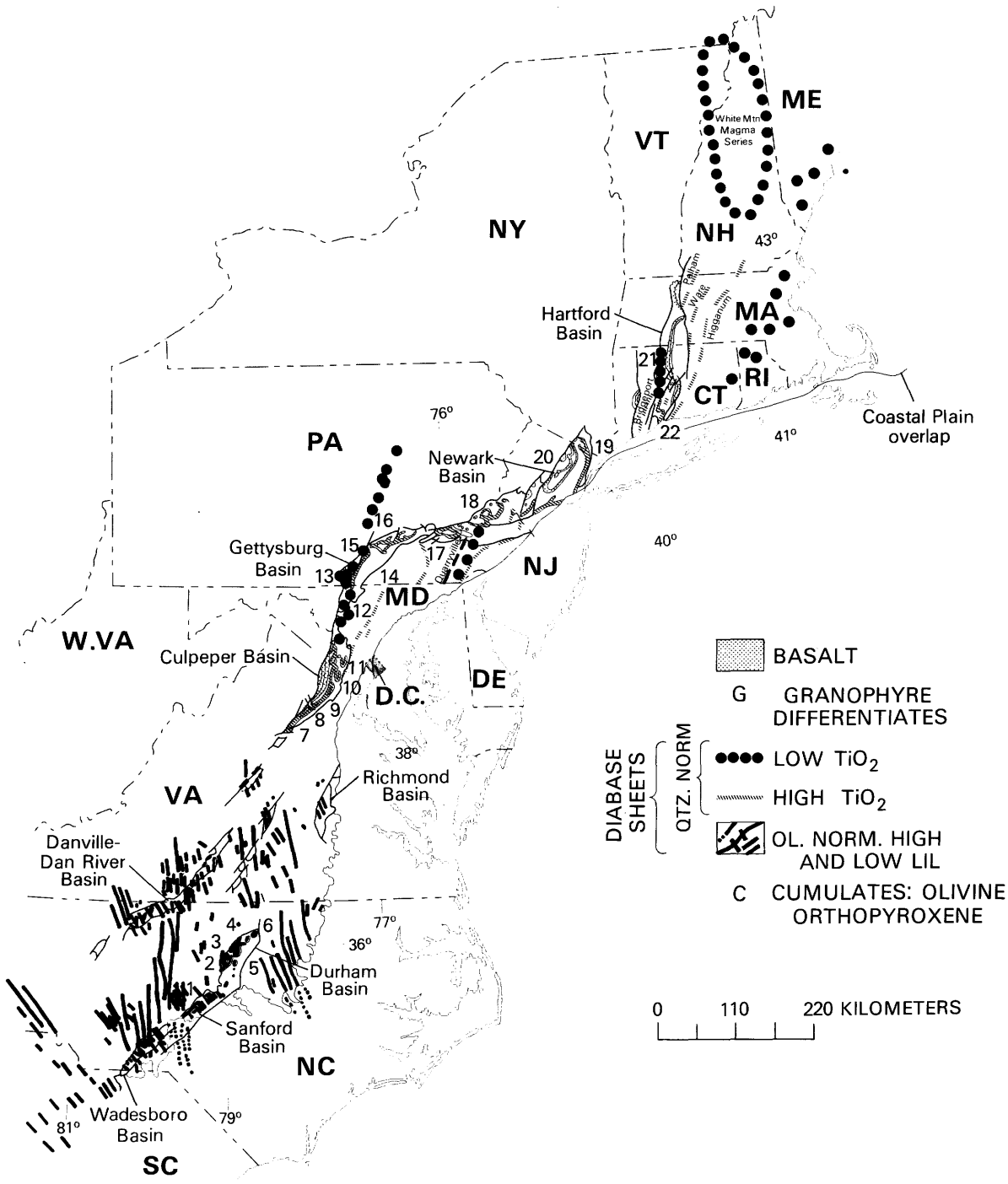

FIGURE 15.1.—Jurassic igneous rocks in exposed Mesozoic basins in the Eastern United States.

event being the extrusion of basalt from fissures, followed by progressive invasion of lower and lower horizons. Carey's (1958b) elegant explanation seems to fit better the pattern of diabase sheets in the Eastern United States, as well as the prevailing distribution of dikes and flows. Roberts (1971) showed that dikes change to sheets where the least principal stress direction changes from horizontal at depth to vertical near the surface due to the decreasing load of the overlying strata.

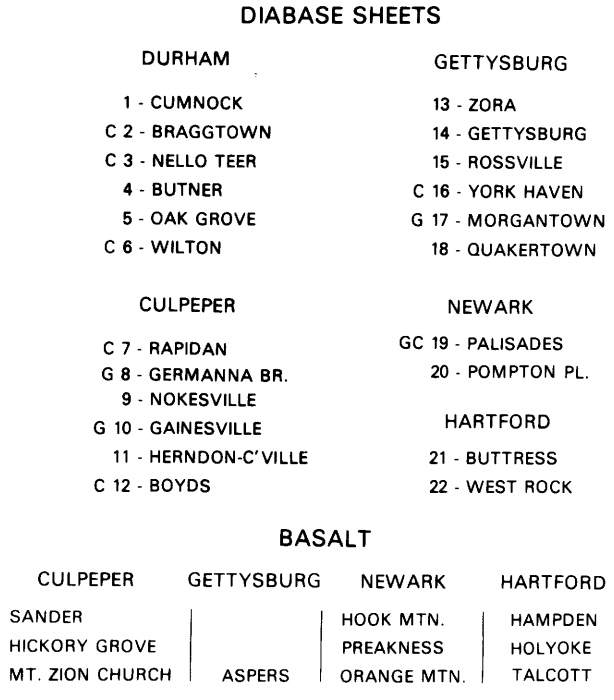

FIGURE 15.1.—Continued.

Hotz (1952) studied many core holes, detailed mine maps, and detailed geophysical surveys and determined that a typical diabase sheet in the Gettysburg basin has the gross shape of a basin or saucer with upturned margins. Smith and others (1975, p. 943) observed that the southeastern parts of typical sheets in the Gettysburg and Newark basins are approximately conformable to bedding of the enclosing gently northwest-dipping Triassic strata but that the other margins commonly cut across bedding. This general form is consistent with what we know of sheets in the Culpeper basin (Va.-Md.), where strata dip uniformly westward, and with the poorly exposed sheets of the Durham and Sanford basins (N.C.) and the Hartford basin (Conn.-Mass.), where the enclosing strata dip east or southeast.

Hotz (1952, p. 384) noted that the dolerite intrusions (subcircular, 10 mi (16 km) in diameter) in the nearly horizontal beds of the Karroo System of South Africa are similar in form to the Gettysburg diabase sheets and that the Karroo sheets (less than 1000 ft (300 m) to more than 3000 ft (900 m) thick) have roughly parallel but markedly undulatory upper and lower surfaces. This is consistent with all observations in the Gettysburg, Newark, and Culpeper basins. Well-developed anticlinal rolls extensively expose the basal portions of the Karroo sheets (with their associated nickeliferous ore deposits), but such structures are extremely rare in early Mesozoic basins of the Eastern United States. The mechanism that controls the basin-like form of the intrusive sheets is still not clearly understood, but it may have been easier for the magma to spread laterally than to rise to higher levels, except along preexisting major fractures. According to Anderson (1938; 1942, p. 23, 142) the thin edge of an advancing magma sheet has a powerful wedging effect by means of which it advances itself. Pollard and others (1975, p. 353) noted that the periphery of the Shonkin Sag sill is extensively fingered, with long, nearly cylindrical tubes that coalesced to form the main body of the sheet. Outcrops and exposures on the margins of the early Mesozoic basin sheets of the Eastern United States are too poor for such precise discrimination of marginal form; however, local relations suggest a very complex injection system. Du Toit (1920, p. 29) suggested that the curving form of Karroo dolerite "may have been partly or wholly determined under stress set up through thermal expansion," and elsewhere (1920, p. 5) he suggested that lateral spread may be aided by water vapor released from the sediments as they are heated by magma. Certainly the studies of Bird and others (1960) on transport phenomena and of Kays (1960) on convective heat and mass transfer bear on the modes of diabase injection. Pollard and others (1975, p. 355-356) pointed out that magma flowing in a horizontal sheet will experience viscous drag, primarily from top and bottom contacts, and that a continuous sheet intrusion may propagate by simply wedging the host rock apart, perhaps with some local compaction. Certainly we can all agree with Eaton (1983, p. 370) that "the emplacement and cooling of magma at shallow depths in the earth's crust result in profound perturbations of the ambient temperature, the fluid pressure, and the stress field of the surrounding rocks."

Whether or not we understand the precise mechanism controlling intrusive form, we can deal with the present forms of sheets using tools we now have: geophysics and, in some areas, modern, accurate geologic maps. Carey (1958a, p. 130–164) developed a potentially useful analytical technique for determining the most likely subsurface shape of surface-breaking diabase bodies and their relationship to enclosing strata, by using isostrats — lines on a map that delineate areas of intrusive contacts above or below a particular mappable horizon (fig. 15.2). Isostrats can, in some cases, be used to differentiate between pre-intrusion and post-intrusion deformation, particularly faulting, as the isostrats may be offset whereas structure contours on the diabase surface are not. Available evidence

indicates that most diabase sheets in the basins of the Eastern United States were intruded before regional tilting, folding, and faulting, but we would like to be able to distinguish individual pre-intrusion major faults that localized diabase feeders and vents.

We would like to conclude with a speculative analytical approach to diabase plumbing systems first postulated for the Culpeper basin: the possibility that a map view of the tilted, asymmetrical, deeply eroded early Mesozoic basins of the Eastern United States offers a natural tangential cross-section. In this model the deepest part of the conical diabase sheets (conformable east and southeast margins) would be situated against the erosional basin margins, connected to

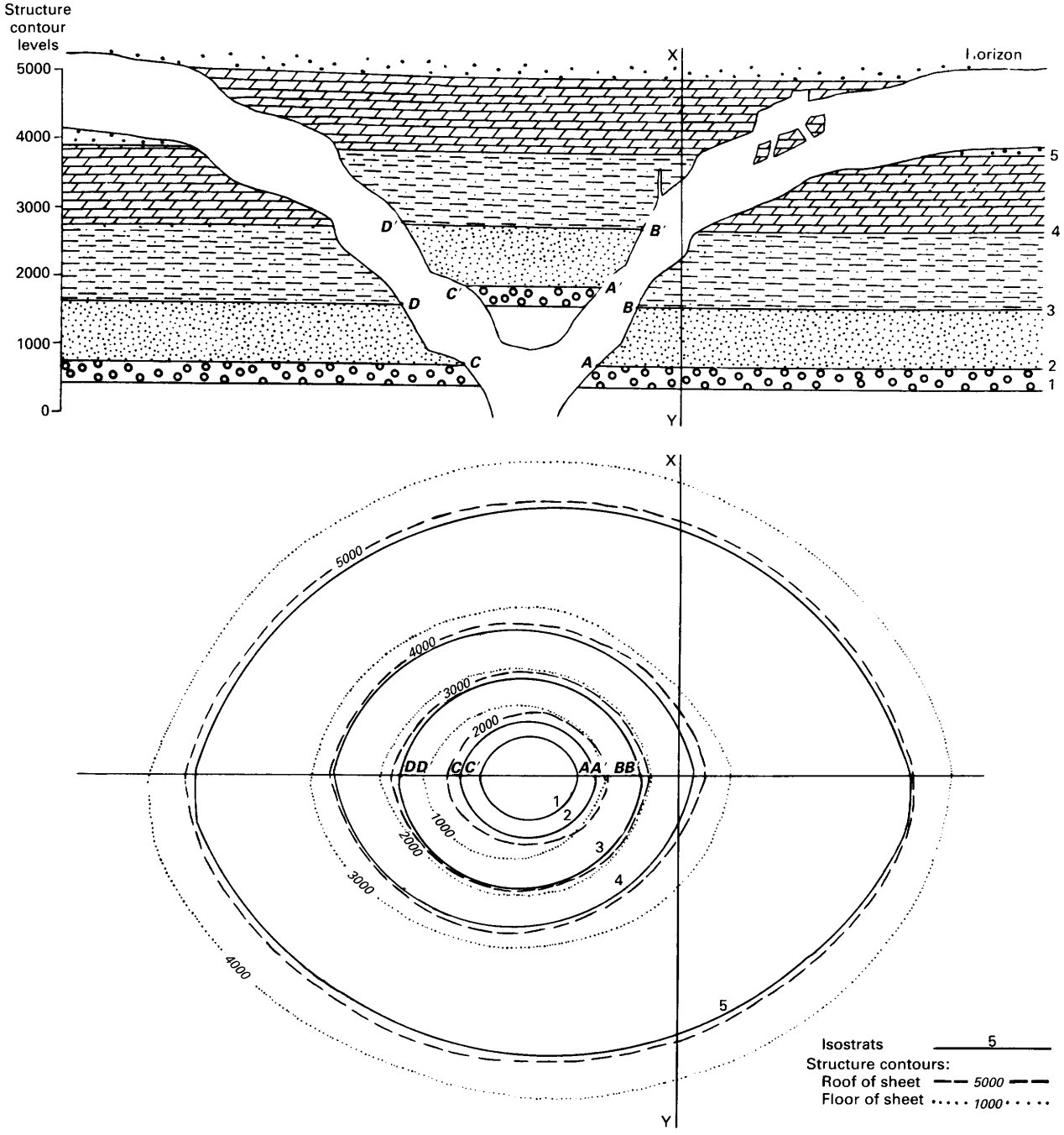

FIGURE 15.2.—Comparison of isostrats and structure contours (from Carey, 1958a).

higher conformable sheets (or stocks) by crosscutting dikes and steeply inclined sheets, finally culminating with feeder dikes to basalt flows against the major border faults (west and northwest margins) (fig. 15.3).

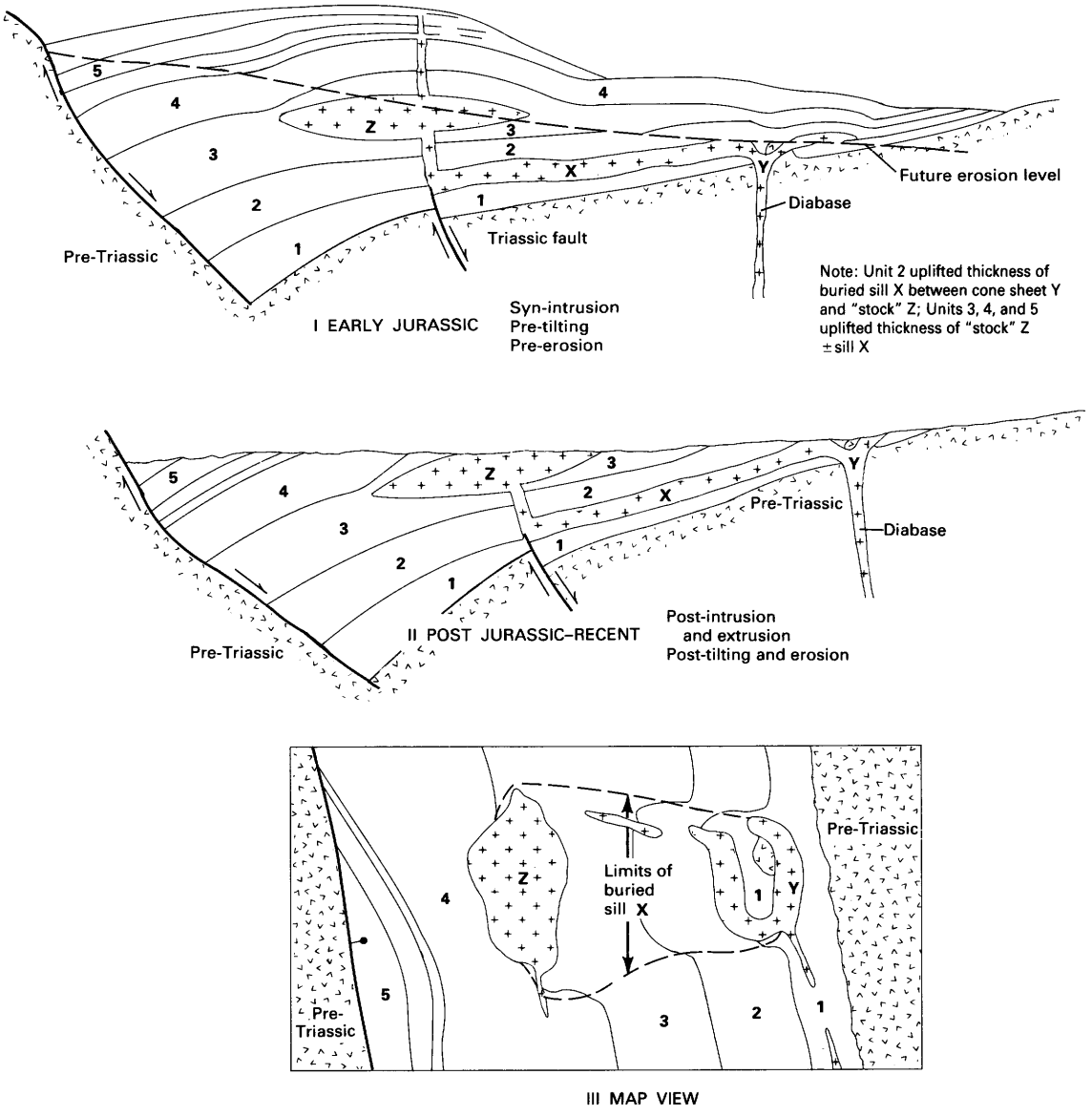

FIGURE 15.3.—Schematic cartoon showing cross sections before (I) and after (II) tilting and erosion; (III) map view of hypothetical early Mesozoic basin containing diabase intrusions and basalt flows.

SELECTED REFERENCES

Anderson, E.M., 1938, The dynamics of sheet intrusion: Royal Society of Edinburgh Proceedings, ser. B, v. 58, no. 3, p. 242–251.

_____1942, The dynamics of faulting and dyke formation with application to Britain: Edinburgh, Oliver and Boyd, 191 p.

Bird, R.B., Stewart, W.E., and Lightfoot, E.N., 1960, Transport phenomena: New York, Wiley, 780 p.

Carey, S.W., 1958a, The isostrat, a new technique for the analysis of the structure of the Tasmanian dolerite, *in* Dolerite, a symposium: Hobart, University of Tasmania, p. 130–164.

_____1958b, Relation of basic intrusions to thickness of sediments, *in* Dolerite, a symposium: Hobart, University of Tasmania, p. 165–169.

Dana, J.D., 1873, On some results of the earth's contraction from cooling, Pt. IV, Igneous injections, volcanoes: American Journal of Science, v. 106, p. 104–115.

De Boer, Jelle, 1967, Paleomagnetic-tectonic study of Mesozoic dike swarms in the Appalachians: Journal of Geophysical Research, v. 71, p. 3567–3576.

Delaney, P.D., 1982, Rapid intrusion of magma into wet rock; ground water flow due to pore pressure increases: Journal of Geophysical Research, v. 87, p. 7739–7756.

Delaney, P.D., and Pollard, D.D., 1981, Deformation of host rocks and flow of magma during growth of minette dikes and breccia-bearing intrusions near Ship Rock, New Mexico: U.S. Geological Survey Professional Paper 1202, 61 p.

Du Toit, A.L., 1920, The Karroo dolerites of South Africa: A study in hypabyssal injection: Geological Society of South Africa Transactions, v. 23, p. 1–42.

Eaton, G.P., 1983, Mineral abundance in the North American Cordillera: American Scientist, v. 72, p. 368–377.

Gottfried, David, Dooley, R.E., and Higgins, M.W., 1983, Geochemistry of lower Mesozoic diabase dikes of the Georgia Piedmont: implications for mantle heterogeneity [abs.]: Geological Society of America Abstracts with Programs, v. 16, no. 6, p. 583.

Hotz, P.E., 1952, The form of diabase sheets in southeastern Pennsylvania: American Journal of Science, v. 250, p. 375–388.

Husch, J.M., Sturgis, D.S., and Bambrick, T.C., 1984, Mesozoic diabases from west-central New Jersey: major and trace element geochemistry of whole-rock samples: Northeastern Geology, v. 5, no. 1, p. 51–63.

Justus, P.S., and Weigand, P.W., 1971, Distribution of dolerite magma types and variations of dike-swarm pattern: clues to tectonic history of Appalachians in Early Mesozoic: Pennsylvania Academy of Science Proceedings, v. 45, p. 202–203.

Kays, W.M., 1960, Convective heat and mass transfer: New York, McGraw-Hill, 387 p.

Lee, K.Y., Leavy, B.D., and Gottfried, David, 1984, Geochemical data for Jurassic diabase and basalt of the northern Culpeper basin, Virginia: U.S. Geological Survey Open-File Report 84–771, 19 p.

McHone, J.G., 1978, Distribution, orientations and ages of mafic dikes in central New England: Geological Society of America Bulletin, v. 89, p. 1645–1655.

Pollard, D.D., 1973, Derivation and evaluation of a mechanical model for sheet intrusions: Tectonophysics, v. 19, no. 3, p. 233–269.

Pollard, D.D., and Muller, O.H., 1976, The effects of gradients in regional stress and magma pressure on the form of sheet intrusions in cross section: Journal of Geophysical Research, v. 81, no. 3, p. 975–984.

Pollard, D.D., Muller, O.H., and Dockstader, D.R., 1975, The form and growth of fingered sheet intrusions: Geological Society of America Bulletin, v. 86, no. 3, p. 351–363.

Ragland, P.C., Brunfelt, A.O., and Weigand, P.W., 1971, Rare-earth abundances in Mesozoic dolerite dikes from eastern United States, *in* Brunfelt, A.O., and Steinnes, Eiliv, eds., Activation analysis in geochemistry and cosmochemistry: Oslo, Universitet Sforlaget, p. 227–235.

Ragland, P.C., and Hatcher, R.D., Jr., 1980, Mesozoic olivine-normative diabase in North Carolina: multiple compositional types and orientations [abs.]: Geological Society of America Abstracts with Programs, v. 12, p. 205.

Ragland, P.C., and Whittington, David, 1983a, "Primitive" Mesozoic diabase dikes of eastern North America: primary or derivative? [abs.]: Geological Society of America Abstracts with Programs, v. 15, p. 92.

———1983b, Early Mesozoic diabase dikes of eastern North America: magma types [abs.]: Geological Society of America Abstracts with Programs, v. 15, no. 6, p. 666.

Roberts, J.L., 1971, On the mechanics of intrusion of sills: discussion: Canadian Journal of Earth Sciences, v. 8, p. 176–179.

Smith, R.C., II, 1973, Geochemistry of Triassic diabase from southeastern Pennsylvania: University Park, Pennsylvania State University, Ph.D. thesis, 262 p.

Smith, R.C., II, and Rose, A.W., 1970, The occurrence and chemical composition of two distinct types of Triassic diabase in Pennsylvania [abs.]: Geological Society of America Abstracts with Programs, v. 2, no. 7, p. 688.

Smith, R.C., II, Rose, A.W., and Lanning, R.M., 1975, Geology and geochemistry of Triassic diabase in Pennsylvania: Geological Society of America Bulletin, v. 86, p. 943–955.

Walker, Frederick, 1940, Differentiation of the Palisades diabase, New Jersey: Geological Society of America Bulletin, v. 51, p. 1059–1105.

———1958, The causes of variation in dolerite intrusions, *in* Dolerite, a symposium: Hobart, University of Tasmania, p. 1–25.

Walker, Frederick, and Poldervaart, Arie, 1949, Karroo dolerites of the Union of South Africa: Geological Society of America Bulletin, v. 60, p. 591–706.

Walker, K.R., 1969, The Palisades sill, New Jersey: A reinvestigation: Geological Society of America Special Paper 111, 178 p.

Weigand, P.W., 1970, Major and trace-element geochemistry of Mesozoic dolerite dikes from eastern North America: Chapel Hill, University of North Carolina, Ph.D. thesis, 162 p.

Weigand, P.W., and Ragland, P.C., 1970, Geochemistry of Mesozoic dolerite dikes from eastern North America: Contributions to Mineralogy and Petrology, v. 29, p. 195–214.

16. GEOCHEMICAL AND PETROLOGIC FEATURES OF SOME MESOZOIC DIABASE SHEETS IN THE NORTHERN CULPEPER BASIN

David Gottfried and Albert J. Froelich

Core samples from three diabase sheets in the northern Culpeper basin were analyzed for major and trace elements, including Ni, Co, Cu, Pt, and Pd. These data combined with field petrologic and petrographic studies may provide guides for the identification of mafic igneous systems, which, in some areas, host magmatic sulfide deposits.

The Nokesville diabase sheet in Prince William County, Va. (fig. 16.1), is part of a composite conformable sheet that intrudes the uppermost Triassic silt-

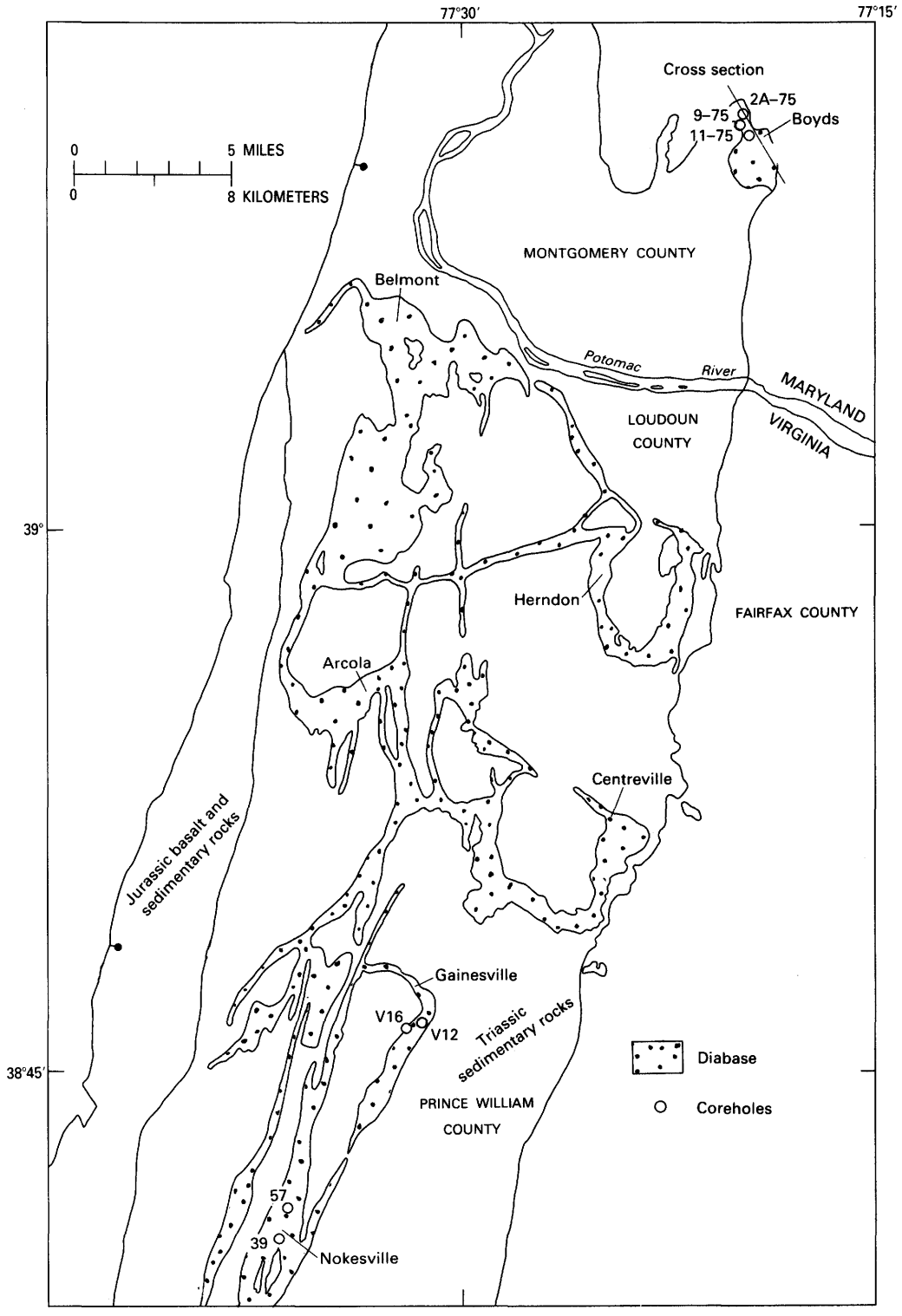

FIGURE 16.1.—Index map of the northern Culpeper basin, Virginia and Maryland, showing locations of principal Mesozoic diabase sheets.

stone, extensively converting it to hornfels. The Gainesville sheet is in the northeast corner of the same diabase trend where the conformable northeast-trending sheet bends abruptly to the west-northwest, cross-cutting Triassic siltstone. Major- and trace-element data indicate wide differences between the two sheets.

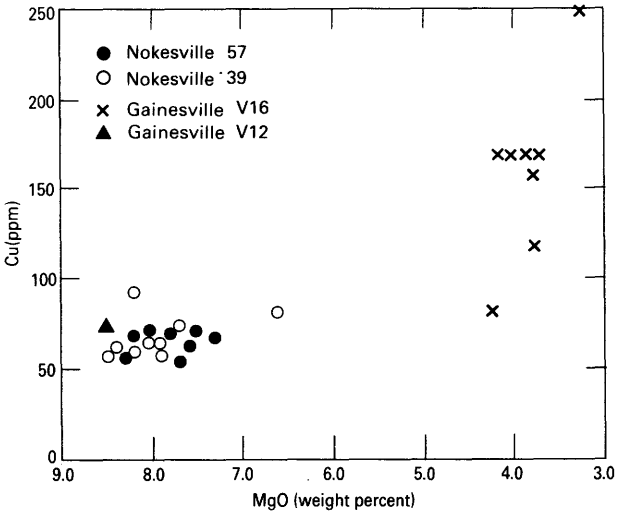

FIGURE 16.2.—Plot of MgO against Cu in samples from Nokesville coreholes 39 and 57 and Gainesville coreholes V12 and V16, Culpeper basin, Virginia.

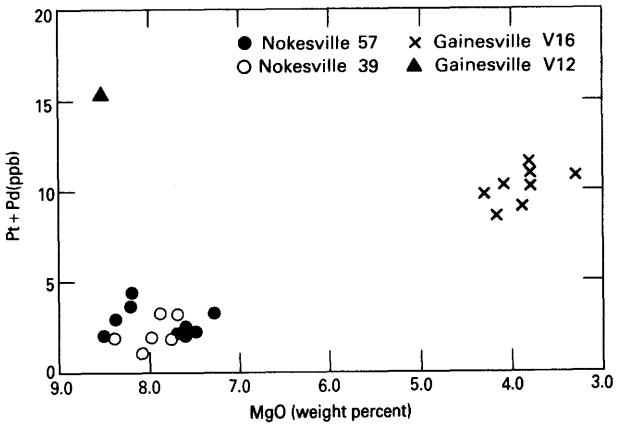

FIGURE 16.3.—Plot of MgO against Pt + Pd in samples from Nokesville coreholes 39 and 57 and Gainesville coreholes V12 and V16, Culpeper basin, Virginia.

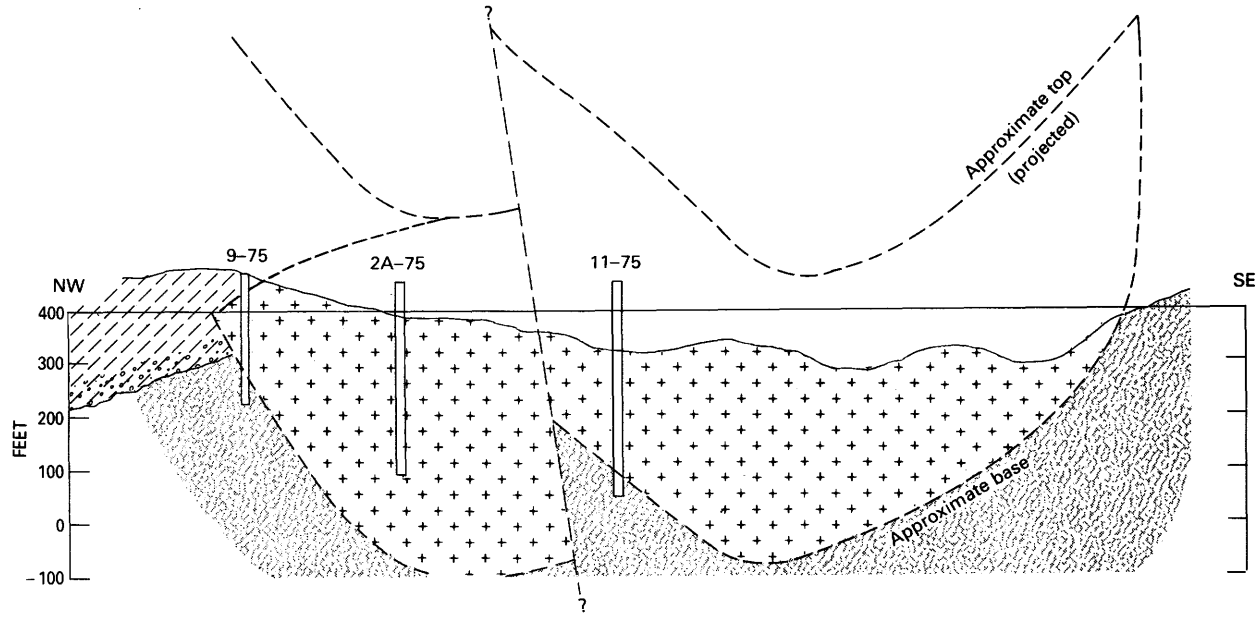

FIGURE 16.4.—Diagrammatic geologic cross section across the Boyds sheet, northern Culpeper basin, Maryland (see fig. 16.1 for line of cross section), showing locations of coreholes 9–75, 2A–75, and 11–75. Vertical exaggeration ×6.

The diabase from the Nokesville sheet is characterized by uniform, relatively high MgO (approximately 8 percent) and low TiO_2 (0.72 percent), Cu, and Pt + Pd contents (fig. 16.2). We tentatively designate this sheet to be of the low-TiO_2 quartz-normative (Rossville) magma type (Smith and others, 1975). The Gainesville sheet has not been adequately sampled. Available petrographic and chemical data on core samples indicate a significant amount (about half the sheet) is relatively coarsely crystalline, fractionated, granophyric diabase of low MgO (3–4 percent) and relatively high Ti, Cu, and Pt + Pd contents (figs. 16.2, 16.3). Geochemical data obtained on the upper chilled margins are virtually the same as these characterizing the high-TiO_2 (1–1.2 percent) quartz-normative (York Haven) magma type. The chilled margin(?) at the apparent base of the sheet

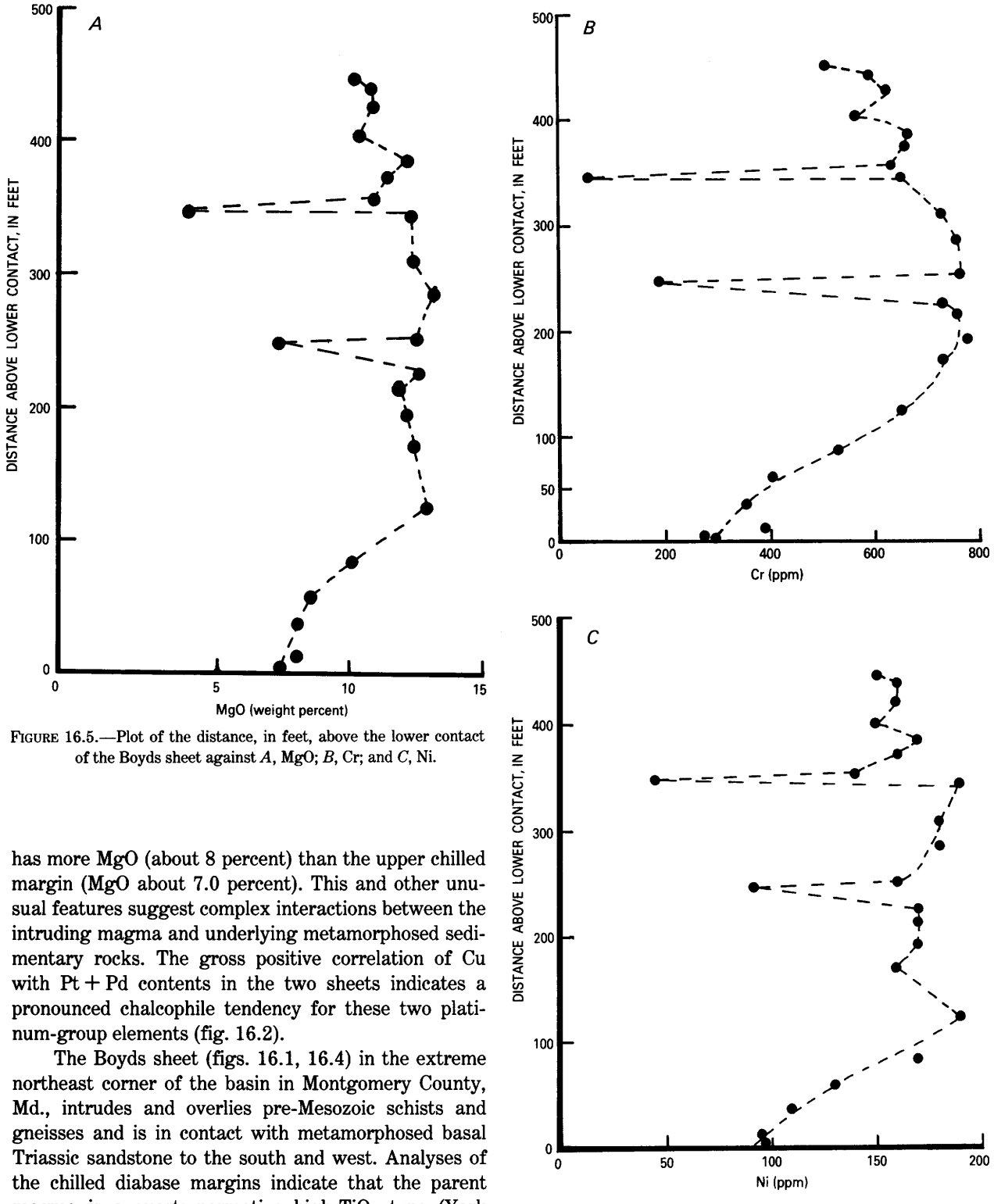

FIGURE 16.5.—Plot of the distance, in feet, above the lower contact of the Boyds sheet against *A*, MgO; *B*, Cr; and *C*, Ni.

has more MgO (about 8 percent) than the upper chilled margin (MgO about 7.0 percent). This and other unusual features suggest complex interactions between the intruding magma and underlying metamorphosed sedimentary rocks. The gross positive correlation of Cu with Pt + Pd contents in the two sheets indicates a pronounced chalcophile tendency for these two platinum-group elements (fig. 16.2).

The Boyds sheet (figs. 16.1, 16.4) in the extreme northeast corner of the basin in Montgomery County, Md., intrudes and overlies pre-Mesozoic schists and gneisses and is in contact with metamorphosed basal Triassic sandstone to the south and west. Analyses of the chilled diabase margins indicate that the parent magma is a quartz-normative high-TiO_2 type (York Haven) containing approximately 7 percent MgO and 1.0 percent TiO_2 (fig. 16.5*A* and 16.6*B*). The bulk of the sheet, however, is characterized by an unusually thick zone of cumulus orthopyroxene, which occurs chiefly as large euhedral crystals. The petrology of this sheet is discussed by Ragland and Arthur (chapter 17, this volume). Although the upper part of the sheet has been removed by erosion, the large difference between

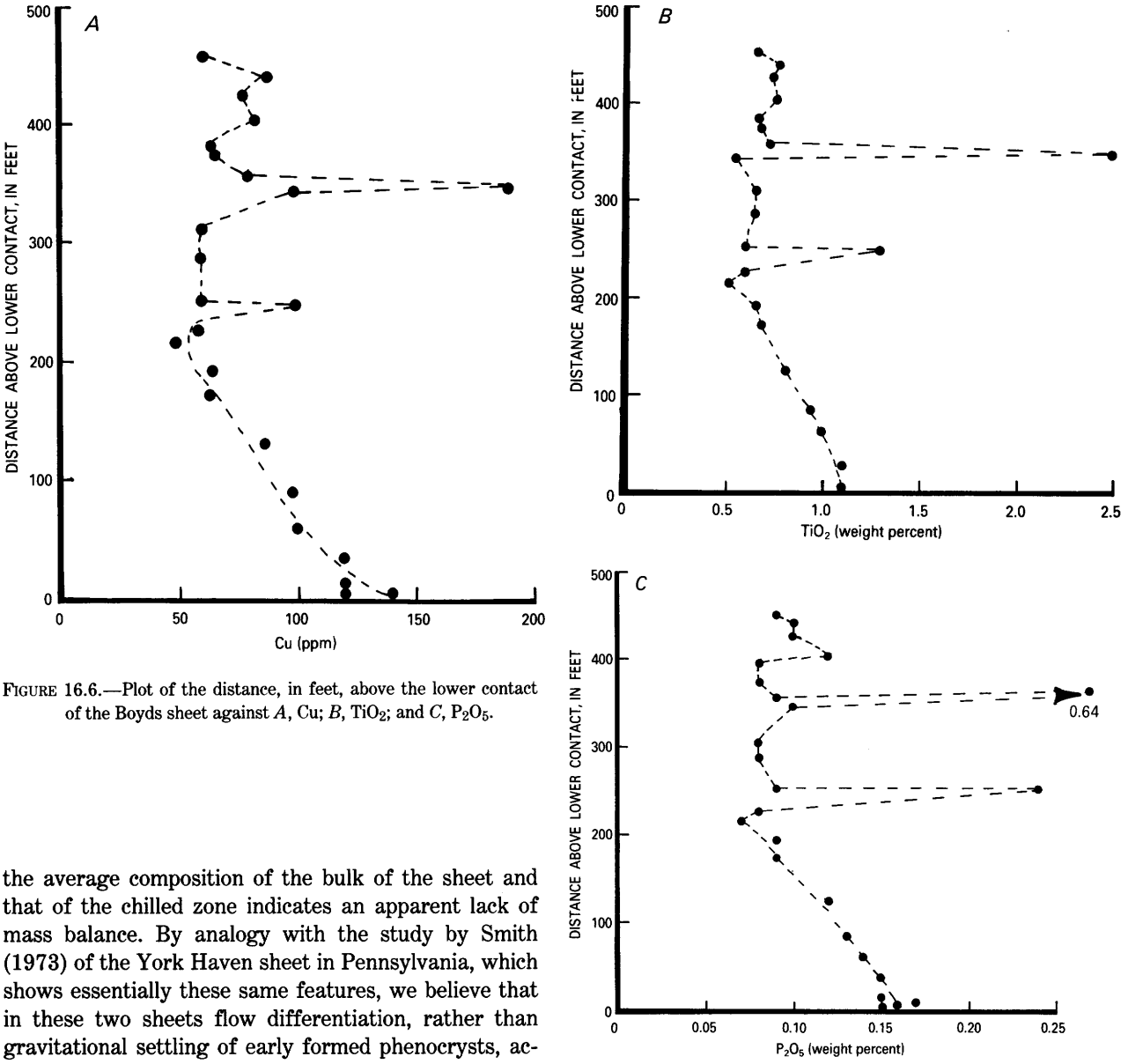

FIGURE 16.6.—Plot of the distance, in feet, above the lower contact of the Boyds sheet against *A*, Cu; *B*, TiO_2; and *C*, P_2O_5.

the average composition of the bulk of the sheet and that of the chilled zone indicates an apparent lack of mass balance. By analogy with the study by Smith (1973) of the York Haven sheet in Pennsylvania, which shows essentially these same features, we believe that in these two sheets flow differentiation, rather than gravitational settling of early formed phenocrysts, accounts for most of the inordinately thick cumulus zones and the absence of any complementary fraction. Elsewhere in the York Haven sheet, the complementary fraction is represented by Fe-rich gabbro and granophyre located several miles from the cumulus zone, apparently as a result of lateral migration of the residual magma. Chemical analyses of the Boyds sheet showing the distribution of MgO, Cr, Ni, Cu, TiO_2, and P_2O_5 are plotted in figures 16.5 and 16.6.

Thus, three supposedly typical diabase sheets in the northern Culpeper basin, originally sampled to provide baseline geochemical and petrologic data, instead display a wide range of eastern North America diabase variants and show striking enrichment and depletion of major and trace elements.

ACKNOWLEDGMENTS

We thank Mr. Joseph A. Gutierrez of Vulcan Materials Company, Winston-Salem, N.C., for providing access to and cores of holes 39 and 57 at Nokesville, Va., and V16 and V12 at Gainesville, Va., as well as his many courtesies in providing entry to the quarries. We also thank Richard F. Langell, consultant, of Germantown, Md., and the staff of Rockville Crushed Stone Corporation for providing cores and descriptions of holes 2A–75, 9–75, and 11–75 at Boyds, Md. Basic research of the U.S. Geological Survey such as that described in this paper would be impossible without the cheerful cooperation of such quarry operators.

REFERENCES

Smith, R.C., II, 1973, Geochemistry of Triassic diabase from southeastern Pennsylvania: University Park, Pennsylvania State University, unpub. Ph.D. thesis, 262 p.

Smith, R.C., II, Rose, A.W., and Lanning, R.M., 1975, Geology and geochemistry of Triassic diabase in Pennsylvania: Geological Society of America Bulletin, v. 86, p. 943–955.

17. PETROLOGY OF THE BOYDS DIABASE SHEET, NORTHERN CULPEPER BASIN, MARYLAND

Paul C. Ragland[8] and Jonathan D. Arthur[8]

INTRODUCTION

The Boyds sheet, an apparently saucer-shaped body of diabasic rock about 3 by 5 km across, crops out in the northeastern corner of the Culpeper basin in Montgomery County, Md. (see Gottfried and Froelich, figs. 16.1, 16.4, this volume). Petrographic descriptions, modal analyses, electron microprobe analyses of mineral phases, and whole-rock chemical analyses (for major and trace elements) have been completed on as many as 22 samples from two cores in this sheet (cores 2A–75 and 11–75; see Gottfried and Froelich, fig. 16.4, this volume). The sheet has apparently been offset by a fault; core 2A–75 is located on the northwest side of the fault and 11–75 on the southeast. The lower 7 samples of the composite section discussed by Gottfried and Froelich (see figs. 16.5, 16.6) and this report (figs. 17.2*A*, 17.2*D*) are from core 11–75, and the upper 15 samples are from core 2A–75. The sheet is exposed, and an unknown thickness has been eroded away (Gottfried and Froelich, fig. 16.4, this volume).

Although no age determinations for the Boyds sheet are available, diabase in the sheet is presumed to be part of the early Mesozoic eastern North American (ENA) petrologic province; Sutter (chapter 21, this volume) has dated diabase dikes and sills in the Culpeper basin as Early Jurassic in age. Compositions of aphyric rocks in the sheet satisfy the chemical criteria of the HTQ (high-Ti, quartz-normative; Weigand and Ragland, 1970; Ragland, 1983) magma type and the equivalent York Haven type (Smith and others, 1975). Modal compositions of the phyric rocks, however, are unusual in that they have abundant orthopyroxene phenocrysts. In fact, since these rocks modally resemble norites, we refer to them as noritic diabase. The lowermost five samples in the section (approximately corresponding to the lower 75 ft) are all aphyric; all samples higher in the section are orthopyroxene-plagioclase phyric.

Gottfried and Froelich (chapter 16, this volume) discuss the trace-element geochemistry of these rocks. This report emphasizes textures, modes, major-element (both whole-rock and mineral) compositions, mass-balance calculations, and incompatible-trace-element trends.

RESULTS

Rocks in the Boyds sheet grade upward in texture from aphyric intergranular, in the lower 75 feet of section, to subophitic porphyritic. Apparently near-liquidus phases ("primocrysts") include plagioclase (An81 (mol percent)), two populations of orthopyroxene (both approximately En78), and very small amounts of clinopyroxene (Wo43En46Fs11). The euhedral plagioclase primocrysts, both zoned and unzoned, average 0.12 × 0.50 mm in size and can occur as phenocrysts and as inclusions in orthopyroxene phenocrysts; these plagioclases are coded as EP in Figure 17.1. Subhedral-anhedral grains of plagioclase, which are similar in size to most euhedral plagioclase phenocrysts, exhibit indistinct extinction and may be normally zoned (they are coded as IP, "indeterminate plagioclase," in fig. 17.1). One population of orthopyroxenes (OPX in fig. 17.1, 1.0–3.5 mm) comprises euhedral-subhedral phenocrysts that are gray to white under crossed nicols. Some appear to exhibit faint twinning and contain clinopyroxene exsolution lamellae, which may indicate inverted pigeonite. The other population

[8]Department of Geology, Florida State University, Tallahassee, Fla. 32306.

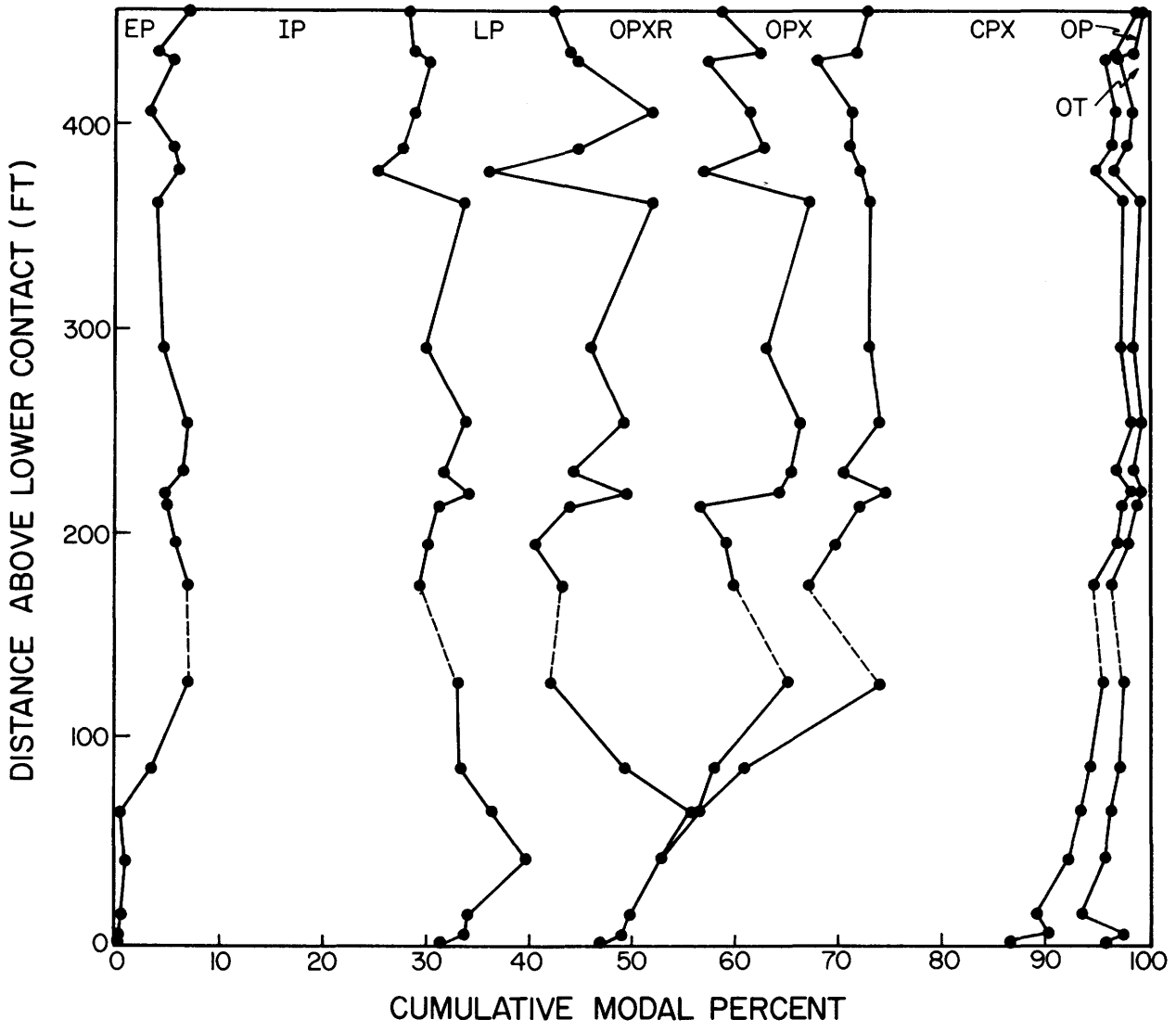

FIGURE 17.1.—Modal analyses, in volume percent, of rocks from the Boyds diabase sheet. EP, apparently early-crystallizing plagioclase; LP, late-crystallizing plagioclase; IP, inderminate plagioclase (that is, very difficult to determine whether early or late); OPXR, orthopyroxene with reaction rims; OPX, orthopyroxene; CPX, clinopyroxene; OP, opaque minerals (generally primary ilmenite, but including some secondary opaque minerals toward the bottom of the sheet); OT, other minerals (including biotite, chlorite, serpentine, K-feldspar, saussurite, sericite). Dashed lines separate rocks of core 2A–75 (upper) from those of 11–75 (lower).

of orthopyroxenes (OPXR in fig. 17.1; also 1.0–3.5 mm) has orthopyroxene reaction rims (average: core En79, rim En66) and occasional clinopyroxene exsolution blebs. The OPXR orthopyroxenes also are generally euhedral-subhedral phenocrysts and typically have slightly higher interference colors than the OPX orthopyroxenes.

Groundmass in the phyric rocks is largely composed of subhedral clinopyroxene in a subophitic relationship with euhedral to subhedral plagioclase (LP in fig. 17.1). Clinopyroxene (Wo36En44Fs20) is inequigranular (0.1–1.0 mm) throughout the sheet; larger grains are twinned. Plagioclase in the groundmass (An74) shows little variation in length (averaging 0.5 mm) throughout the sheet. Toward the base, however, plagioclase grains become much narrower (0.025 mm) than in the phyric rocks above (0.125 mm). In addition to the acicular form of plagioclase toward the base of the sheet, spherulitic textures are observed within 2 feet of the lower contact.

Late-stage crystallization includes intersertal, indistinctly twinned or untwinned plagioclase and K-feldspar, the latter occasionally symplectitic with quartz. Deuteric alteration products include biotite, chlorite, saussurite, sericite, serpentine, and secondary opaque minerals.

Modal analyses are given in figure 17.1. One thousand points were counted on each slide. All orthopyroxenes are primocrysts and almost all clinopyroxenes are part of the groundmass, as are most primary opaque minerals (generally ilmenite). The phenocrystic clinopyroxenes are found throughout the sheet but are rare in all rocks. Plagioclases, however, have a more diverse history in the sheet, crystallizing both early (EP plus some IP, fig. 17.1) and late (LP plus some IP, fig. 17.1). The lower five samples are clearly aphyric, but the ratios of plagioclase to orthopyroxene and OPXR to OPX in the primocrysts and of plagioclase to clinopyroxene in the groundmass have no clearly discernible trends upsection (fig. 17.1).

Opaque minerals decrease upsection, apparently as a result of alteration; primary opaque minerals normally total less than 2 percent in these rocks. Secondary alteration rapidly increases in the lower 75 feet of the sheet as the lower contact is approached (fig. 17.2). This alteration has primarily affected the clinopyroxene in the aphyric zone; plagioclase remains fairly fresh throughout this zone. The oxidation ratio $((Fe_2O_3 \times 100)/(Fe_2O_3 + FeO))$ of about 15 percent in the upper 375 feet suggests that these rocks are only slightly altered, if at all. Oxidation ratios for fresh, unaltered basalts normally are 10–15 percent. Thus the average of about 12 percent hydrous altered minerals in the top 375 feet may indicate deuteric alteration in which the redox conditions of the solutions were similar to those in the magma.

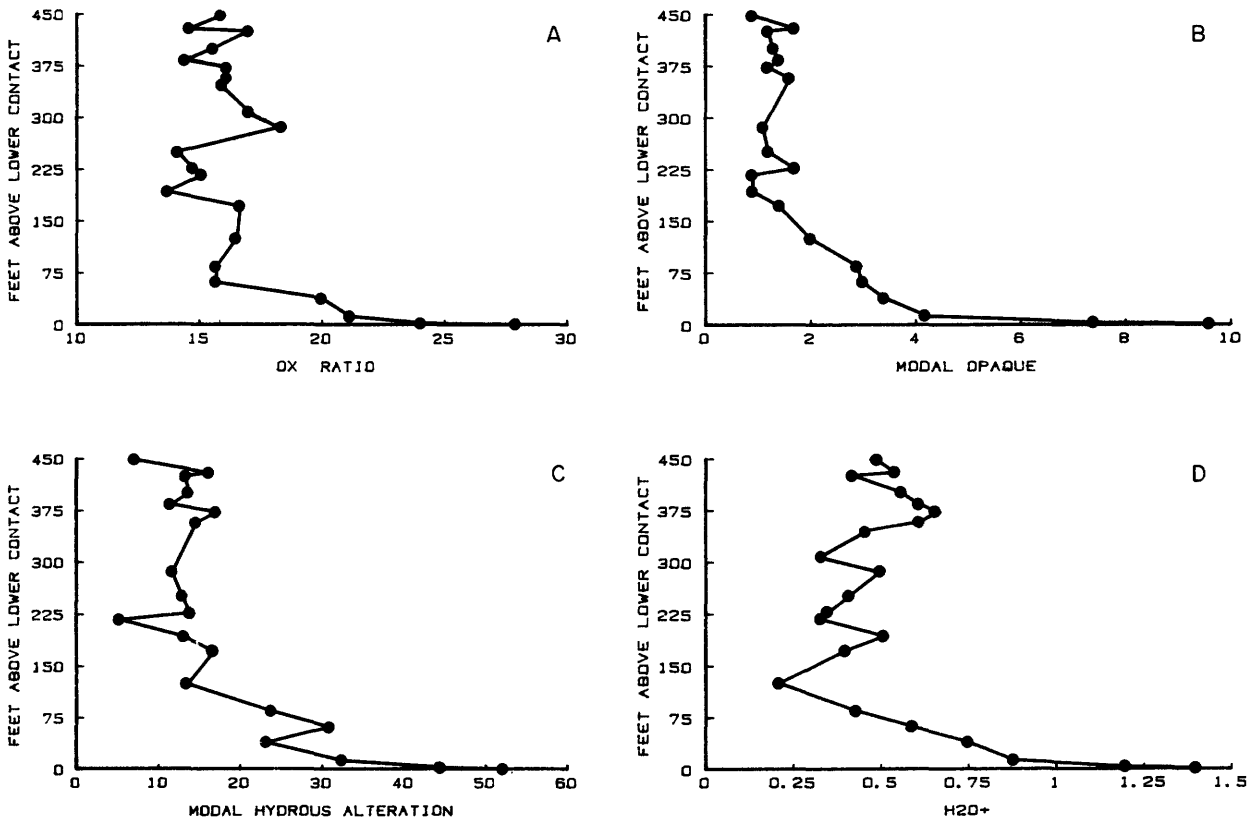

FIGURE 17.2.—Plots of distance above lower contact of Boyds sheet (in feet) against various measures of degree of secondary alteration: *A*, oxidation ratio — $(Fe_2O_3 \times 100)/(Fe_2O_3 + FeO)$ (weight percent); *B*, modal opaque minerals (volume percent), dominantly primary opaque minerals from 75 to 450 feet above base, increasingly secondary below 75 feet; *C*, modal hydrous altered minerals (volume percent), dominantly biotite, chlorite, saussurite, sericite, serpentine; *D*, H_2O^+ (structural H_2O, weight percent).

Figures 17.3 and 17.4 compare the geochemistry of rocks of the Boyds sheet with that of similar rocks reported in the literature. With the exception of one olivine-normative sample (124 feet above lower contact), all samples are quartz-normative (fig. 17.3). The trend is subparallel to the plagioclase-hypersthene "join," in contrast to more typical trends, which are approximately normal to this "join" and are probably controlled by olivine + plagioclase ± clinopyroxene. Figure 17.4 compares rocks of the Boyds sheet with quartz-normative magma types defined by Weigand and Ragland (1970) — now recognizing that HFQ magma types are probably derivatives of HTQ magmas. The most TiO_2-rich aphyric samples fall very near the HTQ field, confirming the similarity of these rocks to the HTQ (Weigand and Ragland, 1970; Ragland, 1983) and equivalent York Haven (Smith and others, 1975) types.

The linear trends for major-element analyses of Boyds sheet rocks (figs. 17.3, 17.4) are qualitatively consistent with orthopyroxene-plagioclase control, for which there is also abundant petrographic evidence. Figure 17.5 shows two examples of an attempt to substantiate and quantify this control. Two-oxide mixing diagrams exhibit remarkably consistent results. A best-fit line through each linear trend of phyric plus aphyric sample points was extrapolated to cut the "tie-line" that connects the average composition of plagioclase primocrysts with that of orthopyroxene primocrysts. The point of intersection of the extrapolated line with the "tie-line" represents the bulk chemical composition of the primocryst assemblage. This implies that the linear trends shown in figures 17.3 and 17.4 can be represented by mixing variable amounts of the aphyric liquid composition with the bulk primocryst assemblage composition. An acceptable solution is achieved if the intersection occurs near the same point on all of the "tie-lines" (two examples are shown in fig. 17.5). The point of intersection ranges from 60 to 70 percent orthopyroxene for all diagrams, quite an acceptable range. For mass-balance calculations described below, we have used a primocryst assemblage of 65 weight percent orthopyroxene (En77) and 35 weight percent plagioclase (An81).

It is interesting to compare this 35 percent plagioclase figure with plagioclase modal percentages shown in figure 17.1. Although the 35 percent is in weight percent and the data in figure 17.1 are in volume percent, densities of these plagioclases and rocks are fairly similar, so that a rough comparison is valid. The EP and IP plagioclases average about 35 percent of the bulk phyric rocks, and the phyric rocks average about 50 percent primocrysts, so about half the IP plagioclases must be near-liquidus phases.

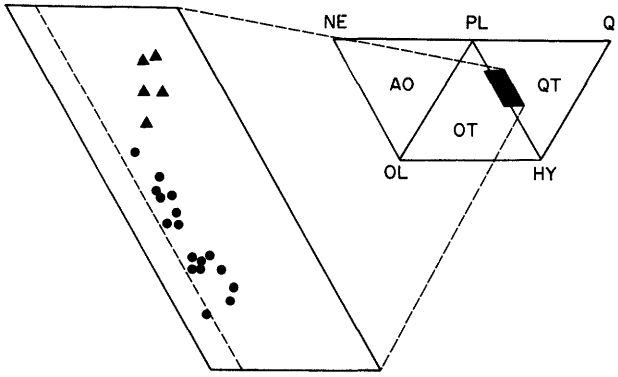

FIGURE 17.3.—CIPW norms of Boyds sheet diabases plotted onto base of basalt tetrahedron. NE, nepheline; OL, olivine; PL, plagioclase; HY, hypersthene; Q, quartz; AO, alkali olivine basalt; OT, olivine tholeiite; QT, quartz tholeiite. In this figure and figures 17.4 and 17.5, triangles represent aphyric samples (five lowermost samples in section), and circles represent orthopyroxene-plagioclase phyric samples. Dashed line in expanded figure is projection of place of silica saturation.

DISCUSSION

At the outset it should be pointed out that these chemical trends in the Boyds sheet are not unique. Although insufficient modal analyses are available, Smith (1973) has found similar trends and orthopyroxene phenocrysts in the York Haven sheet of the Gettysburg basin. Apparently less of the top of the York Haven sheet has been eroded away relative to the Boyds sheet, because more symmetrical chemical patterns have been observed in the York Haven sheet (Smith, 1973). Other sheets in the area may exhibit trends similar to the Boyds and York Haven sheets.

Before consideration of petrogenesis, an important question is whether or not groundmass compositions vary in any systematic manner upsection. Since (1) all orthopyroxenes are primocrysts, (2) a fairly consistent ratio of 65/35 exists for orthopyroxene/plagioclase primocrysts, (3) reasonably accurate modal and normative analyses of orthopyroxene are available, and (4) compositions of both plagioclase and orthopyroxene primocrysts are known, a mass-balance equation can be solved to calculate groundmass compositions. The equation is

$$C_B = W_O C_O + W_P C_P + W_G C_G$$

where W_O, W_P, and W_G are weight fractions of orthopyroxene, plagioclase, and groundmass, respectively; C_B, C_O, C_P, and C_G are compositions in weight

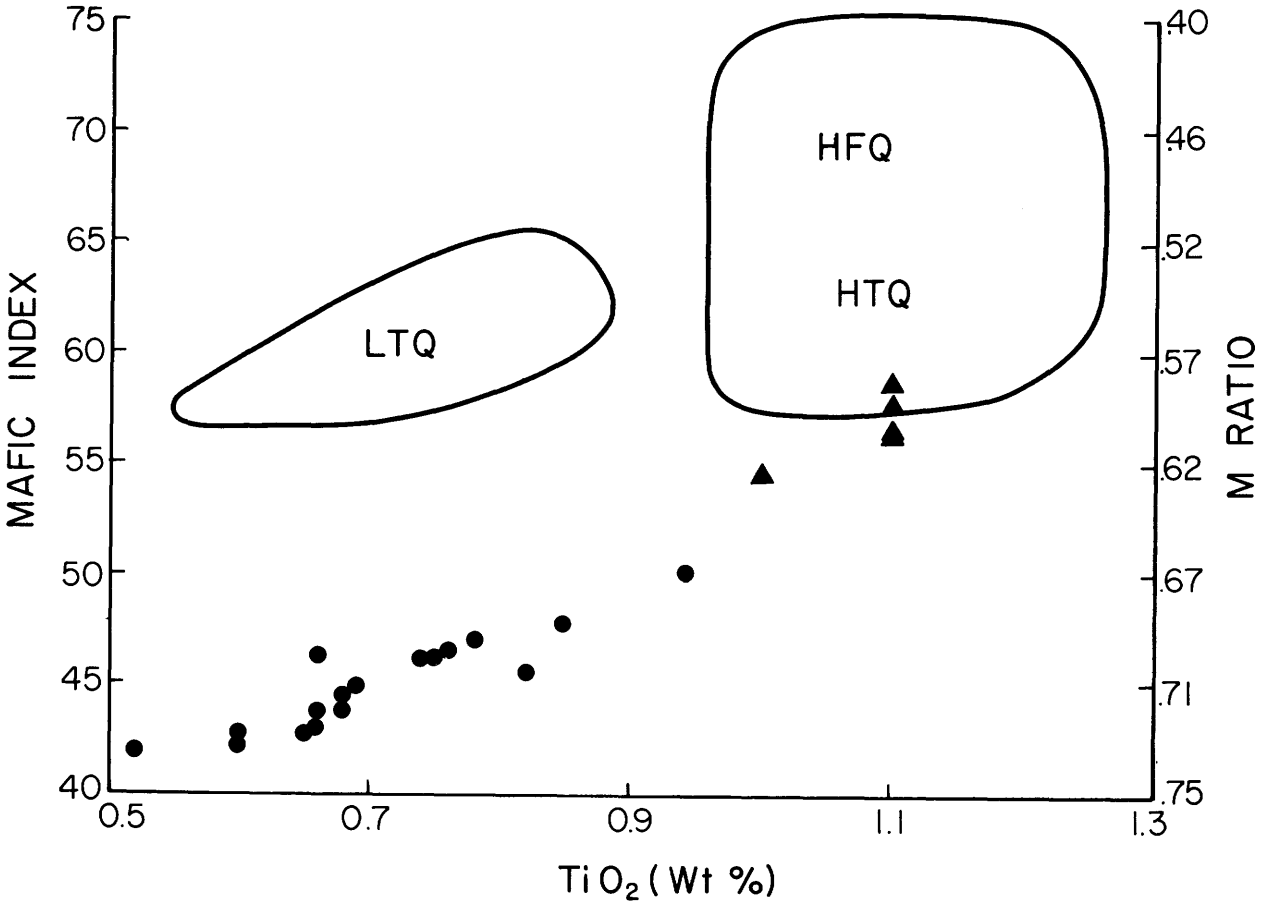

FIGURE 17.4.—Mafic index ((FeO + Fe_2O_3) × 100/(FeO + Fe_2O_3 + MgO), weight percent) and M-ratio (Mg/(Mg + Fe^{2+}), mole percent) plotted against TiO_2 (weight percent). Figure modified from Weigand and Ragland (1970). LTQ, low-Ti, quartz-normative diabase; HFQ, high-Fe, quartz-normative diabase; HTQ, high-Ti, quartz-normative diabase.

percent of bulk rock, orthopyroxene, plagioclase, and groundmass, respectively. Taking an orthopyroxene/plagioclase ratio of 65/35, allowing for conversion of volume percent to weight percent orthopyroxene, collecting terms, and rearranging yields an equation to approximate the groundmass composition:

$$C_G = (d_B C_B - d_O V_O C_O - 0.54 d_O V_O C_P)/d_B - 1.54 d_O V_O$$

where V_O is volume fraction orthopyroxene; d_B and d_O are densities of bulk rock and orthopyroxene, respectively; other terms are defined above.

Results of these calculations for several incompatible elements in the groundmass of phyric samples and whole rocks for aphyric samples are given in figure 17.6. Since no trace-element microprobe analyses are possible, only incompatible elements with effectively zero concentrations in orthopyroxene and plagioclase were examined. Results indicate that the calculated intercumulus liquid compositions show slight cyclical variation with depth, with the development of at least four zones of incompatible-element enrichment (fig. 17.6). This pattern is corroborated by some microprobe data indicating increasingly sodic groundmass plagioclase in the areas of incompatible element enrichment. A closer sampling might reveal more than four of the intercumulus liquid cyclical variation units; in fact, the uppermost unit may be divided in two. Note that a mafic pegmatite is located near the region of culmination (region of highest incompatible-element concentration) of two of these units (fig. 17.6); unsampled pegmatites may exist near other regions of culmination. Table 17.1 demonstrates that pegmatites are greatly enriched in these elements relative to the groundmass. This variation in intercumulus liquid composition is apparently caused by in situ fractionation and migration

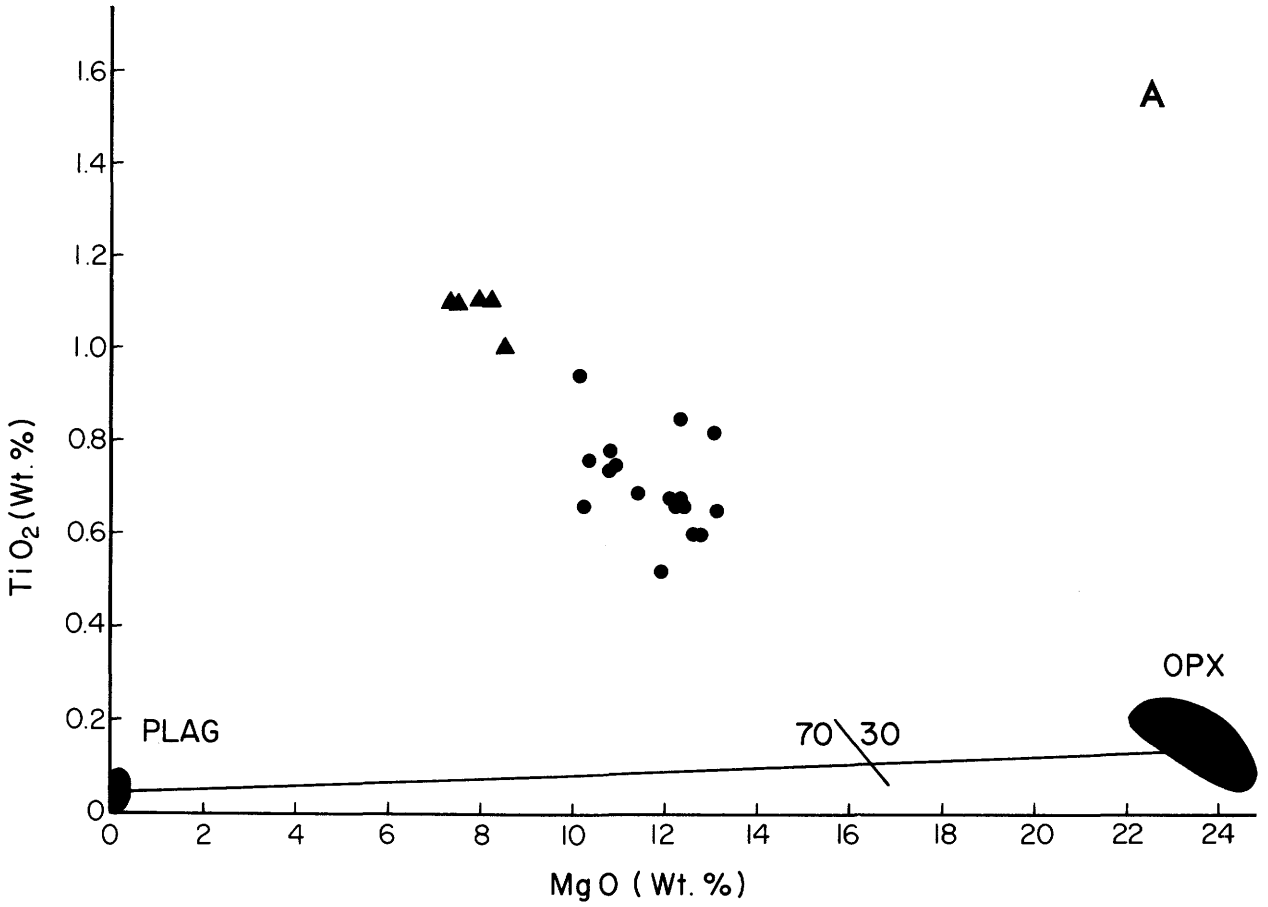

FIGURE 17.5.—Two-oxide mixing diagrams. Dark areas represent microprobe analyses of early-crystallizing (near-liquidus) plagioclase and orthopyroxene ("primocrysts").

of intercumulus liquid in the sheet, but the physical and mechanical processes causing this variation are not presently understood.

Although the trends observed in figure 17.6 delineate multiple cycles of intercumulus liquid variation in the sheet, they do not explain the distribution of primocrysts. Evidence for minor gravity settling and the accumulation of primocrysts in the interior of the sheet can be found in figures 16.5 and 16.6 (Gottfried and Froelich, this volume). Flow differentiation (Bhattacharji and Smith, 1964) may have occurred, but flow differentiation in its simplest form cannot explain all the observations. Simple physical flowage differentiation of primocrysts in a crystal mush toward the center of the conduit cannot cause the chemical trends in the groundmass shown in figure 17.6, assuming the calculated groundmass compositions accurately represent liquid compositions. Such a process would lead to similar groundmass compositions throughout the section without further in situ differentiation.

TABLE 17.1.—*Incompatible-element contents of mafic pegmatites in Boyds sheet diabase*

[343 and 248 are distance above lower contact, in feet; P_2O_5 in percent; Nb, Hf, Th, Ce in parts per million]

	343	209
P_2O_5	0.64	0.24
Nb	25.	9.9
Hf	8.17	3.38
Th	8.28	3.14
Ce	75.4	30.8

Figure 17.2 clearly shows an increasing degree of alteration toward the bottom of the sheet in the lower 75 feet of section. Did this alteration affect chemical trends other than H_2O^+ and Fe_2O_3/FeO? Elements plotted in figure 17.6 apparently were not affected by alteration, because their concentrations in the phyric and aphyric zones are similar. Recall that alteration

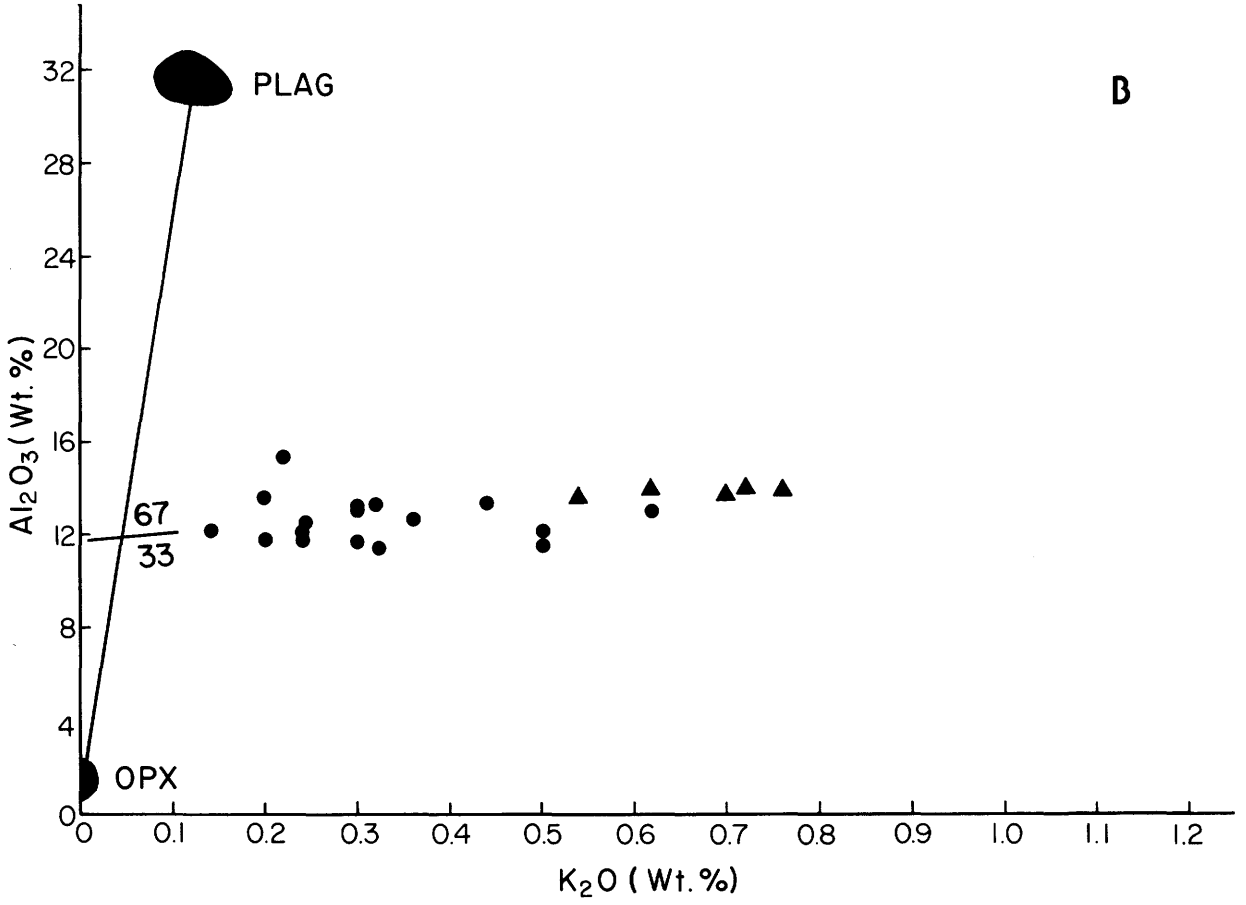

FIGURE 17.5.—Continued.

increases downward in the phyric zone (fig. 17.2) and affects clinopyroxene primarily. Table 17.2 shows that clinopyroxene (including fresh and altered) increases downward in the aphyric zone but MgO decreases, as does CaO. Since these aphyric rocks contain only two major primary minerals, plagioclase and clinopyroxene, the only explanation for the MgO trend is selective leaching and removal of Mg during alteration. Calcium was probably removed as well. Iron was not, because one of the alteration products of the clinopyroxene breakdown was a secondary iron oxide.

Up to this point the term "chill margin" has been conspicuously omitted from this report. The five lowermost samples, although aphyric, represent 75 feet of section and thus clearly cannot represent a chill margin. Although average lengths of groundmass crystals are similar in both the phyric and aphyric rocks, the aphyric groundmass crystals are more acicular, suggesting more rapid rates of undercooling. Spherulitic structures in the aphyric rocks offer further evidence for more rapid undercooling. The sample nearest the lower contact is the finest grained of all and thus is the best candidate for a true chill margin. However, the aphyric samples do not have the same bulk composition as the weighted average of the entire sheet, implying either that they do not represent a parental magma composition or that the Boyds sheet has lost a significant amount of evolved intercumulus liquid from the center of the sheet. We favor the first explanation for the reasons given below.

TABLE 17.2.—*Whole-rock contents of clinopyroxene (CPX, in volume percent) and selected oxides (in weight percent) in the lower six samples of Boyds sheet diabase*

[D, distance above lower contact (in feet); FeO*, total Fe expressed as FeO]

D	CPX	MgO	CaO	FeO*
84	32.5	8.7	11.5	10.6
61	36.4	8.4	10.8	10.1
38	38.5	8.1	10.9	10.3
12	39.3	8.0	10.5	10.2
2	41.1	7.4	10.6	10.2
0	39.1	7.5	10.2	10.1

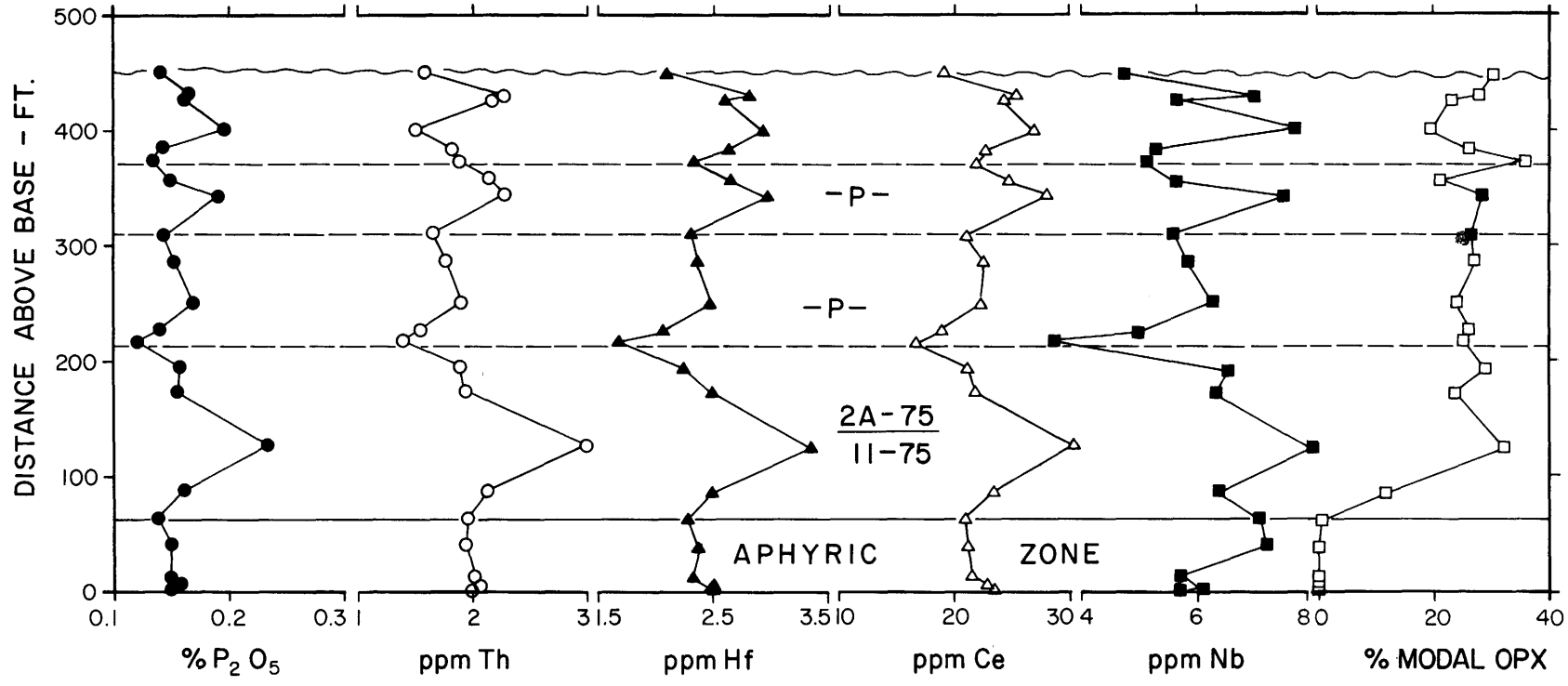

FIGURE 17.6.—Plots of distance above lower contact of Boyds sheet (in feet) against several incompatible-element groundmass compositions for phyric rocks and whole-rock compositions for aphyric rocks. Solid squares in the OPX against depth plot are estimated values. Horizontal dashed lines separate the four zones of incompatible-element enrichment. Locations of mafic pegmatites are marked by "P"; 2A–75 is core from upper part of sheet and 11–75 is core from lower part. See text for further explanation.

Although the top of the Boyds sheet is eroded away, we assume symmetrical bulk-rock compositional trends similar to those in the York Haven sheet (Smith, 1973). When elements not affected by alteration are considered, "chill-margin" (aphyric-zone) compositions are almost identical to the weighted average of phyric-zone groundmass compositions (fig. 17.6). The weighted average M-ratio (molar MgO/(MgO + FeO) ratio) for the entire sheet is close to 0.70, the value that is commonly thought to represent a "primary" basaltic melt in equilibrium with a peridotitic mantle. Thus we envision a deeper magma chamber, with a parental magma composition equivalent to the average composition of the sheet undergoing orthopyroxene + plagioclase (+ minor clinopyroxene) crystallization and crystal settling. At the time of sheet emplacement, the liquid phase was apparently similar in composition throughout the chamber, as evidenced by lack of a significant trend in groundmass compositions throughout the sheet. The magma at the top of the chamber, devoid of primocrysts but possibly enriched in H_2O, was emplaced first and formed the aphyric zone. Subsequent intrusion of the main mass of the sheet (above the preserved aphyric zone), followed by in situ fractionation associated with minor movement of intercumulus liquid, accompanied final crystallization of the sheet. Other aspects of the Boyds sheet, such as determining the depth of orthopyroxene crystallization, await further work.

REFERENCES

Bhattacharji, S., and Smith, C.H., 1964, Flowage differentiation: Science, v. 145, p. 150–153.

Ragland, P.C., 1983, Early Mesozoic diabase dikes of eastern North America: magma types [abs.]: Geological Society of America Abstracts with Programs, v. 15, p. 666.

Smith, R.C., II, 1973, Geochemistry of Triassic diabase from southeastern Pennsylvania: University Park, Pennsylvania State University, unpub. Ph.D. thesis, 262 p.

Smith, R.C., II, Rose, A.W., and Lanning, R.M., 1975, Geology and geochemistry of Triassic diabase in Pennsylvania: Geological Society of America Bulletin, v. 86, p. 943–955.

Weigand, P.W., and Ragland, P.C., 1970, Geochemistry of Mesozoic dolerite dikes from eastern North America: Contributions to Mineralogy and Petrology, v. 29, p. 195–214.

18. GEOCHEMICAL RECONNAISSANCE OF DIABASE FROM VULCAN MATERIALS QUARRY IN THE CULPEPER MESOZOIC BASIN NEAR MANASSAS, VIRGINIA

J.A. Philpotts, D. Gottfried, F.W. Brown, Z.A. Brown, W.B. Crandell, A.F. Dorrzapf, Jr., J.D. Fletcher, D.W. Golightly, L. Mei, and N. Rait

This note presents analytical data on the chemical compositions of Early Jurassic diabase and Late Triassic hornfels from the Vulcan Materials quarry as discussed at the USGS workshop on early Mesozoic basins of the Eastern United States. The quarry is located (lat 38°46′ N., long 77°31′ W., Gainesville 7.5′ quadrangle) in one of the easternmost diabase sheets (the Gainesville diabase sheet) of the central Culpeper basin, just west of Manassas at Rixlew, Va. (see Gottfried and Froelich, chapter 16, this volume). Geochemical study of these samples complements study of drill core from hole V16 (Gottfried and Froelich, this volume) located on the southeast rim of the quarry, a few hundred meters from the present sampling sites. Analyses to date of samples from hole V16 have identified only rocks containing less than 5 percent MgO. In addition, TiO_2, which is highly useful for petrogenetic interpretation, has variable concentrations in samples from the V16 core. The quarry results elucidate the chemical nature of the diabase sheet at this locality and provide a context for interpreting the core data.

In accord with the reconnaissance nature of this study, sample locations were recorded only approximately (see table 18.1). Hornfels GS 15 and fine-grained diabases GS 16, 17, 18, 19, and 20 were all collected within 1–2 m of the southwestward-dipping chilled upper contact of the diabase sheet. Medium-grained diabases GS 22 and 23 were collected an estimated 15 m below this contact. Samples GS 26 and 35 are coarse-grained diabases containing pyroxene crystals more than 2 cm long; although GS 35 is float, it is included here as a possible example of a late differentiate.

Analytical results on the chemical compositions of these samples are presented in tables 18.1 and 18.2. The major-element-oxide abundances reported in table

TABLE 18.1.—*Major-oxide and normative mineral compositions, in weight percent, for hornfels and diabase from the Vulcan Materials Quarry, central Culpeper basin, Virginia*
[m.g., medium-grained; c.g., coarse-grained. Mole % An, mole percentage of anorthite in the normative feldspar; mafic Mg#, mole ratio Mg/(Mg + Fe) for mafic minerals in the norm]

	Locality #1-on highest bench about 15 m below soil level and 600 m NNW of quarry office building			#2-on second cut bench about 10 m down and 30 m SW of #1		#3-on third bench about 10 m below #2		#4-about 10m down and 150 m SE from #3			#5-about 15 m down and 150 m SW from #4	
	GS-15	GS-16	GS-17	GS-19	GS-20	GS-22	GS-23	GS-24	GS-25	GS-26	GS-35	GS-37
	Hornfels	Chilled diabase	Chilled diabase	Chilled diabase	Chilled diabase	m.g. diabase	m.g. diabase	m.g. diabase	m.g. pinkish diabase	c.g. pink diabase	c.g. pinkish diabase float	m.g. diabase
SiO_2	53.7	50.5	51.0	51.3	52.1	51.8	52.5	50.6	50.9	53.7	59.3	52.0
Al_2O_3	18.7	14.5	14.5	14.5	14.5	16.8	14.9	14.6	15.5	12.1	12.0	14.9
Fe_2O_3	5.6	3.9	2.9	3.0	2.5	0.9	2.6	3.0	1.8	3.0	3.0	3.0
FeO	2.7	6.7	7.3	7.4	7.8	8.7	7.2	10.1	10.0	9.4	7.5	9.5
MgO	4.7	7.3	6.9	6.7	6.8	5.3	6.3	3.9	3.6	3.3	1.6	3.5
CaO	3.8	10.3	10.3	10.4	10.3	10.6	11.0	8.9	6.7	6.9	5.7	8.8
Na_2O	5.2	2.5	2.0	2.2	2.1	2.5	2.3	2.6	3.5	3.7	3.8	2.8
K_2O	2.2	0.60	0.51	0.60	0.62	0.57	0.89	0.96	2.0	1.6	2.1	1.0
H_2O+	1.1	1.3	1.4	0.54	0.80	0.60	0.72	1.1	2.2	1.7	1.1	0.94
H_2O-	0.50	0.62	0.84	0.32	0.08	0.16	0.22	0.43	0.18	0.35	0.16	0.26
TiO_2	1.0	1.2	1.2	1.2	1.1	0.92	1.2	2.0	1.7	2.1	1.6	1.8
P_2O_5	0.26	0.14	0.15	0.20	0.18	0.12	0.14	0.21	0.23	0.35	0.52	0.23
MnO	0.11	0.26	0.20	0.18	0.18	0.17	0.17	0.19	0.18	0.23	0.15	0.18
CO_2	0.08	0.04	0.03	0.02	0.02	0.03	0.02	0.04	0.03	0.08	0.03	0.02
TOTAL	99.7	99.9	99.2	99.2	98.7	99.2	100.2	98.7	98.5	98.5	98.6	98.9
Opaques	10	8	7	7	6	3	6	8	6	9	8	8
Feldspar	76	52	50	51	51	58	53	55	65	54	56	56
Diopside	0	19	18	19	18	16	21	15	10	18	13	15
Orthopyx.	12	17	19	18	20	20	15	16	18	12	6	14
Olivine	0	0	0	0	0	0	0	0	1	0	0	0
Quartz	1	3	6	5	6	3	4	5	0	7	16	7
Mole % An	42	70	76	74	75	75	73	68	57	41	36	67
Mafic Mg#	--	76	71	70	68	56	69	50	45	48	37	48

TABLE 18.2.—*Semiquantitative trace-element abundances, in parts per million by weight, for hornfels and diabase from the Vulcan Materials Quarry, central Culpeper basin, Virginia*

[m.g., medium-grained; c.g., coarse-grained. Precision: S, Pd, Pt ± 20 percent; other elements + 50 percent, −33 percent. —, not detected]

	GS-15 Hornfels	GS-16 Chilled diabase	GS-17 Chilled diabase	GS-19 Chilled diabase	GS-20 Chilled diabase	GS-22 m.g. diabase	GS-23 m.g. diabase	GS-24 m.g. diabase	GS-25 m.g. pinkish diabase	GS-26 c.g. pink diabase	GS-35 c.g. pinkish diabase float	GS-37 m.g. diabase
S	--	200	200	300	200	100	100	100	100	200	300	900
Pd	--	0.004	0.006	0.004	0.004	0.004	0.004	0.007	0.007	0.002	0.015	--
Pt	--	--	0.008	0.003	0.003	0.007	--	--	--	0.003	0.003	--
Ag	0.18	0.41	0.37	0.30	0.34	0.29	0.34	0.33	0.36	6.2	0.30	0.51
B	65	12	7.3	7.8	8.6	12	17	9.2	65	150	310	17
Ba	300	59	81	110	94	86	120	150	210	190	350	200
Be	3.1	--	--	--	--	--	--	--	--	1.4	2.3	1.1
Ce	46	--	--	--	--	--	--	--	--	44	63	--
Co	24	41	42	41	43	34	38	38	34	35	28	42
Cr	91	270	240	220	200	26	59	1.9	2.1	--	--	2.5
Cu	2	210	110	160	98	80	160	180	150	170	82	210
Dy	--	--	--	35	--	--	--	26	--	--	--	--
Ga	28	8.9	14	11	12	13	11	15	16	16	21	20
La	41	21	--	25	31	--	--	24	28	42	47	43
Mo	--	1.2	1.4	1.4	1.2	1.4	1.5	1.3	--	1.8	--	2.4
Nb	12	9.3	8.9	7.4	9.9	8.2	8.1	13	7.4	13	14	14
Ni	63	100	110	89	85	59	83	39	30	28	7.9	36
Pb	22	17	12	13	15	14	16	17	11	11	16	17
Sc	17	28	30	30	29	24	32	23	23	31	20	28
Sn	5.9	--	--	--	--	--	--	--	--	--	6.3	--
Sr	410	200	230	260	210	270	240	310	520	320	260	310
V	160	220	220	220	220	180	230	270	200	190	59	230
Y	22	18	19	20	18	14	18	19	22	43	46	27
Yb	4.3	2.3	2.7	2.9	3.5	2.3	2.7	3.9	4	7.2	7.9	4.8
Zn	160	220	110	130	150	130	100	170	100	100	100	180
Zr	68	52	66	67	60	46	61	59	71	280	130	110

18.1 were determined by inductively coupled plasma (ICP) analysis, except K_2O, which was determined by atomic absorption (AA) analysis. Precision (relative standard deviation) for the major-element determinations is typically about 3 percent. For elements with concentrations less than 1 percent, precision can exceed 10 percent. Normative mineralogy, calculated by the method of Morse (1973), is also given in table 18.1; the "mafic Mg#" is the mole percent Mg/(Mg + Fe) in the mafic normative phases. Abundances of S (by Leco analysis), Pd and Pt (by fire assay), and other trace elements (by semiquantitative DC arc-emission spectroscopy) are presented in table 18.2. Precision is estimated to be about 20 percent for the S, Pt, and Pd determinations. For the emission spectrographic data, precision is quoted as + 50 percent, −33 percent. For a relatively homogeneous set of samples such as the present diabases, actual precisions may be better.

The chemical composition of the hornfels (sample GS 15) is not grossly dissimilar to that of the diabase. Sample GS 15 is higher in Al_2O_3 and Na_2O and lower in FeO, MnO, and CaO than any of the diabase samples; it also has 1 percent normative corundum, a distinctly high ferric/ferrous iron ratio, and one hundred times lower Cu than the diabase. Sample GS 19 was thought to be hornfels in the field. The chemical composition, however, indicates diabase. This underscores the difficulty of exactly pinpointing the diabase-hornfels contact at this locality (or in the drill core).

Components such as alkalis, H_2O^+, and CO_2, which are sensitive to alteration, indicate that the igneous rocks are relatively unaltered. However, samples GS 22 and GS 25 have high Al_2O_3 and low ferric/ferrous iron ratios that yield high normative feldspar and low normative opaque minerals, diopside, quartz, and mafic Mg#. These two compositions may not reflect those of the primary igneous rocks. In general the diabases appear to belong to a differentiation suite and show quite a range in MgO (1.6–7.3 percent). The lower MgO diabases have higher P_2O_5, TiO_2, and K_2O and lower CaO contents. Pegmatitic diabase GS 35 has even more P_2O_5, and K_2O enrichment; Na_2O shows a somewhat larger increase in relative abundance than does TiO_2. In general, as MgO contents decrease through the suite, Nb, Zr, Na_2O, K_2O, Ba, La, Ce, Yb, and Y contents all increase. It is reassuring to see that potentially mobile elements like Na, K, and Ba appear to retain primary signatures in these diabases. Later differentiates tend to be strongly enriched in the small cations Si, B, and Be. At the other extreme, Cr declines precipitously as MgO decreases in the high-MgO diabases. Ni shows a more regular decline over the whole series. Sr goes through a distinct maximum. CaO, Co, and Sc show little change in the diabases then decline in the most evolved samples. Although there is considerable scatter, Zn, Cu, and Pb appear to behave in a similar fashion. Al_2O_3, V, and MnO are not too different except for flatter or even rising trends in the intermediate diabases, followed by depletion. P_2O_5, TiO_2, and FeO exaggerate this trend; they are distinctly higher in the low-MgO diabases than in the high-MgO diabases. Ti/P is quite uniform (11 ± 2) in the diabases but falls to a value of 4 in GS 35. With one exception, Ti/Nb is also uniform in the diabases and pegmatitic diabases (800 ± 200). It is perhaps worth noting again that the spectroscopic data are semiquantitative, and absolute concentrations are only approximate (for example, for zirconium).

The quarry diabase samples may be sorted into two compositional groups — a high-MgO group (samples GS 16, 17, 19, 20, 22, and 23) and a low-MgO group (GS 24, 25, 26, and 37). Samples from the V16 core are also low in MgO. The low-MgO diabase differs from the high-MgO diabase also in having approximately 4 percent more normative feldspar, variably lower percentages of An in the feldspar, and a 20 percent lower mafic Mg#. Both diabase groups belong to Weigand and Ragland's (1970) high-Ti quartz-normative type. The low-MgO magma may well have evolved from the high-MgO magma by removal of early-formed crystals. However, it is not clear from what is known at present of the geographic distribution that such differentiation has taken place in situ. Indeed, the lack of any obvious cumulates in the quarry and the extensive occurrence of low-MgO diabase (in both the quarry and V16 core), whose composition differs significantly from that of the high-MgO chilled diabase at the quarry, appear to argue against all or even most of the differentiation having taken place in situ. It is possible that a compositionally zoned source magma was tapped or that there were two or more pulses of magma injection at this locality and that the complementary fraction, which appears to be missing, is located elsewhere in the sheet or its feeder system. The general picture emerging from current studies of Mesozoic diabase sheets is not the textbook example of a sill undergoing quiet gravitational differentiation in place but rather a more complicated model showing considerable lateral heterogeneity and multiple injection of magma that has undergone fractionation elsewhere.

ACKNOWLEDGMENTS

We thank the management of Vulcan Materials Company for allowing access to the quarry. The field guidance of Al Froelich (U.S. Geological Survey) is much appreciated.

REFERENCES

Morse, S.A., 1973, Basalts and phase diagrams: Amherst, University of Massachusetts, 158 p.

Weigand, P.W., and Ragland, P.C., 1970, Geochemistry of Mesozoic dolerite dikes of eastern North America: Contributions to Mineralogy and Petrology, v. 29, p. 195–214.

19. SOME COMPOSITIONAL ASPECTS OF MESOZOIC DIABASE SHEETS FROM THE DURHAM AREA, NORTH CAROLINA

Z.A. Brown, P.J. Aruscavage, F.W. Brown, L. Mei, P.P. Hearn, and J.A. Philpotts

INTRODUCTION AND SAMPLES

The Braggtown, Nello Teer, and Butner diabase sheets, which may be interconnected, occur within 20 km of each other just north of Durham, N.C., in association with other Mesozoic rocks of the Durham basin (see fig. 15.1, Froelich and Gottfried, this volume). The present note reports progress presented at the second USGS workshop on early Mesozoic basins of the Eastern United States regarding analytical data we have obtained for these three diabase bodies that addresses a number of questions of specific geochemical interest. The general geology of the area and of the three locations is outside the limited scope of the present report; no accompanying maps are presented.

One aspect of the work is to evaluate how useful cuttings might be, compared with drill core, for determining diabase composition and thereby to obtain some information on the chemistry of the Butner sheet and its lateral and depth variation. Cutting chips, segregated into 10-ft intervals, had been obtained by drilling of holes ATH 4 and ATH 9 in the southeast corner of the Butner diabase sheet. ATH 9 (elevation 310 ft) is located about 0.5 km west of ATH 4 (elevation 350 ft). The cuttings were washed in demineralized water, and the few obvious pieces of soil and vegetation mixed in with the samples were removed before crushing.

Another question being considered is the nature of the "knobby-weathering" diabase, which is prevalent at the Nello Teer Quarry and the nearby Braggtown Quarry. A field interpretation was that this "knobby" diabase might represent a basal cumulate. To evaluate this interpretation we analyzed sample pairs of "knobby" diabase and of normal (non-knobby) diabase, collected nearby, from both the Braggtown and the Nello Teer Quarries. The Braggtown Quarry is the location from which the rock standard DNC–1 (Dolerite, North Carolina) was obtained (Flanagan, 1984). Unfortunately, the exact collection site of DNC–1 is not certain at this time, and there is considerable local variation in the aspect of the diabase and in grain size; DNC–1 has high abundances of Pt and Pd, which other samples from the site have failed to corroborate. The knobby–non-knobby analyzed pair (samples GS 109 and 107, respectively) were obtained at the northwest corner of the Braggtown Quarry. To gain additional insight on local compositional variations, we analyzed a medium-grained diabase (GS 110) from the foot of the steps about 100 m to the southeast on the south side of the quarry and a diabase (GS 112) from the northeast corner, about 0.3 km away. Total relief at the locality is only about 10 m. Pt and Pd abundances of these four samples were also determined. The knobby–non-knobby pair from the Nello Teer Quarry came from the lowest diabase exposed in the main pit. For comparison, the uppermost diabase from this pit and a fine-grained chilled diabase, collected 1 m from the contact with metavolcanics in the smaller pit to the east, have also been analyzed. The knobby diabase (sample GS 124) was collected on the floor of the main pit at an elevation of about 170 feet at a point about 500 m due north of the Nello Teer offices at the entrance to the quarry. The non-knobby sample, GS 126 (elevation about 200 ft), was collected about 80 m north of GS 124. The uppermost diabase, GS 133, was collected at soil level (elevation about 270 ft) at a location about 250 m north-northeast of GS 126. Sample GS 121 was collected 300 m to the east-southeast at an elevation of about 200 feet.

RESULTS

The major-element compositions of these diabases are presented in table 19.1. The samples were analyzed by our standard "rapid-rock" procedure: fusion followed by inductively coupled plasma (ICP) analysis, except that K_2O is determined by atomic absorption analysis. Some of the P_2O_5 values appeared a little high; colorimetric determinations were therefore made on the same solutions used for ICP and are reported in table 19.1. The average of four values for all elements in standard diabase run with these samples agrees with the abundances given by Flanagan (1984) to within 1 percent relative. Normative compositions, calculated by the method of Morse (1973), are also given in table 19.1. "Mole % An" is the mole percentage of anorthite in the normative feldspar. "Mafic Mg#" is the mole ratio Mg/(Mg + Fe) for the mafic minerals in the norm.

Abundances of Ba, Cr, Co, Cu, Nb, Ni, Sr, V, Y, Zn, and Zr determined by ICP on more concentrated solutions than those used for the major elements are reported in table 19.2. Note that these data are preliminary. For example, the solutions for the trace-element determinations were made by acid dissolution and, for some rocks, this procedure does not put all the Zr into solution. P_2O_5 determinations by ICP are not shown but were in good agreement with the colorimetric values. MnO abundances determined by ICP on the more concentrated solutions were within 0.01 percent absolute of the values given in table 19.1 except for one sample. Precisions for the trace-element determinations, estimated on the basis of weighing errors, volumetric errors, and instrumental errors, are given in table 19.2. For the ranges given, the better precision values correspond with the higher abundance values. Pt and Pd abundances were determined by fire assay for the four Braggtown samples and are also given in table 19.2; estimated precision (relative standard deviation) is 20 percent.

DISCUSSION

Pt and Pd are almost equal in abundance and show little variation in the four Braggtown diabase samples analyzed. The Pt and Pd values are similar to those we usually obtain for the rock standards W–1 and W–2. However, although Pd values of 17 and 7 ppb respectively for DNC–1 and W–2 (analyzed concurrently with the unknowns) are consistent with our previous determinations, Pt values of 23 and 3.6 ppb respectively appear low by about 5 or 6 ppb. Our Braggtown Pt values therefore may well be low by such an amount. However, the abundances of Pt and Pd are clearly lower than those in DNC–1. In terms of major-element composition, DNC–1 is within the range shown by the analyzed samples and may perhaps have been collected towards the middle of the quarry.

Concerning the question of any compositional feature associated with the knobby texture, both the Braggtown and Nello Teer knobby diabases have distinctly lower Al_2O_3 than their associated normal diabases. However, all other intrapair differences are less than one percent. We conclude that knobby weathering at these sites does not appear to be any obvious function of chemical composition and may be a textural or structural feature. In particular it appears that the absence of knobby weathering cannot be used to discriminate noncumulate rocks from cumulates. The possibility remains that this texture forms, if at all, only in rocks that are (partial) cumulates. Comparison of the lower two diabases from the Nello Teer main quarry with the uppermost diabase shows relatively little change in major- or trace-element composition. In terms of normative composition, all three are quite distinct from the chilled diabase from the smaller pit to the east, particularly in having less orthopyroxene, more olivine, and higher mole % An and Mg#. These differences might indicate a later, more primitive melt for the main pit samples. More likely, however, these three are partial cumulates introduced as a later magma containing more phenocryst material than the chilled diabase sample.

The abundances of Na_2O, K_2O, H_2O^+, and CO_2, which can be sensitive to alteration, indicate that the Butner samples (like the Braggtown and Nello Teer samples) represent reasonably unaltered diabase. Although we have confirmed by energy-dispersive X-ray scanning electron microscope analysis that a white efflorescence common on Nello Teer diabase is a sodium sulfate (probably mirabilite), the Nello Teer diabase samples analyzed have no obvious indication of excess sodium. For the Butner samples, we conclude that such cuttings can provide useful chemical information. There are some small compositional differences among the ATH 9 samples, but these do not appear to be a simple function of depth for most elements. The ATH 4 samples are surprisingly homogeneous considering that they were obtained over a depth of 40 feet. Diabase from ATH 9 has somewhat higher mole % An and Mg# and might represent a more primitive melt. However, the presence and variation of normative olivine probably indicates partial accumulation in ATH 9 diabases.

TABLE 19.1.—*Major-oxide and normative mineral compositions, in weight percent, for diabase from the Butner, Braggtown, and Nello Teer diabase sheets, near Durham, N.C.*
[Mole % An, mole percentage of anorthite in the normative feldspar; mafic Mg#, mole ratio Mg/(Mg + Fe) for mafic minerals in the norm]

	BUTNER								BRAGGTOWN				NELLO TEER			
	HOLE ATH #9				HOLE ATH # 4				NON-KN	KNOBBY	SOUTH	NORTHEAST	CHILL	KNOBBY	NON-KN	UPPER
	10'- 20'	20'- 30'	40'- 50	50'- 60'	30'- 40'	40'- 50'	50'- 60'	60'- 70'	GS 107	GS 109	GS 110	GS 112	GS 121	GS 124	GS 126	GS 133
SiO_2	48.9	48.8	49.2	49.8	49.8	49.4	49.6	49.6	48.7	48.8	49.3	46.3	47.7	46.7	45.8	47.0
Al_2O_3	17.0	16.5	16.8	16.9	16.7	16.6	16.8	16.6	18.7	17.0	15.7	14.7	16.5	18.5	19.6	17.8
Fe_2O_3	1.5	1.5	1.8	2.0	2.2	2.1	2.0	2.2	2.0	2.6	2.9	2.6	2.5	1.5	1.1	1.8
FeO	6.2	6.6	6.2	6.2	6.5	6.3	6.5	6.6	6.1	6.8	7.3	7.8	8.3	7.1	6.9	6.9
MgO	10.1	10.5	10.1	9.7	8.4	8.2	8.2	8.3	7.5	8.1	7.4	12.9	7.6	11.0	11.3	11.4
CaO	12.1	11.9	11.9	11.8	11.7	11.8	11.6	11.3	12.8	12.2	12.1	10.6	11.2	11.3	11.1	11.6
Na_2O	1.8	1.8	1.8	1.9	2.0	2.0	2.1	2.0	2.0	1.9	2.1	1.6	2.1	1.8	1.6	1.7
K_2O	.27	.26	.26	.27	.32	.34	.33	.41	.16	.17	.22	.10	.31	.15	.12	.21
H_2O+	.55	.49	.58	.61	.78	.74	.72	1.6	.73	.88	.95	1.3	1.1	.83	.78	1.1
H_2O-	.33	.31	.32	.31	.46	.49	.41	.52	.33	.50	.35	.21	.39	.37	.24	.52
TiO_2	.39	.40	.43	.46	.54	.52	.54	.55	.33	.46	.53	.39	.72	.42	.33	.41
P_2O_5	.08	.08	.09	.10	.10	.11	.12	.11	.06	.09	.10	.07	.12	.07	.07	.06
MnO	.15	.15	.15	.15	.16	.16	.16	.16	.15	.17	.18	.18	.18	.14	.13	.14
CO_2	.01	.01	.01	.01	.02	.02	.04	.01	.02	.04	.04	.04	.02	.06	.02	.01
TOTAL	99.4	99.3	99.6	100.2	99.7	98.8	99.1	100.0	99.6	99.7	99.2	98.8	98.7	99.9	99.1	100.6
Wt% Norm																
Opaques	3	3	3	4	4	4	4	4	3	5	5	5	5	3	2	4
Feldspar	55	54	54	55	55	56	56	56	60	55	53	48	56	59	61	56
Diopside	18	18	17	17	18	19	18	17	17	19	22	16	17	11	7	13
Orthopyx.	16	16	18	20	22	21	21	23	14	20	19	15	16	9	9	9
Olivine	8	9	6	4	0	0	1	0	4	1	0	17	5	18	20	17
Quartz	0	0	0	0	0	0	0	0	0	0	0	0	0	0	0	0
Mole % An	82	82	82	82	80	80	79	80	82	81	78	82	79	84	86	84
Mafic Mg#	77	77	78	78	74	75	74	74	73	73	70	78	67	76	77	78

TABLE 19.2.—*Trace-element abundances, in parts per million by weight, for diabase from the Butner, Braggtown, and Nello Teer diabase sheets, near Durham, N.C.*

	BUTNER		BRAGGTOWN				NELLO TEER				ESTIMATED PRECISION
	HOLE ATH 9	HOLE ATH 4	NON-KN	KNOBBY	SOUTH	NORTHEAST	CHILL	KNOBBY	NON-KN	UPPER	
	40'- 50'	40'- 50'	GS 107	GS 109	GS 110	GS 112	GS 121	GS 124	GS 126	GS 133	
Ba	80	102	52	65	96	41	143	83	70	72	5 - 10%
Cr	580	420	360	350	320	930	250	440	230	520	5 - 20%
Co	43	41	42	46	45	67	53	58	59	59	5 - 10%
Cu	65	71	68	76	92	84	143	85	62	92	5 - 10%
Nb	1.3	1.9	1.1	1.4	1.7	1.1	2.4	1.2	0.9	1.0	10 - 20%
Ni	180	122	114	120	88	410	130	310	330	330	5 - 10%
Sr	148	158	120	116	123	86	148	142	145	141	5 - 10%
V	180	210	156	210	250	200	250	148	123	158	5 - 10%
Y	19	23	15	21	24	19	32	17	13	16	10 - 15%
Zn	57	62	59	68	80	74	84	59	55	59	10 - 15%
Zr	36	44	23	33	31	26	46	30	25	28	5 - 10%
Pt			.0059	.0086	.0076	.0083					20%
Pd			.0060	.0068	.0080	.0072					20%

ATH 4 diabase might be reasonably representative of parental magma of the Butner sheet.

None of the 16 diabase samples analyzed has quartz in the norm. It may be significant that the Butner ATH 4 samples and two of the Braggtown samples have little if any normative olivine. All of the diabases have low TiO_2 contents, although the Nello Teer chilled diabase has somewhat higher TiO_2 than the other samples. As a group, the diabases are similar in major- and trace-element composition to the olivine-normative dike rocks analyzed by Weigand and Ragland (1970). Some of the present samples have high Al_2O_3. The compositional similarity of the diabases from Butner, Braggtown, and Nello Teer, particularly in such characteristics as mole % An and Mg#, suggest that these three diabase sheets may well be comagmatic.

ACKNOWLEDGMENTS

We very much appreciate the help of Jim Sprinkle and the Nello L. Teer Company in the collection of the Butner and Nello Teer Quarry samples. The field acuity of Al Froelich (U.S. Geological Survey) is gratefully acknowledged.

REFERENCES

Flanagan, F.J., 1984, Three USGS mafic rock reference samples, W-2, DNC-1, and BIR-1: U.S. Geological Survey Bulletin 1623, 54 p.

Morse, S.A., 1973, Basalts and phase diagrams: Amherst, University of Massachusetts Press, 157 p.

Weigand, P.W., and Ragland, P.C., 1970, Geochemistry of Mesozoic dolerite dikes from eastern North America: Contributions to Mineralogy and Petrology, v. 29, no. 3, p. 195–214.

20. RECENT PETROLOGIC STUDIES OF MESOZOIC IGNEOUS ROCKS IN CONNECTICUT

A.R. Philpotts[9]

RELATIVE AGES OF DIKES AND FLOWS IN CONNECTICUT

The relative ages of the Mesozoic dikes in eastern North America and their relation to basalt flows in the early Mesozoic basins is, in most cases, unknown or uncertain. Recent studies in Connecticut, however, have established the precise relation between these dikes and flows in part of New England. A considerable thickness of Jurassic sedimentary rocks overlies the basalts in the Hartford basin. Diabase dikes cut the Mesozoic strata beneath the basalts, but none has yet been found to cut the overlying sedimentary rocks, suggesting that the dikes are of the same general age as the flows (fig. 20.1). Dike-flow-sediment relations are similar in the Newark and Culpeper basins, where thick sections of sedimentary rocks also overlie basalts (Olsen, 1983; A.J. Froelich, oral commun., 1985). In addition, exposures in Connecticut have been found where two of the dikes actually connect with and feed their respective flows in the Hartford basin. Correlation of the dikes with the three flows provides an important means of establishing the relative ages of these dikes; when combined with absolute numbers of years between eruptions determined from the cyclical lacustrine sediments between the flows (Van Houten, 1964; Olsen, 1984), the dikes provide a unique opportunity to investigate the genesis of a significant compositional range of continental tholeiitic magmas where there are tight geographical and temporal constraints.

REGIONAL RELATIONS, PETROGRAPHY, AND CHEMICAL COMPOSITION

Three major northeast-trending regional dike systems traverse southern New England (fig. 20.1). Petrographic and chemical characteristics reveal that each dike system is distinct and that the westernmost one (Bridgeport-Pelham) can be related to the youngest flow series, the Hampden Basalt; the central dike (Buttress-Ware), to the middle flow series, the Holyoke Basalt; and the easternmost one (Higganum), to the oldest flow series, the Talcott Basalt. A shorter fourth dike system (Fairhaven), which occurs only in the Hartford basin, has been found to connect with and feed the Talcott Basalt. This dike is compositionally identical with the Higganum dike, which is restricted entirely to the eastern highlands. Petrographically, however, the Fairhaven dike contains euhedral phenocrysts of olivine and some large partly resorbed phenocrysts of orthopyroxene, whereas the Higganum dike contains euhedral orthopyroxene phenocrysts and no olivine. These two dikes are separated by the eastern border fault of the Hartford basin. One geometrical reconstruction suggests that the Fairhaven dike may be the downfaulted upper part of the Higganum dike; if a dip on the fault of 55° is accepted, post-Jurassic cumulative vertical displacement on the border fault may be as much as 10 km. (A shallower dip would of course mean less displacement.) Differences in the phenocrysts between the dikes are consistent with the pressure differences resulting from the different levels of crystallization and subsequent exposure in the two dikes.

Although the compositions of the dikes closely match the basalt flows they fed, there are important differences. The Bridgeport-Pelham dike compositions overlap the compositions of the Hampden Basalt but extend to less evolved (more magnesian) compositions. All Buttress-Ware dike samples have compositions that are less evolved than those of the Holyoke Basalt but clearly lie on the same differentiation trend. In both these cases the flows and dikes appear to have formed from the emptying of zoned magma chambers. The flows consist of magma that rose first from the top of the chambers, whereas the dikes are filled with the last material to rise from the lower part of the chambers. In contrast, the Fairhaven and Higganum dikes have compositions identical with the Talcott Basalt composition, indicating that this period of igneous activity did not tap a differentiated magmatic source. The Talcott magma may therefore be primary.

DIFFERENTIATION OF BASALTS

The Talcott Basalt, oldest of the three flow series, contains small euhedral olivine and plagioclase phenocrysts and less abundant, large orthopyroxene phenocrysts that are rimmed by augite and olivine. The

[9]Department of Geology and Geophysics, University of Connecticut, Storrs, Conn. 06268.

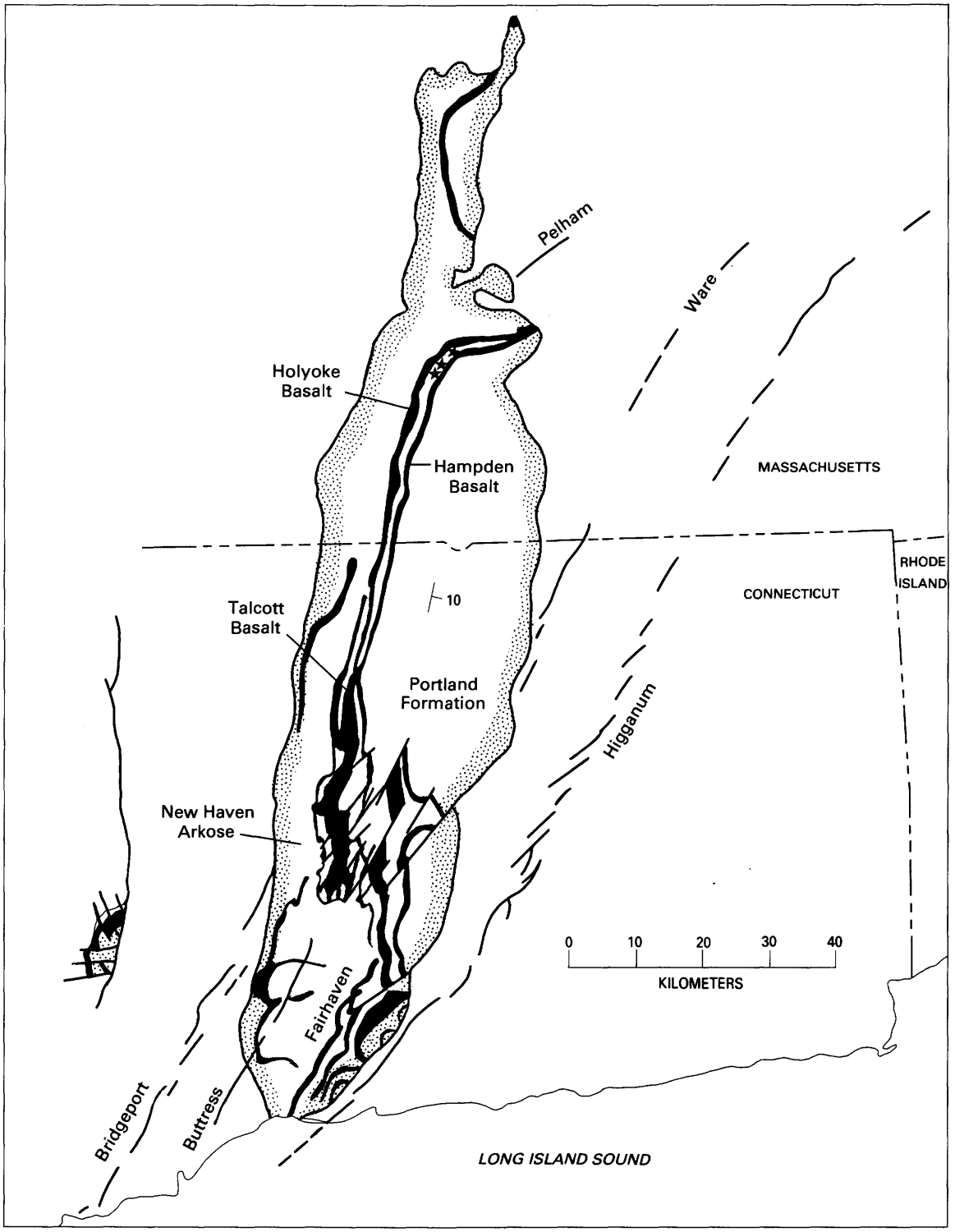

FIGURE 20.1.—The Hartford Mesozoic basin and diabase dike system. The Talcott, Holyoke, and Hampden Basalts are shown in black extending along the central part of the basin and dipping eastward. Dikes are labeled from west to east, the Bridgeport-Pelham, Buttress-Ware, Fairhaven, and Higganum. Volcanic plugs in Massachusetts related to the Hampden Basalt are marked by an asterisk. Data from the State geological maps of Connecticut (Rodgers, 1985) and Massachusetts (Zen and others, 1983).

orthopyroxene has a remarkably constant composition (En_{84}) and is Cr-rich. The unusual texture of orthopyroxene rimmed by olivine is a clear indication that these orthopyroxene crystals were derived from considerable depth where high pressure would expand the primary liquidus field of orthopyroxene. Material balance calculations using the phenocryst compositions indicate that the second flow series (Holyoke) can be derived from a Talcott magma by addition of 7.8 percent orthopyroxene and removal of 7.9 percent olivine, 15 percent clinopyroxene, and 13.3 percent plagioclase. The youngest basalt (Hampden) cannot be derived from a Holyoke magma by any reasonable fractionation scheme but can be derived from a Talcott magma by removal of 4.4 percent olivine, 12.0 percent clinopyroxene, and 14.3 percent plagioclase.

One-atmosphere melting experiments (fig. 20.2; see also Philpotts and Reichenbach, 1985) under controlled oxygen fugacities indicate successively lower liquidus temperatures for Talcott, Holyoke, and Hampden basalts. Both the Talcott and Holyoke have olivine and plagioclase on the liquidus simultaneously, with augite and pigeonite appearing approximately 15°C and 25°C below the liquidus, respectively. The Hampden has plagioclase alone on the liquidus, with olivine and augite appearing only 5°C below this.

Orthopyroxene is not present in the low-pressure experiments but, by analogy with experimental work on other basaltic systems, would have been stable on the liquidus at depths corresponding to pressures exceeding 8 kbar. If the Holyoke magma was derived from Talcott magma, assimilation of orthopyroxene and crystallization of other phases must have taken place at depth. Because the low-pressure phases obtained in the experiments are those required to produce the Hampden from the Talcott magma, this fractionation likely occurred in a shallow magma chamber.

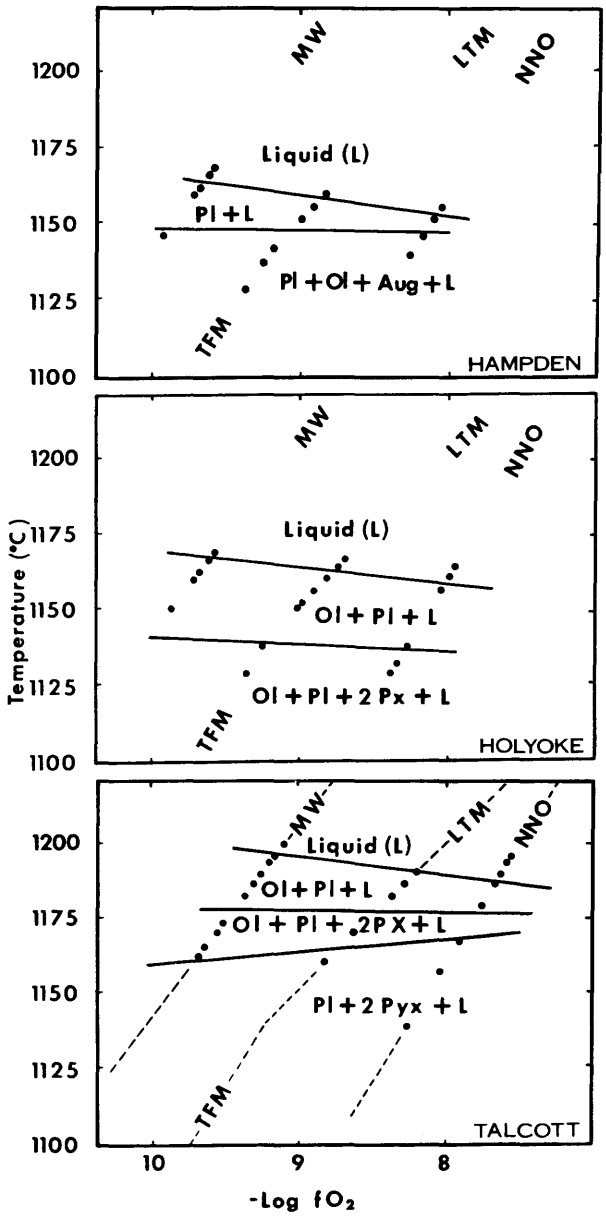

FIGURE 20.2.—Results of melting experiments on Talcott, Holyoke, and Hampden Basalts under the oxygen buffers magnetite-wustite (MW), tridymite-fayalite-magnetite (TFM), liquid-tridymite-magnetite (LTM), and nickel-nickel oxide (NNO).

SULFIDE IMMISCIBILITY IN THE HOLYOKE BASALT

The mesostasis of the Holyoke Basalt contains evidence of three coexisting liquids in the form of abundant droplets of immiscible sulfide liquid (mostly pyrrhotite) enclosed in a two-phase silicate glass. Pyroxene crystals surrounding patches of mesostasis grew with euhedral morphology until the residual liquid unmixed into iron-rich and silica-rich liquids, whereupon the crystals continued to grow with convoluted faces due to the attachment of iron-rich droplets. Immiscible sulfide spheres are trapped in the outer part of pyroxene crystals, suggesting that sulfide unmixing from the silicate melt was triggered by the unmixing of the silicate liquids.

REFERENCES

Olsen, P.E., 1983, Relationship between biostratigraphic subdivisions and igneous activity in the Newark Supergroup [abs.]: Geological Society of America Abstracts with Programs, v. 15, p. 93.

———1984, Periodicity of lake-level cycles in the Late Triassic Lockatong Formation of the Newark Basin (Newark Supergroup, New Jersey and Pennsylvania), *in* Berger, Andre, Imbrie, John, Hays, James, Kukla, George, and Saltzman, Barry, eds., Milankovitch and climate, NATO Symposium: D. Reidel, Dordrecht, Part 1, p. 129–146.

Philpotts, A.R., and Reichenbach, Ingrid, 1985, Differentiation of Mesozoic basalts of the Hartford basin, Connecticut: Geological Society of America Bulletin, in press.

Rodgers, John, 1985, Bedrock geological map of Connecticut: Connecticut Geological and Natural History Survey, 2 sheets, scale 1:125,000.

Van Houten, F.B., 1964, Cyclic lacustrine sedimentation, Upper Triassic Lockatong Formation, central New Jersey and adjacent Pennsylvania: Kansas Geological Survey Bulletin 169, p. 497–531.

Zen, E-an, editor, and Goldsmith, Richard, Ratcliffe, N.M., Robinson, Peter, and Stanley, R.S., compilers, 1983, Bedrock geologic map of Massachusetts: Reston, Va., U.S. Geological Survey, 3 sheets, scale 1:250,000.

21. PROGRESS ON GEOCHRONOLOGY OF MESOZOIC DIABASES AND BASALTS

John F. Sutter

Mesozoic diabases and basalts of the circum-Atlantic margin have been the subject of geochronologic research for over two decades (Erikson and Kulp, 1961; Larochelle and Wanless, 1966; de Boer, 1968; Armstrong and Besancon, 1970; Dalrymple and others, 1975; Dallmeyer, 1975; Manspeizer and others, 1978; Sutter and Smith, 1979; Westphal and others, 1979; Hodych and Hayatsu, 1980; Dooley and Smith, 1982; Lanphere, 1983; Seidemann and others, 1984). They have also proven to be among the most difficult crystalline rocks of the earth's crust to date accurately. At present, the only dating methods that have met with even moderate success are the K-Ar technique and its more recent variation, the $^{40}Ar/^{39}Ar$ age-spectrum technique.

K-Ar ages for these rocks have generally been measured either on whole-rock samples or on plagioclase separates. The apparent ages on these materials range from about 135 Ma to more than 1,000 Ma, the vast majority being between 175 Ma and 225 Ma. Every K-Ar age measured and reported for these rocks is suspect because, when multiple samples of the same unit are measured, the variation in apparent ages has always exceeded the analytical errors common to the technique. This type of behavior indicates geological error, meaning that these materials do not satisfy all the criteria necessary for a rock or mineral to be dated by the K-Ar technique. In general K-Ar researchers have suggested the cause for this anomalous behavior of the K-Ar isotopic system is (1) inhomogeneous distribution of K and Ar in the material (Armstrong and Besancon, 1970); (2) variable amounts of $^{40}Ar^*$ loss after initial crystallization and cooling (Armstrong and Besancon, 1970); (3) incorporation of variable amounts of "excess" $^{40}Ar^*$ during the intrusion, crystallization, and cooling process (Dalrymple, Gromme, and White, 1975; Sutter and Smith, 1979; Seidemann and others, 1984); or (4) the fact that the initial (trapped) $^{40}Ar/^{36}Ar$ ratio for the rock is significantly different (lower) than the accepted value of 295.5 used for correcting out atmospheric argon contamination (Hodych and Hayatsu, 1980). Suffice it to say that none of the K-Ar studies on these diabases and basalts has been able to decipher all of the causes of the anomalous behavior of the K-Ar isotopic system.

In an effort to shed more light on the possible causes of variation in ages outside of normal analytical errors, several workers have tried to apply the $^{40}Ar/^{39}Ar$ age-spectrum technique of K-Ar dating (Dalrymple, Gromme, and White, 1975; Dallmeyer, 1975; Sutter and Smith, 1979; Lanphere, 1983; Seidemann and others, 1984). This technique is potentially able to identify anomalous behavior of K-Ar systems, and, under favorable conditions, the cause for the anomalous behavior can be suggested. The results of these studies so far suggest that the irreproducibility of K-Ar ages results from a nonuniform distribution of ^{40}K and $^{40}Ar^*$ in the samples, usually the result of minor loss of $^{40}Ar^*$, gain of $^{40}Ar^*$ (excess ^{40}Ar), or minor gain of ^{40}K. No two workers are in total agreement on the relative importance of these three possible causes, although most workers in North America believe that "excess ^{40}Ar" is at least part of the problem. This belief is reinforced by the fact that apparent ages are usually much more reproducible when the analyzed samples intrude or are interbedded with sedimentary rocks rather than intruding older crystalline rocks. So far, however, the $^{40}Ar/^{39}Ar$ age-spectrum results on whole-rock or plagioclase mineral concentrates from Mesozoic diabase and basalt have not been able to yield ages for

these rocks that are reproducible to the current level of analytical precision.

Our recent $^{40}Ar/^{39}Ar$ work in the intrusions and flows of the Culpeper basin in Virginia is probably the best constrained age data that exist at the present time for these rocks (Sutter and others, 1983). Six whole-rock samples from sills and dikes have total-gas $^{40}Ar/^{39}Ar$ ages (essentially equivalent to K-Ar ages) that range from 192 to 207 Ma. The $^{40}Ar/^{39}Ar$ age spectra for these samples define near "plateau" ages that range from 193 to 201 Ma and, except for sample RA–A1, cannot be distinguished from one another at the 95 percent confidence level (fig. 21.1). These five "plateau" ages yield a mean age of 198.4 ± 2.1 Ma (2 sigma), which is interpreted as the best estimate for the age of intrusion and crystallization of these sills and dikes. In addition, paleomagnetic data from these same samples suggest a paleopole that plots near the apparent polar-wander path for North America at about 200 Ma (Raymond and others, 1982). Preliminary chemical and petrologic data suggest that these six samples represent at least two of the common magma types recognized in the Mesozoic igneous province of eastern North America and that were thought to possibly be temporally separated. We see no evidence for a significant separation in the time of intrusion of these diverse magma types. However, there is a problem. Using the $^{40}Ar/^{39}Ar$ age-spectrum dating technique for samples that are closed K-Ar systems, we have been able to show that our normal analytical uncertainties should result in a "plateau age" that has an uncertainty of 0.5–1.0 Ma in 200 Ma. Clearly the data that have been generated on these rocks greatly exceed that value, except for sample MS–A1, and therefore geologic error is indicated; in other words, these rocks are not "datable," strictly speaking, by this technique. This situation is worse for basalt flows than for dikes or sills (fig. 21.2). The probable reason is that chemical alteration of ground mass in basalts causes an even more open system behavior in flows than in intrusives. It is my opinion that no reliable ages for basalt flows in any of the circum-Atlantic Mesozoic basins exist and, using current techniques, none are possible. The temporal resolution needed to help solve problems of chronology from basin to basin and within the entire province is on the order of 1–2 Ma, certainly possible in samples that are closed K-Ar systems.

Two separate approaches to the geochronology of these rocks is needed for the future. First is to try to understand more fully the cause of open-system behavior in these rocks in an attempt to find samples that most closely approximate closed K-Ar systems. The best way to do this appears to be a chemical and petrographic screening technique. To this end, Dave Gottfried and I are comparing notes on chemical and petrographic data for potential samples for $^{40}Ar/^{39}Ar$ age spectrum dating. Second, and probably more productive, is to try to identify materials for dating that have a good potential for being closed K-Ar systems or open systems that have a good potential for being understood. This approach needs the cooperation of all those involved in the project, especially those individuals looking at the igneous rocks and their margins. For instance, many sills and some of the thicker dikes and flows have undergone enough differentiation that they contain small amounts of granophyric segregations. Some of the segregations contain either hornblende or orthoclase as one of their constituent minerals. Hornblende is one of the best minerals for closed system behavior in the K-Ar technique and valuable age information can often be gleaned from the $^{40}Ar/^{39}Ar$ age spectra for hornblendes that exhibit some degree of open-system behavior (Harrison, 1981). Orthoclase is not nearly as well known as hornblende in terms of its K-Ar systematics, but we are learning more about it all the time; its future use in $^{40}Ar/^{39}Ar$ geochronology is promising (Harrison and McDougall, 1982). In addition, the contact metamorphic rocks (hornfels) associated with sills, dikes, and some flows may contain minerals that are potentially datable with fairly high precision, such as monoclinic K-feldspar (sanidine), biotite, muscovite, and hornblende. It is also possible that in some cases microcline in detrital sediments might have been sufficiently heated by intrusion or extrusion to have at least partially reset its K-Ar isotopic system. This happens at a relatively low temperature, and because we know that ^{40}Ar is lost from microcline by volume diffusion (Harrison and McDougall, 1982), it is often possible, using the $^{40}Ar/^{39}Ar$ age-spectrum method, to determine quite precisely the timing of that heating event and thus, indirectly, the age of the igneous intrusion. Sanidine is also a very reliable $^{40}Ar/^{39}Ar$ geochronometer, and a recent report by Stoddard (1983) of alkali-rich dikes, containing sanidine and anorthoclase phenocrysts, in Northampton County, N.C., demonstrates that material that can be precisely dated by $^{40}Ar/^{39}Ar$ techniques probably exists. If these rocks could then be inferred, on chemical, paleomagnetic, and petrologic grounds, to be coeval with diabase dikes, the diabases would be dated by inference.

The current state of geochronology of igneous rocks in the Eastern U.S. Mesozoic province is such that no temporal resolution is possible among basalt flows, sills, and dikes. All igneous rocks of this province

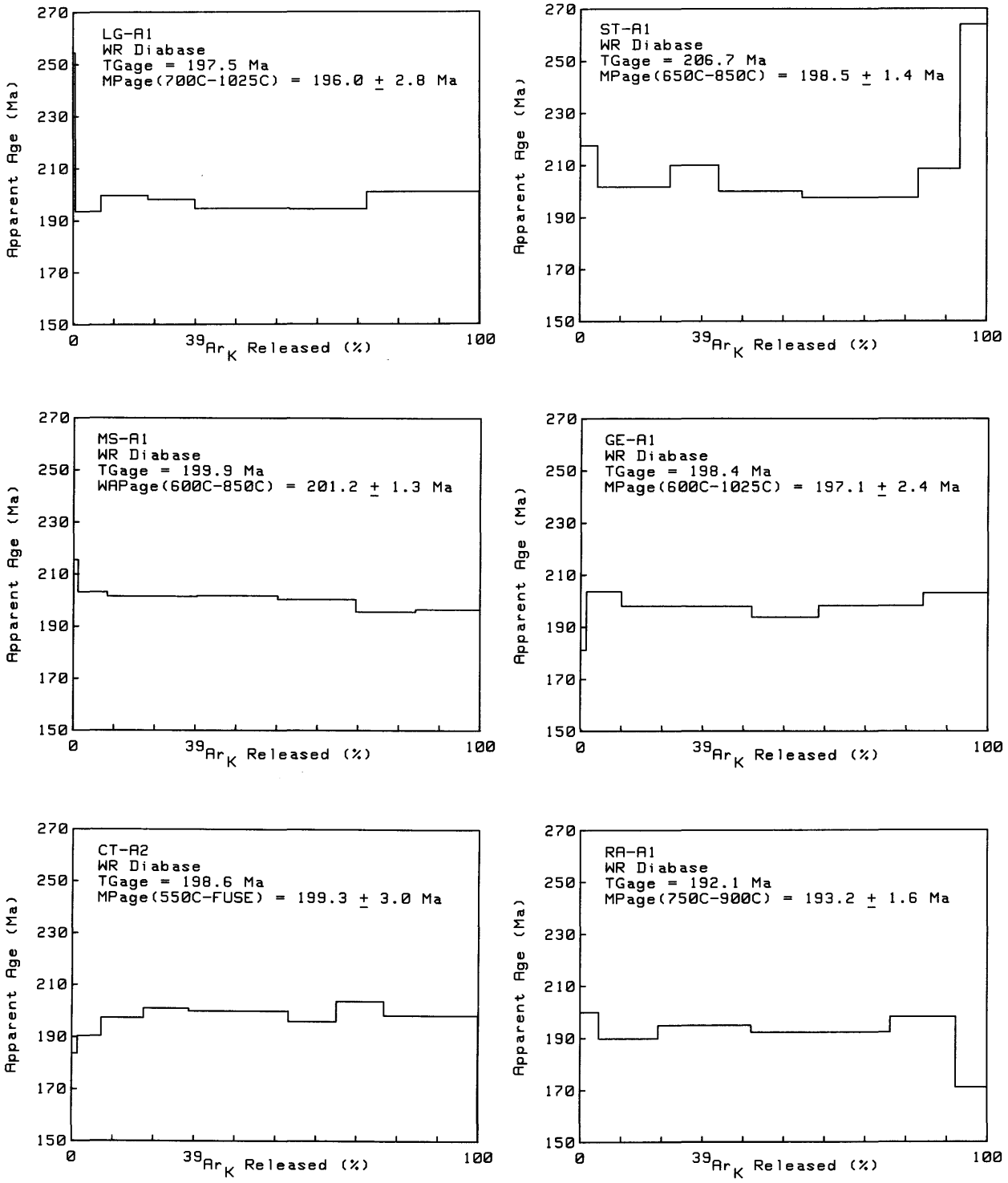

FIGURE 21.1.—$^{40}Ar/^{39}Ar$ age-spectrum diagrams of diabase dikes and sills from the Culpeper basin, Virginia. WR, whole-rock sample; TGage, total-gas age (essentially equivalent to K-Ar age); MPage, most preferred age (near plateau); WAPage, weight-average plateau age. Uncertainties in ages represent 1-sigma values (67 percent confidence level).

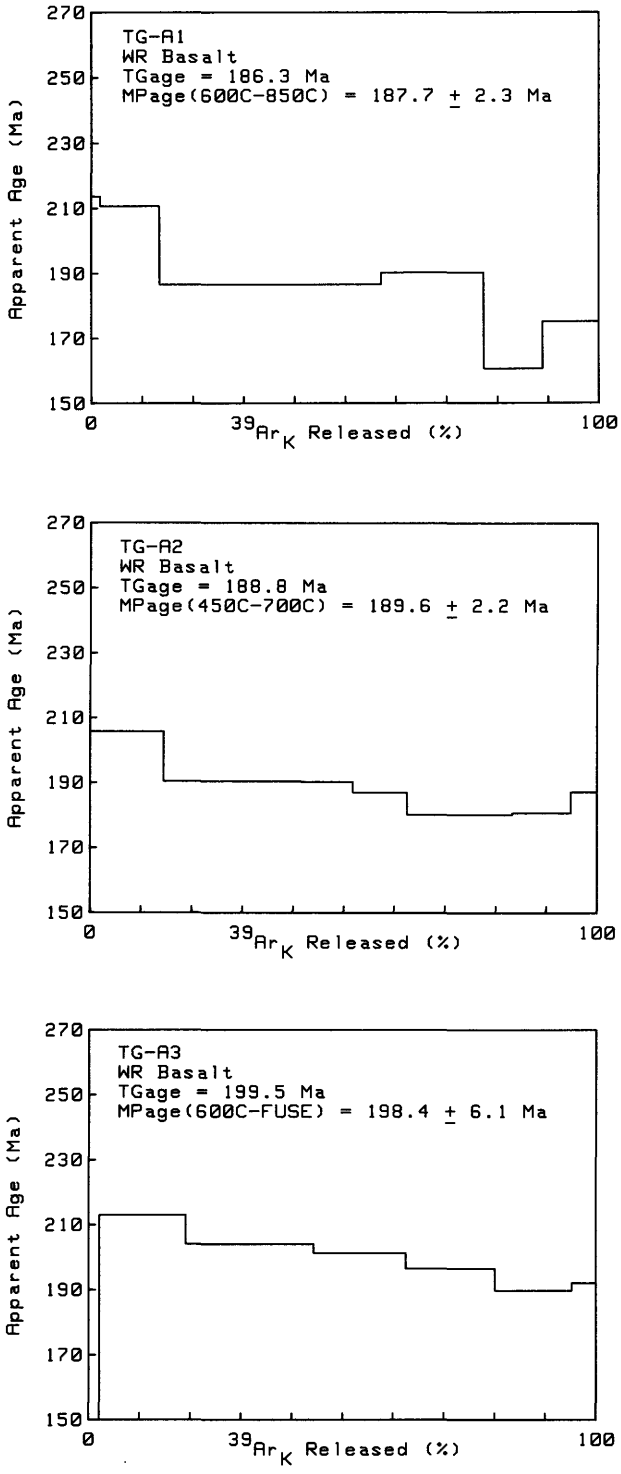

FIGURE 21.2.—$^{40}Ar/^{39}Ar$ age-spectrum diagrams of basalt flows from the Culpeper basin, Virginia. Abbreviations as in figure 21.1.

appear to have crystallized in the general time span of 175–200 Ma and probably closer to the older end of this range. However, until we can analyze materials that give apparent ages that are reproducible within the general analytical precision of the $^{40}Ar/^{39}Ar$ method, no significant contributions to the detailed geochronology of the Eastern U.S. Mesozoic igneous province are possible.

SELECTED REFERENCES

Armstrong, R.L., and Besancon, J., 1970, A Triassic time scale dilemma: K-Ar dating of Upper Triassic mafic igneous rocks, eastern U.S.A. and Canada and post-Upper Triassic plutons, western Idaho, U.S.A.: Eclogae Geologicae Helvetiae, v. 63, p. 15–28.

Dallmeyer, R.D., 1975, The Palisades sill: A Jurassic intrusion? Evidence from $^{40}Ar/^{39}Ar$ incremental release ages: Geology, v. 3, p. 243–245.

Dalrymple, G.B., Gromme, C.S., and White, R.W., 1975, Potassium argon age and paleomagnetism of diabase dikes and sills in Liberia: Initiation of central Atlantic rifting: Geological Society of America Bulletin, v. 86, p. 399–411.

de Boer, J., 1968, Paleomagnetic differentiation and correlation of the Late Triassic volcanic rocks in the central Appalachians (with special reference to the Connecticut Valley): Geological Society of America Bulletin, v. 79, p. 609–626.

DeLorey, C.M., Dooley, R.E., Ressetar, R., Fullagar, P.D., and Stoddard, E.F., 1982, Paleomagnetism and isotope geochronology of early Mesozoic rhyolite porphyry dikes, eastern Southern Appalachian Piedmont [abs.]: EOS, v. 63, no. 18, p. 309.

Dooley, R.E., and Smith, W.A., 1982, Age and magnetism of diabase dikes and tilting of the Piedmont: Tectonophysics, v. 90, p. 283–307.

Dooley, R.E., and Wampler, J.M., 1983, Potassium-argon relations in diabase dikes of Georgia — The influence of excess ^{40}Ar on the geochronology of early Mesozoic igneous and tectonic events, *in* Gohn, G.S., ed., Studies related to the Charleston, South Carolina, earthquake of 1886 — Tectonics and seismicity: U.S. Geological Survey Professional Paper 1313–M, p. M1–M24.

Erikson, G.P., and Kulp, J.L., 1961, Potassium-argon measurements on the Palisades Sill, New Jersey: Geological Society of America Bulletin, v. 72, p. 649–652.

Evans, C.R., and Tarney, J., 1964, Isotopic ages of Assynt dykes: Nature, v. 204, p. 638.

Fitch, F.J., and Miller, J.A., 1967, The age of the Whin Sill: Geological Journal, v. 5, p. 233.

Gidskehaug, A., Creer, K.M., and Mitchell, J.G., 1975, Paleomagnetism and K-Ar ages of the southwest African basalts and their bearing on the time of initial rifting of the south Atlantic Ocean: Geophysical Journal of the Royal Astronomical Society, v. 42, p. 1–20.

Hailwood, E.A., and Mitchell, J.G., 1971, Paleomagnetic and radiometric dating results from Jurassic intrusions in south Morocco: Geophysical Journal of the Royal Astronomical Society, v. 24, p. 351–364.

Harrison, T.M., 1981, The diffusion of ^{40}Ar in hornblende: Contributions to Mineralogy and Petrology, v. 78, p. 324–331.

Harrison, T.M., and McDougall, I., 1982, The thermal significance of potassium feldspar K-Ar ages inferred from $^{40}Ar/^{39}Ar$ age spectrum results: Geochimica et Cosmochimica Acta, v. 46, p. 1811–1820.

Hayatsu, A., 1979, K-Ar isochron age of the North Mountain basalt, Nova Scotia: Canadian Journal of Earth Sciences, v. 16, p. 973–975.

Hodych, J.P., and Hayatsu, A., 1980, K-Ar isochron age and paleomagnetism of diabase along the trans-Avalon aeromagnetic lineament — Evidence of Late Triassic rifting in Newfoundland: Canadian Journal of Earth Sciences, v. 17, p. 491–499.

Houlick, C.W., Jr., and Laird, H.S., 1977, Mesozoic wrench tectonics and the development of the northern Newark Basin [abs.]: Geological Society of America Abstracts with Programs, v. 9, p. 275.

Lanphere, M.A., 1983, $^{40}Ar/^{39}Ar$ ages of basalt from Clubhouse Crossroads test hole #2, near Charleston, South Carolina, *in* Gohn, G.S., ed., Studies related to the Charleston, South Carolina, earthquake of 1886 — Tectonics and seismicity: U.S. Geological Survey Professional Paper 1313–B, p. B1–B8.

Larochelle, A., and Wanless, R.K., 1966, The paleomagnetism of a Triassic diabase dike in Nova Scotia: Journal of Geophysical Research, v. 71, p. 4949–4953.

Lee, K.Y., Leavy, B.D., and Gottfried, D., 1984, Geochemical data for Jurassic diabase and basalt of the northern Culpeper basin, Virginia: U.S. Geological Survey Open-File Report 84–758, 19 p.

McHone, J.G., 1978, Distribution, orientations, and ages of mafic dikes in central New England: Geological Society of America Bulletin, v. 89, p. 1645–1655.

Manspeizer, Warren, Puffer, J.H., and Cousminer, H.L., 1978, Separation of Morocco and eastern North America: A Triassic-Liassic stratigraphic record: Geological Society of America Bulletin, v. 89, p. 901–920.

Raymond, C.A., Ellwood, B.B., Chaves, Lisa, and Leavy, B.D., 1982, Paleomagnetic analyses of lower Mesozoic diabase and basalt from the central and southern Appalachians [abs.]: Geological Society of America Abstracts with Programs, v. 14, p. 76.

Reesman, R.H., Filbert, C.R., and Krueger, H.W., 1973, Potassium-argon dating of the Upper Triassic lavas of the Connecticut Valleys, New England [abs.]: Geological Society of America Abstracts with Programs, v. 5, p. 211.

Seidemann, D.E., Masterson, W.D., Dowling, M.P., and Turekian, K.K., 1984, K-Ar dates and $^{40}Ar/^{39}Ar$ age spectra for Mesozoic basalt flows of the Hartford Basin, Connecticut, and the Newark Basin, New Jersey: Geological Society of America Bulletin, v. 95, p. 594–598.

Stoddard, E.F., 1983, A compositionally bimodal, alkali-rich suite of early Mesozoic dikes, eastern North Carolina Piedmont [abs.]: Geological Society of America Abstracts with Programs, v. 15, p. 698.

Sutter, J.F., 1976, Timing and tectonic significance of post-Paleozoic igneous activity in the central and southern Appalachians [abs.]: Geological Society of America Abstracts with Programs, v. 8, p. 281.

Sutter, J.F., Arth, J.G., and Leavy, B.D., 1983, $^{40}Ar/^{39}Ar$ age spectrum dating and strontium isotope geochemistry of diabase sills from the Culpeper Basin, Virginia [abs.]: Geological Society of America Abstracts with Programs, v. 15, p. 92.

Sutter, J.F., and Smith, T.E., 1979, $^{40}Ar/^{39}Ar$ ages of diabase intrusions from Newark trend basins in Connecticut and Maryland: Initiation of central Atlantic rifting: American Journal of Science, v. 279, p. 808–831.

Thuizat, R., 1976, Ages potassium-argon de dolerites mésozoïques du Maroc [K-Ar ages of Mesozoic dolerites of Morocco]: Réunion Annuelle des Sciences de la Terre, no. 4, p. 379.

Thuizat, R., and Montigny, R., 1978, Ages potassium-argon du filon doleritique de l'Alentejo-Plasencia et leur signification géologique [K-Ar ages of the doleritic dike of Alentejo-Plasencia and their geologic significance]: Réunion Annuelle des Sciences de la Terre, no. 6, p. 389.

Wampler, J.M., and Dooley, R.E., 1975, Potassium-argon determination of Triassic and Eocene igneous activity in Rockingham County, Virginia [abs.]: Geological Society of America Abstracts with Programs, v. 7, p. 547.

Wanless, R.K., Stevens, R.D., LaChance, G.R., and Delabio, R.N., 1972, Age determinations and geological studies, K-Ar isotopic ages: Report 10: Geological Survey of Canada Paper 71–2, p. 72–73.

Westphal, M., Montigny, R., Thuizat, R., Bardon, C., Bossert, A., Hamzeh, R., and Rolley, J.P., 1979, Pal´eomagnetisme et datation du volcanisme permien, triasique et crétace du Maroc [Paleomagnetism and dating of Permian, Triassic, and Cretaceous volcanism in Morocco]: Canadian Journal of Earth Sciences, v. 16, p. 2150–2164.

Zartman, R.E., Brock, M.R., Heyl, A.V., and Thomas, H.H., 1967, K-Ar and Rb-Sr ages of some alkalic intrusive rocks from central and eastern United States: American Journal of Science, v. 265, p. 848–870.

22. PEARCE-CANN DISCRIMINANT DIAGRAMS APPLIED TO EASTERN NORTH AMERICAN MESOZOIC DIABASE

John A. Philpotts

Pearce-Cann discrimination diagrams (see, for example, Pearce and Cann, 1973) are widely used as a means of attempting to determine paleotectonic environment. Not all those who employ these diagrams, however, are as careful as were Pearce and co-workers about analytical quality or about freshness of samples. Mobile elements such as K, Sr, and Ba are potentially highly informative but tend to have disturbed abundances in older rocks for which magma-tectonic interpretations might be most needed (Pearce and Cann,

1973; Pearce and others, 1975). There are also more fundamental problems. Pearce and Cann (1973) pointed out that individual rocks can yield false information on tectonic setting in these diagrams and stressed the importance of studying suites. They also mentioned that polygenetic magma suites can further complicate the results. However, Pearce and Cann suggested that, in most cases, these diagrams can be used to determine the tectonic setting of eruption of Phanerozoic volcanic rocks. Nevertheless, the geochemical literature contains numerous cases of rock data plotting in the "wrong" field. A number of these are directly germane to the consideration of Mesozoic diabase of eastern North America (ENA). For example, Holm (1982) found that continental tholeiites (including the Avalon dike, which is the northern extension of the ENA diabase province) plotted in the calc-alkali basalt fields of the Ti-Zr-Y discrimination diagram rather than in the putative continental basalt field. For the Karroo diabase, Cox (1983) has samples plotting in both the continental and calc-alkali fields in this diagram.

The fields for ENA Mesozoic diabase are plotted in various discrimination diagrams in figures 22.1 through 22.4. The first three diagrams are from Pearce and Cann (1973), and the fourth diagram is from Pearce (1975). The diabase data used are from Weigand and Ragland (1970), Smith and others (1975), Puffer and others (1981), and my unpublished analyses. In the Ti-Zr-Y diagram (fig. 22.1), ENA diabase plots in fields B and C; if a single setting is appropriate, a relationship with calc-alkalic basalt is indicated. Some diabases may be partially accumulative in origin, and this may slightly distort the diabase field. Pearce and others (1977) pointedly excluded intrusive rocks from consideration on the grounds of crystal fractionation. Inasmuch as many lavas have also undergone crystal fractionation, and in some cases flows and chilled material from feeder dikes are identical in petrography and chemical composition, filtering on this basis may be suspect. Nevertheless, phenocryst-rich rocks, cumulates and partial cumulates, are more common in hypabyssal than in extrusive rocks and can disturb discriminant diagrams, particularly plots of element pairs, such as figure 22.2. ENA diabase plots in all four fields of the Ti-Zr diagram proposed for discriminating altered plate-margin basalts (fig. 22.2). These results may indicate that it is inappropriate to apply this particular discriminant diagram to these continental basalts. Alternatively, of course, the results could be interpreted as indicating a variety of tectonic magma types within the diabase province. Similar interpretations are possible for figure 22.3, the Ti-Zr-Sr diagram (intended only for unaltered rocks), which also shows ENA diabase overlapping all three fields. The right end of the diabase field is defined by rocks that may be partially accumulative in origin and hence not entirely appropriate for such discriminant diagrams; the presence of cumulate plagioclase, for example, would result in higher Sr contents.

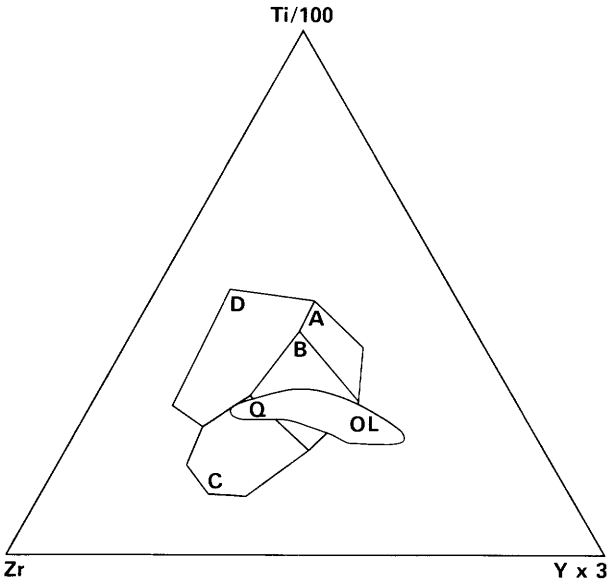

FIGURE 22.1.—Field for eastern North American (ENA) diabase plotted on a Ti/100–Zr–Y×3 discrimination diagram. Q, quartz-normative diabase. OL, olivine-normative (or non-quartz-normative) diabase. Within-plate (ocean island and continental) basalts supposedly plot in field D, low-potassium tholeiites in A and B, ocean-floor basalts in B, and calc-alkali basalts in fields B and C.

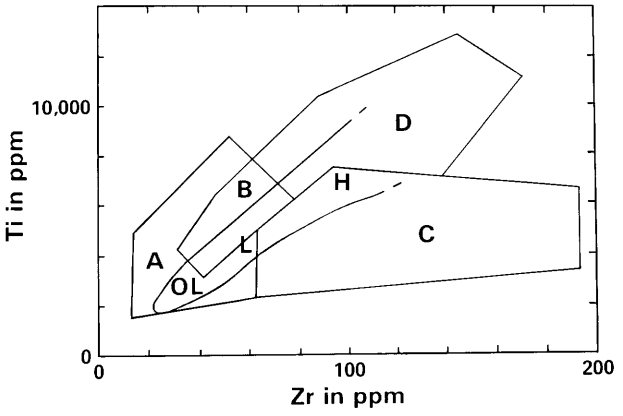

FIGURE 22.2.—Field for ENA diabase plotted on a Ti-Zr discrimination diagram. H, high-iron and high-titanium diabase. L, low-titanium diabase. OL, olivine-normative (or non-quartz-normative) diabase. Low-potassium tholeiites plot in fields A and B, calc-alkali basalts in C and B, and ocean-floor basalts in fields D and B.

In many ways the Ti-Cr diagram (fig. 22.4) may be most significant for diabase interpretation. The plot is equivalent in many ways to Ti-Mg plots, which have long been used (Chayes and Metais, 1964) to distinguish ocean-island from circum-oceanic (for example, Andean) rocks, except that Cr shows a much more dramatic drop for early crystallization of mafic phases than does Mg. Plagioclase accumulation would move data points towards the origin, whereas mafic phases plot to the lower right. The locations shown in figure 22.4 for the various diabase types are probably quite reasonable however. Further subdivision is possible; for example, the later differentiated high-iron types have both high-titanium representatives, such as the Hampden and Hook Mountain (Third Watchung) Basalts, and low-titanium representatives, such as the Holyoke Basalt. The normal high-Ti diabase and the olivine-normative diabase plot in Pearce's (1975) ocean-floor basalt field, although only the former group has Ti and Cr contents similar to those in ocean-floor basalts. The olivine-normative grouping represented in figures 22.1, 22.2, and 22.4 might better be termed "non-quartz-normative" because some of these diabases contain little or no normative olivine. The normal low-Ti diabase plots in the island-arc tholeiite field. Although such designations must be taken with a grain of salt for the diabases, it is difficult to tie all the diabase groups together in any simple differentiation scheme. Again a number of different sources appears indicated.

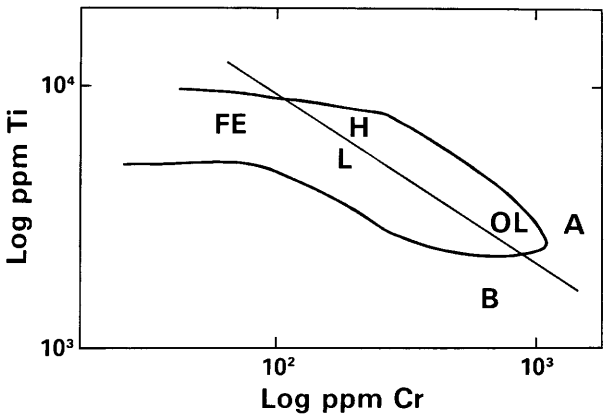

FIGURE 22.4.—Field for ENA diabase plotted on a Ti-Cr discrimination diagram. FE, high-iron diabase. H, high-titanium diabase. L, low-titanium diabase. OL, olivine-normative (or non-quartz-normative) diabase. Ocean-floor basalts plot in field A, island-arc tholeiites in field B.

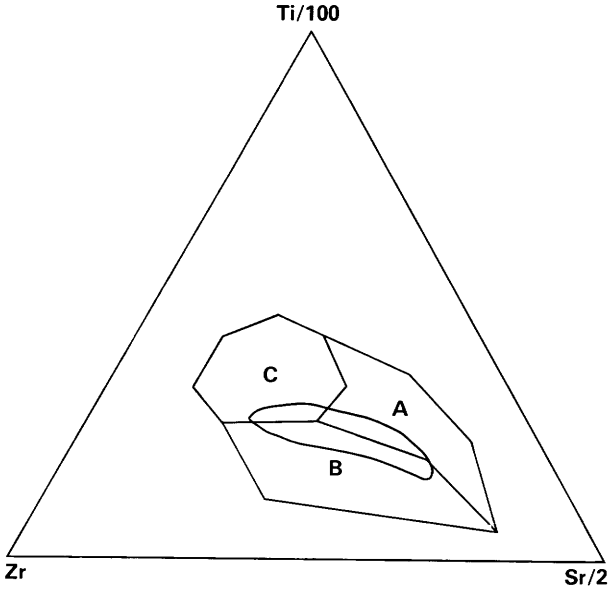

FIGURE 22.3.—Field for ENA diabase plotted on a Ti/100–Zr–Sr/2 discrimination diagram. Ocean-floor basalts plot in field C, low-potassium tholeiites in A, and calc-alkali basalts in B.

Pearce and others (1975) proposed a TiO_2-K_2O-P_2O_5 diagram as a method of discriminating between oceanic and non-oceanic basalts and explicitly applied it to diabase. ENA diabase falls mostly in the continental field in this diagram, but a few samples plot in the oceanic field. Both the physical meaning of this discriminant and its efficacy are open to question. The average continental basalts of Europe, North America, and Africa plot close to the discriminant line, and Scoresby Sund and Deccan Trap continental basalts plot decidedly in the oceanic field. Pearce and others (1975) offered an explanation for the Deccan Trap discrepancy, but this is interpretation not discrimination. The FeO-MgO-Al_2O_3 discriminant diagram, which uses data from intermediate rocks (Pearce and others, 1977), paradoxically places most Mesozoic diabase in the ocean-floor field rather than the orogenic or continental fields. So it goes. At present, we do not appear particularly close to having reliable and universal discriminants. For ENA Mesozoic diabase, very little evidence of any kind relates the province either to the alkalic igneous activity commonly associated with rifts or to mid-ocean-ridge basalt. Perhaps the best current interpretation for ENA Mesozoic diabase calls for a number of source regions, perhaps subduction-related as proposed recently by Pegram (1983) to account for the isotopic data. The conflicting results of the discriminant diagrams and the lack of both quartz and olivine in many diabase norms may indicate a relatively unusual (little sampled) thermal-tectonic regime during

generation of the Mesozoic diabases. The extension of the diabase field beyond the Pearce-Cann fields in figure 22.1, for example, might also be giving such an indication.

REFERENCES

Chayes, Felix, and Metais, D., 1964, Discriminant functions and petrographic classification: oceanic-island and circum-oceanic basalts: Carnegie Institution of Washington Year Book 63, p. 179–182.

Cox, K.G., 1983, The Karroo province of southern Africa: origin of trace element enrichment patterns, *in* Hawkesworth, C.J., and Norry, M.J., eds., Continental basalts and mantle xenoliths: Nantwich, Shiva Publishing Ltd., p. 139–157.

Holm, P.E., 1982, Non-recognition of continental tholeiites using the Ti-Y-Zr diagram: Contributions to Mineralogy and Petrology, v. 79, p. 308–310.

Pearce, J.A., 1975, Basalt geochemistry used to investigate past tectonic environments on Cyprus: Tectonophysics, v. 25, p. 41–67.

Pearce, J.A., and Cann, J.R., 1973, Tectonic setting of basic volcanic rocks determined using trace element analyses: Earth and Planetary Science Letters, v. 19, p. 290–300.

Pearce, J.A., Gorman, B.E., and Birkett, T.C., 1975, The TiO_2-K_2O-P_2O_5 diagram: a method of discriminating between oceanic and non-oceanic basalts: Earth and Planetary Science Letters, v. 12, p. 339–349.

———1977, The relationship between major element chemistry and tectonic environment of basic and intermediate volcanic rocks: Earth and Planetary Science Letters, v. 36, p. 121–132.

Pegram, W.J., 1983, Isotopic characteristics of the Mesozoic Appalachian tholeiites [abs.]: Geological Society of America Abstracts with Programs, v. 15, p. 660.

Puffer, J.H., Hurtubise, D.O., Geiger, F.J., and Lechler, Paul, 1981, Chemical composition and stratigraphic correlation of the Mesozoic basalt units of the Newark basin, New Jersey, and the Hartford basin, Connecticut: Geological Society of America Bulletin, v. 92, p. 515–553.

Smith, R.C., II, Rose, A.W., and Lanning, R.M., 1975, Geology and geochemistry of Triassic diabase in Pennsylvania: Geological Society of America Bulletin, v. 86, p. 943–955.

Weigand, P.W., and Ragland, P.C., 1970, Geochemistry of Mesozoic dolerite dikes from eastern North America: Contributions to Mineralogy and Petrology, v. 29, p. 196–214.

23. ORE DEPOSIT MODELS AND MINERAL RESOURCE STUDIES IN THE EARLY MESOZOIC BASINS OF THE EASTERN UNITED STATES

Gilpin R. Robinson, Jr.

INTRODUCTION

Mineral deposits of strategic economic importance (such as nickel, cobalt, and platinum-group elements) and energy-related deposits (such as coal, uranium, oil, and gas) are known to occur in intracontinental rift settings. This relationship targets the Triassic-Jurassic basins in the Eastern United States as an attractive area to test, evaluate, and refine genetic models of these deposits in a setting that has undergone only minor post-rifting deformation.

Our mineral resource studies will primarily focus on assessing the potential for (1) magmatic sulfide deposits associated with Mesozoic diabase sheets, (2) sediment-hosted stratiform and stratabound sulfide deposits, (3) base-metal vein deposits, and (4) magnetite-skarn deposits (containing copper and recoverable cobalt and gold) associated with these basins. The geologic settings of these deposit types are shown schematically in figure 23.1.

Models developed for these types of ore deposit can be applied to the Eastern U.S. early Mesozoic basins (EMB) to identify regional exploration targets. Significant ore deposits of these types are presently unknown in the EMB but have been found in other intracontinental rift-basin tectonic settings. The models define regional targets by (1) identifying associations of deposit types likely to be found in a given area and (2) providing criteria to locate favorable geologic and tectonic settings and to identify types of chemical transport, alteration, and fractionation associated with mineralization.

RESEARCH STRATEGY

The goal is to develop a synthesis of the geologic, structural, depositional, intrusive, and metamorphic history of the early Mesozoic basins of the Eastern United States in order to develop, test, and evaluate

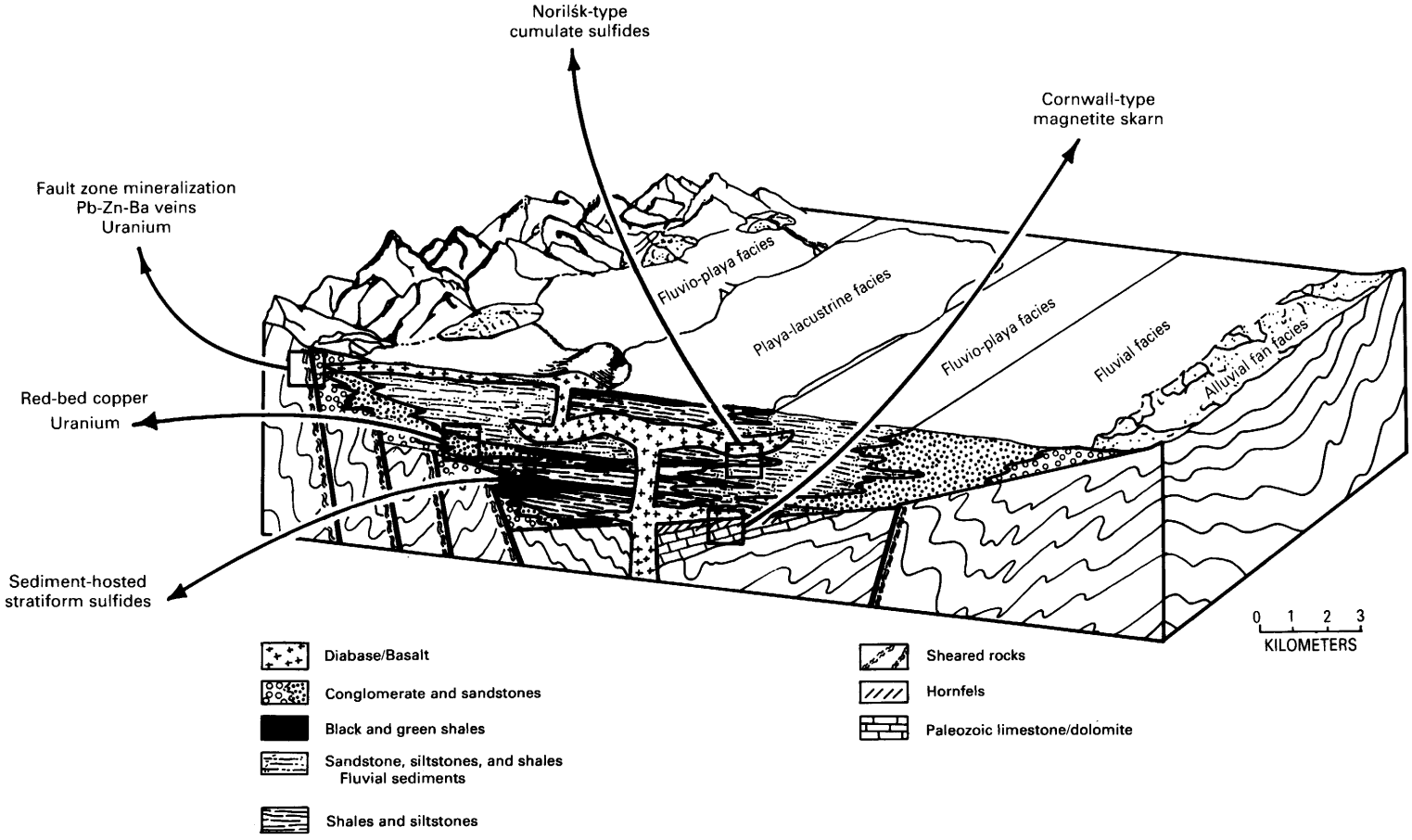

FIGURE 23.1.—Schematic distribution of facies in the early Mesozoic basins in the Eastern United States, showing some potential mineral resources. (Modified from Turner-Peterson, C.E., 1980, Short Course Notes, Rocky Mountain Section of Society of Economic Paleontologists and Mineralogists, p. 149–175.)

the ore-deposit models. The problem requires a regional approach and the interaction of geologic, geochemical, geophysical, and mineral resource disciplines. The following section provides an overview of the models developed for (1) magmatic sulfide deposits and (2) sediment-hosted stratiform sulfide deposits. Key elements of the research strategy are outlined and preliminary results are given.

Rift-related magmatic nickel-copper sulfide deposits.—Important deposits of this type occur in the Noril'sk district, U.S.S.R., and minor deposits occur in the Duluth Complex, Minn., and Insizwa Complex, Transkei, South Africa. These deposits are associated with basaltic intrusions in rift zones. The nickel and associated copper, cobalt, and platinum-group elements (PGE) are in sulfide segregations near the base of the intrusions, commonly in depressions. The sulfide segregations formed when the magma became saturated with sulfur, causing an immiscible sulfide liquid to separate from the basaltic magma and sink to the bottom of the igneous body. The sulfide liquid acts as a collector for the nickel, copper, cobalt, and PGE. In the Duluth and Noril'sk deposits, assimilation of sulfur from adjacent country rocks is related to mineralization. In the Noril'sk and Insizwa deposits, but not the Duluth deposits, the initial formation and segregation of the sulfide liquid precedes the final emplacement of the magma in the sheet-like body hosting the ore deposit. Sulfide segregations in these deposits occur near dike systems feeding the epizonal diabase sheet complexes.

Target areas for diabase-hosted sulfide mineralization in the EMB, defined on the basis of systematic nickel, cobalt, and copper trace-element variations, are diabase sheets with geochemical trends indicating sulfide fractionation (see Gottfried, chapter 25, this volume). Additional features favorable for economic mineralization in diabase sheets exhibiting sulfide fractionation include (1) sulfur isotopic and other geochemical signatures indicating contamination with crustal material and (2) cumulate zones, granophyric differentiates, and abundant metasedimentary inclusions. Assessment for potential deposits involves

(1) Geochemical and petrological studies to identify igneous suites exhibiting sulfide fractionation and crustal contamination;
(2) Structural and morphologic studies to identify likely sites for sulfide accumulation; and
(3) Geophysical studies to identify anomalies (magnetic, electromagnetic, gravity, and so on) that may indicate geologic sites favorable for sulfide accumulations.

The preliminary geochemical investigations (summarized by Gottfried, chapter 25, this volume) indicate that sulfide fractionation processes appear to have affected the magma chemistry of Jurassic quartz-normative tholeiites in Connecticut, New Jersey, Virginia, North Carolina, and South Carolina. Therefore, on a regional scale, the early Mesozoic basin province in the Eastern United States appears to have potential for the occurrence of magmatic sulfide deposits. However, no occurrences of anomalous metal enrichments or sulfide segregations associated with these diabase sheets are known at present.

Sediment-hosted stratiform sulfide deposits.—Sediment-hosted deposits of lead, zinc, and copper are characterized by essentially stratiform sulfide mineralization in sediments deposited in tectonically active intracratonic basins. Mineralization is commonly in black or gray shales in stratigraphic sections containing marine strata, lacustrine beds, and (or) red beds. Some deposits contain economic silver (Rammelsberg, West Germany; Mt. Isa, Australia; Polish deposits), cobalt (Zaire-Zambia copper belt, Mt. Isa), or PGE (Kupferschiefer, East and West Germany; Dzhezkazan, U.S.S.R.). The deposits appear to form a continuum between low-temperature diagenetic replacement deposits (usually copper-rich) and higher temperature syngenetic-diagenetic deposits (usually lead-zinc-rich). Some of the lead-zinc-rich deposits may originate from the exhalation of metal-rich brines onto the subaqueous basin floor. Transport of metal-bearing brines from within the basin to shallow sites of sulfide precipitation (possibly along syndepositional faults) appears important to the development of the deposits. Favorable factors for mineralization include (1) syndepositional-postdepositional faults, (2) lacustrine and marine sections with redox changes, (3) anomalous copper, lead, zinc, barium, boron, or silica mineralization, and (4) lead-zinc-copper-barium vein occurrences. Assessment for potential deposits involves

(1) Compilation of regional stratigraphic information on the distribution of lithologies, rock types, and known mineral occurrences;
(2) Geochemical, experimental, and theoretical studies of sources, transport, and deposition of base metals in sedimentary basins, with particular emphasis on diagenesis;
(3) Regional geochemical studies to identify anomalies; and

(4) Characterization of the depositional, tectonic, and thermal histories of the sedimentary basins.

Occurrences of sandstone-hosted stratabound copper-silver mineralization and vein lead-zinc-copper-barium mineralization are widespread in the EMB and are believed to have formed from the transport of basinal brines to shallow sites of mineral deposition in the Jurassic to Early Cretaceous. Promising target areas for more extensive sediment-hosted stratiform mineralization include Late Triassic to Jurassic lacustrine sections in the Hartford, Newark, and Culpeper basins and basal marine sections overlying buried Triassic basins in South Carolina, Georgia, and Florida.

24. MODES OF URANIUM OCCURRENCE IN BLACK MUDSTONES IN THE NEWARK BASIN, NEW JERSEY AND PENNSYLVANIA

Christine E. Turner-Peterson, P.E. Olsen, and Vito F. Nuccio

INTRODUCTION

The Newark basin in eastern Pennsylvania, central New Jersey, and southern New York is an early Mesozoic rift-related basin that formed in Late Triassic time and continued to receive sediment through Early Jurassic time (see fig. 24.1). Anomalous concentrations of uranium occur in sandstone of the Stockton Formation (Turner-Peterson, 1980) and mudstone of the Stockton and Lockatong Formations (fig. 24.2).

Mudstone-hosted uranium deposits, discussed in this report, occur as thin (less than 0.5 m) but laterally continuous uraniferous zones in certain types of black mudstone. The usual grade in these mineralized mudstones is 0.01–0.02 percent uranium oxide as U_3O_8 (Turner-Peterson, 1980); locally higher grades (as high as 0.29 percent) are known. These uranium values are higher than values for other uranium occurrences in black shale reported in the literature. Black-shale uranium occurrences in the Devonian and Mississippian Chattanooga Shale and the Alum Shale in Sweden average 0.006 and 0.03 percent, respectively (Davidson, 1961; Chase, 1979). In all the black-shale occurrences, uranium was probably fixed at or near the sediment-water interface, representing a nearly syngenetic concentration of uranium within reduced lake-bottom sediments.

NEW RESULTS

As a result of recent work, uranium mineralization in the Lockatong black mudstones can now be tied to portions of lacustrine cycles defined originally by Van Houten (1964) and refined by Olsen (1980a, 1984). Highest uranium contents occur in division 2 (of the detrital short cycle of Olsen, 1984), which is characterized by fine, calcareous laminated black siltstone (fig. 24.3). High uranium content correlates with high organic carbon and high sulfide sulfur contents. The uranium is commonly, but not always, associated with conchostracans, coprolites, ostracodes, and fish fossils.

One of the uranium anomalies has been located at precisely the same stratigraphic interval in the Lockatong at three widely spaced localities spanning a lateral distance of approximately 60 km. The widespread lateral extent of these black-shale uranium occurrences in the Lockatong Formation suggests syndepositional mineralization. This feature may also be useful for stratigraphic correlation.

A newly discovered anomaly in the Stockton Formation is of particular interest because the uranium occurs in a shaley black mudstone containing lacustrine fossils that resembles many of the uranium-bearing black shales of the Lockatong. Abundant conchostracans occur in the mineralized interval, indicating a lacustrine environment for the mineralization. Organic-carbon contents range from 0.05 to 0.66 percent, and uranium achieves a maximum grade of 0.29 percent uranium oxide, which is ore grade (table 24.1).

DISCUSSION

Because uranium occurrences are commonly associated with organic material in both sandstone and shale, a discussion of the types of organic matter that occur in the Newark basin is of interest. In general,

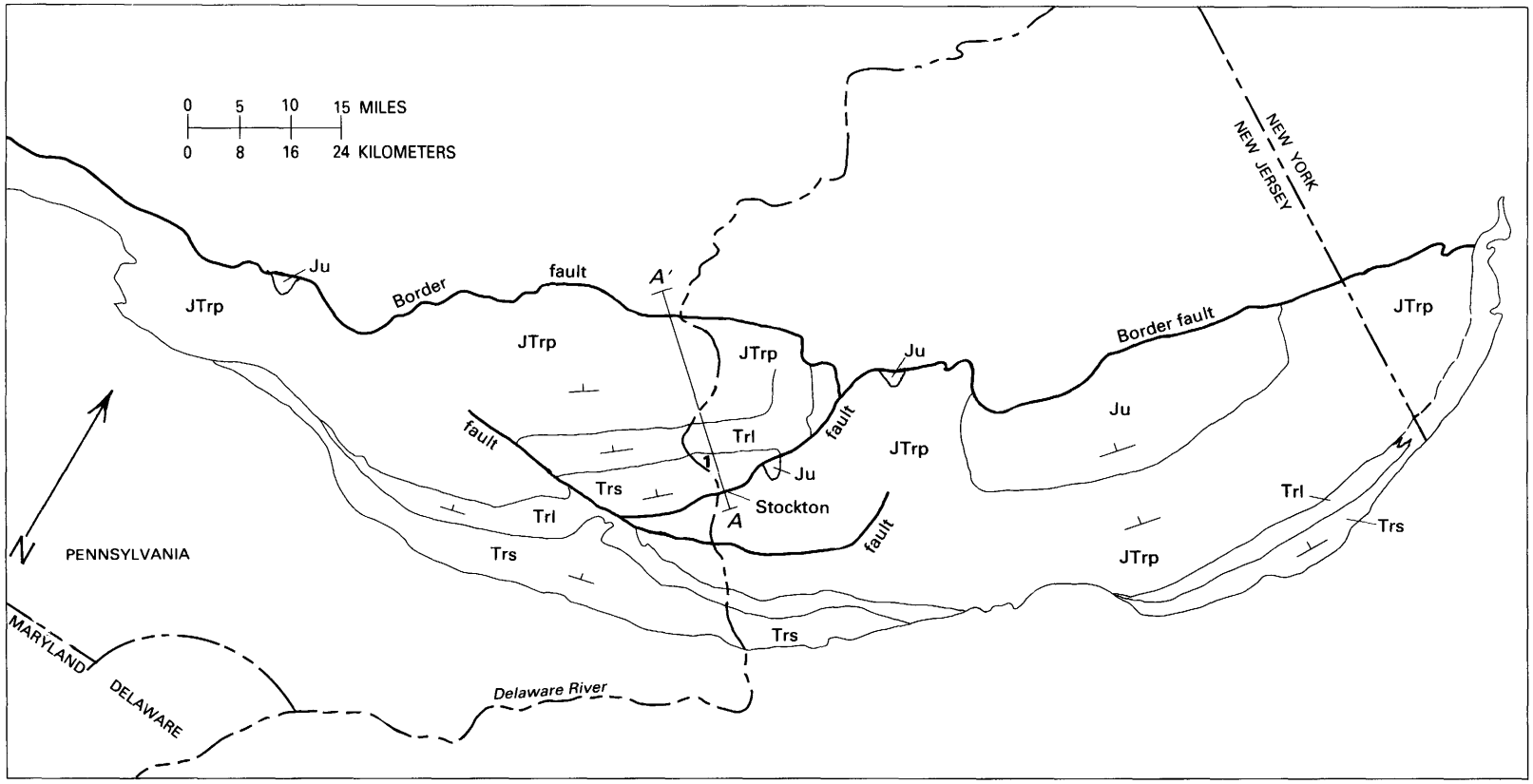

FIGURE 24.1.—Generalized geologic map of Newark basin (modified from Glaeser, 1966). Units dip to the north and northwest toward the northern border fault, and the section is repeated by faulting near the Delaware River. The stratigraphic units shown are the Stockton (Trs), Lockatong (Trl), and Passaic (JTrp) Formations and the Jurassic basalts and interbedded sedimentary rocks, shown here as Jurassic undifferentiated (Ju). Location 1 shows site of a newly discovered uranium anomaly in a gray mudstone of the Stockton Formation (see table 24.1). Cross section A–A' shown in figure 24.2.

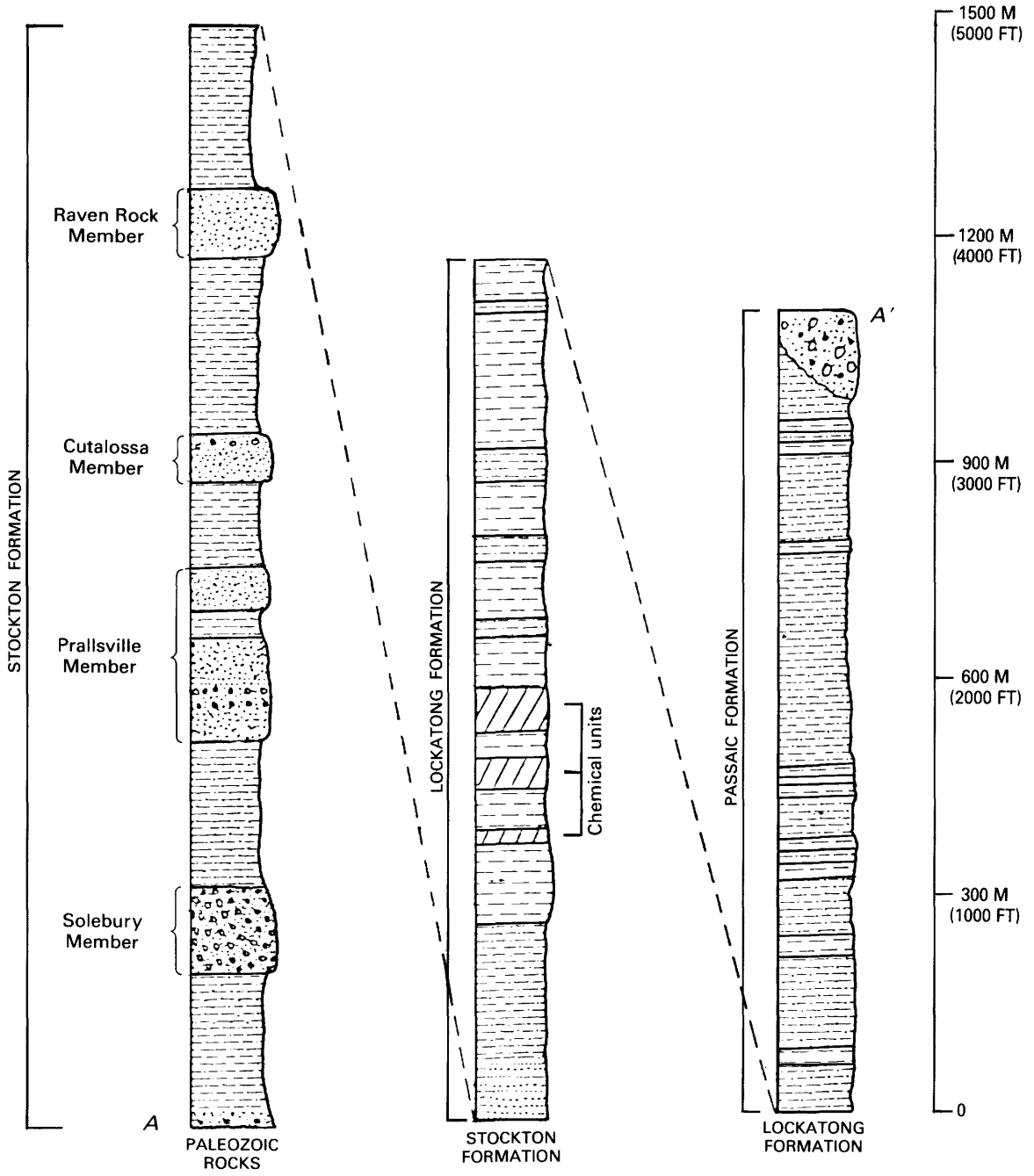

FIGURE 24.2.—Stratigraphic section of the Newark Supergroup along the Delaware River from Stockton, N.J., northward (modified from Van Houten, 1969). Section measured along *A–A'* (fig. 24.1).

organic material that is characterized by numerous oxygen-bearing functional groups has a greater affinity for metals than do other types of organic material (Schnitzer and Khan, 1978). Humic substances, in particular, are known to be effective concentrators of uranium (Szalay, 1958), whereas hydrocarbons generally are not (Andreyev and Chumachenko, 1964). New data indicate that many of the Jurassic lacustrine beds in the Newark basin have organic characteristics and thermal maturity making them suitable as hydrocarbon source beds (Olsen, 1984; Hatcher and Romankiw, chapter 11, this volume; Pratt and others, chapter 13,

this volume), but humic substance contents in these samples are low, and thus these beds are not favorable for uranium mineralization. Lacustrine beds in the Triassic Lockatong Formation also contain only small amounts of terrestrial plant material and thus are inferred not to contain much humic material. In fact, visual examination of the kerogen in typical black mudstone of division 2 in the Lockatong Formation shows that detrital plant debris makes up only a minor fraction of the total organic material present (Olsen, 1984). However, the presence of thin coaly beds and detrital plant fragments in other parts of the basin indicates that humic-substance-producing organic material (terrestrial plant debris) was available and present in the lake basin. Visual inspection of kerogen from the Stockton anomaly site during vitrinite reflectance studies showed that type 3 (terrestrial plant material derivative) is abundant in the samples enriched in uranium (table 24.1). Even though the organic matter in the Stockton anomaly is apparently rich in humic substances favorable for fixing uranium, it is unclear at this point whether the organic matter played an active role in the fixing of uranium. Fixation of uranium could occur by complexing with humic matter or by precipitation in response to reducing conditions near the sediment-water interface. The mechanism is of particular concern as the Lockatong uranium occurrences are in black mudstones that apparently do not contain large quantities of terrestrial plant debris, which contribute humic substances. The extremely high grade (0.29 percent uranium oxide) of the Stockton black mudstone, however, may reflect the influence of an unusual abundance of terrestrial plant material in this particular unit.

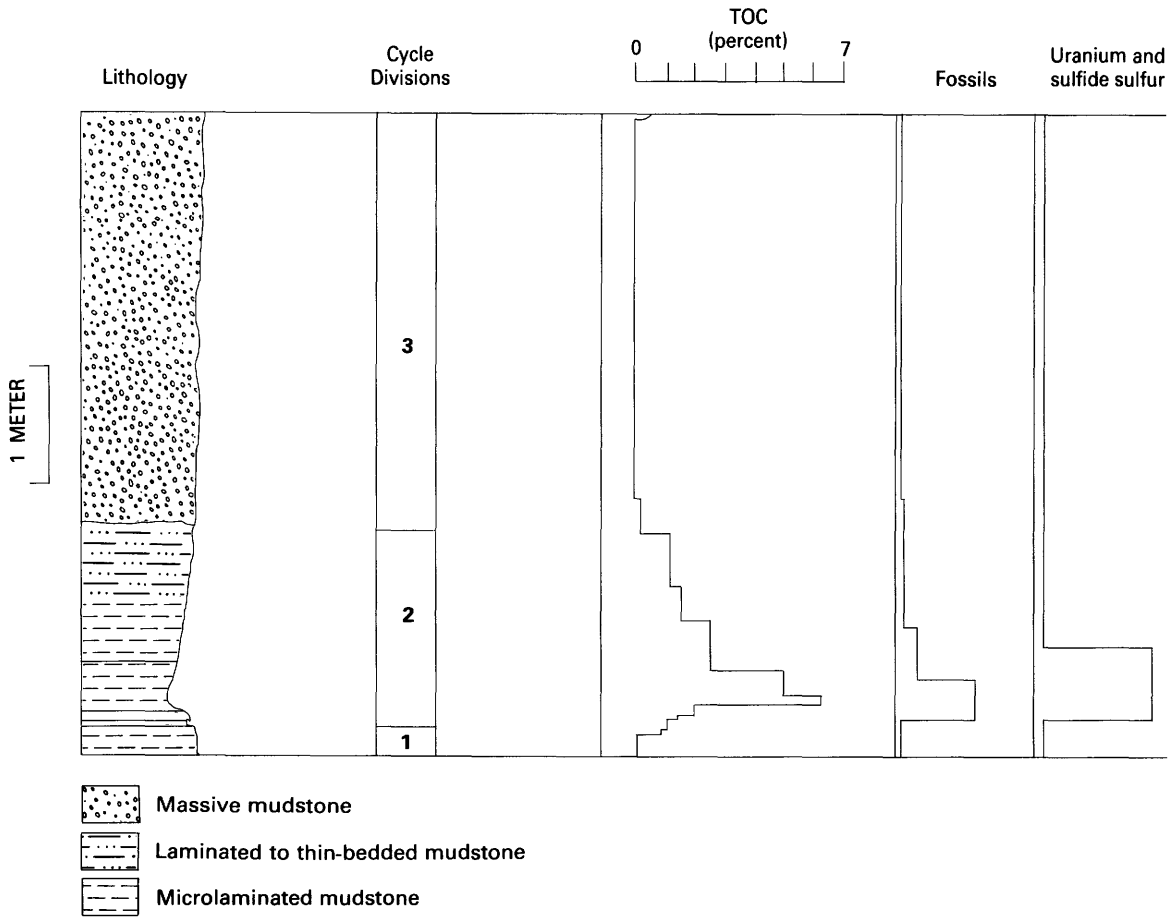

FIGURE 24.3.—Typical detrital cycle in the Lockatong Formation. Note that total organic carbon (TOC) is highest in division 2. Most uranium anomalies in this formation are associated with the lower part of division 2, which commonly contains coprolites, conchostracans, ostracodes, and fish remains. TOC values are from Olsen (1984). Fossil content is intended to be schematic and is summarized from Olsen (1984). Uranium and sulfur contents are also schematic.

TABLE 24.1.—*Vertical section (120 cm) across zone of uraniferous mudstone in the Stockton Formation. Units generally 2.5–15 cm thick; sample 6 is from a 2.5-cm-thick unit. See figure 24.1 for location*

[U_3O_8 in percent; determined by delayed neutron activation analysis. Organic carbon in percent; determined by difference (total organic carbon minus carbonate carbon). Vitrinite reflectance in percent; —, not determined]

Sample number	Lithology	U_3O_8	Organic carbon	Vitrinite reflectance
13	Dark red siltstone	<0.01	0.02	—
12	Medium gray mudstone	<.01	.03	—
11	Medium gray mudstone	<.01	.02	—
10	Medium gray mudstone	<.01	.02	—
9	Medium gray sandstone	<.01	.03	—
8	Dark gray siltstone	<.01	<01	—
7	Dark gray siltstone	<.01	.08*	—
6	Medium gray claystone	.29	.10**	—
5	Black mudstone	.04	.66**	0.68
4	Light gray claystone	.01	.05	—
3	Black mudstone	.01	.33	1.15
2	Light gray claystone	<.01	.10	—
1	Black mudstone	<.01	.23	.66

*Contains plant fragments. **Contains conchostracans.

CONCLUSIONS

Some Triassic black lacustrine mudstones of the Newark basin are rich in uranium, with contents commonly in the range of 0.01–0.02 weight percent uranium oxide. High uranium concentrations in these black mudstones correlate with high organic carbon and high total sulfur contents. This uranium enrichment is interpreted to be syndepositional and possibly related to precipitation in response to reducing conditions at the sediment-water interface. The occurrence of uranium enrichment at the same stratigraphic position in the Lockatong Formation at three widely separated localities supports this model.

A newly discovered uranium anomaly in the Stockton Formation is of particular interest because of the high uranium content (0.29 percent U_3O_8). High uranium concentrations occur in gray to black lacustrine mudstones with locally high contents of organic matter, similar to the associations observed elsewhere. This site is distinctive in that the mineralized horizon contains a high proportion of terrestrial organic matter.

REFERENCES

Andreyev, P.F., and Chumachenko, A.P., 1964, Reduction of uranium by natural organic substances: Geochemical International, v. 1, p. 3–7.

Chase, C.K., 1979, The Chattanooga and other Devonian shales — the United States' largest uranium source; Symposium Papers, Synthetic Fuels from Oil Shale: Chicago, Illinois, Institute of Gas Technology, p. 547–578.

Davidson, C.F., 1961, The kolm deposits of Sweden: Mining Magazine, v. 105, p. 201–207.

Glaeser, J.D., 1966, Provenance, dispersal, and depositional environments of Triassic sediments in the Newark-Gettysburg basin: Pennsylvania Geological Survey Bulletin G43, 168 p.

Olsen, P.E., 1980a, Fossil great lakes of the Newark Supergroup in New Jersey, *in* Manspeizer, Warren, ed., Field studies in New Jersey geology and guide to field trips, 52nd Annual Meeting, New York State Geological Association: Newark, N.J., Rutgers University Press, p. 352–398.

———1980b, The latest Triassic and Early Jurassic formations of the Newark basin (eastern North America, Newark Supergroup): Stratigraphy, structure, and correlation: New Jersey Academy of Science Bulletin 25, p. 25–51.

———1984, Comparative paleolimnology of the Newark Supergroup — A study of ecosystem evolution: New Haven, Conn., Yale University, unpub. Ph.D. dissertation, 726 p.

Szalay, A., 1958, The significance of humus in the geochemical enrichment of uranium: Proceedings of the Second International Conference on the Peaceful Uses of Atomic Energy, Geneva, v. 2, p. 182–186.

Schnitzer, M., and Khan, S.U., 1978, Soil organic matter: New York, Elsevier, 319 p.

Turner-Peterson, C.E., 1980, Sedimentology and uranium mineralization in the Triassic-Jurassic Newark basin, *in* Turner-Peterson, C.E., ed., Uranium in sedimentary rocks — Application of the facies concept to exploration: Short Course Notes, Rocky Mountain Section of Society of Economic Paleontologists and Mineralogists, p. 149–175.

Van Houten, F.B., 1964, Cyclic lacustrine sedimentation, Upper Triassic Lockatong Formation, central New Jersey and adjacent Pennsylvania: Kansas Geological Survey Bulletin 169, p. 497–531.

25. COPPER, NICKEL, AND COBALT FRACTIONATION PATTERNS IN MESOZOIC THOLEIITIC MAGMAS OF EASTERN NORTH AMERICA — EVIDENCE FOR SULFIDE FRACTIONATION [10]

David Gottfried

During fractional crystallization of silicates from tholeiitic magmas, Ni concentrations decrease sharply, Co concentrations decrease slightly, and Cu concentrations increase in the residual liquids. Tholeiitic suites illustrating this fractionation trend (Palisades sill, N.J.; Dillsburg intrusion, Pennsylvania; most of the Great Lake sheet, Tasmania; Alae lava lake, Hawaii) show an increase of Cu as the Ni/Co ratio decreases (trend 1, fig. 25.1). Published and new data on tholeiitic dikes and flows in Triassic-Jurassic basins in eastern North America show a contrasting tendency of decreasing Cu with decreasing Ni/Co ratio (trend 2, fig. 25.1). Cu content in the trend 2 group is as much as one-half to one-third lower than it is in rocks of virtually identical major and stable lithophile trace-element composition. Geochemical features of trend 2 rocks are attributed to the strong partitioning of Cu and Ni into an immiscible sulfide melt that separated from the magmas during ascent. Most tholeiitic basalts showing the largest amounts of Cu depletion are in North and South Carolina. These contrasting trends of Ni/Co versus Cu can identify mafic rocks in which fractionation of Ni- and Cu-bearing sulfide liquids took place and thus can be a guide in the exploration for magmatic Ni-Cu deposits.

[10]This paper is reprinted, with modifications, from Gottfried (1983, Geological Society of America Abstracts with Programs, v. 15, no. 2, p. 92.)

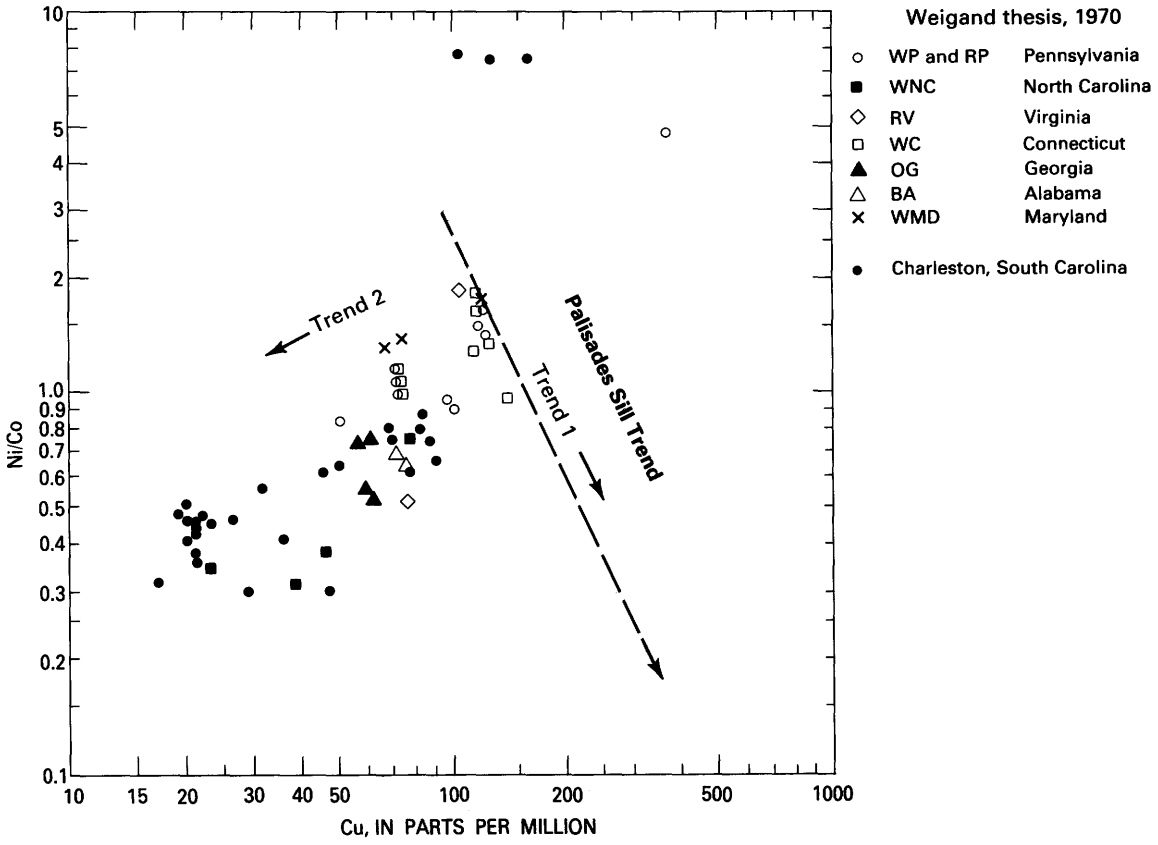

FIGURE 25.1.—Plot showing contrasting patterns of Cu versus Ni/Co abundances in Triassic and Jurassic diabase dikes and lava flows in the Eastern United States. Sample letters from Weigand (1970, Ph.D. thesis, Chapel Hill, University of North Carolina, 162 p.). Trend 1 data from Walker (1969, Geological Society of America Special Paper 111, 178 p.). Charleston data from Gottfried and others (1977, U.S. Geological Survey Professional Paper 1028, p. 91–113; 1983, U.S. Geological Survey Professional Paper 1313, p. A1–A19).

26. MAGNETITE SKARN DEPOSITS OF THE CORNWALL (PENNSYLVANIA) TYPE — A POTENTIAL COBALT, GOLD, AND SILVER RESOURCE

Gilpin R. Robinson, Jr.

This study provides an overview of the geologic setting of Mesozoic magnetite skarn deposits in the Gettysburg basin, Pennsylvania, and is part of a series of presentations at the workshop applying topical geological, geophysical, and geochemical studies to mineral resource exploration in the Gettysburg basin. The magnetite skarn deposits in the Gettysburg basin were a domestic source of iron ore from colonial times until the 1960's. Although such deposits in the Eastern U.S. Mesozoic basins are presently considered uneconomic, the association of elements of strategic importance (Co, Au) with the skarns warrants further investigation into their potential as a future low-grade resource for these elements.

Magnetite skarn deposits associated with Eastern U.S. Triassic-Jurassic basins, such as the classic Cornwall mine, Pennsylvania, are all spatially associated with Mesozoic diabase sheets, and most deposits are associated with carbonate host rocks. Deposits in the Cornwall and Morgantown districts are replacements of limestone, dolomitic limestone, and dolomite (fig. 26.1). Deposits in the Dillsburg and Boyertown districts are replacements of limey shale, limestone conglomerate, and siltstone.

The typical ore is magnetite containing accessory to trace amounts of pyrite, chalcopyrite, pyrrhotite, and sphalerite. In general, magnetite appears to preferentially replace calcite; diopside, actinolite, iron-rich chlorite, and accessory sulfides appear to preferentially replace dolomite. Approximately 1.5×10^6 tons of ore were mined from many small scattered deposits in the Dillsburg district. About 1×10^8 tons of ore were mined from a few concentrated deposits in the Cornwall district, and at least 1×10^8 tons of ore were mined from several concentrated deposits in the Morgantown district (mainly the Grace mine), where substantial reserves probably remain.

Interest in these deposits today centers around trace metals (Co, Au, and Ag) associated with sulfides. The Cornwall deposit was once a major domestic cobalt source, and both the Cornwall and Grace mines apparently have produced significant amounts of gold and silver (possibly 1×10^6 oz. Ag and a similar amount of Au at the Grace Mine; Cornwall produced approximately 1×10^5 oz. Au and 7.5×10^5 oz. Ag; A.V. Heyl, 1984, oral commun.). Table 26.1 provides average assay values for sulfide concentrates at the Grace and Cornwall mines.

Copper, gold, and silver(?) are localized predominately in chalcopyrite. Pyrite is the dominant carrier of cobalt in the Cornwall deposit. Another sulfide phase (possibly pyrrhotite) carries substantial cobalt at the Grace mine. Sulfides are more abundant in the Cornwall and Dillsburg district deposits than in the Morgantown district deposits.

The large magnetite skarn deposits in the Gettysburg basin are localized along the basin margins, where diabase sheets are in contact with pre-Mesozoic carbonate units; however, smaller deposits in the Dillsburg and Boyertown districts replace Triassic limestone and limestone conglomerate. Lapham and Gray (1972) noted a number of characteristic features of these deposits:

(1) Ore is generally, *but not always*, above diabase sheets.
(2) The distribution of late differentiates (granophyres and ferrogabbros) is commonly spatially unrelated to the loci of ore bodies or ore channels.
(3) Diabase chilled margins adjacent to ore are hydrothermally altered, and mineralized veins sometimes cut diabase.
(4) Chlorite, actinolite, sulfides, and trace cations (Ag, Au, Ni, Co) are closely associated.

These deposits appear to be a variant of the calcic magnetite skarn type of Einaudi and others (1981). Lithostatic pressure, estimated from stratigraphic evidence, must have been low, approximately 1500 bars (Sims, 1968). The initial skarn alteration occurs at approximately 600–700°C. The main period of oxide and sulfide ore deposition generally occurs at lower temperature (500°C or less) and is accompanied by the beginning of hydrous alteration of early skarn minerals and the associated intrusion. The accessory sulfides appear to be associated with chlorite-actinolite-rich layers (originally dolomite?) (Lapham and Gray, 1972). Pyrite often forms both contemporaneously with and later than magnetite. Chalcopyrite appears to replace magnetite. Late sulfide deposition may be structurally controlled and cut across earlier skarn patterns.

Eugster and Chou (1979) and Rose and others (1985) have developed models describing the formation

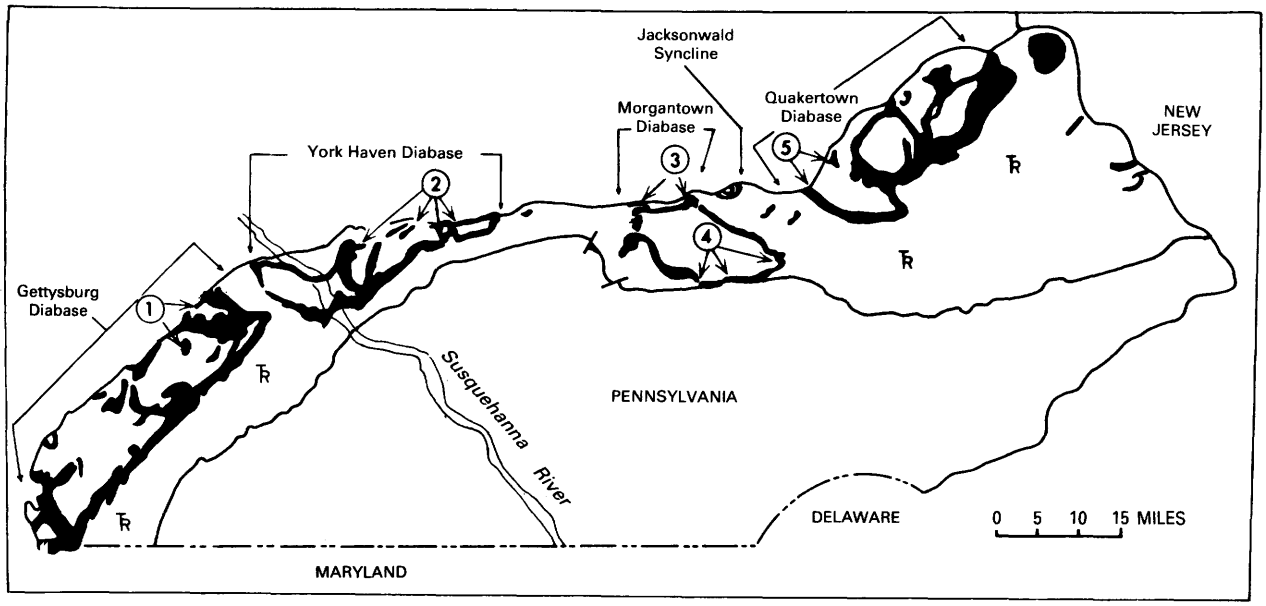

FIGURE 26.1.—Map of diabase-magnetite ore districts in the Pennsylvania Triassic belt (from Lapham and Gray, 1972, Pennsylvania Geological Survey Bulletin M–56, ser. 4, p. 281). 1, Dillsburg; 2, Cornwall, including, from west to east, Hummelstown, Carper, Cornwall, and Doner mines; 3, Wheatfield, including, from west to east, Wheatfield and Ruth mines, Fritz Island, and Esterly (in Jacksonwald syncline); 4, Morgantown-French Creek, including, from west to east, Morgantown, Jones, Hopewell, and French Creek mines; 5, Boyertown. All districts are now inactive.

of Cornwall-type magnetite skarn deposits. Their models assume the presence of a convective hydrothermal cell driven by temperature gradients developed by the intrusive diabase sheet. The hydrothermal fluid must be saline (chloride-rich) to transport dissolved iron and sulfur. The preferred interpretation is that the ore solutions were formed by circulation and heating of connate or meteoric fluids, although the chloride-rich fluids could be produced from late-stage diabase differentiates or granophyres (Smith and Rose, 1972). As mentioned above, however, distribution of these late differentiates is spatially unrelated to loci of ore bodies or ore channels (Lapham and Gray, 1972). Magnetite mineralization occurs through a series of coupled reactions between fluids, source rocks, and host rocks. At high temperatures, the fluids transport iron along with some H_2S. This fluid cools and reacts with calcite marble, raising fluid pH and depositing magnetite and sulfides (Eugster and Chou, 1979).

Sulfide deposition appears to be related to the waning period of the hydrothermal cell. Sulfur isotope values for the Cornwall, Dillsburg, and French Creek deposits (+ 5 to + 17) are typically heavier than normal magmatic sulfur values and are similar to values for sulfides from nearby non-igneous country rock (Lapham and Gray, 1972, p. 132), implying a sedimentary sulfur source. Sulfide abundances in typical ore are less than 10 weight percent.

Critical features for these deposits include

(1) Diabase sheets of sufficient thickness to set up hydrothermal circulation;

TABLE 26.1.—*Average sulfide concentrate ore assay of bulk ore and pyrite separates from Pennsylvania*

[Sulfide, Co, Ni, Cu, Zn, Pb in weight percent; Au, Ag in parts per million. —, not determined]

	Sulfide	Co	Ni	Cu	Zn	Pb	Au	Ag
Cornwall ore	6.5	1.14	0.13	4.5	—	—	0.5	4
Pyrite separate	—	1.3	.10	—	—	—	—	—
Grace ore	4	.68	.26	1.41	0.22	0.20	—	7
Pyrite separate	—	.51	—	—	—	—	—	—

(2) The presence (at an appropriate time) of saline brines to carry metals;
(3) The presence of replaceable carbonate units in the proper geometry to hydrothermal circulation to buffer fluid pH and channel fluid flow; and
(4) External source of sulfur to cause sulfide deposition.

Magnetite-poor and sulfide-rich variants of this deposit type may exist, possibly associated with hornfels and skarns developed in Mesozoic dolomitic marls in the basins.

REFERENCES

Einaudi, M.T. and others, 1981, Skarn deposits: Economic Geology, v. 75, p. 317–391.

Eugster, H.P., and Chou, I-M., 1979, A model for deposition of Cornwall-type magnetite deposits: Economic Geology, v. 74, p. 763–744.

Lapham, D.M., and Gray, Carlyle, 1972, The geology and origin of the Triassic magnetite deposit and diabase at Cornwall, Pennsylvania: Pennsylvania Geological Survey Bulletin M–56, ser. 4, 343 p.

Rose, A.W., Herrick, D.C., and Deines, Peter, 1985, An oxygen and sulfur isotope study of skarn-type magnetite deposits of the Cornwall type, southeastern Pennsylvania: Economic Geology, v. 80, p. 418–443.

Sims, S. J., 1968, The Grace mine magnetite deposit, Berks County, Pennsylvania, *in* Ore deposits of the United States; 1933–1967: New York, American Institute of Mining, Metallurgical, and Petroleum Engineers, v. 1, p. 108–124.

Smith, R.C., II, and Rose, A.W., 1972, Major and trace elements in differentiates of Triassic diabase and their relationships to Cornwall-type deposits [abs.]: Geological Society of America Abstracts with Programs, v. 4, p. 671.

27. GRAVIMETRIC CHARACTER AND ANOMALIES IN THE GETTYSBURG BASIN, PENNSYLVANIA — A PRELIMINARY APPRAISAL

David L. Daniels

The digital gravity data set assembled for the study area in the Gettysburg basin consists of 3400 stations. The largest source of data is a new USGS gravity survey, which significantly increases station density compared with the U.S. Department of Defense gravity data in the western part of the area. After removal of clearly spurious data, the contoured Bouguer gravity data (fig. 27.1) show a major east-west gradient, a segment of the regional Appalachian gravity gradient, dominating the southern half of the map. To reduce the dominance of this gradient and enhance local features, a high-pass filter was prepared from a radially averaged power spectrum of the gridded data. The resulting high-pass residual contour map is shown in figure 27.2.

Positive gravity anomalies within the basin are associated with diabase intrusive rocks and are consistent with the large density contrast (0.25–0.55 g/cm^3) between diabase (2.95–3.05 g/cm^3) and the sedimentary rocks (2.5–2.7 g/cm^3). Four major intrusive bodies are present at the surface: the Gettysburg, York Haven, Morgantown, and Quakertown, listed from west to east and shown as G, Y, M, and Q on figure 27.2, following the usage of Sumner (1977). The form of the intrusives is locally complex, but in general they are largely sheetlike and only the southeast edge of the sheet is partly conformable to the bedding of the enclosing sedimentary rocks (Hotz, 1952). Each diabase intrusive is composed of multiple, interconnected and irregular bodies with ring-like outcrop patterns (see Robinson, fig. 26.1, this volume). An early gravity study by Hersey (1944) showed that an anomaly maximum occurs over the sedimentary rocks in the center of the ring of outcropping Quakertown diabase (Q, fig. 27.2), which can be explained by a structure described as "an elongated spoon shape" with a central maximum thickness of more than 500 m. Central anomaly maxima are also present over the Gettysburg and York Haven bodies (G and Y, fig. 27.2), which probably have similar structures. The Morgantown body (M, fig. 27.2) is an exception, having a deep gravity low in the central area. The low indicates that diabase is absent or very thin in the subsurface beneath the center of the ring. The Morgantown body is also unique in that it spans the basin making contact with both borders, whereas the other sheets are situated along the northern edge. Maximum thickness of the Morgantown body, as inferred from the gravity data, follows the complex southern limb of exposed diabase and also an area of Paleozoic and Precambrian rocks, which lie within the ring of diabase (X, fig. 27.2) and appear to have been faulted or rafted upwards by intrusion of diabase.

Correlation is strongest between anomalies on the high-pass map and Mesozoic diabase bodies in the area south of Harrisburg (H, fig. 27.2) where the station

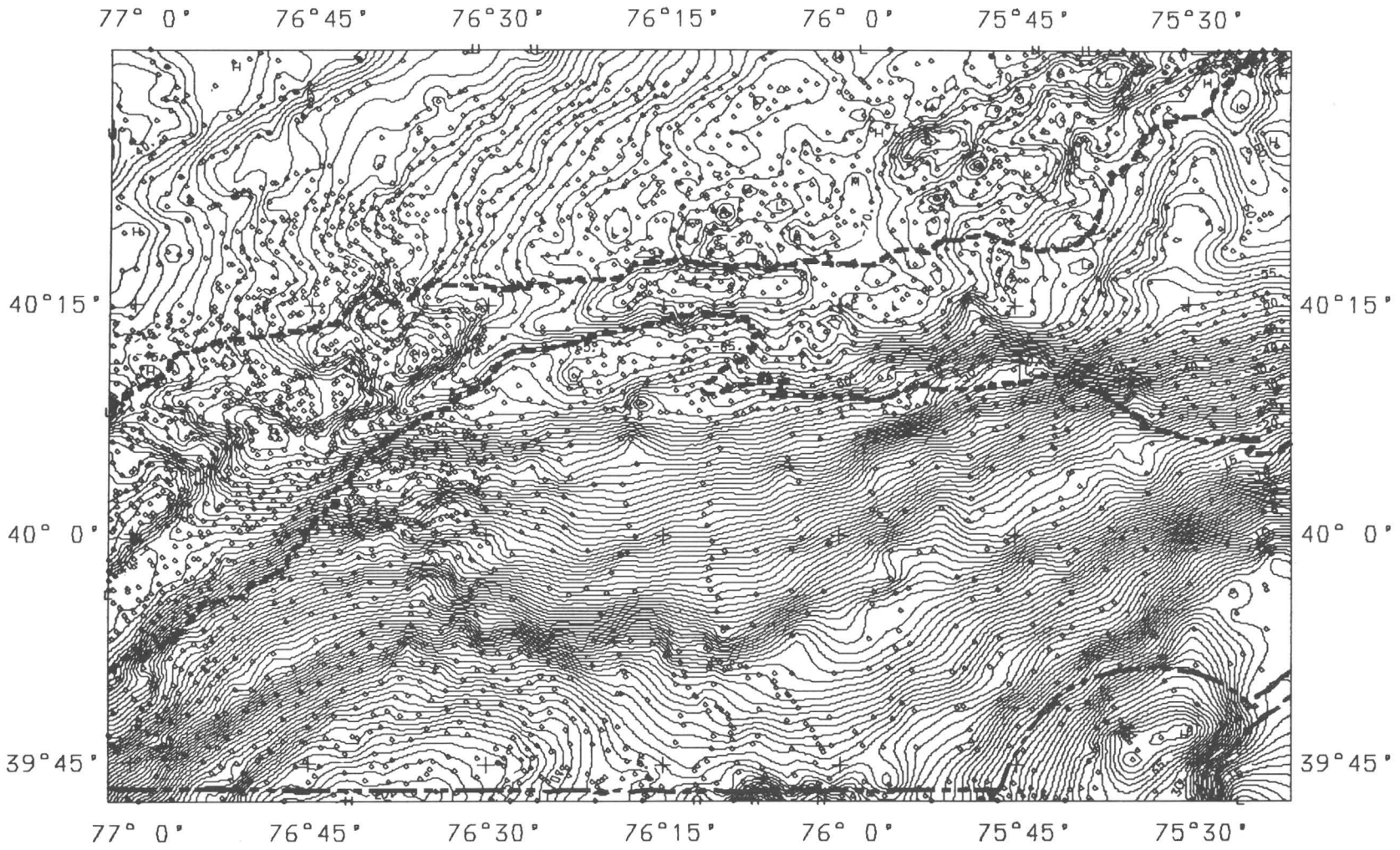

FIGURE 27.1.—Bouguer gravity anomaly map of part of the Gettysburg-Newark basin and vicinity. Contour interval 1 mgal; stations shown with diamond symbol; basin boundaries shown as short dashed line.

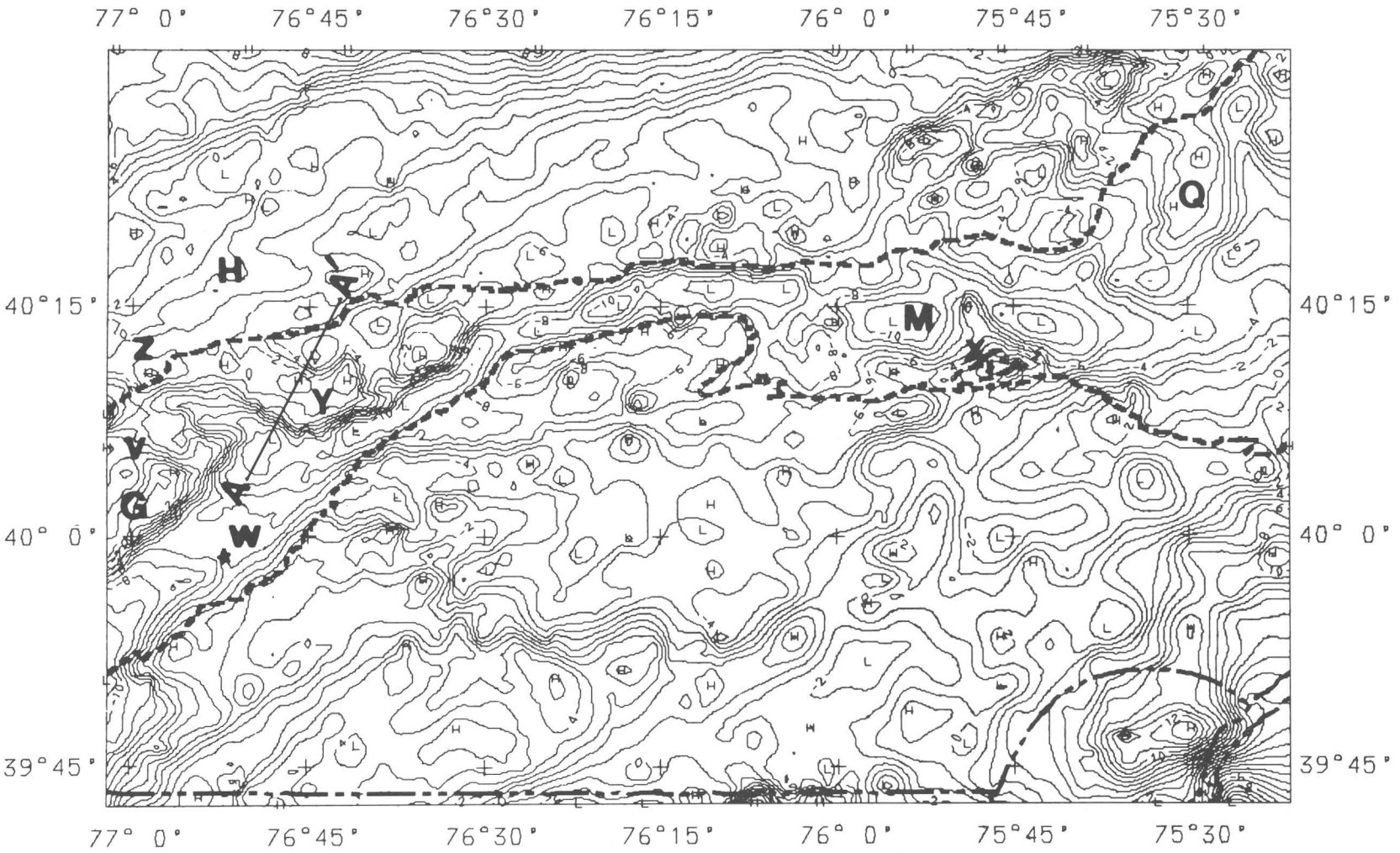

FIGURE 27.2.—Residual gravity map derived from data shown in figure 27.1. Contour interval 1 mgal; basin boundaries shown as short dashed lines; letters mark locations discussed in text; location of profile (fig. 27.3) shown by line *A-A'*.

density is highest. The York Haven body was selected for more detailed study by gravity modelling. Along a north-northeast-trending profile (*A–A'*, fig. 27.2; shown in fig. 27.3), a single body with maximum thick-

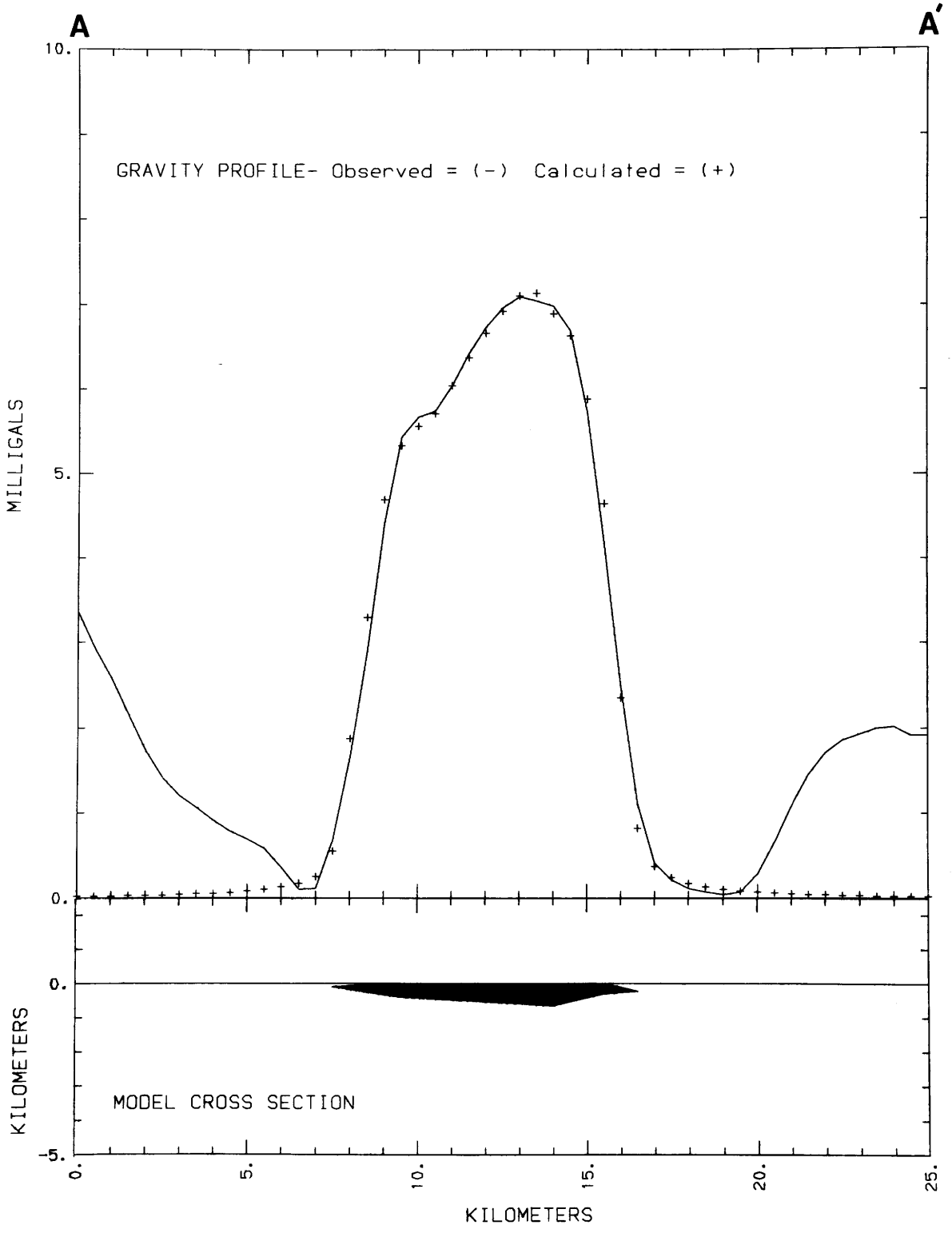

FIGURE 27.3.—Residual gravity profile and associated cross-sectional model of part of the York Haven diabase body (fig. 27.2, *A-A'*).

ness of 640 m can match the observed gravity, assuming a density contrast of 0.35 g/cm^3 between the diabase and sedimentary rocks. Along the profile, diabase is present at the surface at 9.0–9.3 km and at 14.8–15.5 km, corresponding to the southern and northern sides of the exposed ring. To match the anomaly with these fixed points required a model that dips outward at shallow depth, reversing to inward dips at greater depths (fig. 27.3). The central area of sedimentary rocks above the diabase in this model is thin (60 m).

The gravity high over the York Haven diabase west of profile A–A' extends beyond the ring of exposed diabase, beyond the edge of the basin, and in part overlies Paleozoic rocks. A small exposure of diabase at the edge of the basin suggests that much of the anomaly within the basin is underlain by diabase. Diabase may also be present beneath the Paleozoic sedimentary rocks outside the basin (Z, fig. 27.2), suggesting potential conditions (diabase and limestone in contact) for the development of Cornwall-type magnetite skarn ore deposits. Alternatively, dense subsurface Precambrian rocks, such as metabasalt, may be the anomaly source in that area.

The marked variation in anomaly amplitude over the York Haven and Gettysburg bodies probably reflects variable thickness of the diabase sheets and possibly the depth of the top of the diabase where it is covered by sedimentary rocks. Contrary to the findings of Sumner (1977), the maximum thickness of the Gettysburg and York Haven bodies appears to be similar. An abrupt change of about 250 m in the thickness of the Gettysburg sheet near Rossville (R, fig. 27.2) is marked by a linear gradient trending northwest across the northeast end of the body, suggesting fault control of the intrusion. Smith and others (1975) have shown that the Gettysburg body encompasses two separate diabase intrusions of slightly different composition, the York Haven and Rossville types. It is not clear at this time whether or not one or both of these bodies thin across the linear gradient.

Residual gravity lows characterize the sedimentary rocks of the basin, and gravity contours parallel the basin boundaries for much of their length except adjacent to the Reading Prong, where local densities may be similar to the sedimentary rocks of the basin. Gravity minima are located axial to the basin boundaries where the diabase is absent, and the spacing of contours generally suggests a symmetrical V-shaped basin cross-section. If the two basin boundary structures have similar dip, then the north-northwestern border probably cannot be represented as a single steeply dipping fault. Either a series of down-to-basin normal faults, each of limited displacement, or a large-displacement shallow-dipping listric normal fault may be more probable. Sumner (1977) modelled the basin with several densities from 2.55 to 2.72 g/cm^3 for the sedimentary rocks and calculated thicknesses in different areas that range from 0.5 to 5.0 km. Accurate density data are critically important for the determination of basin thickness by gravity methods. Complicating factors include the presence of the diabase, the selection of the regional gradient, the validity of reported density determinations (especially of the basin sedimentary rocks), and the variety of lithologies and densities that make up the enclosing "basement" rocks. A well that may have reached pre-Mesozoic basement penetrated over 2.8 km of sedimentary rocks (Shaub, 1975) southeast of the Gettysburg diabase (W, fig. 27.2). Residual gravity is about -5 mgal at this location, whereas at several locations within the basin, values are less than -10 mgal. This suggests that the basin reaches depths significantly greater than that indicated at the well location.

REFERENCES

Hersey, J.B., 1944, Gravity investigation of central-eastern Pennsylvania: Geological Society of America Bulletin, v. 55, p. 417–444.

Hotz, P.E., 1952, Form of diabase sheets in southeastern Pennsylvania: American Journal of Science, v. 250, p. 375–388.

Shaub, F.J., 1975, Interpretation of a gravity profile across the Gettysburg Triassic basin: University Park, Pennsylvania State University, M.S. thesis, 65 p.

Smith, R.C., II, Rose, A.W., and Lanning, R.M., 1975, Geology and geochemistry of Triassic diabase in Pennsylvania: Geological Society of America Bulletin, v. 86, p. 943–955.

Sumner, J.R., 1977, Geophysical investigation of the structural framework of the Newark-Gettysburg Triassic basin, Pennsylvania: Geological Society of America Bulletin, v. 88, p. 935–942.

28. AEROMAGNETIC CHARACTER AND ANOMALIES OF THE GETTYSBURG BASIN AND VICINITY, PENNSYLVANIA — A PRELIMINARY APPRAISAL

Jeffrey D. Phillips

Published USGS aeromagnetic quadrangle maps for the Gettysburg basin and vicinity have been digitized and compiled into a regional aeromagnetic map (fig. 28.1). The map represents the total field anomaly at 150 m (500 ft) above the terrain. A least-squares planar surface was removed from the data before contouring. The basin boundaries, which are faulted on the north and unconformable on the south, are represented by heavy dashed lines.

Patterns of aeromagnetic anomalies in the Gettysburg basin region are strongly correlated with mapped lithologies. The Triassic sandstones and shales of the basin produce low-amplitude anomalies and smooth, broadly spaced magnetic contours, as do the Paleozoic limestones and shales outside the basin. Where these two rock types are in contact, the basin boundary is poorly defined by the aeromagnetic data. The larger diabase sheets within the basin, and their associated thermal metamorphic (hornfels) zones, produce moderate-amplitude anomalies and closely spaced magnetic contours. Longer wavelength anomalies associated with the diabase bodies suggest that many of the northern limbs of these sheets dip to the south. A reduced-to-the-pole aeromagnetic map (not shown) suggests that nearly all limbs of the sheets dip inward, toward the centers of the bodies. This is in agreement with drill-hole data (Hotz, 1952).

Outside the basin, Precambrian and lower Paleozoic metamorphic rocks produce noisy patterns of closely spaced contours and moderate- to high-amplitude magnetic anomalies. The characteristic circular anomaly pattern observed north of the basin in the northeast corner of the map is produced by the Precambrian hornblende and granitic gneisses of the Reading Prong. The northwestern limit of this imbricate stack of basement thrust sheets is defined by the abrupt change from this circular anomaly pattern to a smooth magnetic low.

The pronounced linear anomaly in the southeast corner of the map is produced by schists of the lower Paleozoic Wissahickon (oligoclase phase) and Peters Creek formations (Socolow, 1974). Although the magnetic contours suggest a south-dipping contact between this magnetic unit and the nonmagnetic (chloritic phase) schist of the Wissahickon to the north (Bromery and Griscom, 1967), this inference is not supported by the reduced-to-the-pole aeromagnetic data, which indicate only that the magnetic unit is thin and has sharp contacts on both sides.

The broad, northeast-trending linear anomaly in the southwest corner of the map is thought to be produced by anticlinally folded Precambrian rocks at depth. These rocks may be related to the exposed Precambrian granites and gneisses that produce a similar broad anomaly to the east (Bromery and Griscom, 1967), or they may be related to the metavolcanic rocks of the Catoctin Formation, which is exposed along the western margins of the early Mesozoic basins in Maryland and Virginia. The circular positive anomalies at the northeastern end of this linear feature are spatially related to exposures of Precambrian metavolcanic rocks (Bromery and Griscom, 1967). The discontinuous narrow band of anomalies south of this broad linear anomaly and curving to the east is produced by units of the Cambrian Chickies Quartzite, Harpers Phyllite, and Antietam Quartzite (Bromery and Griscom, 1967; Socolow, 1974).

On the eastern side of the map, the broad, low-amplitude anomaly produced by Precambrian granites and gneisses appears to cross the southern boundary of the basin. Superimposed shorter wavelength anomalies are attenuated at the basin margin. With this exception, anomalies produced by the older metamorphic rocks rarely extend across the basin boundaries. This suggests either that the basin is exceptionally thick or, more likely, that much of the basement beneath the Mesozoic rocks of the basin is composed of a thick sequence of nonmagnetic Paleozoic sedimentary rocks.

Long-wavelength magnetic anomalies support this last suggestion. The west-central third of the map is dominated by a broad magnetic low, corresponding to exposures of Paleozoic limestones and shales. The only significant magnetic anomalies in this region are those produced by diabase bodies within the basin, by a thin sheet of Precambrian gneiss just across the northern boundary of the basin (Bromery and Griscom, 1967; Socolow, 1974), and by an isolated industrial plant in Lancaster, Pa. By implication, nonmagnetic rocks must extend to considerable depth in this region.

Most known iron ore (magnetite) deposits, both inside and outside the basin, produce positive circular anomalies on the aeromagnetic map (Socolow, 1974). The Rittenhouse Gap magnetite district (R, fig. 28.1) is north of the basin, in the Precambrian gneisses of the

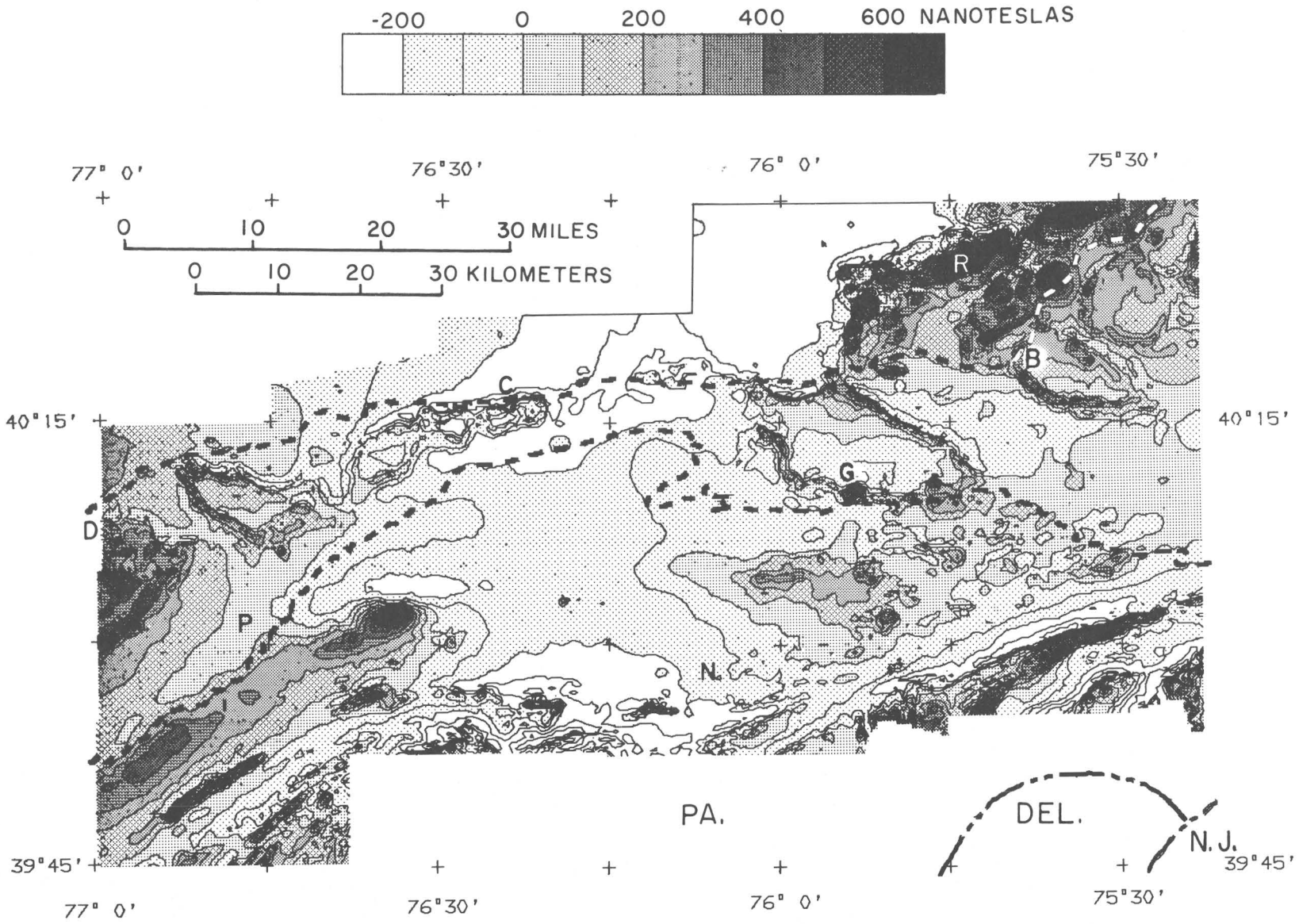

FIGURE 28.1.—Aeromagnetic map of the Gettysburg basin and vicinity. Heavy dashed lines mark basin boundaries. R, Rittenhouse Gap magnetite district; C, Cornwall iron mines; B, Boyertown iron mines; G, Grace mine; D, Dillsburg orebodies; N, Gap Nickel deposit; P, small copper prospect.

Reading Prong. The Rittenhouse Gap orebody produces the highest amplitude positive magnetic anomaly on the map. More than 100 mines were active in this district during the 1870's and 1880's (Socolow, 1974). Other high-amplitude positive magnetic anomalies within the Reading Prong are produced by disseminated magnetite within the Precambrian gneisses.

The Cornwall iron mines (C) lie on a diabase-limestone contact along the northern margin of the Mesozoic basin. The large Cornwall orebodies are characterized by relatively small magnetic anomalies, a fact most often attributed to a strong remanent magnetization directed at right angles to the present geomagnetic field (Bromery and Griscom, 1967; Socolow, 1974). The Boyertown iron mines (B), also at the northern margin of the basin, are centered under a large, isolated magnetic anomaly (Bromery and Griscom, 1967; Socolow, 1974). At the southern margin of the basin, a circular anomaly lies over the Grace mine (G), a concealed magnetite deposit that was discovered through the use of aeromagnetic data (Jensen, 1951). Numerous small iron ore prospects are also present around the diabase body southeast of Dillsburg (D) (Stose and Jonas, 1939). Like the Cornwall orebodies, the Boyertown, Grace, and Dillsburg orebodies result from magnetite replacement of Paleozoic limestone or Triassic limestone conglomerate (Socolow, 1974), presumably during and immediately following the intrusion of the adjacent diabase bodies.

Magnetic anomalies are conspicuously absent over the Gap Nickel deposit (N), south of the basin (Socolow, 1974), and over a small copper prospect (P) within the Triassic strata southeast of Dillsburg (Stose and Jonas, 1939). North-northeast-trending diabase dikes, such as the Quarryville dike, which passes near both the Gap Nickel deposit and the Grace mine, also do not appear in the aeromagnetic data, perhaps owing in part to their narrow widths (less than 50 m wide) and in part to their orientation, which is subparallel to the north-south flight-lines.

REFERENCES

Bromery, R.W., and Griscom, A., 1967, Aeromagnetic and generalized geologic map of southeastern Pennsylvania: U.S. Geological Survey Geophysical Investigations Map GP-577, 2 sheets, scale 1:125,000.

Hotz, P. E., 1952, Form of diabase sheets in southeastern Pennsylvania: American Journal of Science, v. 250, no. 5, p. 375–388.

Jensen, H., 1951, Aeromagnetic survey helps find new Pennsylvania iron orebody: Engineering and Mining Journal, v. 152, no. 8, p. 56–59.

Socolow, A.A., 1974, Geologic interpretation of aeromagnetic maps of southeastern Pennsylvania: Pennsylvania Geological Survey Information Circular 77, 85 p.

Stose, G.W., and Jonas, A.I., 1939, Geology and mineral resources of York County, Pennsylvania: Pennsylvania Geological Survey Bulletin C–67, 199 p., 1 map, scale 1:62,500.

29. HYDROGEOCHEMICAL EXPLORATION IN THE EARLY MESOZOIC BASINS OF SOUTHEASTERN PENNSYLVANIA

W.H. Ficklin, J.B. McHugh, and James M. McNeal

The most important mineral occurrences in the early Mesozoic basins of southeastern Pennsylvania are the magnetite skarn deposits at Morgantown and Cornwall. Mines at these two locations have been productive until recent years. Some small lead mines were located near Phoenixville, and a mine near Gap, Pa., was the major nickel supply for the United States for a short time after the Civil War. Currently there is very little mining in the region. However, the geologic environment is appropriate for this type of skarn deposit throughout the area.

Fresh surface rocks are scarce in southeastern Pennsylvania because of the deep weathering that takes place in a humid climate. The region is densely populated, making stream sediment sampling subject to contamination from cultural activities. However, a potentially useful sample medium is ground water. Almost every residence and business outside of a community has a well as a domestic water supply, so a reconnaissance of a large area can be made by collecting ground water samples.

Hydrogeochemical exploration has been made easier and more reliable in recent years with the introduction of several new analytical methods, namely graphite furnace atomic absorption spectrometry and ion chromatography. With these techniques a relatively

small amount of sample can be used to obtain a large number of determinations for major and trace constituents (Miller, Ficklin, and Learned, 1982).

The water samples used for this study were collected mainly during April and May 1984; a few samples were collected in October 1983. Samples were collected from an area within the Newark basin between 75°30′ W. and 76°15′ W. Each 7.5–min quadrangle was divided into nine cells of 2.5 min on a side, where one or more samples were collected.

The location of the sample in each cell was randomly selected. In some cells three samples were collected to provide estimates of error due to local variation. Analytical duplicates were made from one of the three samples from those cells where three samples were collected.

We collected 135 water samples and 24 duplicates from domestic wells, usually the water supply for a home or small business. The samples were collected after the water had been running for at least five minutes. Temperatures and pH were measured at the time of sample collection. All samples were placed in a random sequence before analysis. The analytical methods used are summarized in Miller, Ficklin, and Learned (1982).

The water was analyzed for sulfate, copper, cobalt, nickel, and zinc. The major constituents and several other trace metals were also determined so that computerized equilibrium calculations and factor analysis could be applied to the results. Abnormally large sulfate concentrations are due in some instances to the oxidation of sulfide deposits. The elements copper, cobalt, nickel, and zinc are generally mobile enough in ground water to indicate where unusually high concentrations are due to ground-water interaction with a mineral deposit. The copper, nickel, cobalt, and zinc concentrations of samples collected near the Gap Nickel mine were all in excess of 100 µg/L, whereas the mean concentration for all samples was less than 5 µg/L. A copper-zinc-cobalt-nickel-sulfate anomaly was found just east of Reading. A cobalt anomaly occurs in samples from four wells along a diabase dike just at the edge of the basin (near Denver, Pa.). Copper-nickel anomalies occur throughout the region, mainly near diabase outcrops or dikes. Some of the domestic water supplies sampled have copper plumbing, which may account for several of the high concentrations of copper and zinc (greater than 100 µg/L); however, most "highs" are probably the result of dissolution of natural mineral occurrences.

The objective of the study was met: water samples were collected and analyzed from a large area within a short span of time. Part of the effort was directed toward determining the usefulness of water as a sample medium in an area where other, more conventional, sample media may not be as useful. Although contamination problems were apparent, the water sampling method was accurate enough to target several areas for further investigation with a more detailed sampling program.

REFERENCE

Miller, W.R., Ficklin, W.H., and Learned, R.E., 1982, Hydrogeochemical prospecting in the tropical marine climate of Puerto Rico: Journal of Geochemical Exploration, v. 16, no. 3, p. 217.

30. THE USE OF SULFUR ISOTOPES AS A GEOCHEMICAL EXPLORATION TECHNIQUE IN THE EARLY MESOZOIC BASINS OF PENNSYLVANIA

James M. McNeal

The tectonic setting of the early Mesozoic basins of the Eastern United States is very similar to that of the Noril'sk area in Siberia (Naldrett, 1981). The sulfides of the magmatic segregation deposits of the Noril'sk area contain Ni, Cu, and platinum-group elements and were apparently formed after the intruding basaltic magma became contaminated by assimilating sedimentary sulfate before emplacement. Subsequent reduction of the sulfate and segregation by crystal settling of the sulfide minerals led to the formation of these deposits (Naldrett, 1981). The assimilated sedimentary sulfate was enriched in ^{34}S (Naldrett, 1981) compared with the sulfur of normal mafic and ultramafic rocks (Ohmoto and Rye, 1979). The purpose of this preliminary study is to report the sulfur isotopic composition of whole-rock diabase, sulfide minerals,

and other sulfur-containing minerals from the early Mesozoic basins of Pennsylvania as a first step in testing, developing, and applying sulfur isotopic compositions of diabase as a geochemical exploration technique.

Normal basaltic magmas do not contain enough sulfur to form sulfide deposits by magmatic segregation. Three of the several methods of causing sulfide minerals to precipitate from basaltic magmas are (1) adding sulfur from an outside source, (2) increasing the concentration of sulfur in the residual melt by magmatic differentiation, and (3) decreasing the sulfur solubility by assimilating silica-rich minerals (Cawthorn, 1980). It is the first of these three methods that led to the formation of the Noril'sk-type deposits (Godlevskii and Grinenko, 1963), and it is the possibility of this having occurred in the early Mesozoic basins of the Eastern United States that serves as the focus of this study.

The sulfur isotopic systematics of sulfide minerals in ultramafic and mafic rocks are straightforward; $\delta^{34}S$ values range from -1 to $+2$ per mil (Ohmoto and Rye, 1979). Deviations from this range are attributed to contamination by sedimentary sulfur (Ohmoto and Rye, 1979), since ^{34}S variations due to magmatic differentiation can be ignored (Ohmoto and Rye, 1979). However, Smitheringale and Jensen (1963) did report minor isotopic enrichment of ^{34}S in late-stage sulfides from diabase of the early Mesozoic basins in the Eastern United States. ^{34}S in sedimentary sulfate in rocks of Jurassic age and older can be expected to range from 10 to 30 per mil, with a mean between 15 and 20 per mil (Holser and Kaplan, 1966). Sulfur isotopes, therefore, offer a means of determining whether diabase has been contaminated with sedimentary sulfate when one is exploring for Noril'sk-type mineral deposits.

In this preliminary study, samples of diabase and of sulfur-bearing minerals from the early Mesozoic basins of Pennsylvania were examined for their sulfur isotopic composition. Samples were collected of the three types of diabase identified by Smith and others (1975): the York Haven type (high TiO_2, quartz tholeiite), the Rossville type (low TiO_2, quartz tholeiite), and the Quarryville type (olivine tholeiite), including both chilled-margin and differentiated material. Sulfide mineral samples were also collected from the Gap Nickel mine (a magmatic segregation of sulfide minerals in an ultramafic host of Precambrian age, which is close to the Quarryville Mesozoic diabase dike), and from several of the Cornwall-type ore bodies (skarn replacement of carbonate by magnetite, Co-bearing pyrite, and chalcopyrite in association with diabase) that occur in Pennsylvania.

The chilled margin of the diabase represents the initial composition of the intruding magma, and the preliminary results suggest whole-rock $\delta^{34}S$ values of about -1.2 per mil for the Rossville type, 1.2 per mil for the York Haven type, and 3.1 per mil for the Quarryville type. Except for the Quarryville, these values are all close to the -1 to $+2$ per mil values for mafic and ultramafic igneous rocks suggested by Ohmoto and Rye (1979). While the $\delta^{34}S$ value for the Quarryville is somewhat high, it may represent a minor extension of the normal range of isotopic composition or minor contamination by a sulfur source enriched in ^{34}S.

Substantial variation of ^{34}S composition was found for the York Haven diabase. The $\delta^{34}S$ values for eight samples from four different localities range from 1.2 per mil, for a chilled-margin sample, to 1.7 and 2.3 per mil for fine-grained samples, 2.0 and 3.0 per mil for medium-grained samples, 5.0 per mil for a coarse-grained sample containing magnetite, and 12.6 per mil for a sample of gabbroic pegmatite. One sample of a bronzite cumulate zone in the lower portion of a sill had a value of 1.7 per mil. The gabbroic pegmatite, which contained sparse hornblende, was the only sample that contained hydrous minerals; the formation of a minor aqueous phase may be responsible for the higher ^{34}S content of the sample, if there is a partitioning of ^{34}S into the aqueous phase. While there is a trend of increasing ^{34}S content with increasing grain size, reflecting a partitioning of ^{34}S due to the early stages of normal differentiation, it may be that later intruded magma of the same event assimilated progressively greater amounts of sulfur enriched in ^{34}S from the underlying sediments.

The results for the Rossville samples suggest that some of the magma became contaminated by sedimentary sulfate or that substantial magmatic differentiation of the S occurred causing unusually high $\delta^{34}S$ values. Four localities of Rossville diabase were sampled; three of the four have rather similar $\delta^{34}S$ values (range -2.7 to -1.0 per mil, median $= -1.6$ per mil, $n = 6$), with no apparent relationship to grain size. Three samples from the fourth locality, the Zora ring complex, have systematically higher $\delta^{34}S$ values (2.4, 4.9, and 5.8 per mil). Unlike the York Haven diabase, the Rossville diabase shows no apparent relation between $\delta^{34}S$ values and grain size. One sample from the ring complex contains magnetite, which occurs near the top of a diabase sheet, suggesting that this sample formed near the end of the magmatic differentiation process. It had an intermediate $\delta^{34}S$ value. This result

suggests that the whole ring complex contains unusually heavy sulfur, because this magnetite-bearing sample would be expected to have the highest $\delta^{34}S$ value if magmatic differentiation were solely responsible for the elevated $\delta^{34}S$ value.

The $\delta^{34}S$ values for the Quarryville-type diabase, which range from 2.5 to 3.1 per mil (n = 3), suggest either that the magma originated from a source with unusually high $\delta^{34}S$ values or that the magma became contaminated with sedimentary sulfur before emplacement. The possibility of extensive local magmatic differentiation can be ruled out because the Quarryville diabase is a dike no more than a few tens of meters wide and about 100 km long. The $\delta^{34}S$ values for two samples of fine-grained diabase collected about 15 km apart are both 2.5 per mil. At one of the localities, a chilled-margin sample was found to have a value of 3.1 per mil. If partitioning of sulfur isotopes occurs such that the later products become enriched in ^{34}S, then the chilled margin would be expected to have a $\delta^{34}S$ value somewhat higher than the next products to crystallize, while the later products would have increasingly greater ^{34}S contents. This may be why the chilled margin of the Quarryville is somewhat heavier than the fine-grained rock.

Studies of the ^{34}S composition of sulfide minerals from the Cornwall-type Morgantown and French Creek deposits by this author and of the Cornwall deposit by Rose and others (1985) suggest by their high $\delta^{34}S$ values that the sulfur of the sulfide minerals had a sedimentary sulfate source. The $\delta^{34}S$ values for the Morgantown and French Creek deposits generally range from 5 to 11 per mil; at the Cornwall deposit, the values range from 6 to 20 per mil. These results are important because they suggest that there is a source of isotopically heavy sulfur (sedimentary sulfate) available for the formation of sulfide minerals and that the sulfur has a distinctly higher ^{34}S content than the associated diabase. It may be that the presumed sedimentary sulfate was a precondition for the formation of the sulfides in the Cornwall-type deposits.

Speculation that the Gap Nickel deposit is a previously unrecognized Noril'sk deposit is not supported by the sulfur isotopic evidence. The sulfide minerals at the Gap Nickel mine were found to be rather light (chalcopyrite, 1.3 to 2.6 per mil, n = 4; pyrrhotite, 1.8 to 2.3 per mil, n = 3) compared with the sulfide minerals from the Cornwall-type deposits. This suggests that the sulfur in the Gap Nickel deposit is not from sedimentary sulfate, as would be necessary to fit the Noril'sk model. The $\delta^{34}S$ values in the Gap deposit approximate those from the nearby Quarryville diabase (2.5 per mil), suggesting, but not proving, that there may be a genetic relationship between the Gap Nickel deposit and the Quarryville diabase.

Sulfur isotopic values of gypsum from quarries in diabase are very heavy, with $\delta^{34}S$ values of 25 and 33 per mil. Values of anhydrite from the Grace mine (a Cornwall-type deposit, near Morgantown, Pennsylvania) are much lighter, with values of 13.2 and 13.9 per mil. Although the gypsum may be a secondary mineral in the quarries, thus accounting for the high $\delta^{34}S$ values, the anhydrite is more likely to have been primary, as it appeared to be bedded in the core samples and is somewhat heavier than the sulfide of the deposit.

Several conclusions can be drawn from these results. First, the sulfur isotopic compositions of the chilled margin of the three kinds of diabase appear to be different. Second, there appears to be some variation in ^{34}S content of York Haven-type diabase due to magmatic differentiation. Third, sedimentary sulfate appears to have been a factor in the formation of the Cornwall-type mineral deposits but not in the formation of the Gap Nickel deposit. Fourth, substantial variation in the ^{34}S content within one type of diabase can occur, as shown by the values for the Zora ring complex, perhaps by local contamination with sedimentary sulfate. Fifth, the use of sulfur isotopes as a geochemical exploration technique for Noril'sk-type deposits in the early Mesozoic basins of Pennsylvania looks encouraging for two reasons. The sulfur isotopic composition of chilled diabase seems rather constant and light for each of the three types of diabase, suggesting that contamination by a sedimentary sulfate source could be readily distinguished. In addition, an example of contamination of diabase by isotopically heavy sulfur, a precondition for the formation of Noril'sk-type deposits, may have occurred at the Zora ring complex; similar contamination may have occurred elsewhere in the early Mesozoic basins of the Eastern United States.

REFERENCES

Cawthorn, R.G., 1980, High-MgO Karroo tholeiite and the formation of nickel-copper sulphide mineralisation in the Insizwa intrusion, Transkei: South African Journal of Science, v. 76, p. 467–470.

Godlevskii, M.N., and Grinenko, L.N., 1963, Some data on the isotopic composition of sulfur in sulfides of the Noril'sk deposit: Geochemistry, v. 1, p. 35–41.
Holser, W.T., and Kaplan, I.R., 1966, Isotope geochemistry of sedimentary sulfates: Chemical Geology, v. 1, p. 93–135.
Naldrett, A.J., 1981, Nickel sulphide deposits: Classification, composition, genesis, *in* Skinner, B.J., ed., Seventy-fifth anniversary volume: El Paso, Tex., Economic Geology Publishing Co., p. 628–685.
Ohmoto, H., and Rye, R.O., 1979, Isotopes of sulfur and carbon, *in* Barnes, H.L., ed., Geochemistry of hydrothermal ore deposits, second edition: New York, Wiley, p. 509–567.
Rose, A.W., Herrick, D.C., and Deines, Peter, 1985, An oxygen and sulfur isotope study of skarn-type magnetite deposits of the Cornwall type, southeastern Pennsylvania: Economic Geology, v. 80, p. 418–443.
Smith, R.C., II, Rose, A.W., and Lanning, R.M., 1975, Geology and geochemistry of Triassic diabase in Pennsylvania: Geological Society of America Bulletin, v. 86, p. 943–955.
Smitheringale, W.G., and Jensen, M.L., 1963, Sulfur isotopic composition of the Triassic igneous rocks of eastern United States: Geochimica et Cosmochimica Acta, v. 27, p. 1183–1207.

31. A PRELIMINARY ANALYSIS OF LINEAR FEATURES OF THE GETTYSBURG BASIN

M.D. Krohn, O.D. Jones, and J.G. Ferrigno

INTRODUCTION

An area in southeastern Pennsylvania (fig. 31.1) was selected as the test site for the multidisciplinary U.S. Geological Survey program studying the Mesozoic basins of the Eastern United States. This area corresponds to a narrow neck of the Mesozoic basins that is the juncture between the Gettysburg basin to the west and the Newark basin to the east. The area is of interest from a physiographic viewpoint, because it covers the transition between the pre-Mesozoic South Mountain and the Blue Ridge province to the south and the Reading Prong and the New England Highland province to the north. The area is the only place along the Appalachians where the Mesozoic basin lies directly against the Paleozoic limestones of the Great Valley. The overall goal of our study is to determine the relationship of linear features observed on Landsat images to regional structures that have affected the location and geologic history of this basin. The purpose of this report is to provide a preliminary analysis of the spatial correlation of linear features to different aspects of the Mesozoic geology.

PRELIMINARY RESULTS

Linear features were compiled on late autumn Landsat MSS (Multispectral Scanner) band 7 images (fig. 31.2). The linear features were digitized and presented as a length-weighted azimuth frequency histogram (fig. 31.3) and a density contour map (fig. 31.4). A minimum in the strike frequency histogram at N. 55° W. indicates a sun-angle bias rather than any geologic feature. The maxima near N. 70° E. represent linear features that in general parallel bedding or foliation trends in the area. Linear features that trend across the strike of the general bedding and foliation orientation display north-northeast and northwest azimuthal maxima at N. 14° E., N. 25° W., and N. 75° W. (fig. 31.5). The north-northeast-trending linear features cluster into several distinctive zones that appear to transect the Mesozoic basin. The N. 14° E. and the N. 75° W. linear features at several places form intersecting orthogonal sets that are not influenced by the Mesozoic basin.

INTERPRETATION OF THE DATA

Previous studies over the past decade have shown that zones of linear features commonly coincide with subsurface regional structural features as evidenced by aligned inflections of contours on isopach, gravity, and aeromagnetic maps (Podwysocki and others, 1982) and in some cases coincide with regional patterns of mineralization (Rowan and Wetlaufer, 1981). Three zones of linear features identified on the Landsat images correlate with different aspects of the geology within and around the Gettysburg basin: structural features, diabase dikes, and ore deposits. However, there is considerable overlap in the geologic expression of these zones.

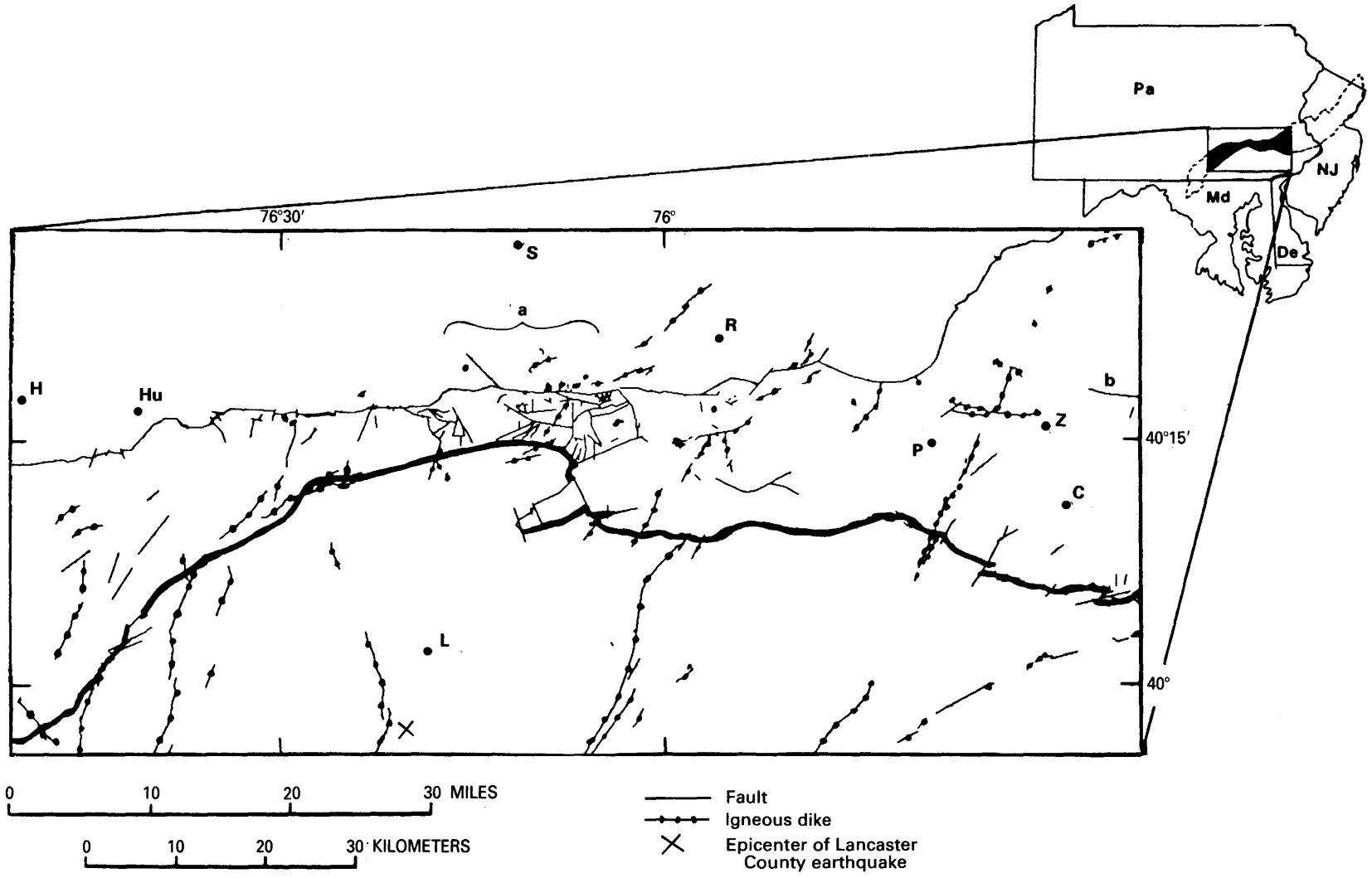

FIGURE 31.1.—Index map of Gettysburg basin showing basin boundaries (heavy lines), faults, and igneous dikes. C, Collegeville; H, Harrisburg; Hu, Hummelstown; L, Lancaster; P, Pottstown; R, Reading; S, Schaefferstown; Z, Zieglerville. Brace marked "a" denotes zone of increased fault density within the Mesozoic basin; b, Chelafont fault.

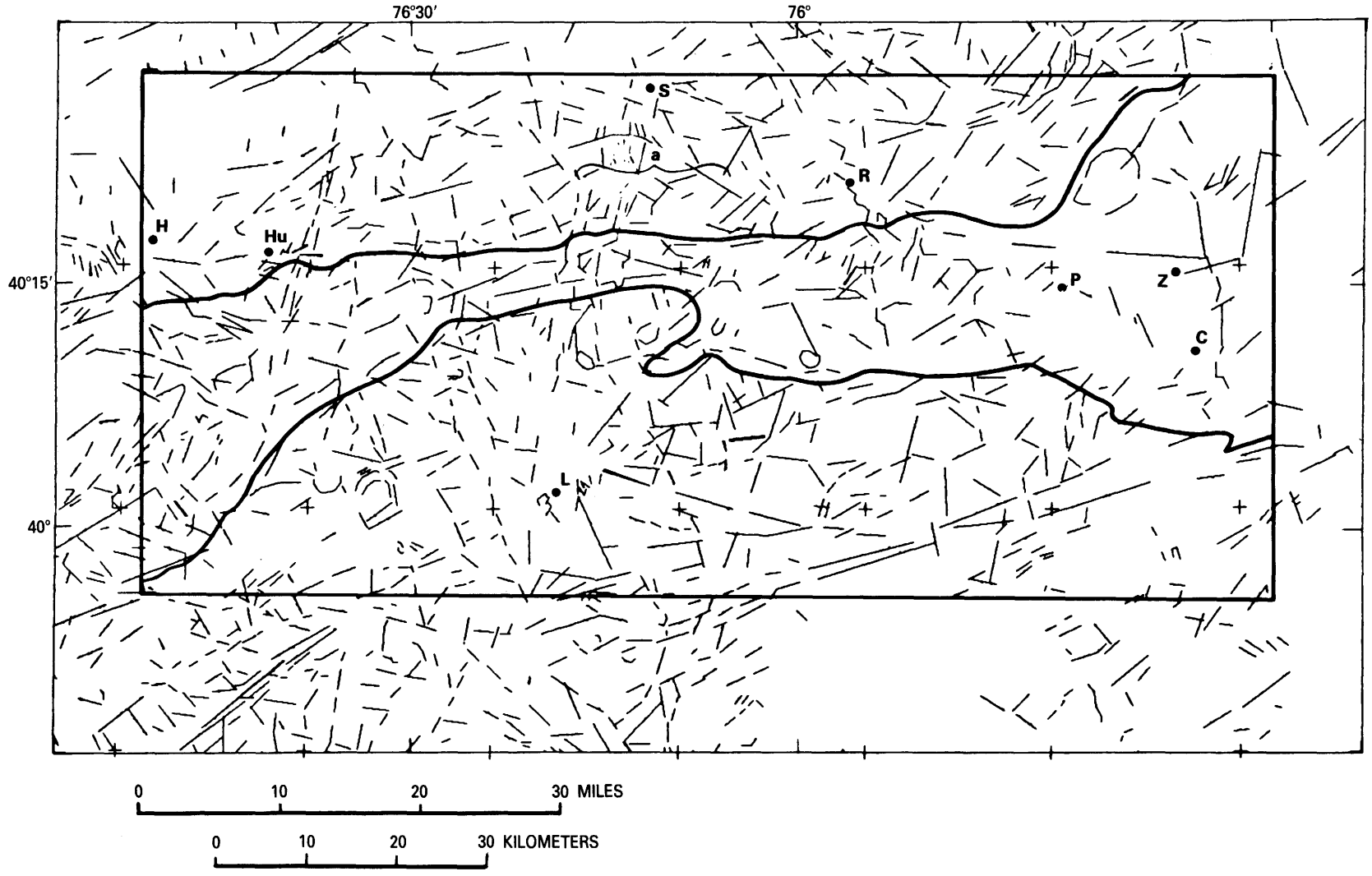

FIGURE 31.2.—Linear features mapped from Landsat Multispectral Scanner (MSS) band 7 (0.8–1.1 micrometers), Landsat scene identification numbers 1080–15185 and 1080–15192. Letter symbols the same as in figure 31.1.

STRUCTURAL FEATURES

A zone of linear features trends N. 14° E. for a distance of 45 miles (72 km) across the study area from near Lancaster (L) to Schaefferstown (S), Pa. (figs. 31.2, 31.5). This zone transects the basin at its narrowest part and corresponds to the western side of an area 10 miles (16 km) wide of increased faulting within the basin (a, fig. 31.1). An anomalous concentration of linear features is observed in this area on the density contour map (a, fig. 31.4). Immediately north of the basin margin, the zone is about 4 miles (6.5 km) wide and includes two diabase dikes that also trend north-northeast.

Several north-northeast-trending structures outside the basin are aligned along this zone. South of the basin, a north-northeast-trending fault is shown on the older geologic map of Pennsylvania (Gray and others, 1960) but not on the newer version (Berg and others, 1980). Original mapping by Jonas and Stose (1930) shows a fault extending over 10 miles (16 km) north-northeast from Lancaster with right-lateral displacement. Later mapping by Meisler and Becher (1970) shows several right-lateral displacements of thrust and normal faults aligned in a north-south orientation; however, they are not mapped as a continuous structure. North of the basin, the Paleozoic limestones show a distinctive north-south cross-fold pattern that transects the general east-west trend of the outcrop pattern. Further north, north-northeast-trending faults cut the Martinsburg Formation (Berg and others, 1980). Gravity data in the area of the north-northeast-trending zone of linear features show a distinct high in an area of roughly constant gradient south of the basin and several inflections of gravity contours north of the basin (Daniels, chapter 27, this volume). The projected epicenter of the Lancaster County earthquake of April 22, 1984, aligns on the eastern edge of the zone and yielded a north-northeast-trending fault-plane solution (Scharnberger, 1984). Furthermore, several of the north-northeast-trending zones of linear features correspond to alignments of diabase dikes (Berg and others, 1980) and seem to show a fairly constant 15-mile (24-km) spacing between zones. The alignment of several separate structures along a common zone of weakness is a characteristic of zones of linear features (Podwysocki and others, 1982).

DIABASE DIKES

Diabase dikes of Mesozoic age are common in the Appalachian region and cut both pre-Mesozoic and Triassic rocks. The dikes are subvertical tabular bodies that show linear surface traces extending for many miles. In addition to the dikes, laterally extensive diabase sheets and extrusive basalt flows may be present.

Near Zieglerville, Pa. (Z, fig. 31.2), a zone of linear features trends N. 86° W. for 20 miles (32 km). This zone aligns with a pair of west-trending dikes, which are approximately 5 miles (8 km) long, and also aligns with a west-trending margin of a diabase sheet (Berg and others, 1980). The N. 86° W. orientation is noteworthy, because it does not correspond to the maxima observed in the strike frequency histogram (fig. 31.3). Moreover, the orientation is unusual for diabase dikes, which in this area generally trend north to northeast.

These west-trending dikes align with other structures and geomorphic features in the area. Immediately south of the dikes is the west-trending stream drainage of Swamp Creek. Four miles (6.5 km) northeast of the dikes is the western edge of the west-trending Chelafont fault (b, fig. 31.1). The Chelafont fault is a normal fault, down to the south, with a maximum displacement of 3500 feet (1000 m) (Willard and others, 1959). The surface trace of the fault is mappable to the east for a distance of more than 20 miles (32 km) (Berg and others, 1980). Drag folds in outcrop indicate that some left-lateral displacement may have occurred (Willard and others, 1959). The combination of diabase dikes, basalt flow margins, linear stream drainages, and normal faults suggests some type of subsurface control for this N. 86° W. zone of linear features.

ORE DEPOSITS

The distribution of ore deposits in the Mesozoic basin, taken from a compilation by Rose (1970) (fig. 31.6), can be used for an initial comparison to the linear features mapped from Landsat data. Rose (1970) grouped the ore deposits into four categories: Pb-Zn vein-type deposits, Cornwall-type skarn deposits, copper deposits adjacent to igneous bodies, and copper deposits away from igneous bodies, although no genetic relationship is implied. The Pb-Zn deposits along the southeastern margin show little correspondence with the individual linear features. This observation runs counter to our initial hypothesis, since these deposits are commonly sited in cross-cutting veins and minor fault zones; higher spatial resolution may be needed. Cornwall-type skarn deposits located along the northern basin margin show some correspondence with

individual linear features. The westernmost skarn deposit in the study area occurs along one of the north-northeast-trending zones of linear features (fig. 31.5) and corresponds to an offset of the northern border fault near Hummelstown, Pa. (Hu, fig. 31.1) (Berg and others, 1980).

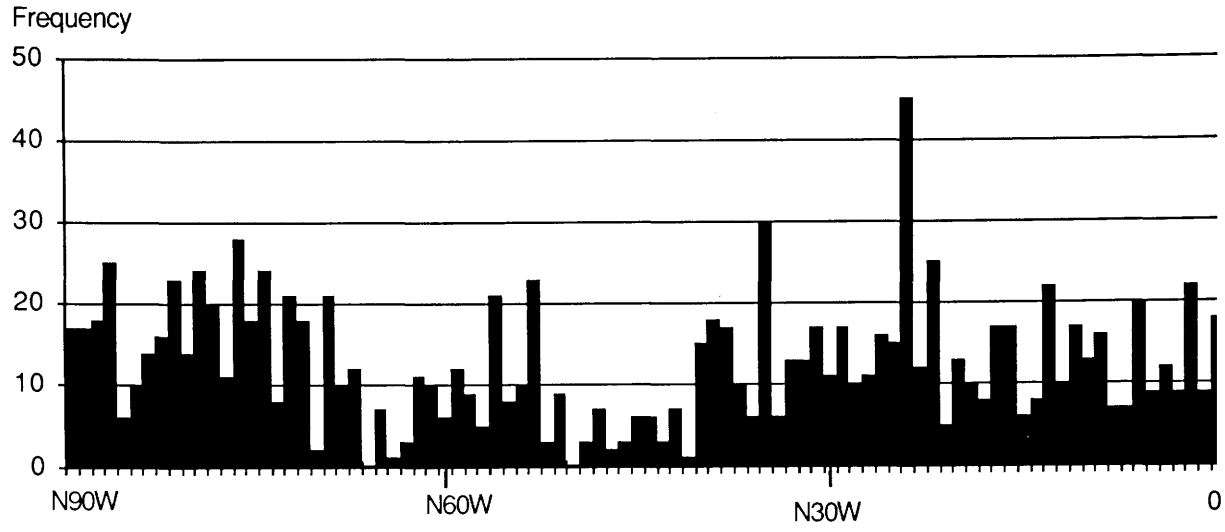

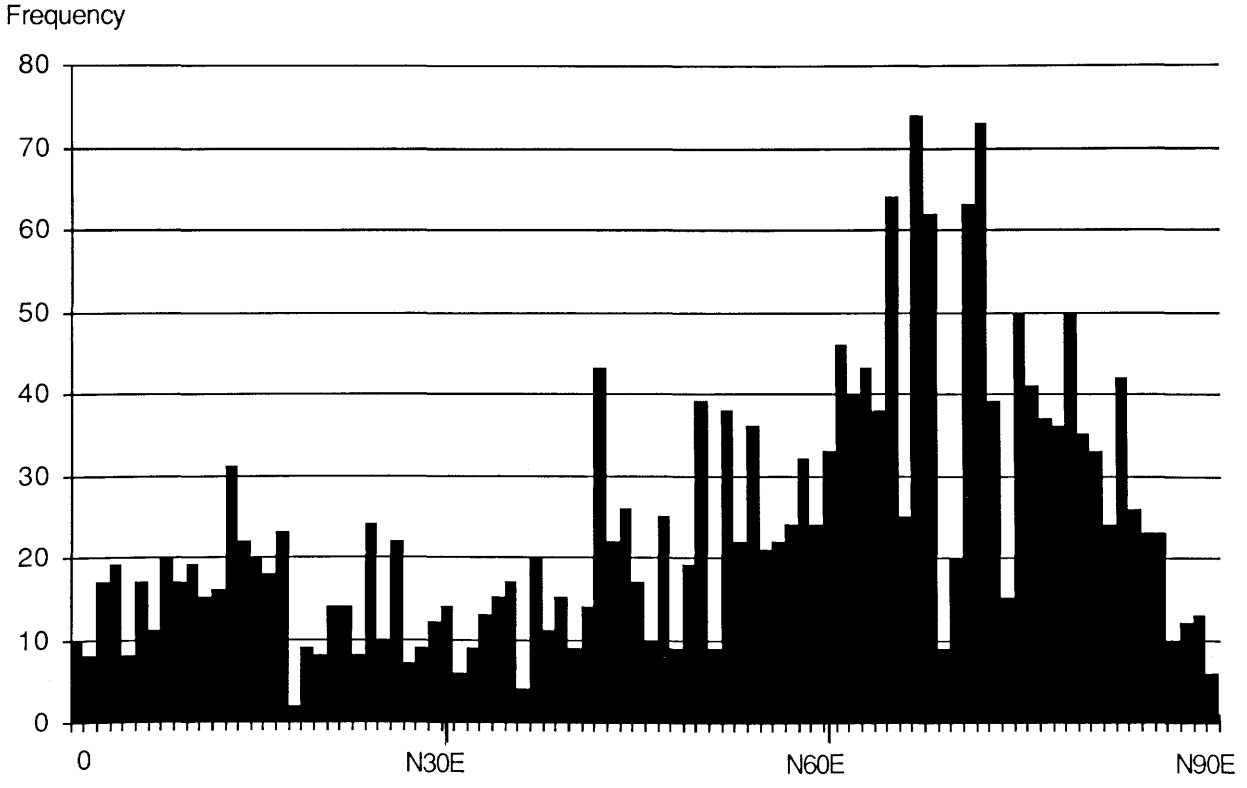

FIGURE 31.3.—Azimuth frequency histogram for linear features observed on MSS band 7.

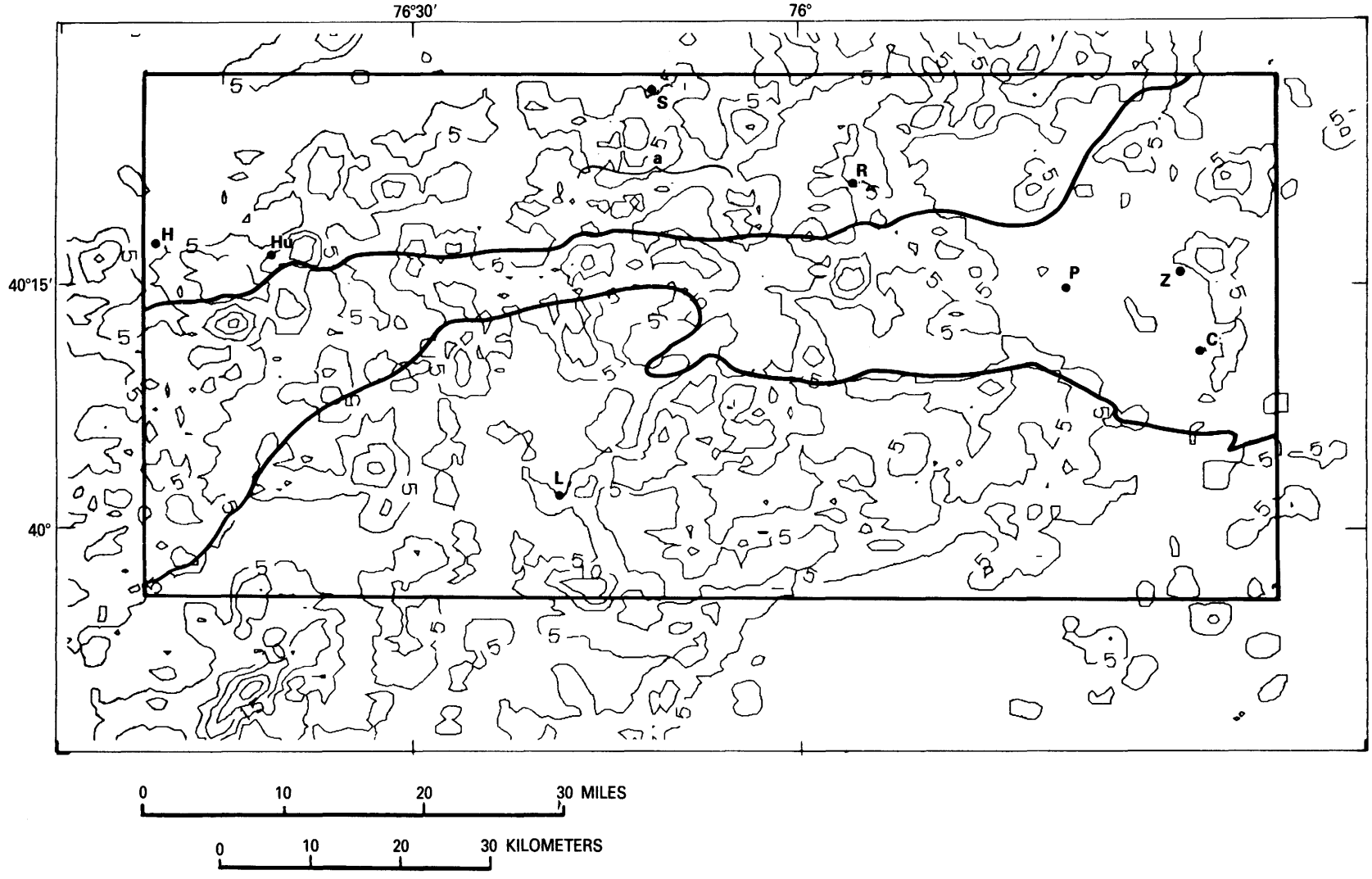

FIGURE 31.4.—Contour map of length-weighted density of linear features. Letter symbols the same as in figure 31.1.

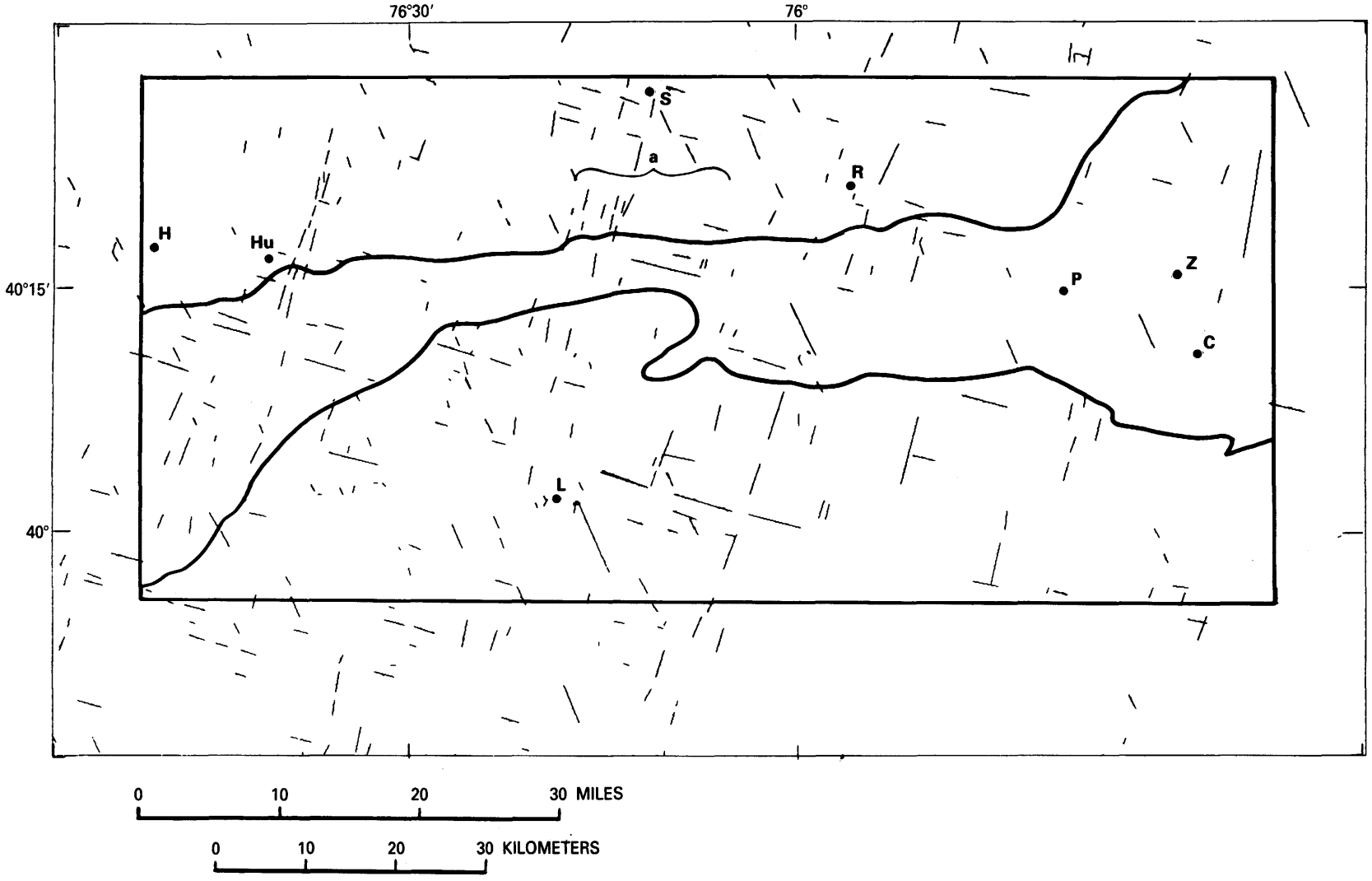

FIGURE 31.5.—Map of north-northeast- and northwest-trending linear features observed on Landsat MSS band 7 images. Azimuthal ranges of linear features plotted are N. 7° E.–N. 25°E., N. 70° W.–N. 80° W., and N. 20° W.–N. 30° W. Letter symbols the same as in figure 31.1.

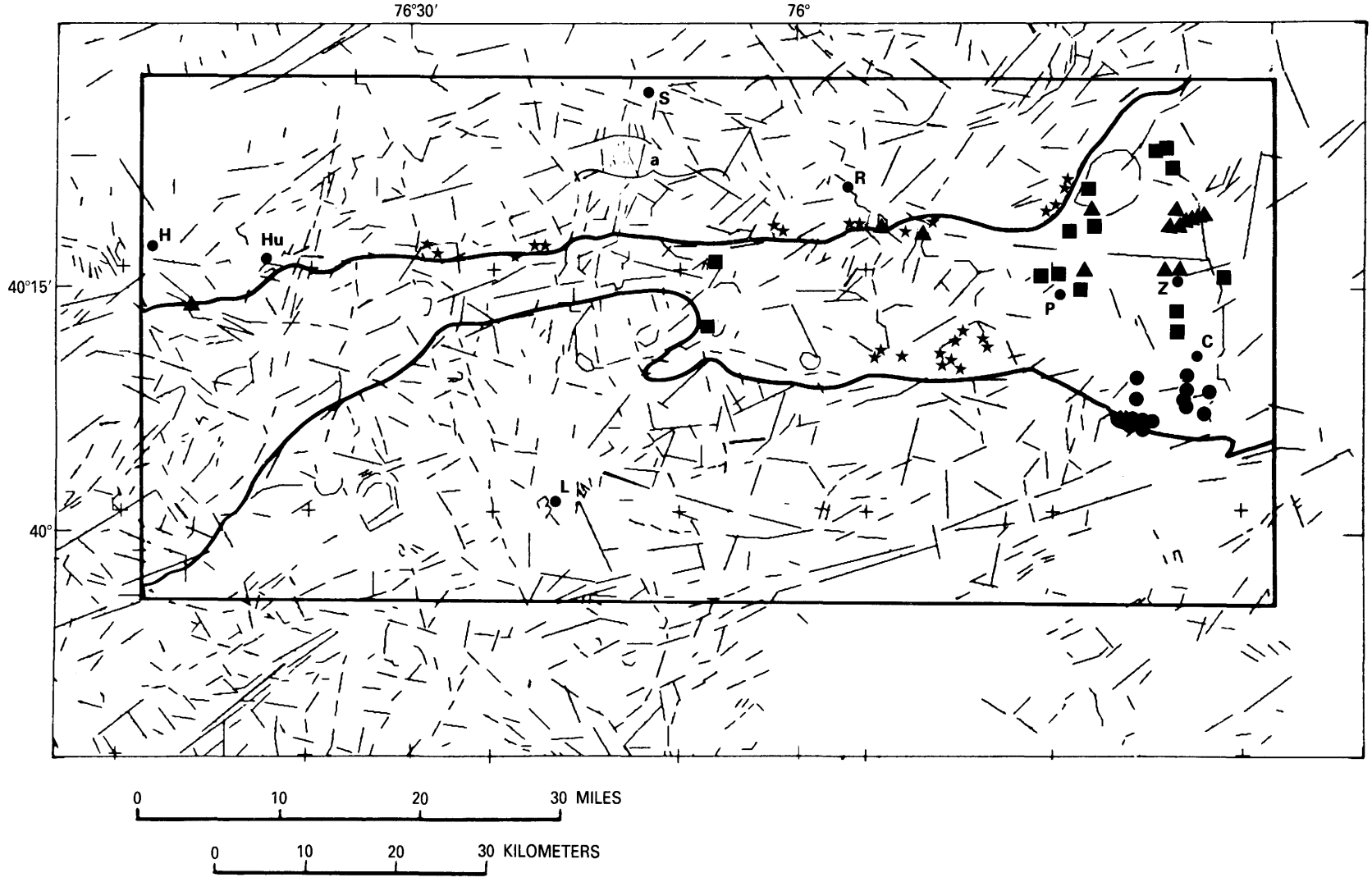

FIGURE 31.6.—Map of ore deposits in the Gettysburg basin (modified from Rose, 1970) superimposed on map of linear features (fig. 31.1). ● , Pb-Zn vein deposits; ★ , Cornwall-type skarn deposits; ▲ , Cu deposits adjacent to igneous bodies; ■ , Cu deposits away from igneous bodies.

Copper deposits in the eastern part of the area are aligned with a north-northwest-trending zone of linear features, near Collegeville, Pa. (C, fig. 31.2), which is partly composed of a linear segment of Perkiomen Creek. A similar north-northwest-trend is present in the density contour map (fig. 31.4). Copper deposits adjacent to igneous bodies cluster in a westerly trend along the margin of a diabase sheet (Berg and others, 1980). Copper deposits away from igneous bodies align with the north-northwest-trending zone of linear features (figs. 31.2, 31.6). This zone changes orientation from N. 5° W. in the south to N. 17° W. in the northern part near Zieglerville, Pa. (Z, fig. 31.2). An extension of this zone of north-northwest-trending linear features can be projected into a group of Pb-Zn deposits; however, most of the Pb-Zn deposits are located along northeast-trending veins (Smith, 1977), and linear features oriented north-northwest do not show any special correspondence to the ore deposits.

The copper deposits not associated with the diabase occur as pore fillings and as secondary replacement fillings of the clastic Triassic sedimentary rocks. The primary copper minerals are chalcopyrite and chalcocite, which are commonly altered by supergene processes into films of malachite and brochantite with secondary calcite (Bascom and others, 1931). The major copper deposit near Mechanicsville, Pa., 4 miles (6 km) northwest of Zieglerville, Pa. (Z, fig. 31.1), is related to a zone of faulting along the axis of a syncline, but other copper deposits do not show any obvious surface expression of structural control. The alignment of north-northwest-trending linear features with copper deposits away from diabase suggests that some type of regional structural control may affect the location of this category of copper deposits.

SUMMARY

A preliminary analysis of the linear features of the Gettsyburg basin mapped from Landsat MSS band 7 images shows several zones of linear features that illustrate different types of relationships to the Mesozoic geology. Three zones of linear features are shown to align with faults, diabase dikes, and ore deposits within the basin, fault offsets along the basin margin, and several different fold and fault structures outside the basin. Plots of linear features whose azimuthal trends correspond to maxima observed in an azimuth frequency histogram show that north-northeast-trending linear features transect the basin in several distinctive zones and form an orthogonal set to N. 75°W.-trending linear features. One north-northeast-trending zone of linear features corresponds to an area of a high density of faults within the basin and a corresponding relatively high concentration of linear features. In addition the zone aligns with several north-northeast-trending fault and fold axes outside the basin. A N. 85°W.-trending zone of linear features aligns with a pair of west-trending diabase dikes. This orientation is uncommon for the diabase dikes in that part of the basin; moreover, the dikes appear to be aligned along the extension of a major west-trending normal fault within the basin. Some replacement copper deposits that are not associated with igneous bodies align with a north-northwest-trending zone of linear features, suggesting that some regional structural control may be present in spite of the absence of mapped surface structures.

REFERENCES

Bascom, F., Wherry, E.T., Stose, G.W., and Jonas, A.I., 1931, Geology and mineral resources of the Quakertown-Doylestown district, Pennsylvania and New Jersey: U.S. Geological Survey Bulletin 828, 62 p.

Berg, Thomas, compiler, and others, 1980, Geologic map of Pennsylvania: Pennsylvania Geological Survey, scale 1:250,000.

Gray, Carlyle, compiler, and others, 1960, Geologic map of Pennsylvania: Pennsylvania Geological Survey, scale 1:250,000.

Jonas, A.I., and Stose, G.W., 1930, Geology and mineral resources of the Lancaster 15′ quadrangle: Pennsylvania Geological Survey, Atlas 168, scale 1:62,500.

Meisler, Harold, and Becher, A.E., 1970, Geologic and hydrologic map of the Lancaster 15-minute quadrangle, southeastern Pennsylvania: Pennsylvania Geological Survey Ground Water Report W–26, scale 1:24,000.

Podwysocki, M.H., Pohn, H.A., Phillips, J.D., Krohn, M.D., Purdy, T.P., and Merrin, I.S., 1982, Evaluation of remote sensing, geological, and geophysical data for south-central New York and north-central Pennsylvania: U.S. Geological Survey Open-File Report 82–319, 43 p.

Rose, A.W., 1970, Atlas of Pennsylvania mineral resources. Part 3, Metal mines and occurrences in Pennsylvania: Pennsylvania Geological Survey, Fourth Series, Bulletin M50, 14 p.

Rowan, L.C., and Wetlaufer, P.H., 1981, Relation between regional lineament systems and structural zones in Nevada: American Association of Petroleum Geologists Bulletin, v. 65, p. 1414–1432.

Scharnberger, C.K., 1984, Lancaster's Easter earthquake: Pennsylvania Geology, v. 15, no. 3, p. 2–5.

Smith, R.C., II, 1977, Zinc and lead occurrences in Pennsylvania: Pennsylvania Geological Survey, Fourth Series, Mineral Resource Report 72, 318 p.

Willard, B., Freedman, J., McLauglin, D.B., Ryan, J.R., Wherry, E.T., Peltier, L.C., and Gault, H.R., 1959, Geology and resources of Bucks County, Pennsylvania: Pennsylvania Geological Survey Bulletin C9, 243 p.

*U.S. GOVERNMENT PRINTING OFFICE: 1985-461-431:20036